REDOX REGULATION IN SKELETAL MUSCLE AGING AND EXERCISE

EDITED BY: Brian McDonagh
PUBLISHED IN: Frontiers in Physiology

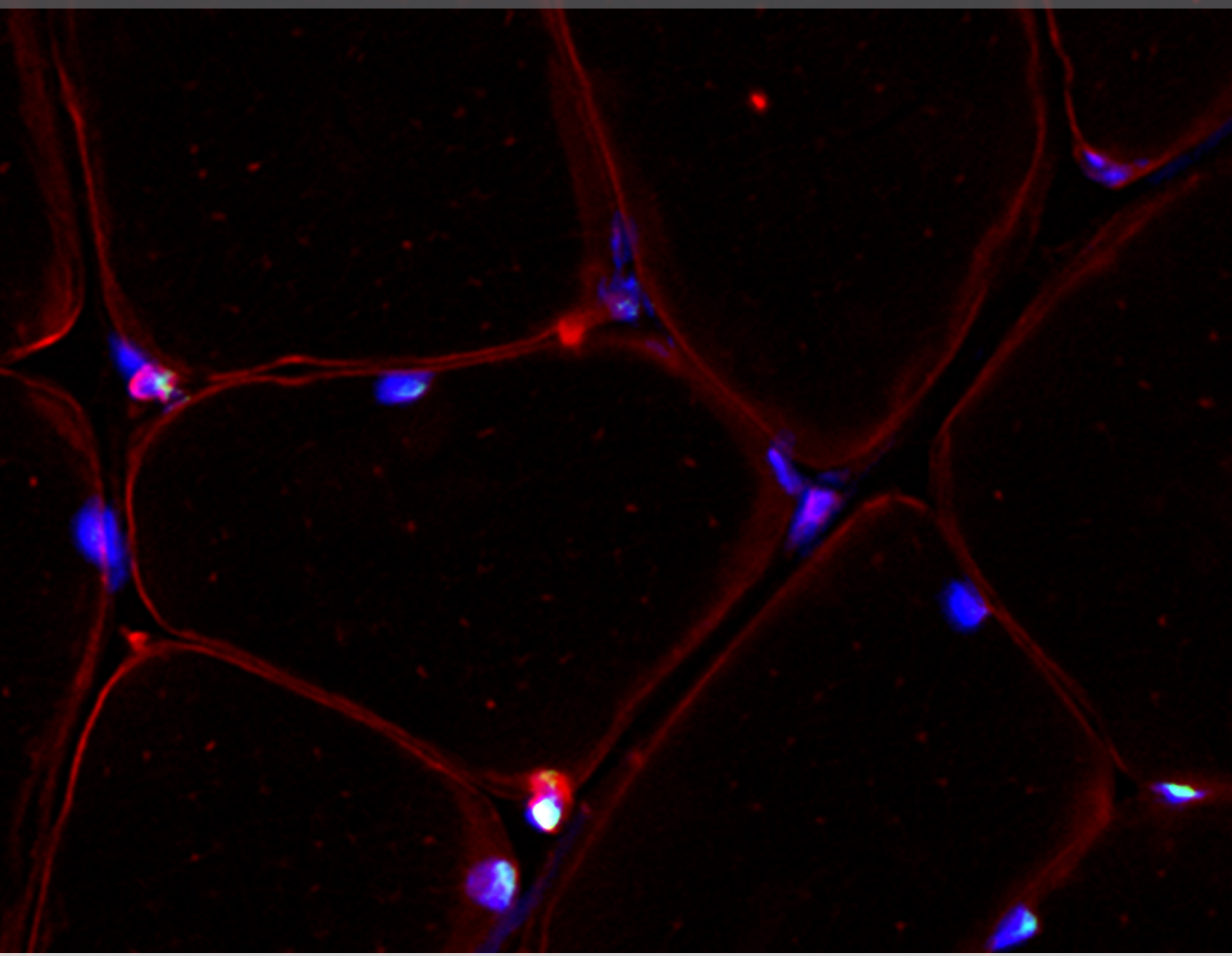

frontiers Research Topics

frontiers

ISSN 1664-8714
ISBN 978-2-88945-196-8
DOI 10.3389/978-2-88945-196-8

About Frontiers

Frontiers is more than just an open-access publisher of scholarly articles: it is a pioneering approach to the world of academia, radically improving the way scholarly research is managed. The grand vision of Frontiers is a world where all people have an equal opportunity to seek, share and generate knowledge. Frontiers provides immediate and permanent online open access to all its publications, but this alone is not enough to realize our grand goals.

Frontiers Journal Series

The Frontiers Journal Series is a multi-tier and interdisciplinary set of open-access, online journals, promising a paradigm shift from the current review, selection and dissemination processes in academic publishing. All Frontiers journals are driven by researchers for researchers; therefore, they constitute a service to the scholarly community. At the same time, the Frontiers Journal Series operates on a revolutionary invention, the tiered publishing system, initially addressing specific communities of scholars, and gradually climbing up to broader public understanding, thus serving the interests of the lay society, too.

Dedication to Quality

Each Frontiers article is a landmark of the highest quality, thanks to genuinely collaborative interactions between authors and review editors, who include some of the world's best academicians. Research must be certified by peers before entering a stream of knowledge that may eventually reach the public - and shape society; therefore, Frontiers only applies the most rigorous and unbiased reviews.
Frontiers revolutionizes research publishing by freely delivering the most outstanding research, evaluated with no bias from both the academic and social point of view.
By applying the most advanced information technologies, Frontiers is catapulting scholarly publishing into a new generation.

What are Frontiers Research Topics?

Frontiers Research Topics are very popular trademarks of the Frontiers Journals Series: they are collections of at least ten articles, all centered on a particular subject. With their unique mix of varied contributions from Original Research to Review Articles, Frontiers Research Topics unify the most influential researchers, the latest key findings and historical advances in a hot research area! Find out more on how to host your own Frontiers Research Topic or contribute to one as an author by contacting the Frontiers Editorial Office: **researchtopics@frontiersin.org**

REDOX REGULATION IN SKELETAL MUSCLE AGING AND EXERCISE

Topic Editor:
Brian McDonagh, Physiology, NUI Galway, Ireland

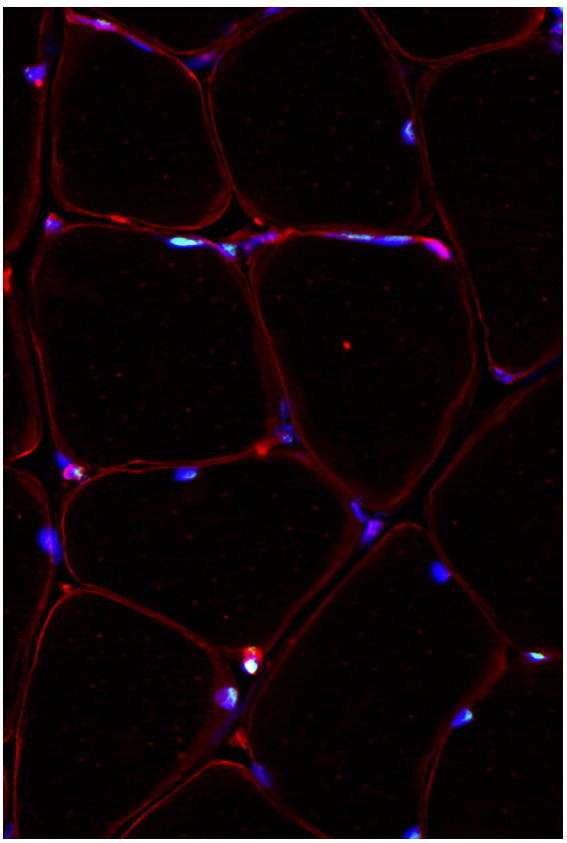

Cross section of fibres obtained from Gastrocnemius muscle from an adult mouse, immuno fluorescence staining for Pax7(green), DAPI (blue) and wheat germ agglutinin (yellow/red). Image courtesy of Ana Soriano Arroquia and Dr. Katarzyna Goljanek Whysall

Skeletal muscle represents the largest organ of the human body and comprises about 40% of total body mass in humans. Even in people who 'age well', there is a noticeable loss of muscle strength and function that accelerates dramatically after the age of 60, a major factor in the reduction in life quality for the aging population. One of the most effective interventions to maintain muscle mass and function is through exercise. Skeletal muscle generates reactive oxygen and reactive

nitrogen (ROS/RNS) species in response to muscle contractions. The concentration and species of ROS/RNS generated can depend on the age and fitness of the individual, muscle fibre type and the intensity of the muscle contractions. ROS/RNS generate unique signaling cascades that are not only essential in skeletal muscle contraction and adaptation but also play a role in a wide array of cell processes including cell proliferation, protein synthesis/degradation, immune response and antioxidant defense. ROS/RNS generated by contractions are involved in a co-ordinated local response that is tightly controlled at all levels from generation to detoxification. This collection of original articles and reviews highlights investigations that measure different aspects of the redox response of skeletal muscle to aging and exercise.

Citation: McDonagh, B., ed. (2017). Redox Regulation in Skeletal Muscle Aging and Exercise. Lausanne: Frontiers Media. doi: 10.3389/978-2-88945-196-8

Table of Contents

frontiers in Physiology

EDITORIAL
published: 22 January 2016
doi: 10.3389/fphys.2016.00005

Editorial: Redox Regulation in Skeletal Muscle Aging and Exercise

Brian McDonagh *

MRC-Arthritis Research UK Centre for Integrated Research into Musculoskeletal Aging, Institute of Ageing and Chronic Disease, University of Liverpool, Liverpool, UK

Keywords: skeletal muscle aging, redox signaling, exercise

The Editorial on the Research Topic

Redox Regulation in Skeletal Muscle Aging and Exercise

Changes in population demographics have seen an increase in human lifespan coupled with an increase in many age associated disorders that determine quality of life including, sarcopenia, and frailty. Closing the gap between life expectancy and healthy aging has now become a research priority in many countries. Skeletal muscle comprises up to 40% of body mass and the inhibition or delay of the progressive loss in muscle mass with age would help maintain mobility, strength and independence. Regular exercise is one of the few interventions known to help maintain both muscle mass and strength with age. The metabolic and structural changes induced by exercise ultimately affect the contractile properties of the muscle fiber. The role of endogenously generated reactive oxygen and reactive nitrogen species (ROS/RNS) as intracellular signaling molecules have been identified as playing a crucial role in the correct adaptation and response to exercise in skeletal muscle. The species, concentration and cellular location of endogenously generated ROS/RNS can directly and indirectly affect the activity of redox regulated proteins and transcription factors with a multitude of downstream effects. There are a number of potential sites for ROS/RNS generation including electron leakage from the electron transport chain, but more recent studies have identified endogenous cytoplasmic sources as a major contributor to ROS/RNS generation within muscle during contractions (Sakellariou et al., 2013; Pal et al., 2014; Pearson et al., 2014). An attractive mechanism for the redox regulation of numerous cellular processes is a redox signaling relay from cytoplasmic generation to a mitochondrial response, through the sequential modification of specific residues in regulatory proteins located in close proximity to the sites of endogenously generated ROS/RNS (McDonagh et al., 2014). Understanding the mechanisms of redox regulation in skeletal muscle and the changes induced during aging or disease are essential to maximize the beneficial effects of exercise. This special topic is a collection of original research and review articles that aims to bring together recent advances in our understanding of redox regulation in skeletal muscle during aging and exercise.

Elevated levels of Sphingomyelinase (SMase) have been detected during aging and in a variety of diseases, SMase induced sphingolipid metabolism results in a decrease in force production, increased fatigue and muscle atrophy (Ferreira et al., 2012). In the article by Lehr and colleagues they utilized redox sensitive green fluorescent probes (roGFP) targeted to Nox2 or the mitochondria allowing the identification of the site specific ROS generation as a result of SMase stimulation in single muscle FDB fibers (Loehr et al.). Results identify Nox2 as the major enzyme responsible for the increase in ROS, which was confirmed by a lack of increased ROS generation in Nox2$^{-/y}$ animals and Nox2 deficiency offers partial protection against SMase induced fatigue (Loehr et al.). Claflin and co-workers have contributed a novel method to assess mitochondrial function in skeletal muscle by fluorescently monitoring NADH/NAD^{+} balance as a reflection of the global mitochondrial redox state (Claflin et al.). They performed lengthening procedures on isolated lumbrical muscles from adult and old mice deficient in CuZnSOD, allowing force measurements and fluorescent monitoring of NADH concentrations (Claflin et al.). A brief period of intense contractions resulted in a large, reproducible fluorescence oscillation of NADH that ultimately returned to pre-contraction levels. Differences in the duration and magnitude of

OPEN ACCESS

Edited and reviewed by:
Paul M. L. Janssen,
Ohio State University, USA

***Correspondence:**
Brian McDonagh
b.mcdonagh@liverpool.ac.uk

Specialty section:
This article was submitted to Striated Muscle Physiology, a section of the journal Frontiers in Physiology

Received: *21 December 2015*
Accepted: *08 January 2016*
Published: *22 January 2016*

Citation:
McDonagh B (2016) Editorial: Redox Regulation in Skeletal Muscle Aging and Exercise. Front. Physiol. 7:5. doi: 10.3389/fphys.2016.00005

oscillations from adult and old mice, was attributed to differences in the ROS buffering capacity of old mice (Claflin et al.). Continuing with mitochondrial redox signaling cascades as a result of skeletal muscle contractions and exercise, Brandauer and colleagues investigated the requirement of AMPK for the exercise induced increase in the mitochondrial deacetylase SIRT3 and its target mitochondrial proteins (Brandauer et al.). Activation of AMPK by exercise or pharmacologically, can increase PGC-1α phosphorylation with subsequent increases in SIRT3 abundance and activation of its downstream targets (Brandauer et al.).

Skeletal muscle T-tubules are essential for excitation-contraction coupling and form triads with adjacent terminal cisternae of the sarcoplasmic reticulum regulating Ca^{2+} release and sequestration. Triads are unusual in that they contain high levels of cholesterol and sphingolipids, the group of Hidalgo has investigated the effects of cholesterol removal and age, on excitation-contraction (E-C) coupling and the protein content of triads in single muscle fibers (Barrientos et al.). A reduction in cholesterol impaired E-C coupling as a result of a modification of the interactions of the cholesterol associated caveolin-3, with Cav1.1 and the ryanodine receptor, interestingly the levels of the cholesterol binding caveolin-3 protein also decreased with age (Barrientos et al.).

Two contributions from the O'Halloran group examine the redox remodeling effects of chronic intermittent hypoxia (CIH) and chronic sustained hypoxia (CH) in sternohyoid muscle (Lewis et al.;Williams et al.). In the article by Williams et al, the authors examined the effects of CIH on rat sternohyoid force and power with complementary analysis of a number of redox parameters and enzymatic activities (Williams et al.). The authors conclude that CIH up-regulates NOX expression with concomitant modest oxidative stress, while constitutive NOX activity decreased sternohyoid muscle force and power (Williams et al.). The sternohyoid muscles of mice exposed to CH, with and without antioxidants, were analyzed by 2D redox proteomics and complimented with force measurements and enzyme activities (Lewis et al.). Alterations in redox and expression changes occurred in metabolic proteins with a functional deficit in sternohyoid function that was prevented by antioxidant supplementation (Lewis et al.).

The special topic also contains a number of selective reviews on redox regulation in skeletal muscle, including a contribution from Edward Debold that discusses potential mechanisms underlying muscle fatigue by ROS/RNS. The author examines studies where pre-treatment with ROS scavengers significantly attenuated the development of fatigue and presents evidence that ROS/RNS mediated fatigue involves modifications of muscle regulatory proteins that results in a decrease in Ca^{2+} sensitivity of these proteins (Debold). In the contribution by Michael P. Wiggs, the author outlines how exercise training or preconditioning can help prevent muscle atrophy due to inactivity (Wiggs). The author presents evidence that exercise induced mild oxidative stress, results in the activation of a number of cellular signaling pathways that can ultimately help protect skeletal muscle from disuse atrophy (Wiggs). Kaltsatou and colleagues present a systematic review on uremic myopathy, they identify studies linking renal failure with progressive muscle weakness and premature fatigue (Kaltsatou et al.). Chronic kidney disease is described as a silent epidemic in many developed countries and this review highlights there is a clear but as yet unexplored link between oxidative stress and uremic myopathy (Kaltsatou et al.).

This special topic highlights important advances in the field for studying redox regulation in skeletal during muscle aging and exercise, including the molecular mechanisms underlying the age related loss of muscle mass and function. I would like to especially thank all the contributors for their insightful and elegant original and review articles. I sincerely hope the Special Topic will help provide colleagues in the musculoskeletal and redox field with a platform that will stimulate ideas and experiments for further research.

AUTHOR CONTRIBUTIONS

The author confirms being the sole contributor of this work and approved it for publication.

FUNDING

BM is supported by the Wellcome Trust ISSF Fund (097826/Z/11/Z).

REFERENCES

Ferreira, L. F., Moylan, J. S., Stasko, S., Smith, J. D., Campbell, K. S., and Reid, M. B. (2012). Sphingomyelinase depresses force and calcium sensitivity of the contractile apparatus in mouse diaphragm muscle fibers. *J. Appl. Physiol. (1985)* 112, 1538–1545. doi: 10.1152/japplphysiol.01269.2011

McDonagh, B., Sakellariou, G. K., Smith, N. T., Brownridge, P., and Jackson, M. J. (2014). Differential cysteine labeling and global label-free proteomics reveals an altered metabolic state in skeletal muscle aging. *J. Proteome Res.* 13, 5008–5021. doi: 10.1021/pr5006394

Pal, R., Palmieri, M., Loehr, J. A., Li, S., Abo-Zahrah, R., Monroe, T. O., et al. (2014). Src-dependent impairment of autophagy by oxidative stress in a mouse model of Duchenne muscular dystrophy. *Nat. Commun.* 5, 4425. doi: 10.1038/ncomms5425

Pearson, T., Kabayo, T., Ng, R., Chamberlain, J., McArdle, A., and Jackson, M. J. (2014). Skeletal muscle contractions induce acute changes in cytosolic superoxide, but slower responses in mitochondrial superoxide and cellular hydrogen peroxide. *PLoS ONE* 9:e96378. doi: 10.1371/journal.pone.0096378

Sakellariou, G. K., Vasilaki, A., Palomero, J., Kayani, A., Zibrik, L., Mcardle, A., et al. (2013). Studies of mitochondrial and nonmitochondrial sources implicate nicotinamide adenine dinucleotide phosphate oxidase(s) in the increased skeletal muscle superoxide generation that occurs during contractile activity. *Antioxid. Redox Signal.* 18, 603–621. doi: 10.1089/ars.2012.4623

Conflict of Interest Statement: The author declares that the research was conducted in the absence of any commercial or financial relationships that could be construed as a potential conflict of interest.

frontiers in PHYSIOLOGY

ORIGINAL RESEARCH ARTICLE
published: 21 January 2015
doi: 10.3389/fphys.2014.00530

Sphingomyelinase promotes oxidant production and skeletal muscle contractile dysfunction through activation of NADPH oxidase

James A. Loehr, Reem Abo-Zahrah, Rituraj Pal and George G. Rodney*

Department of Molecular Physiology and Biophysics, Baylor College of Medicine, Houston, TX, USA

Edited by:
Brian McDonagh, University of Liverpool, UK

Reviewed by:
Francisco H. Andrade, University of Kentucky College of Medicine, USA
George K. Sakellariou, University of Liverpool, UK

****Correspondence:***
George G. Rodney, Department of Molecular Physiology and Biophysics, Baylor College of Medicine, One Baylor Plaza-BCM335, Houston, TX 77030, USA
e-mail: rodney@bcm.edu

Elevated concentrations of sphingomyelinase (SMase) have been detected in a variety of diseases. SMase has been shown to increase muscle derived oxidants and decrease skeletal muscle force; however, the sub-cellular site of oxidant production has not been elucidated. Using redox sensitive biosensors targeted to the mitochondria and NADPH oxidase (Nox2), we demonstrate that SMase increased Nox2-dependent ROS and had no effect on mitochondrial ROS in isolated FDB fibers. Pharmacological inhibition and genetic knockdown of Nox2 activity prevented SMase induced ROS production and provided protection against decreased force production in the diaphragm. In contrast, genetic overexpression of superoxide dismutase within the mitochondria did not prevent increased ROS production and offered no protection against decreased diaphragm function in response to SMase. Our study shows that SMase induced ROS production occurs in specific sub-cellular regions of skeletal muscle; however, the increased ROS does not completely account for the decrease in muscle function.

Keywords: ROS, skeletal muscle, Nox2, sphingomyelinase, force

INTRODUCTION

A variety of chronic diseases such as chronic heart failure (Doehner et al., 2007; Empinado et al., 2014), inflammatory disease (Wong et al., 2000), and sepsis (Okazaki et al., 2014) have been correlated with muscle weakness. Shingomyelinase (SMase), an enzyme involved in sphingolipid metabolism, has been shown to be elevated during these conditions (Wong et al., 2000; Claus et al., 2005; Empinado et al., 2014). Sphingolipids are abundant in skeletal muscle and their metabolites affect a wide variety of molecular processes (Nikolova-Karakashian and Reid, 2011). SMase induced sphingolipid metabolism results in an increase in ceramide production which has been shown to decrease force production and increase fatigue and muscle atrophy (Ferreira et al., 2010, 2012; De et al., 2012; Empinado et al., 2014).

Reactive oxygen species (ROS) have been shown to play a key role in modulating muscle function (Reid et al., 1993). In contracting skeletal muscle, mitochondria have traditionally been thought to be the major source of ROS; however, more recent evidence indicates that NADPH Oxidase (Nox2) may play a predominant role in ROS generation (Michaelson et al., 2010; Pal et al., 2013, 2014b; Sakellariou et al., 2013, 2014). In non-muscle cells, SMase has been shown to increase both mitochondrial and Nox2-dependent ROS (Sawada et al., 2004; Reinehr et al., 2005); while in skeletal muscle the mitochondria appear to be the primary source (Ferreira et al., 2012).

Until recently, there has been no reliable method to determine the sub-cellular origins of ROS. Traditionally, dichlorofluorescein (DCFH), in combination with various antioxidants, has been used to assess intracellular ROS production and extrapolate oxidant origin. While DCFH is useful for measuring general cytosolic ROS production, it is an irreversible dye that cannot differentiate between subcellular sources of ROS or determine redox state within the cell. Therefore, redox-sensitive green fluorescent probes (roGFP) with an artificial dithiol-disulfide pair inserted into the GFP (Hanson et al., 2004) were developed to function as reversible redox sensors and evaluate the local redox balance within the cell (Dooley et al., 2004; Hanson et al., 2004; Pal et al., 2013). We have shown that ro-GFPs specifically targeted to Nox2 (p47-roGFP) or the mitochondria (mito-roGFP) allow for measurement of site-specific ROS production within skeletal muscle (Michaelson et al., 2010; Pal et al., 2013, 2014a). Therefore, the aim of this project was to determine the specific subcellular site of ROS production in response to SMase stimulation. Our data indicate that Nox2 is a major contributor to ROS production in skeletal muscle (Michaelson et al., 2010; Pal et al., 2013, 2014b; Sakellariou et al., 2013, 2014); therefore, we hypothesized that SMase would induce Nox2-specific ROS and impair muscle function.

MATERIALS AND METHODS

IN-VIVO ELECTROPORATION

C57Bl/6J wild type (WT) and Nox2 knockout ($Nox2^{-/y}$) were purchased from Jackson Laboratories (Bar Harbor, ME) and bred following their breeding strategy. Mitochondrial SOD (MnSOD) transgenic mice were a kind gift from Dr. Pautler and were genotyped by PCR as previously described to verify transgene overexpression (Massaad et al., 2009). Redox sensitive GFP probes were transfected into the flexor digitorum brevis (FDB) of male WT,

$Nox2^{-/y}$, and MnSOD mice as previously described (Michaelson et al., 2010) and in accordance with National Institutes of Health guidelines and with the approval of the Institutional Animal Care and Use Committee of Baylor College of Medicine. Briefly, mice between 8 and 12 weeks of age were anesthetized with isoflurane (2%) and hyaluronidase (0.5 mg/ml) dissolved in sterile saline was injected subcutaneously into the foot pad of both hindlimb feet. Two hours later each foot was injected with 20–30 μg of rDNA in PBS; typically the right foot with p47-roGFP and the left foot with mito-roGFP. Two electrodes were placed subcutaneously at the proximal and distal FDB tendons to deliver 20 pulses of 150 V, 20 ms in duration at a frequency of 1 Hz with a square pulse stimulator (S48; Grass Technologies, West Warwick, RI). Mice were returned to their home cage and FDB muscle fibers were isolated 6–8 days later.

ISOLATION OF FDB FIBERS

Mice were deeply anesthetized by isofluorane (2%) inhalation and euthanized by rapid cervical dislocation. FDB muscles were surgically isolated and incubated at 37°C in minimal essential media containing 1% Pen Strep (Life Technologies, Grand Island, NY) and 0.4% Collagenase A (Roche Applied Science, Indianapolis, IN) for 2.0 h. FDB muscles were transferred to a serum containing media (10%, Atlanta Biologicals) without collagenase and triturated gently to release single fibers. Single fibers were then incubated in 21% O_2/5% CO_2 at 37°C until used, typically 12–36 h later.

ROS MEASUREMENTS

Prior to experiments, fibers were plated in 96 well dishes (Greiner Bio One, Monroe, NC) on ECM gel from Engelbreth-Holm-Swarm murine sarcoma (Sigma, St. Louis, MO). Intracellular ROS, in unstimulated FDB fibers, was measured using 6-carboxy-2′,7′-dichlorodihydrofluorescein diacetate (DCFH-DA) (Invitrogen, Carlsbad, CA) or electroporated site-specific subcellular redox sensitive ROS probes targeted to Nox2 (p47-roGFP) or the mitochondria (mito-roGFP). All FDB fibers were imaged at baseline (no drug) and then incubated for 30 min at 37°C with either vehicle control (0.13% Glycerol final) or SMase (0.5 U/ml). Cells were imaged after 30 min, placed back in the incubator for another 30 min and imaged again at 60 min. To obtain maximal oxidation, p47-roGFP and mito-roGFP electroporated fibers were exposed to 100 μM H_2O_2 for 5 min followed by dithiothreitol (DTT, 10 mM) to obtain maximum reduction. Regions of interest (ROI) were drawn on the cell and in the background. Ratio images (403/470) were created by subtracting the mean background ROI from the mean cell ROI.

DCFH-DA LOADING AND TREATMENT OF SINGLE FDB FIBERS

Plated FDB fibers were washed with 4-(2-Hydroxyethyl) piperazine-1-ethanesulfonic acid (HEPES) buffered Ringer's solution containing (in mM): 146 NaCl, 4.7 KCl, 0.6 MgSO4, 1.8 CaCl, 1.6, NaHCO3, 0.13 NaH2PO4, 7.8 glucose, 20.0 HEPES, pH 7.3 and incubated with DCFH-DA (5 μM) for 30 min at 37°C. The fibers were then washed with Ringer's solution and the dye was allowed to de-esterify for 20 min at 37°C prior to fluorescence microscopy. To prevent light induced oxidation of DCFH, all cell-loading and imaging was performed in the dark. In a subset of conditions, prior to DCFH-DA incubation, cells were incubated with a Nox2 peptide inhibitor, gp-91 ds (5 μM; Biosynthesis Inc., Lewisville, TX), for 45 min at 37°C.

MICROSCOPY

A Sutter Lamda DG-5 Ultra high speed wavelength switcher was used to excite DCF (480 nm) and ro-GFP (403/12 nm and 470/20 nm) fluorescence. DCFH-DA and ro-GFP emission intensity was collected at 510 nm and 535/48 nm, respectively, on a charge coupled device (CCD) Camera (CoolSNAP MYO, Photometrics, Tucson, AZ) attached to an Axio Observer (Zeiss) inverted microscope (40× H_2O objective, 1.2 NA) at a rate of 0.1 Hz.

EX VIVO FORCE MEASUREMENTS

Diaphragm muscle was surgically dissected from mice and sectioned into diaphragm strips with one end attached to a fixed hook and the other to a force transducer (F30, Harvard Apparatus) using silk suture (4-0) in a physiological saline solution continuously gassed with 95% O_2–5% CO_2 at 25°C. Diaphragm strips were incubated at 37°C for 15 min and optimal muscle length (L_o) and voltage (V_{max}) were adjusted to elicit maximum twitch force. SMase (0.5 U/ml) or vehicle control (0.13% glycerol final) was administered to the muscle bath and force at 300 Hz was monitored over time at 0, 30, and 60 min with pulse and train durations of 0.5 and 400 ms, respectively. After 60 min of incubation force-frequency characteristics were measured at stimulation frequencies of 1, 5, 10, 20, 40, 60, 80, 120, 150, 200, and 300-Hz every minute with pulse and train durations of 0.5 and 250 ms. Following a 5 min rest period fatigue was assessed using a matched force protocol in which frequency was adjusted so force generated by drug treated tissue matched the force of vehicle control at 40 Hz with pulse and train durations of 0.5 and 400 ms and a train rate of 0.5 Hz. ROS has been suggested to decrease force by altering Ca^{2+} sensitivity; therefore a frequency on the steep part of the force frequency relationship (40 Hz) was chosen to determine if inhibiting SMase induced ROS protected against decreased muscle force. At the end of the contractile protocol muscle length was measured using a hand-held electronic caliper, fiber bundles were removed from the bath and trimmed of excess bone and connective tissue, blotted dry, and weighed. Muscle weight and Lo were used to estimate cross-sectional area and absolute forces expressed as N/cm^2 (Close, 1972).

DATA ANALYSIS

Data are reported as mean ± SEM, unless otherwise specified. A One-Way RM ANOVA was used to measure statistical differences within a group and a Two-Way RM ANOVA was used for between group differences. Tukey's *post-hoc* test was used when statistical differences were identified. Statistical analysis was performed in Origin Pro (OriginLab Corporation, Northhampton, MA) with significance set *a priori* at $p \leq 0.05$.

RESULTS

EFFECT OF SMase STIMULATION ON GENERAL ROS PRODUCTION

To assess the role of Nox2 in general non-specific intracellular ROS production, we measured changes in DCF fluorescence in

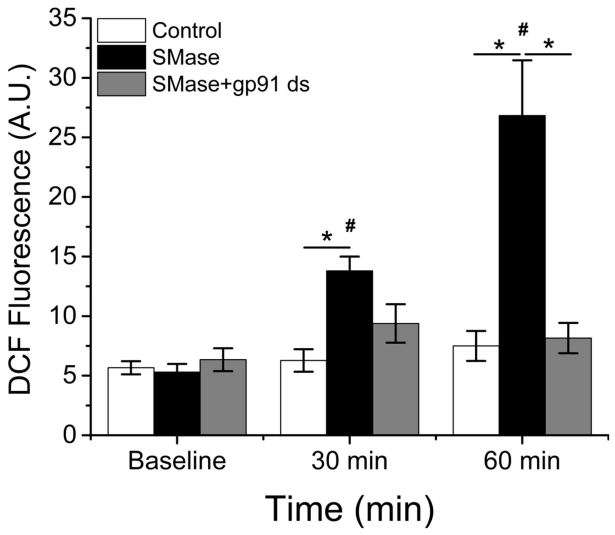

FIGURE 1 | SMase increases ROS production through Nox2 in FDB fibers. SMase increased DCF fluorescence in WT FDB fibers (black bars), which could be completely inhibited upon pre-incubation with gp91-ds (gray bars). There was no time-dependent change in the absence of SMase (white bars). $p \leq 0.05$ *significantly different from vehicle treated control, #significantly different from baseline in at least $n_{animals} = 3$, $n_{cells} = 31$.

FDB fibers in the presence or absence of the Nox2 specific peptide inhibitor gp91-ds (Rey et al., 2001; Csanyi et al., 2011; Pal et al., 2013). SMase resulted in an increase ($p \leq 0.05$) in DCF fluorescence at 30 min and a further increase at 60min, which was inhibited by pre-incubation with gp91-ds (**Figure 1**). There was no change in control fibers over the same time. These data suggest that in skeletal muscle, SMase stimulates Nox2 dependent ROS production.

SUBCELLULAR ROS SENSORS TARGETED TO NADPH OXIDASE (Nox2) AND THE MITOCHONDRIA

While our data indicate a role for Nox2 in SMase induced ROS production, others have indicated a potential role for mitochondrial ROS generation (Sawada et al., 2004; Nikolova-Karakashian and Reid, 2011; Ferreira et al., 2012). Therefore, we used redox sensitive GFP probes targeted to Nox2 (p47-roGFP) and the mitochondria (mito-roGFP) to determine the localization of subcellular ROS production. Similar to DCFH, in the absence of SMase, we saw no time dependent effects of ROS production using the p47-roGFP or mito-roGFP ROS sensors (data not shown). SMase exposure increased Nox2 derived ROS following 30 and 60 min (**Figure 2C**), while it had no effect on increasing mitochondrial oxidant burden (**Figure 2D**). Representative images demonstrate the change in fluorescence of both p47-roGFP (**Figure 2A**) and mito-roGFP (**Figure 2B**) in response to SMase. The use of site-specific redox probes further confirms ROS is produced through Nox2, with no additional mitochondrial contribution.

GENETIC ABLATION OF Nox2 PREVENTS INCREASED ROS PRODUCTION

Our data indicate that Nox2 plays a central role in SMase induced ROS production in skeletal muscle. To further confirm the role of Nox2 we assessed the effects of SMase stimulated ROS production in FDB fibers from Nox2 deficient ($Nox2^{-/y}$) mice. SMase induced oxidation of p47-roGFP was completely abolished (**Figure 3A**) and, consistent with our previous findings, there was no change in the oxidation of mito-roGFP (**Figure 3B**). The lack of ROS production in $Nox2^{-/y}$ animals further supports the role of Nox2 as the source of ROS production in adult skeletal muscle exposed to SMase.

MnSOD OVEREXPRESSION DOES NOT PREVENT SMase INDUCED ROS PRODUCTION

Previous data have shown increased mitochondrial ROS in response to SMase stimulation (Ferreira et al., 2012). Genetically overexpressing mitochondrial superoxide dismutase (MnSOD) in mice has been shown to reduce contraction induced mitochondrial ROS in skeletal muscle (McClung et al., 2010); therefore, we next wanted to determine if MnSOD overexpression had any effect on ROS production in response to SMase. A representative DNA gel image, verifying MnSOD transgene overexpression, is shown in **Figure 4A**. In FDBs from MnSOD overexpressing mice, SMase induced an increase in Nox2 (p47-roGFP) ROS production (**Figure 4B**), while no difference was detected in mitochondrial ROS production (**Figure 4C**). These results provide further support that SMase increases ROS production through Nox2, while mitochondrial ROS production is not altered.

GENETIC DELETION OF Nox2 PARTIALLY PROTECTS AGAINST SMase INDUCED FORCE DECREMENT

SMase induced ROS has been shown to decrease force in skeletal muscle (Ferreira et al., 2010, 2012). Our previous data indicate decreased ROS production in $Nox2^{-/y}$ animals in response to SMase; therefore, we wanted to determine whether genetically inhibiting Nox2-dependent ROS production would provide protection against SMase induced force depression in diaphragm strips. In the absence of SMase, there was a non-significant (<4%) time dependent change in force over 60 min (**Figures 5A,B**). SMase decreased tetanic force ($p \leq 0.05$) in diaphragm strips from WT, $Nox2^{-/y}$, and MnSOD overexpressing mice compared to their respective controls at 30 and 60 min (**Figures 5A,B**). Nox2 deficient animals conferred partial protection against the force decrement observed in the diaphragm of WT mice at 60 min (**Figure 5A**), while the MnSOD overexpressing mice offered no protection in force decrement (**Figure 5B**). While not statistically significant ($p \leq 0.08$), there was a trend toward protection against force decrement in the $Nox2^{-/y}$ animals at 30 min.

SMase induced force decrements were observed across all frequencies of stimulation (**Figure 6**) Genetic deletion of Nox2 protected against SMase induced force loss at all frequencies of stimulation, with an approximate 51 and 55% protection against twitch and peak tetanic force loss, respectively (**Figure 6A**). Interestingly, diaphragm from $Nox2^{-/y}$ mice displayed enhanced force production compared to WT animals at higher frequencies of stimulation (**Figure 6A**), suggesting that Nox2 specific ROS regulates muscle function even under basal conditions. Unlike the protection observed by eliminating Nox2 dependent ROS, no protection was evident in muscle from MnSOD overexpressing mice (**Figure 6B**), confirming our previous data that SMase does not result in a significant increase in ROS production from the

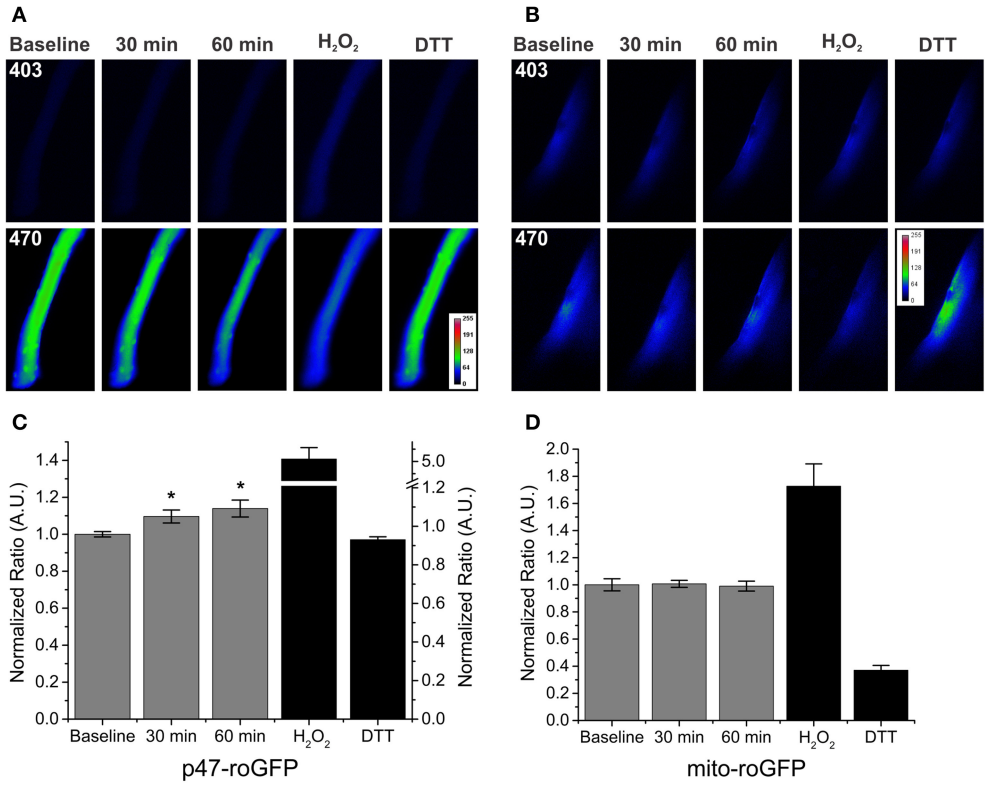

FIGURE 2 | SMase increased Nox2 ROS production in WT FDB fibers with no effect on mitochondrial ROS. (A,B) Representative images of SMase induced changes in p47-roGFP and mito-roGFP fluorescence, respectively. **(C)** Nox2 ROS (p47-roGFP) in FDBs from WT animals was elevated following SMase at both 30 and 60 min. H_2O_2 and DTT (100 μM and 10 mM, black bars) resulted in further oxidation and reduction of p47-roGFP. **(D)** Mitochondrial ROS (mito-roGFP) did not change in response to SMase. H_2O_2 and DTT (100 μM and 10 mM, black bars) resulted in further oxidation and reduction of mito-roGFP. Fluorescence values were normalized to non-drug treated baseline measurements. $p \leq 0.05$ *significantly different from baseline in at least $n_{animals} = 4$, $n_{cells} = 11$.

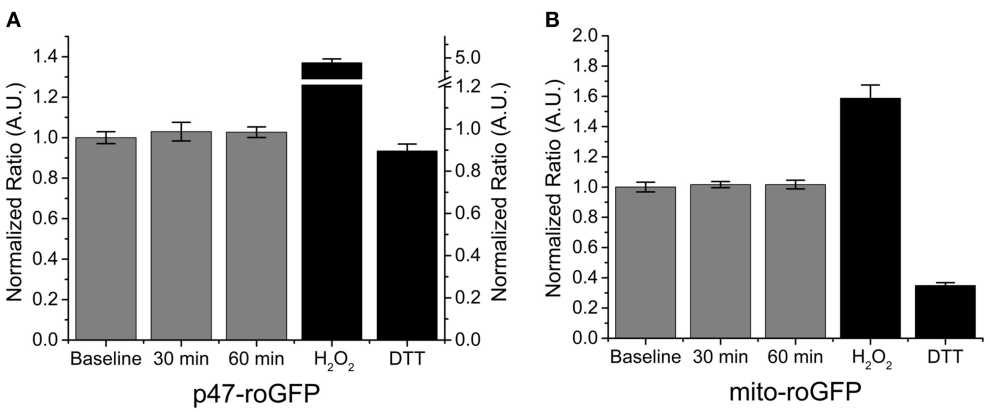

FIGURE 3 | Genetic deletion of Nox2 prevents SMase induced ROS. (A) Nox2 ROS (p47-roGFP) was not altered with SMase in FDBs from Nox2$^{-/y}$ mice. **(B)** Mitochondrial ROS (mito-roGFP) did not change in response to SMase. H_2O_2 and DTT (100 μM and 10 mM, black bars) resulted in further oxidation and reduction of both p47-roGFP and mito-roGFP. Fluorescence values were normalized to non-drug treated baseline measurements in at least $n_{animals} = 4$, $n_{cells} = 12$.

mitochondria. Our data indicate that eliminating SMase stimulated Nox2-dependent ROS confers protection against force decrement and that Nox2-specific ROS may play a role in basal muscle function.

Nox2 DOES NOT CONFER PROTECTION AGAINST SMase INDUCED FATIGUE

Oxidants have been shown to promote skeletal muscle fatigue (Moopanar and Allen, 2005; Bruton et al., 2008) and SMase has

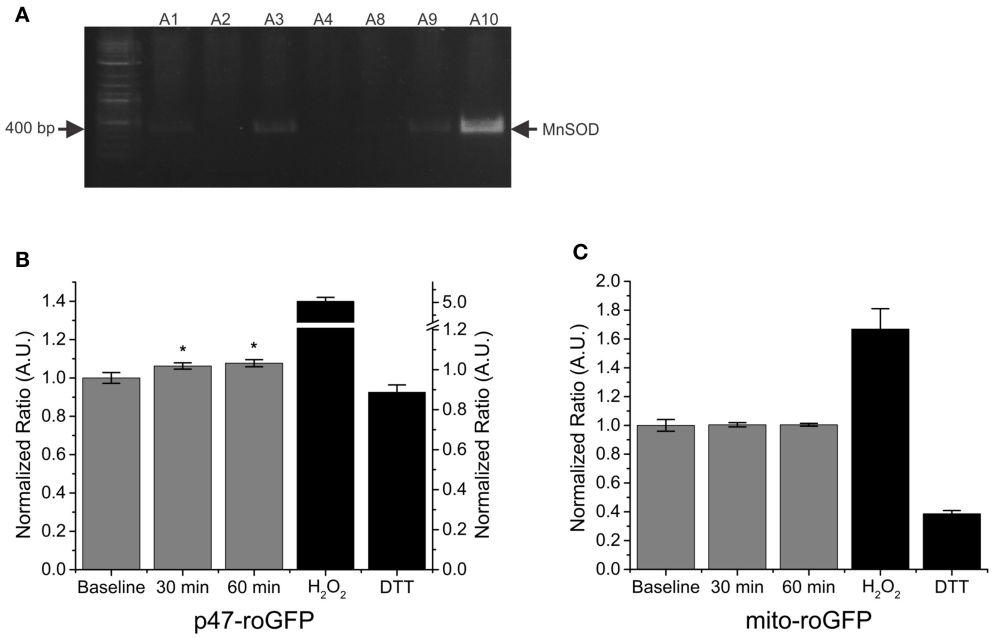

FIGURE 4 | SMase increased Nox2 ROS production in FDB fibers from MnSOD overexpressing mice. (A) Representative DNA gel verifying MnSOD transgene overexpression. **(B)** SMase increased Nox2 ROS (p47-roGFP) in muscle from MnSOD overexpressing animals at both 30 and 60 min. **(C)** Mitochondrial ROS (mito-roGFP) did not change in response to SMase. H_2O_2 and DTT (100 μM and 10 mM, black bars) resulted in further oxidation and reduction of both p47-roGFP and mito-roGFP. Fluorescence values were normalized to non-drug treated baseline measurements. $p \leq 0.05$ *significantly different from baseline in at least $n_{animals} = 3$, $n_{cells} = 10$.

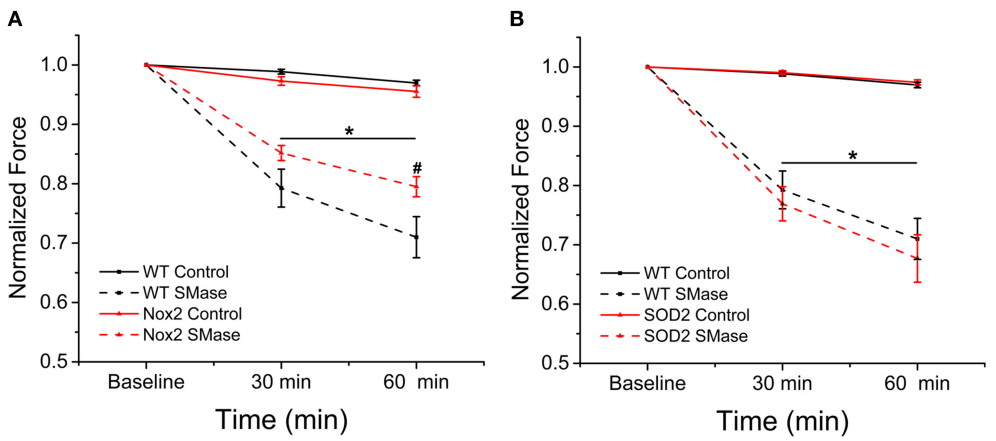

FIGURE 5 | Genetic deletion of Nox2 protected against diaphragm force decrement over time. Peak tetanic force was decreased at both 30 and 60 min following SMase administration compared with respective controls. **(A)** Genetic deletion of Nox2 protected against SMase induced force loss compared with WT. Black solid = WT control, Black dash = WT SMase, Red solid = $Nox2^{-/y}$ control, Red dash = $Nox2^{-/y}$ SMase. **(B)** Overexpressing MnSOD did not affect force decrement compared to WT. Black solid = WT control, Black dash = WT SMase, Red solid = MnSOD control, Red dash = MnSOD SMase. Force values at 30 and 60 min were normalized to force measured in the absence of SMase (baseline). $p \leq 0.05$ *All genotypes significantly different from respective control, #$Nox2^{-/y}$ SMase significantly different from WT SMase in at least $n_{animals} = 6$.

been shown to increase fatigue in an oxidant dependent manner (Ferreira et al., 2010). Our results show that Nox2 deficiency decreases SMase induced oxidant production and offers partial protection against the decrease in force observed in WT animals; therefore, we wanted to determine if it also would protect against SMase induced fatigue. In the vehicle treated control groups, neither diaphragm from the $Nox2^{-/y}$ nor the MnSOD overexpressing mice showed altered fatigue compared with WT. Following SMase administration, there was an increase in the rate of fatigue for diaphragm from WT, $Nox2^{-/y}$ and MnSOD overexpressing mice (**Figures 7A,B**). Neither the Nox2 knockout nor the MnSOD overexpressing mice conferred any protection against

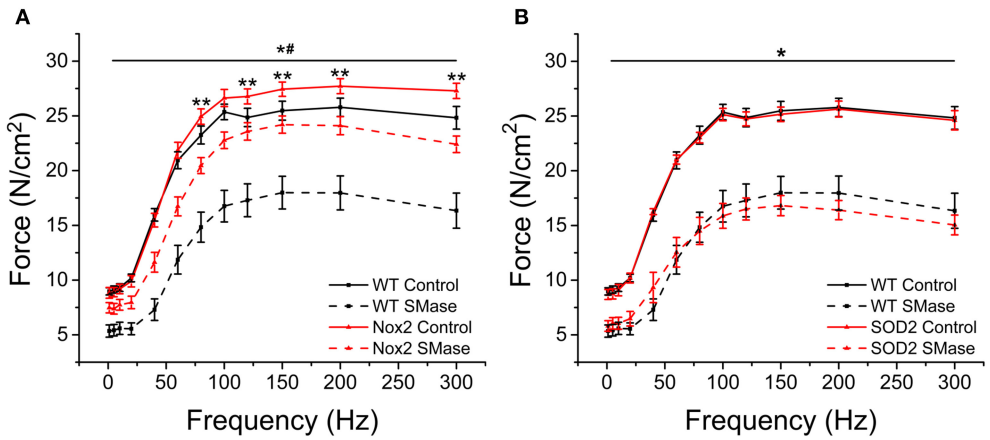

FIGURE 6 | Nox2 deletion protected against SMase induced decreased force. Force was decreased at all frequencies following SMase administration compared with respective controls. **(A)** SMase induced force loss was prevented in diaphragm muscle from Nox2$^{-/y}$ mice compared to WT at all frequencies. Nox2$^{-/y}$ controls produced greater force at higher frequencies compared with WT control. Black solid = WT control, Black dash = WT SMase, Red solid = Nox2$^{-/y}$ control, Red dash = Nox2$^{-/y}$ SMase. **(B)** MnSOD overexpression did not prevent force loss at any frequency compared to WT SMase. Black solid = WT control, Black dash = WT SMase, Red solid = MnSOD control, Red dash = MnSOD SMase. $P \leq 0.05$ *All genotypes significantly different from respective control, #Nox2$^{-/y}$ SMase significantly different from WT SMase, **Nox2 control significantly different from WT control in at least $n_{animals} = 4$.

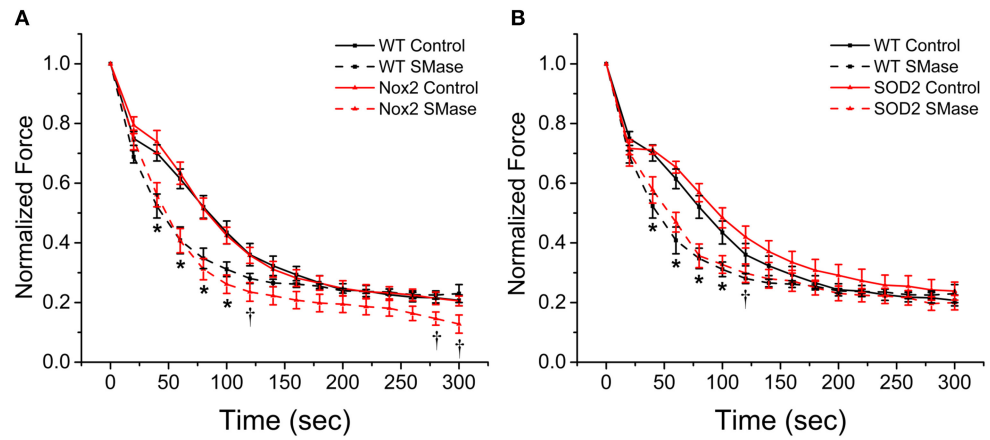

FIGURE 7 | Genetic ablation of Nox2 or MnSOD overexpression does not protect against SMase induced fatigue. All genotypes fatigued approximately 75–80%. SMase induced an increased rate of fatigue in diaphragm from WT (**A,B**, black dashed), Nox2$^{-/y}$ (**A**, red dashed), and MnSOD (**B**, red dashed) compared with their respective controls (solid lines). All force values were normalized to initial force. $p \leq 0.05$ *All genotypes significantly different from respective control, †Nox2$^{-/y}$ and MnSOD significantly different from respective controls in at least $n_{animals} = 6$.

increased rate of fatigue (**Figures 7A,B**). The fatigue index, calculated as the last tetanus divided by the first tetanus, indicated diaphragm strips from all animals fatigued approximately 75–80%. These data suggest that fatigue observed in the presence of SMase is likely independent of ROS.

DISCUSSION

SMase, an enzyme which catalyzes the production of metabolites that affect a number of cellular functions (Nikolova-Karakashian and Reid, 2011), has been shown to be elevated in response to a variety of diseases (Wong et al., 2000; Claus et al., 2005; Empinado et al., 2014). Increased SMase results in increased ROS production, which has been thought to negatively impact muscle force and promote fatigue (Ferreira et al., 2010, 2012). Previous research has shown that SMase can induce either mitochondrial or Nox2 ROS in non-muscle cells (Sawada et al., 2004; Reinehr et al., 2005) while recent indirect evidence suggests SMase induced ROS in skeletal muscle was generated by the mitochondria (Ferreira et al., 2012). The majority of ROS production in skeletal muscle has generally been assumed to be mitochondrial; however, more recent evidence by our lab and others implicate Nox2 as a major source of ROS in skeletal muscle (Michaelson et al., 2010; Pal et al., 2013, 2014b; Sakellariou et al., 2013, 2014). Using site-specific subcellular redox sensors and various genetic

animal models, we have shown that SMase induces ROS through Nox2 and eliminating Nox2-dependent ROS partially recovers muscle function.

Using the general ROS probe, DCFH, and a Nox2-specific peptide inhibitor (gp91-ds), we show that Nox2 plays a significant role in SMase induced ROS production. However, since DCFH is a non-specific, irreversible probe that does not allow for the evaluation of cellular redox homeostasis, there is still uncertainty as to the source of ROS within the cell and whether there is a true shift in the redox balance upon SMase exposure. The recent development of reversible, site-specific subcellular redox probes allows for a more thorough evaluation of the source of ROS production and redox balance in response to various stimuli or in response to different disease states. Using ROS sensors specifically targeted to Nox2 (p47-roGFP) and the mitochondria (mito-roGFP), we were able to show that SMase increased Nox2 ROS production, but had no effect on mitochondrial ROS in mouse FDB muscle. The lack of response of mito-roGFP to SMase cannot be attributed to the failure of the probe to respond, as the fluorescence ratio increased approximately two-fold upon oxidation (100 μM H_2O_2). These findings are in disagreement with other reports, which suggest SMase induces mitochondrial ROS production in the mouse diaphragm. Using an antioxidant peptide targeted to the inner mitochondrial membrane (SS-31) Reid and colleagues have suggested that SMase induces ROS generation from the mitochondria in mouse diaphragm muscle, which then diffuses into the cytosol where it is detected by the non-specific ROS probe DCFH (Ferreira et al., 2012). While SS-31 has been shown to localize to the mitochondria Szeto and colleagues have also shown that it also localizes to the cytosol (Zhao et al., 2004). This would allow SS-31 to act as a cytosolic ROS scavenger; reducing SMase induced ROS production generated by Nox2. Using pharmacological inhibition of Nox2 (gp91-ds) and genetic deletion of Nox2 ($Nox2^{-/y}$), our results confirm that SMase induces ROS production by activating Nox2 in skeletal muscle. Furthermore, MnSOD overexpressing mice did not confer protection against SMase induced oxidation of our Nox2 redox biosensor.

Another potential confounding variable is that mitochondrial content varies in different muscles based on fiber type composition. Ferreira et al. (2012) used mouse diaphragm, which is comprised of 42–49% oxidative (Type I and IIA) fibers with the mitochondria encompassing approximately 34% of the fiber volume (Gamboa and Andrade, 2010; Guido et al., 2010; Pal et al., 2014b). We evaluated ROS production in FDB fibers, which have been reported to contain approximately 30% oxidative fibers (Gonzalez et al., 2003) with a mitochondrial volume between 10 and 36% of the fiber volume (Bruton et al., 2003; Laker et al., 2014). However, if SMase was able to induce a shift in the mitochondrial redox balance in muscle with a higher mitochondrial content (i.e., diaphgram), one would predict that overexpressing MnSOD would protect against SMase induced dysfunction, which was not observed in our studies. Therefore, we believe that differences in fiber type or mitochondrial content do not affect SMase induced mitochondrial ROS production.

ROS has been shown to be a potent modifier of skeletal muscle contractility and fatigue by modulating myofilament calcium sensitivity (Reid et al., 1993; Andrade et al., 1998; Callahan et al., 2001; Moopanar and Allen, 2005; Bruton et al., 2008). In the present study, eliminating SMase induced ROS provided partial protection against decreased force and had no effect on fatigue. It is unlikely that reactive nitrogen species, another source of oxidants in skeletal muscle, could account for the continued force decrement, as SMase had no effect on NO activity and blocking NO activity had no effect on SMase induced force decrement (Ferreira et al., 2010). Sarcoplasmic reticulum (SR) calcium release has been shown to play an important role in skeletal muscle function (Ortenblad et al., 2000; Allen et al., 2008). The direct metabolite of SMase activity, ceramide, can be further metabolized by ceramidase into sphingosine. Sphingosine has been shown to decrease SR calcium release (Betto et al., 1992; Sabbadini et al., 1992; McDonough et al., 1994) by decreasing ryanodine receptor open probability (Needleman et al., 1997; Sabbadini et al., 1999). Increased levels of sphingosines have also been shown to decrease myocyte calcium transients, cell shortening, and contractile function, (Webster et al., 1994; Oral et al., 1997; Friedrichs et al., 2002; Favory et al., 2004) in addition to promoting muscle fatigue (Danieli-Betto et al., 2000). Therefore, SMase may affect muscle function through a non-ROS dependent mechanism. We are currently investigating the role of these potential mechanisms in skeletal muscle force depression and fatigue.

In summary, we have shown that SMase increases Nox2 dependent ROS and has no effect on mitochondrial ROS production. Genetically deleting or pharmacologically inhibiting Nox2 reduced SMase stimulated ROS production to control levels. In addition, Nox2 inhibition provided protection against decreased force production induced by SMase; however, there was no effect on muscle fatigue. This indicates that SMase, through its downstream metabolites, may affect contractile function in a ROS independent manner, potentially through modifying SR calcium release.

ACKNOWLEDGMENTS

We thank Dr. Robia Pautler and Deric Griffin for providing and genotyping the MnSOD overexpression mice. Research reported in this publication was supported by the National Institute of Arthritis and Musculoskeletal and Skin Diseases of the National Institutes of Health under Award Number R01 AR061370 to George G. Rodney, the National Institute of Neurological Disorders and Stroke of the National Institutes of Health under Award Number R21 NS085208 to George G. Rodney, the National Heart, Lung, and Blood Institute of the National Institutes of Health under Award Number T32 HL007676 to James A. Loehr, and a Gillson Longenbaugh Foundation Award to George G. Rodney.

REFERENCES

Allen, D. G., Lamb, G. D., and Westerblad, H. (2008). Impaired calcium release during fatigue. *J. Appl. Physiol. (1985)* 104, 296–305. doi: 10.1152/japplphysiol.00908.2007

Andrade, F. H., Reid, M. B., Allen, D. G., and Westerblad, H. (1998). Effect of hydrogen peroxide and dithiothreitol on contractile function of single skeletal muscle fibres from the mouse. *J. Physiol.* 509(Pt 2), 565–575. doi: 10.1111/j.1469-7793.1998.565bn.x

Betto, R., Teresi, A., Fachechi-Cassano, G., Salviati, G., and Sabbadini, R. A. (1992). Sphingosine inhibits calcium release from sarcoplasmic reticulum membranes. *Adv. Exp. Med. Biol.* 311, 403–404. doi: 10.1007/978-1-4615-3362-7_55

Bruton, J. D., Dahlstedt, A. J., Abbate, F., and Westerblad, H. (2003). Mitochondrial function in intact skeletal muscle fibres of creatine kinase deficient mice. *J. Physiol.* 552, 393–402. doi: 10.1113/jphysiol.2003.050732

Bruton, J. D., Place, N., Yamada, T., Silva, J. P., Andrade, F. H., Dahlstedt, A. J., et al. (2008). Reactive oxygen species and fatigue-induced prolonged low-frequency force depression in skeletal muscle fibres of rats, mice and SOD2 overexpressing mice. *J. Physiol.* 586, 175–184. doi: 10.1113/jphysiol.2007.147470

Callahan, L. A., She, Z. W., and Nosek, T. M. (2001). Superoxide, hydroxyl radical, and hydrogen peroxide effects on single-diaphragm fiber contractile apparatus. *J. Appl. Physiol. (1985)* 90, 45–54.

Claus, R. A., Bunck, A. C., Bockmeyer, C. L., Brunkhorst, F. M., Losche, W., Kinscherf, R., et al. (2005). Role of increased sphingomyelinase activity in apoptosis and organ failure of patients with severe sepsis. *FASEB J.* 19, 1719–1721. doi: 10.1096/fj.04-2842fje

Close, R. I. (1972). Dynamic properties of mammalian skeletal muscles. *Physiol. Rev.* 52, 129–197.

Csanyi, G., Cifuentes-Pagano, E., Al Ghouleh, I., Ranayhossaini, D. J., Egana, L., Lopes, L. R., et al. (2011). Nox2 B-loop peptide, Nox2ds, specifically inhibits the NADPH oxidase Nox2. *Free Radic. Biol. Med.* 51, 1116–1125. doi: 10.1016/j.freeradbiomed.2011.04.025

Danieli-Betto, D., Germinario, E., Esposito, A., Biral, D., and Betto, R. (2000). Effects of fatigue on sarcoplasmic reticulum and myofibrillar properties of rat single muscle fibers. *J. Appl. Physiol. (1985)* 89, 891–898.

De, L. J., Zufferli, A., Serra, F., Isidori, A. M., Naro, F., Dessalle, K., et al. (2012). TNF-alpha- and tumor-induced skeletal muscle atrophy involves sphingolipid metabolism. *Skelet. Muscle* 2:2. doi: 10.1186/2044-5040-2-2

Doehner, W., Bunck, A. C., Rauchhaus, M., von, H. S., Brunkhorst, F. M., Cicoira, M., et al. (2007). Secretory sphingomyelinase is upregulated in chronic heart failure: a second messenger system of immune activation relates to body composition, muscular functional capacity, and peripheral blood flow. *Eur. Heart J.* 28, 821–828. doi: 10.1093/eurheartj/ehl541

Dooley, C. T., Dore, T. M., Hanson, G. T., Jackson, W. C., Remington, S. J., and Tsien, R. Y. (2004). Imaging dynamic redox changes in mammalian cells with green fluorescent protein indicators. *J. Biol. Chem.* 279, 22284–22293. doi: 10.1074/jbc.M312847200

Empinado, H. M., Deevska, G. M., Nikolova-Karakashian, M., Yoo, J. K., Christou, D. D., and Ferreira, L. F. (2014). Diaphragm dysfunction in heart failure is accompanied by increases in neutral sphingomyelinase activity and ceramide content. *Eur. J. Heart Fail.* 16, 519–525. doi: 10.1002/ejhf.73

Favory, R., Lancel, S., Marchetti, P., Mordon, S., Chopin, C., Formstecher, P., et al. (2004). Endotoxin-induced myocardial dysfunction: evidence for a role of sphingosine production. *Crit. Care Med.* 32, 495–501. doi: 10.1097/01.CCM.0000109452.36271.FA

Ferreira, L. F., Moylan, J. S., Gilliam, L. A., Smith, J. D., Nikolova-Karakashian, M., and Reid, M. B. (2010). Sphingomyelinase stimulates oxidant signaling to weaken skeletal muscle and promote fatigue. *Am. J. Physiol. Cell Physiol.* 299, C552–C560. doi: 10.1152/ajpcell.00065.2010

Ferreira, L. F., Moylan, J. S., Stasko, S., Smith, J. D., Campbell, K. S., and Reid, M. B. (2012). Sphingomyelinase depresses force and calcium sensitivity of the contractile apparatus in mouse diaphragm muscle fibers. *J. Appl. Physiol. (1985)* 112, 1538–1545. doi: 10.1152/japplphysiol.01269.2011

Friedrichs, G. S., Swillo, R. E., Jow, B., Bridal, T., Numann, R., Warner, L. M., et al. (2002). Sphingosine modulates myocyte electrophysiology, induces negative inotropy, and decreases survival after myocardial ischemia. *J. Cardiovasc. Pharmacol.* 39, 18–28. doi: 10.1097/00005344-200201000-00003

Gamboa, J. L., and Andrade, F. H. (2010). Mitochondrial content and distribution changes specific to mouse diaphragm after chronic normobaric hypoxia. *Am. J. Physiol. Regul. Integr. Comp. Physiol.* 298, R575–R583. doi: 10.1152/ajpregu.00320.2009

Gonzalez, E., Messi, M. L., Zheng, Z., and Delbono, O. (2003). Insulin-like growth factor-1 prevents age-related decrease in specific force and intracellular Ca^{2+} in single intact muscle fibres from transgenic mice. *J. Physiol.* 552, 833–844. doi: 10.1113/jphysiol.2003.048165

Guido, A. N., Campos, G. E., Neto, H. S., Marques, M. J., and Minatel, E. (2010). Fiber type composition of the sternomastoid and diaphragm muscles of dystrophin-deficient mdx mice. *Anat. Rec. (Hoboken.)* 293, 1722–1728. doi: 10.1002/ar.21224

Hanson, G. T., Aggeler, R., Oglesbee, D., Cannon, M., Capaldi, R. A., Tsien, R. Y., et al. (2004). Investigating mitochondrial redox potential with redox-sensitive green fluorescent protein indicators. *J. Biol. Chem.* 279, 13044–13053. doi: 10.1074/jbc.M312846200

Laker, R. C., Xu, P., Ryall, K. A., Sujkowski, A., Kenwood, B. M., Chain, K. H., et al. (2014). A novel MitoTimer reporter gene for mitochondrial content, structure, stress, and damage *in vivo*. *J. Biol. Chem.* 289, 12005–12015. doi: 10.1074/jbc.M113.530527

Massaad, C. A., Washington, T. M., Pautler, R. G., and Klann, E. (2009). Overexpression of SOD-2 reduces hippocampal superoxide and prevents memory deficits in a mouse model of Alzheimer's disease. *Proc. Natl. Acad. Sci. U.S.A.* 106, 13576–13581. doi: 10.1073/pnas.0902714106

McClung, J. M., Deruisseau, K. C., Whidden, M. A., Van, R. H., Richardson, A., Song, W., et al. (2010). Overexpression of antioxidant enzymes in diaphragm muscle does not alter contraction-induced fatigue or recovery. *Exp. Physiol.* 95, 222–231. doi: 10.1113/expphysiol.2009.049650

McDonough, P. M., Yasui, K., Betto, R., Salviati, G., Glembotski, C. C., Palade, P. T., et al. (1994). Control of cardiac Ca^{2+} levels. Inhibitory actions of sphingosine on Ca^{2+} transients and L-type Ca^{2+} channel conductance. *Circ. Res.* 75, 981–989. doi: 10.1161/01.RES.75.6.981

Michaelson, L. P., Shi, G., Ward, C. W., and Rodney, G. G. (2010). Mitochondrial redox potential during contraction in single intact muscle fibers. *Muscle Nerve* 42, 522–529. doi: 10.1002/mus.21724

Moopanar, T. R., and Allen, D. G. (2005). Reactive oxygen species reduce myofibrillar Ca^{2+} sensitivity in fatiguing mouse skeletal muscle at 37 degrees C. *J. Physiol.* 564, 189–199. doi: 10.1113/jphysiol.2005.083519

Needleman, D. H., Aghdasi, B., Seryshev, A. B., Schroepfer, G. J. Jr., and Hamilton, S. L. (1997). Modulation of skeletal muscle $Ca^{2(+)}$-release channel activity by sphingosine. *Am. J. Physiol.* 272, C1465–C1474.

Nikolova-Karakashian, M. N., and Reid, M. B. (2011). Sphingolipid metabolism, oxidant signaling, and contractile function of skeletal muscle. *Antioxid Redox Signal.* 15, 2501–2517. doi: 10.1089/ars.2011.3940

Okazaki, T., Liang, F., Li, T., Lemaire, C., Danialou, G., Shoelson, S. E., et al. (2014). Muscle-specific inhibition of the classical nuclear factor-kappaB pathway is protective against diaphragmatic weakness in murine endotoxemia. *Crit. Care Med.* 42, e501–e509. doi: 10.1097/CCM.0000000000000407

Oral, H., Dorn, G. W., and Mann, D. L. (1997). Sphingosine mediates the immediate negative inotropic effects of tumor necrosis factor-alpha in the adult mammalian cardiac myocyte. *J. Biol. Chem.* 272, 4836–4842. doi: 10.1074/jbc.272.8.4836

Ortenblad, N., Sjogaard, G., and Madsen, K. (2000). Impaired sarcoplasmic reticulum $Ca^{(2+)}$ release rate after fatiguing stimulation in rat skeletal muscle. *J. Appl. Physiol.* 89, 210–217.

Pal, R., Basu, T. P., Li, S., Minard, C., and Rodney, G. G. (2013). Real-time imaging of NADPH oxidase activity in living cells using a novel fluorescent protein reporter. *PLoS ONE* 8:e63989. doi: 10.1371/journal.pone.0063989

Pal, R., Monroe, T. O., Palmieri, M., Sardiello, M., and Rodney, G. G. (2014a). Rotenone induces neurotoxicity through Rac1-dependent activation of NADPH oxidase in SHSY-5Y cells. *FEBS Lett.* 588, 472–481. doi: 10.1016/j.febslet.2013.12.011

Pal, R., Palmieri, M., Loehr, J. A., Li, S., Abo-Zahrah, R., Monroe, T. O., et al. (2014b). Src-dependent impairment of autophagy by oxidative stress in a mouse model of Duchenne muscular dystrophy. *Nat. Commun.* 5:4425. doi: 10.1038/ncomms5425

Reid, M. B., Khawli, F. A., and Moody, M. R. (1993). Reactive oxygen in skeletal muscle. III. Contractility of unfatigued muscle. *J. Appl. Physiol. (1985)* 75, 1081–1087.

Reinehr, R., Becker, S., Eberle, A., Grether-Beck, S., and Haussinger, D. (2005). Involvement of NADPH oxidase isoforms and Src family kinases in CD95-dependent hepatocyte apoptosis. *J. Biol. Chem.* 280, 27179–27194. doi: 10.1074/jbc.M414361200

Rey, F. E., Cifuentes, M. E., Kiarash, A., Quinn, M. T., and Pagano, P. J. (2001). Novel competitive inhibitor of NAD(P)H oxidase assembly attenuates vascular O(2)(-) and systolic blood pressure in mice. *Circ. Res.* 89, 408–414. doi: 10.1161/hh1701.096037

Sabbadini, R. A., Betto, R., Teresi, A., Fachechi-Cassano, G., and Salviati, G. (1992). The effects of sphingosine on sarcoplasmic reticulum membrane calcium release. *J. Biol. Chem.* 267, 15475–15484.

Sabbadini, R. A., Danieli-Betto, D., and Betto, R. (1999). The role of sphingolipids in the control of skeletal muscle function: a review. *Ital. J. Neurol. Sci.* 20, 423–430. doi: 10.1007/s100720050062

Sakellariou, G. K., Jackson, M. J., and Vasilaki, A. (2014). Redefining the major contributors to superoxide production in contracting skeletal muscle. The role of NAD(P)H oxidases. *Free Radic. Res.* 48, 12–29. doi: 10.3109/10715762.2013.830718

Sakellariou, G. K., Vasilaki, A., Palomero, J., Kayani, A., Zibrik, L., McArdle, A., et al. (2013). Studies of mitochondrial and nonmitochondrial sources implicate nicotinamide adenine dinucleotide phosphate oxidase(s) in the increased skeletal muscle superoxide generation that occurs during contractile activity. *Antioxid Redox Signal.* 18, 603–621. doi: 10.1089/ars.2012.4623

Sawada, M., Kiyono, T., Nakashima, S., Shinoda, J., Naganawa, T., Hara, S., et al. (2004). Molecular mechanisms of TNF-alpha-induced ceramide formation in human glioma cells: P53-mediated oxidant stress-dependent and -independent pathways. *Cell Death Differ.* 11, 997–1008. doi: 10.1038/sj.cdd.4401438

Webster, R. J., Sabbadini, R. A., Dettbarn, C. A., and Paolini, P. J. (1994). Sphingosine effects on the contractile behavior of skinned cardiac myocytes. *J. Mol. Cell Cardiol.* 26, 1273–1290. doi: 10.1006/jmcc.1994.1147

Wong, M. L., Xie, B., Beatini, N., Phu, P., Marathe, S., Johns, A., et al. (2000). Acute systemic inflammation up-regulates secretory sphingomyelinase *in vivo*: a possible link between inflammatory cytokines and atherogenesis. *Proc. Natl. Acad. Sci. U.S.A.* 97, 8681–8686. doi: 10.1073/pnas.150098097

Zhao, K., Zhao, G. M., Wu, D., Soong, Y., Birk, A. V., Schiller, P. W., et al. (2004). Cell-permeable peptide antioxidants targeted to inner mitochondrial membrane inhibit mitochondrial swelling, oxidative cell death, and reperfusion injury. *J. Biol. Chem.* 279, 34682–34690. doi: 10.1074/jbc.M402999200

Conflict of Interest Statement: The authors declare that the research was conducted in the absence of any commercial or financial relationships that could be construed as a potential conflict of interest.

Received: 31 October 2014; accepted: 27 December 2014; published online: 21 January 2015.

Citation: Loehr JA, Abo-Zahrah R, Pal R and Rodney GG (2015) Sphingomyelinase promotes oxidant production and skeletal muscle contractile dysfunction through activation of NADPH oxidase. Front. Physiol. ***5****:530. doi: 10.3389/fphys.2014.00530*

This article was submitted to Striated Muscle Physiology, a section of the journal Frontiers in Physiology.

frontiers in
PHYSIOLOGY

ORIGINAL RESEARCH ARTICLE
published: 04 February 2015
doi: 10.3389/fphys.2015.00021

Age affects the contraction-induced mitochondrial redox response in skeletal muscle

Dennis R. Claflin[1,2]*, Malcolm J. Jackson[3] and Susan V. Brooks[1,4]

[1] *Department of Biomedical Engineering, University of Michigan, Ann Arbor, MI, USA*
[2] *Department of Surgery, Section of Plastic Surgery, University of Michigan, Ann Arbor, MI, USA*
[3] *Department of Musculoskeletal Biology, Institute of Ageing and Chronic Disease, University of Liverpool, Liverpool, UK*
[4] *Department of Molecular and Integrative Physiology, University of Michigan, Ann Arbor, MI, USA*

Edited by:
Li Zuo, Ohio State University, USA

Reviewed by:
Kunihiro Sakuma, Toyohashi University of Technology, Japan
Feng He, Skidmore College, USA
Fuchun Yang, The First Affiliated Hospital of The Guangxi Medical University, China

****Correspondence:***
Dennis R. Claflin, Department of Surgery, Section of Plastic Surgery, University of Michigan, 109 Zina Pitcher Place, Ann Arbor, MI 48109, USA
e-mail: claflin@umich.edu

Compromised mitochondrial respiratory function is associated with advancing age. Damage due to an increase in reactive oxygen species (ROS) with age is thought to contribute to the mitochondrial deficits. The coenzyme nicotinamide adenine dinucleotide in its reduced (NADH) and oxidized (NAD^+) forms plays an essential role in the cyclic sequence of reactions that result in the regeneration of ATP by oxidative phosphorylation in mitochondria. Monitoring mitochondrial NADH/NAD^+ redox status during recovery from an episode of high energy demand thus allows assessment of mitochondrial function. NADH fluoresces when excited with ultraviolet light in the UV-A band and NAD^+ does not, allowing NADH/NAD^+ to be monitored in real time using fluorescence microscopy. Our goal was to assess mitochondrial function by monitoring the NADH fluorescence response following a brief period of high energy demand in muscle from adult and old wild-type mice. This was accomplished by isolating whole lumbrical muscles from the hind paws of 7- and 28-month-old mice and making simultaneous measurements of force and NADH fluorescence responses during and after a 5 s maximum isometric contraction. All muscles exhibited fluorescence oscillations that were qualitatively similar and consisted of a brief transient increase followed by a longer transient period of reduced fluorescence and, finally, an increase that included an overshoot before recovering to resting level. Compared with the adult mice, muscles from the 28 mo mice exhibited a delayed peak during the first fluorescence transient and an attenuated recovery following the second transient. These findings indicate an impaired mitochondrial capacity to maintain NADH/NAD^+ redox homeostasis during contractile activity in skeletal muscles of old mice.

Keywords: skeletal muscle, contraction, fluorescence, mitochondria, reactive oxygen species, NADH

INTRODUCTION

Mitochondria are the main source of the adenosine triphosphate (ATP) required to support skeletal muscle contractile function. The mitochondrial processes that result in the regeneration of ATP also give rise to reactive oxygen species (ROS). If ROS levels are not sufficiently controlled by intrinsic antioxidant defense systems, oxidative damage to various cellular systems can accumulate and this process is thought to contribute to the age-related reductions in muscle mitochondrial function (Conley et al., 2000; Mansouri et al., 2006; Peterson et al., 2012).

The coenzyme nicotinamide adenine dinucleotide (NAD) in its reduced (NADH) and oxidized (NAD^+) forms plays an essential role in the cyclic sequence of reactions that result in the regeneration of ATP by oxidative phosphorylation in mitochondria. NADH fluoresces when excited with ultraviolet (UV-A) light and NAD^+ does not, allowing the NAD redox state to be monitored using fluorescence spectroscopy (Chance and Jobsis, 1959). Because the fluorescence captured during whole cell or tissue UV excitation is dominated by mitochondrial NADH (Mayevsky and Rogatsky, 2007), tracking the fluorescence response of skeletal muscle following a maximum tetanic contraction provides a view of mitochondrial function and mitochondrial NAD redox status during recovery from an episode of high energy demand. Moreover, since the mitochondrial NAD redox state reflects the global mitochondrial redox state (Mayevsky and Rogatsky, 2007; Zorov et al., 2014) which, in turn, is an indicator of the probability of ROS formation (Zorov et al., 2014), the fluorescence response serves as a continuous, real-time signal that predicts the development of oxidative stress.

In skeletal muscles from adult rats (Wendt and Chapman, 1976) and toads (Godfraind-De Becker, 1972), the fluorescence response following a brief isometric tetanic contraction is a large, damped oscillation that slowly returns to the pre-contraction steady-state level. Since advancing age is known to compromise mitochondrial function, we hypothesized that the mitochondrial redox response as reported by NADH fluorescence is altered in muscles from old mice following a brief period of high-intensity energy demand. Using fluorescence microscopy to monitor the redox response of isolated whole skeletal muscles from adult and old mice, we found that advanced age is associated with a change

in the balance between the rates of NAD reduction and oxidation in muscle mitochondria following a brief increase in energy demand.

MATERIALS AND METHODS

ANIMALS AND OPERATIVE PROCEDURE

Male wild-type mice, aged 16–17 mo (adult) or 26–33 mo (old), were obtained from the Jackson Laboratory (Bar Harbor, ME) and Dr. Holly Van Remmen at the University of Texas Health Science Center, San Antonio. Mice were deeply anesthetized with an intraperitoneal injection of tribromoethanol (Avertin, 400 mg/kg). The hind paws were removed and whole lumbrical (LMB) muscles were dissected from the medial side of digit 2 while immersed in a chilled bathing solution, composition (in mM): 137 NaCl, 11.9 $NaHCO_3$, 5.0 KCl, 1.8 $CaCl_2$, 0.5 $MgCl_2$, 0.4 NaH_2PO_4. The mice were then euthanized by an overdose of the anesthetic followed by a bilateral thoracotomy. All experimental procedures were approved by the University Committee for the Use and Care of Animals at the University of Michigan and were in accordance with the Guide for Care and Use of Laboratory Animals (Public Health Service, 19965, NIH Pub. No. 85–23).

CONTRACTILE PROPERTIES

Details of the apparatus and procedures for assessing the contractile properties of isolated mouse LMB muscles have been described previously (Claflin and Brooks, 2008). Briefly, freshly dissected muscles were transferred to a chamber that was perfused at a rate of 2 exchanges/min with Tyrode solution (mM): NaCl, 121; KCl, 5.0; $CaCl_2$, 1.8; $MgCl_2$, 0.5; NaH_2PO_4, 0.4; $NaHCO_3$, 24; glucose, 5.5; EDTA, 0.10. The temperature of the solution was held at 25°C and oxygenation and pH 7.3 were maintained by bubbling with a 95% O_2, 5% CO_2 mix. Activation was by electrical stimulation via platinum plate electrodes placed on either side of and parallel to the muscle. Muscles were mounted horizontally in the chamber with one end attached to a stationary post and the other to a force transducer (Aurora Scientific, Inc., modified Model 400A). The small size of the LMB muscle permitted visualization of sarcomere-based striations using standard brightfield microscopy. This allowed real-time monitoring of sarcomere length with a high-speed video system (model 901A, Aurora Scientific, Inc.), which was used to adjust resting sarcomere length to 2.5 μm for all experiments. The LMB muscle was then stimulated continuously for 2, 5, or 10 s at 125 pulses/s, a rate sufficient to elicit maximum isometric force. Each of the stimulus pulses was 0.2 ms in duration and exceeded the intensity required for maximum force production by approximately 25%. Force and NADH fluorescence (see below) were recorded continuously throughout the protocol.

NADH FLUORESCENCE

The floor of the experimental chamber was made of polished quartz, which allowed unattenuated transmission of ultraviolet (UV) excitation light. The chamber was placed on the stage of an inverted microscope (Zeiss Axiovert 100). Fluorescence was elicited by epi-illumination from a 75 W xenon lamp and detected using a photomultiplier tube (Hamamatsu, model R1527 PMT). The wavelengths for excitation were centered at 361 nm (2 nm bandwidth), selected using a diffraction grating monochromator (Deltascan 4000, Photon Technology International). The emitted fluorescence passed through a 460 nm band-pass filter (50 nm bandwidth) before reaching the photomultiplier tube. Fluorescence responses were collected from a 0.23 mm by 0.92 mm rectangular area, centered on the muscle, with the long axis of the rectangle coinciding with the long axis of the muscle. Exposure of the muscle to UV light was minimized by controlling a light-blocking shutter to open only when fluorescence measurements were actively being acquired.

EXPERIMENTAL PROCEDURE

After attachment to the experimental apparatus, the LMB muscle was lengthened until just taut and subjected to 3–5 single stimulus pulses of increasing amplitude, separated by 10 s. The purpose of this sequence was to determine supramaximal stimulus intensity by monitoring peak twitch forces. Sarcomere length was then set to 2.5 μm by adjusting the length of the muscle while monitoring the output of the video sarcomere length analyzer. System background fluorescence was determined by moving the microscope stage just enough to remove the muscle from the microscopic field and was subtracted from all subsequent fluorescence measurements. A minimum of 10 min was allowed to elapse between the final twitch of the sequence and any fluorescence measurements to allow NADH to return to its resting level. Simultaneous continuous recording of muscle force and fluorescence was then initiated and 3 min of baseline recording was acquired before the tetanic stimulus was applied. Following the tetanic contraction, recording continued for an additional 17 min. Sample rate was 10/s throughout. For a subset of experiments (6 of 8 adult, 4 of 10 old), the chamber perfusion was stopped and the solution was replaced with a Tyrode solution to which sodium cyanide (5 mM), an electron transport inhibitor, had been added. Introduction of the cyanide resulted in a rapid increase in fluorescence that reached a plateau level within 8–10 min (see **Figure 1B**). The maximum fluorescence level was interpreted as corresponding to the maximum possible ratio of NADH to total NAD ($NADH + NAD^+$), or the maximally reduced mitochondrial redox state. For experiments in which the maximum fluorescence level was not determined, it was estimated using the average age-specific ratio of maximum fluorescence to resting fluorescence established in the subset of experiments in which the cyanide incubation step was carried out. Although system background fluorescence was removed from all responses (described above), no attempt was made to determine the contributions of non-NADH fluorescence through the use of uncouplers such as carbonylcyanide-p-trifluoromethoxy phenylhydrazone (FCCP) (Eng et al., 1989; Minezaki et al., 1994; Brandes and Bers, 1996; Gandra et al., 2012). Because fluorescence results are all presented after normalization by either resting or maximum fluorescence, and any non-NADH fluorescence that is present is not accounted for, non-NADH fluorescence would have the effect of reducing all reported amplitudes. The peak values, Δ-peak values, and peak-peak values presented here should therefore be considered lower-bound estimates of the true values.

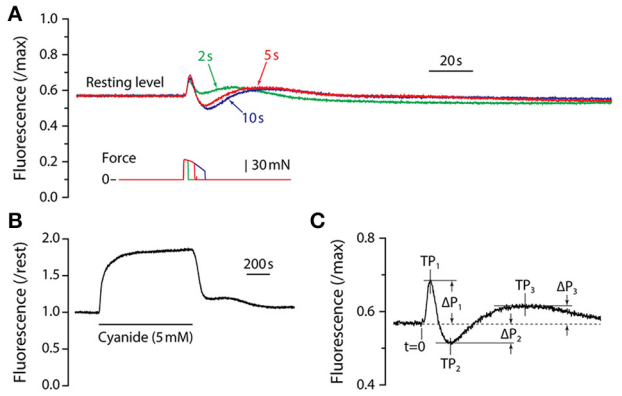

FIGURE 1 | NADH fluorescence responses. (A) Fluorescence responses of adult mouse LMB muscle for tetanic contractions of 2, 5, and 10 s duration. All responses are from the same muscle and are scaled by the maximum fluorescence as determined by exposure to cyanide. Corresponding tetanic force responses are shown beneath the fluorescence traces and are plotted using the same time-base. Note that all fluorescence responses from adult muscle exhibit the same qualitative time-course consisting of a sharp, brief increase followed by an abrupt decline, then a recovery that exceeds baseline level. Fluorescence then declines to a sub-resting level before returning slowly to the pre-contraction level. **(B)** Response of LMB muscle to sodium cyanide (5 mM). The solid horizontal line beneath the fluorescence record indicates the duration of the cyanide exposure. **(C)** Parameter definitions for the first three fluorescence oscillation peaks are indicated. Peak times (TP_1, TP_2, TP_3) were measured relative to $t = 0$, the time at which the contraction was initiated. Peak amplitudes (ΔP_1, ΔP_2, ΔP_3) were measured relative to the pre-contraction resting level (dashed line).

STATISTICS

Statistical analyses were performed using JMP software (SAS Institute, Inc.). Student's *t*-test was used to identify differences between means. Significance was set *a priori* at $p < 0.05$.

RESULTS

Typical fluorescence responses to maximum isometric tetanic contractions of 2, 5, and 10 s are shown in **Figure 1A** scaled relative to the maximum fluorescence level as determined by exposure to cyanide (**Figure 1B**). The earliest observed fluorescence change was a large, rapid increase that began approximately 1 s after the initiation of the contraction and reached a peak ("P_1") approximately 2 s later. The fluorescence intensity then reversed and fell rapidly, reaching a minimum level ("P_2"). From the minimum, fluorescence recovered slowly to a third peak ("P_3"), and then declined again before gradually returning to resting level. Fluorescence response amplitude (P) and time (T) parameters are defined in **Figure 1C**. In preliminary experiments, fluorescence responses to tetanic contraction durations of up to 20 s were recorded. Responses to all tetanus durations were qualitatively similar, exhibiting damped oscillations consisting of three distinct peaks followed by a gradual return to resting level. For contractions that were longer than 3 s, P_1 occurred during force generation and its amplitude and timing were therefore independent of tetanus duration. The fluorescence reversal that defined P_2 did not begin until shortly after a contraction ended, thus both its amplitude ($|\Delta P_2|$) and time-to-peak (T_2) increased with contraction duration. The time required for the entire damped fluorescence oscillation to return to resting level depended on the duration of the contraction and was approximately 10 min for a 5 s tetanus and 15 min for a 10 s tetanus. Based upon these preliminary experiments, a 5 s tetanic contraction was chosen as the test condition for the remainder of the study as it resulted in a robust, characteristic fluorescence response without the large decline in force observed during longer contractions. With the exception of **Figure 1A**, all results reported are responses to 5 s maximum isometric tetanic contractions.

Representative fluorescence responses to a 5 s maximum isometric tetanic contraction in LMB muscles from adult and old mice are shown in **Figure 2**. In **Figure 2A**, the fluorescence is scaled by the maximum cyanide-induced level and illustrates the finding that, relative to maximum, the resting level in muscles from old mice was higher than that in adult mice. For all experiments in which maximum fluorescence levels were determined, the resting level in muscles from adult mice, expressed as a fraction of maximum, was 0.53 ± 0.03 (mean ± SEM, $n = 6$) whereas the resting level for old mice was 0.63 ± 0.02 ($n = 4$), significantly higher ($p = 0.026$). In **Figure 2B** the fluorescence records shown in **Figure 2A** have been normalized by their respective resting levels to facilitate temporal comparisons. This representation serves to illustrate the blunted fluorescence recovery of old muscles from P_2 to P_3, the most striking difference observed between the responses of muscles from adult and old mice.

Peak fluorescence amplitudes are presented either as ΔP, the difference between resting level and peak level, or as the peak-to-peak difference between consecutive peaks, all normalized by maximum fluorescence and shown in **Figure 3**. Values for ΔP_1, ΔP_2, and P_1–P_2 were not affected by the age of the mouse. In contrast, ΔP_3 and P_3–P_2 were significantly smaller in muscles from old mice compared with adult mice. The time intervals between the initiation of contraction and P_2 and between P_1 and P_2 were not affected by age. However, the time required to reach P_1 was increased and the time to reach P_3 was decreased in old compared with adult, as was the time interval from P_2 to P_3 (**Figure 4**).

DISCUSSION

Following a brief (5 s) period of intense contractile activity by LMB muscles of mice, the NADH fluorescence response shows a rapid increase to an initial peak (P_1), followed by a similarly rapid decline to a minimum (P_2) that is below resting level, followed by a slower recovery to another local peak (P_3) before gradually returning to resting level. While this response was qualitatively similar for muscles of adult and old animals, significant quantitative differences were observed. Most pronounced was the attenuation, for muscles from old mice, of the duration and magnitude of the recovery from P_2 to P_3. Under the conditions used in the present study, the fluorescence response is dominated by fluctuations in mitochondrial [NADH] (Mayevsky and Rogatsky, 2007). Because mitochondrial [NADH] is the net result of NAD oxidation and reduction activities, this finding indicates that, following a brief period of high energy demand, mitochondria

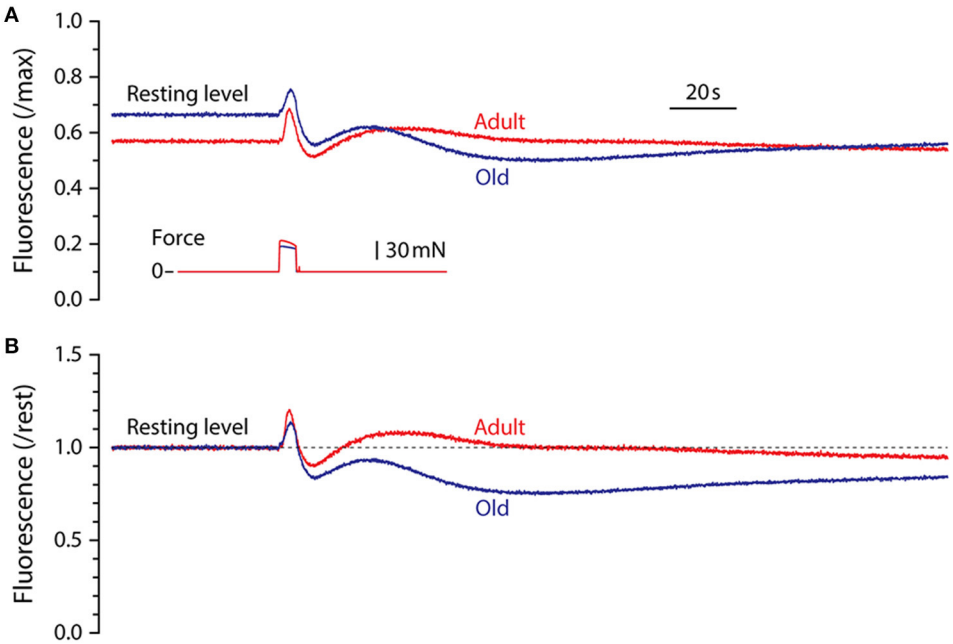

FIGURE 2 | Representative NADH fluorescence responses for LMB muscles from adult and old mice. (A) Superimposed NADH fluorescence responses during 5 s maximum tetanic contractions in LMB muscles from adult and old mice. Records are scaled by the maximum fluorescence as determined by exposure to cyanide (see **Figure 1B**). Corresponding tetanic force responses are shown beneath the fluorescence traces. **(B)** The fluorescence responses shown in **(A)** have been re-scaled relative to pre-contraction resting levels (dashed line) to facilitate comparison of their time courses. All fluorescence and force responses shown in **(A)** and **(B)** are plotted using the same time-base.

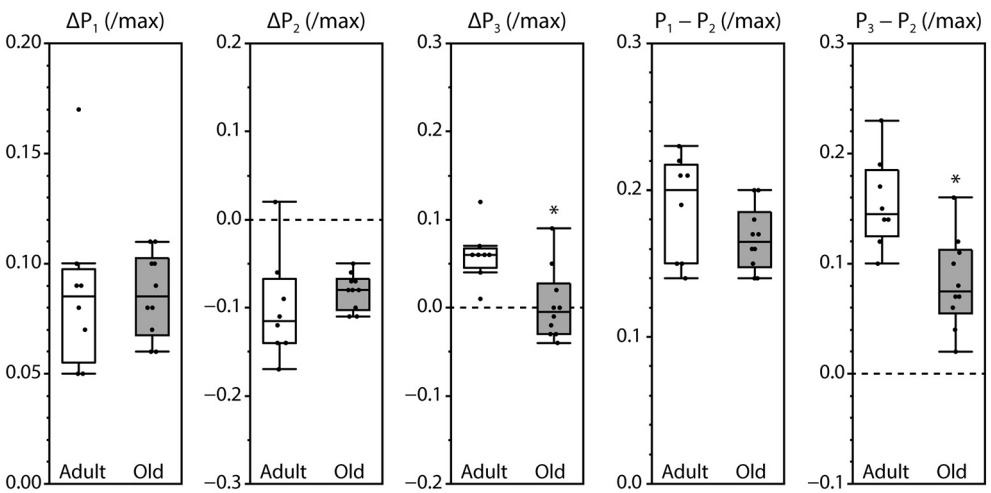

FIGURE 3 | Amplitudes of the fluorescence oscillations in LMB muscles from adult and old mice. Definitions for the amplitude parameters are shown in **Figure 1C**. Box plots indicate the median and the 25th and 75th quartiles. The vertical lines that originate from the top and bottom surfaces of the boxes extend to the outermost data points that fall within 1.5× the difference between the 75th and 25th quartiles. Asterisks indicate significant differences ($p < 0.05$). Data were collected from $n = 8$ and $n = 10$ LMB muscles from adult and old mice, respectively.

from old mice exhibit a decreased rate of NAD^+ reduction, an increased rate of NADH oxidation, or both. Two clear advantages of this approach support its usefulness for assessing mitochondrial function. First, the speed inherent in fluorescence measurements provides a highly resolved view of the temporal relationship between contractile activity and the dynamics of the mitochondrial response, information impossible to obtain from traditional biochemical techniques. Second, mitochondrial function is monitored within the relevant physiological environment of living contracting muscle fibers. Thus, our findings provide new insight into the effects of aging on mitochondrial function.

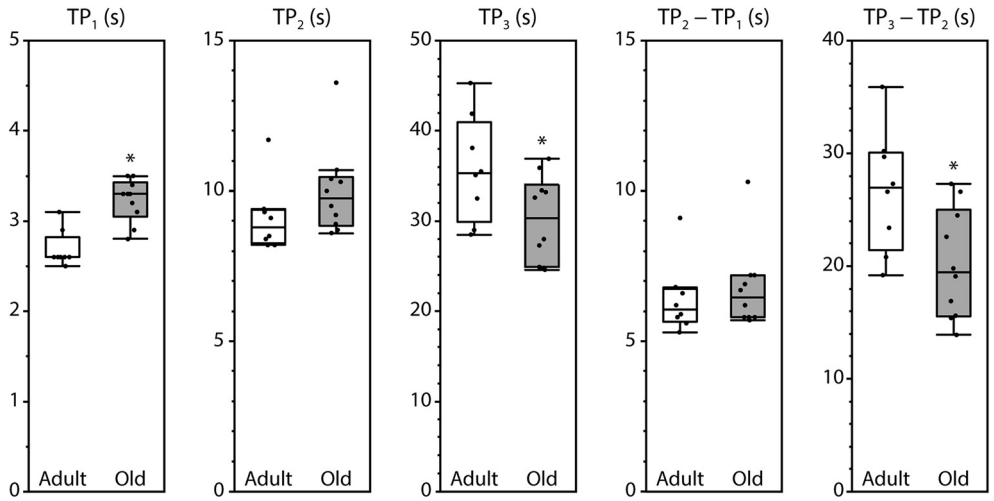

FIGURE 4 | Timing of the fluorescence oscillation peaks in LMB muscles from adult and old mice. Definitions for the time parameters are shown in **Figure 1C**. Box plots indicate the median and the 25th and 75th quartiles. The vertical lines that originate from the top and bottom surfaces of the boxes extend to the outermost data points that fall within 1.5× the difference between the 75th and 25th quartiles. Asterisks indicate significant differences ($p < 0.05$). Data were collected from $n = 8$ and $n = 10$ LMB muscles from adult and old mice, respectively.

INITIAL INCREASE IN NADH (P_1)

The brief, early increase in mitochondrial [NADH] following tetanic contractions (P_1) has been observed in toad skeletal muscles (Godfraind-De Becker, 1972) and in rat soleus muscles (Wendt and Chapman, 1976). Extensor digitorum longus (EDL) muscles of rats reportedly lack the initial increase in [NADH] following a tetanic contraction (Wendt and Chapman, 1976), perhaps due to differences in fiber type composition of rat soleus (predominantly type 1) and EDL (predominantly type 2) muscles (Ariano et al., 1973). The LMB muscle of the mouse hind paw contains both type 1 and type 2 fibers, although type 1 fibers occupy only ≈10% of the cross-sectional area (Smith et al., 2013). Based on this small fraction of type 1 fibers, type 2 fiber subtypes likely also contribute to the robust P_1 response observed in the present study. P_1 is abolished by iodoacetic acid, a specific inhibitor of glyceraldehyde-3-phosphate dehydrogenase (Godfraind-De Becker, 1972; Wendt and Chapman, 1976), indicating that the initial increase in mitochondrial [NADH] is a result of increased glycolytic activity, although the mechanism has not been established. Among the possibilities are increases in mitochondrial availability of pyruvate and/or the activity of NADH shuttle systems.

TRANSITIONS TO P_2 AND P_3

In cardiac muscle, an abrupt increase in energy demand by myofibrillar and sarcoplasmic reticulum ATPases causes ADP levels to rise and mitochondrial [NADH] levels to fall in response to ADP-induced activation of the electron transport system (Brandes and Bers, 2002). Recovery of mitochondrial [NADH] follows, even in the presence of continued high energy demand, as the result of a delayed increase in the activity of tricarboxylic acid (TCA) cycle dehydrogenases driven by a gradually increasing mitochondrial [Ca^{2+}] (Brandes and Bers, 2002). Computational models that include [ADP]-controlled modulation of NADH oxidation rates and time-delayed [Ca^{2+}]-controlled modulation of NAD^+ reduction rates by TCA cycle activity reproduce the oscillations associated with abrupt changes in energy demand in cardiac muscle (Cortassa et al., 2006). Our interpretations of the [NADH] oscillations in skeletal muscle are based, in part, upon the findings in cardiac muscle. Specifically, we attribute the rapid decline in mitochondrial [NADH] following P_1 to ADP-induced activation of the electron transport system, resulting in an increased rate of NADH oxidation. As mitochondrial [ADP] then begins to fall due to an increase in oxidative phosphorylation, its influence on the electron transport system declines, reducing the rate of NADH oxidation by that pathway. Simultaneous with the falling NADH oxidation rate, an increase in mitochondrial [Ca^{2+}] activates mitochondrial dehydrogenases, promoting an increase in the reduction of NAD^+ to NADH by the TCA cycle. The net result of these opposing NAD oxidation and reduction activities is P_2, where mitochondrial [NADH] reaches a nadir and begins to recover. The recovery continues to P_3, where NADH oxidation rates again exceed NAD^+ reduction rates and another local peak occurs.

RESPONSE IN MUSCLES FROM OLD MICE

The most striking differences between the NADH responses of muscles from adult and old mice are the declines in the duration and magnitude of the recovery from the minimum level (P_2) to the next local maximum (P_3). If this recovery is driven by delayed Ca^{2+}-activation of TCA cycle activity as suggested by experiments on cardiac tissue (Brandes and Bers, 2002) and by computational models (Cortassa et al., 2006), then the muted response in muscles from old mice suggests diminished TCA cycle capacity or an attenuated intramitochondrial [Ca^{2+}] increase in response to the preceding tetanic contraction. In support of the latter, the myoplasmic Ca^{2+} response is reduced in skeletal muscle from old humans (Delbono et al., 1995) and mice (Gonzalez et al., 2003;

Umanskaya et al., 2014). Normal tetanic myoplasmic Ca^{2+} levels can be restored in old mice by overexpression of the antioxidant catalase, implicating an increase in ROS as a factor contributing to the diminished response (Umanskaya et al., 2014). Another factor that could contribute to the weak NADH recovery is increased "uncoupling" of NADH oxidation (i.e., oxidation that does not result in ATP generation), which has also been proposed to occur with aging (Conley et al., 2000; Johannsen et al., 2012). Finally, the observation that rat soleus and EDL muscles produce different NADH responses to contractions (Wendt and Chapman, 1976) raises the possibility that changes with aging in the fiber type composition contribute to the differences in NADH responses observed in the present study. We did not analyze fiber type composition of the muscles used in this study, but no changes in fiber types are observed with aging in the fore paw LMB muscle (Russell et al., manuscript under review) and minimal age-related shifts in fiber types are reported in other hind limb muscles of mice (Phillips et al., 1993; Fry et al., 2015).

A second difference between the age groups was a significant age-associated elevation in resting NADH. The observation of higher NADH for muscles of old mice is consistent with reports that the ratio of NADH to total NAD is increased in heart, lung, liver and kidney tissue from old rats (Braidy et al., 2011) and skin from older humans (Massudi et al., 2012). The elevated resting NADH indicates that the NADH-NAD^+ pair is more reduced in old than in adult mice suggesting a more reduced mitochondrial redox environment in old mice (Mayevsky and Rogatsky, 2007; Zorov et al., 2014), although not all mitochondrial redox couples exhibit age-related changes (Dimauro et al., 2012). A more reduced mitochondrial environment in muscles of old mice increases the probability of ROS formation during cellular respiration (Zorov et al., 2014). Consistent with this possibility, mitochondria from skeletal muscles of old mice produce significantly more hydrogen peroxide (Mansouri et al., 2006), have elevated levels of regulatory proteins associated with ROS removal (Dimauro et al., 2012), and have higher antioxidant enzyme activities (Vasilaki et al., 2006) than those from adult mice. An increase in the NADH/NAD^+ ratio is thought to be caused in part by increased activity of the NAD^+-consuming poly (ADP-ribose) polymerase (PARP) DNA repair proteins (Braidy et al., 2011; Massudi et al., 2012), and the relative scarcity of NAD^+ that results could have implications for other cellular enzyme systems (Sauve et al., 2006; Stein and Imai, 2012).

FLUORESCENCE-BASED NADH MEASUREMENTS

Monitoring mitochondrial NADH levels by measuring fluorescence offers a non-invasive means for tracking, in real-time, the mitochondrial redox state of a cell or collection of cells (Mayevsky and Rogatsky, 2007). The NADH fluorescence can thus report instantaneously the response of the mitochondrial oxidative machinery to changes in energy demand such as those that occur frequently in skeletal muscle. In addition, because the mitochondrial NADH-NAD^+ balance is thought to reflect the global redox status of the mitochondria under study (Mayevsky and Rogatsky, 2007; Zorov et al., 2014), the fluorescence response provides valuable insights into the myriad mitochondrial functions that are affected by the redox environment and/or the availability of NADH or NAD^+, such as calcium release by the sarcoplasmic reticulum (Zima et al., 2004), the tendency for ROS formation (Zorov et al., 2014), and the activity of sirtuin proteins (Sauve et al., 2006; Stein and Imai, 2012). Comparing fluorescence responses of skeletal muscle from adult and old mice therefore allows insights into the effects of aging on mitochondrial function and redox homeostasis and all mitochondrial processes known to be affected by redox imbalance.

STUDY LIMITATIONS

Recordings of mitochondrial NADH fluctuations yield the most information when the full potential of the dynamic range of the response is known. This is typically determined by applying an inhibitor of the mitochondrial electron transport chain activity such as cyanide to maximize [NADH], and then applying an "uncoupler" such as FCCP to minimize [NADH] (Eng et al., 1989; Minezaki et al., 1994; Brandes and Bers, 1996; Gandra et al., 2012). In this study maximum NADH levels were determined by application of cyanide, but no attempt was made to assess minimum levels. Thus, an increase in non-NADH fluorescence could be contributing to the increase in resting fluorescence in muscles from old mice reported. Future experiments in which NADH levels are minimized will definitively determine resting NADH fluorescence. In addition, motion can contribute undesirable artifacts during optical recordings in muscle tissue (Godfraind-De Becker, 1972; Brandes et al., 1992; Morgan et al., 1997), but only P_1 occurs during contractile activity making TP_1 and ΔP_1 the only measurements potentially affected by motion. Finally, NADPH is excited and fluoresces at the same wavelengths as NADH, but the contribution of NADPH fluorescence to total tissue fluorescence is reported to be small (Mayevsky and Rogatsky, 2007).

SUMMARY/CONCLUSIONS

We have shown that, compared with adult mice, the resting fluorescence level and dynamic fluorescence response to an energetic challenge differ substantially in skeletal muscles of old mice. The differences suggest an aging-associated hyper-reduced cellular environment and blunted mitochondrial NADH recovery.

ACKNOWLEDGMENTS

Financial support for this work was provided by National Institute on Aging Grant AG-020591 (Susan V. Brooks).

REFERENCES

Ariano, M. A., Armstrong, R. B., and Edgerton, V. R. (1973). Hindlimb muscle fiber populations of five mammals. *J. Histochem. Cytochem.* 21, 51–55.

Braidy, N., Guillemin, G. J., Mansour, H., Chan-Ling, T., Poljak, A., and Grant, R. (2011). Age related changes in NAD^+ metabolism oxidative stress and Sirt1 activity in wistar rats. *PLoS ONE* 6:e19194. doi: 10.1371/journal.pone.0019194

Brandes, R., and Bers, D. M. (1996). Increased work in cardiac trabeculae causes decreased mitochondrial NADH fluorescence followed by slow recovery. *Biophys. J.* 71, 1024–1035. doi: 10.1016/S0006-3495(96)79303-7

Brandes, R., and Bers, D. M. (2002). Simultaneous measurements of mitochondrial NADH and Ca^{2+} during increased work in intact rat heart trabeculae. *Biophys. J.* 83, 587–604. doi: 10.1016/S0006-3495(02)75194-1

Brandes, R., Figueredo, V. M., Camacho, S. A., Massie, B. M., and Weiner, M. W. (1992). Suppression of motion artifacts in fluorescence spectroscopy of perfused hearts. *Am. J. Physiol.* 263, H972–H980.

Chance, B., and Jobsis, F. F. (1959). Changes in fluorescence in a frog sartorius muscle following a twitch. *Nature* 184, 195–196. doi: 10.1038/184195a0

Claflin, D. R., and Brooks, S. V. (2008). Direct observation of failing fibers in muscles of dystrophic mice provides mechanistic insight into muscular dystrophy. *Am. J. Physiol. Cell Physiol.* 294, C651–C658. doi: 10.1152/ajpcell.00244.2007

Conley, K. E., Jubrias, S. A., and Esselman, P. C. (2000). Oxidative capacity and ageing in human muscle. *J. Physiol.* 526(Pt 1), 203–210. doi: 10.1111/j.1469-7793.2000.t01-1-00203.x

Cortassa, S., Aon, M. A., O'rourke, B., Jacques, R., Tseng, H. J., Marban, E., et al. (2006). A computational model integrating electrophysiology, contraction, and mitochondrial bioenergetics in the ventricular myocyte. *Biophys. J.* 91, 1564–1589. doi: 10.1529/biophysj.105.076174

Delbono, O., O'rourke, K. S., and Ettinger, W. H. (1995). Excitation-calcium release uncoupling in aged single human skeletal muscle fibers. *J. Membr. Biol.* 148, 211–222.

Dimauro, I., Pearson, T., Caporossi, D., and Jackson, M. J. (2012). *In vitro* susceptibility of thioredoxins and glutathione to redox modification and aging-related changes in skeletal muscle. *Free Radic. Biol. Med.* 53, 2017–2027. doi: 10.1016/j.freeradbiomed.2012.09.031

Eng, J., Lynch, R. M., and Balaban, R. S. (1989). Nicotinamide adenine dinucleotide fluorescence spectroscopy and imaging of isolated cardiac myocytes. *Biophys. J.* 55, 621–630. doi: 10.1016/S0006-3495(89)82859-0

Fry, C. S., Lee, J. D., Mula, J., Kirby, T. J., Jackson, J. R., Liu, F., et al. (2015). Inducible depletion of satellite cells in adult, sedentary mice impairs muscle regenerative capacity without affecting sarcopenia. *Nat. Med.* 21, 76–80. doi: 10.1038/nm.3710

Gandra, P. G., Nogueira, L., and Hogan, M. C. (2012). Mitochondrial activation at the onset of contractions in isolated myofibres during successive contractile periods. *J. Physiol.* 590, 3597–3609. doi: 10.1113/jphysiol.2012.232405

Godfraind-De Becker, A. (1972). Heat production and fluorescence changes of toad sartorius muscle during aerobic recovery after a short tetanus. *J. Physiol.* 223, 719–734.

Gonzalez, E., Messi, M. L., Zheng, Z., and Delbono, O. (2003). Insulin-like growth factor-1 prevents age-related decrease in specific force and intracellular Ca^{2+} in single intact muscle fibres from transgenic mice. *J. Physiol.* 552, 833–844. doi: 10.1113/jphysiol.2003.048165

Johannsen, D. L., Conley, K. E., Bajpeyi, S., Punyanitya, M., Gallagher, D., Zhang, Z., et al. (2012). Ectopic lipid accumulation and reduced glucose tolerance in elderly adults are accompanied by altered skeletal muscle mitochondrial activity. *J. Clin. Endocrinol. Metab.* 97, 242–250. doi: 10.1210/jc.2011-1798

Mansouri, A., Muller, F. L., Liu, Y., Ng, R., Faulkner, J., Hamilton, M., et al. (2006). Alterations in mitochondrial function, hydrogen peroxide release and oxidative damage in mouse hind-limb skeletal muscle during aging. *Mech. Ageing Dev.* 127, 298–306. doi: 10.1016/j.mad.2005.11.004

Massudi, H., Grant, R., Braidy, N., Guest, J., Farnsworth, B., and Guillemin, G. J. (2012). Age-associated changes in oxidative stress and NAD^+ metabolism in human tissue. *PLoS ONE* 7:e42357. doi: 10.1371/journal.pone.0042357

Mayevsky, A., and Rogatsky, G. G. (2007). Mitochondrial function *in vivo* evaluated by NADH fluorescence: from animal models to human studies. *Am. J. Physiol. Cell Physiol.* 292, C615–C640. doi: 10.1152/ajpcell.00249.2006

Minezaki, K. K., Suleiman, M. S., and Chapman, R. A. (1994). Changes in mitochondrial function induced in isolated guinea-pig ventricular myocytes by calcium overload. *J. Physiol.* 476, 459–471.

Morgan, D. L., Claflin, D. R., and Julian, F. J. (1997). The relationship between tension and slowly varying intracellular calcium concentration in intact frog skeletal muscle. *J. Physiol.* 500, 177–192.

Peterson, C. M., Johannsen, D. L., and Ravussin, E. (2012). Skeletal muscle mitochondria and aging: a review. *J. Aging Res.* 2012, 194821. doi: 10.1155/2012/194821

Phillips, S. K., Wiseman, R. W., Woledge, R. C., and Kushmerick, M. J. (1993). Neither changes in phosphorus metabolite levels nor myosin isoforms can explain the weakness in aged mouse muscle. *J. Physiol.* 463, 157–167

Sauve, A. A., Wolberger, C., Schramm, V. L., and Boeke, J. D. (2006). The biochemistry of sirtuins. *Annu. Rev. Biochem.* 75, 435–465. doi: 10.1146/annurev.biochem.74.082803.133500

Smith, I. C., Gittings, W., Huang, J., McMillan, E. M., Quadrilatero, J., Tupling, A. R., et al. (2013). Potentiation in mouse lumbrical muscle without myosin light chain phosphorylation: is resting calcium responsible? *J. Gen. Physiol.* 141, 297–308. doi: 10.1085/jgp.201210918

Stein, L. R., and Imai, S. (2012). The dynamic regulation of NAD metabolism in mitochondria. *Trends Endocrinol. Metab.* 23, 420–428. doi: 10.1016/j.tem.2012.06.005

Umanskaya, A., Santulli, G., Xie, W., Andersson, D. C., Reiken, S. R., and Marks, A. R. (2014). Genetically enhancing mitochondrial antioxidant activity improves muscle function in aging. *Proc. Natl. Acad. Sci. U.S.A.* 111, 15250–15255. doi: 10.1073/pnas.1412754111

Vasilaki, A., McArdle, F., Iwanejko, L. M., and McArdle, A. (2006). Adaptive responses of mouse skeletal muscle to contractile activity: the effect of age. *Mech. Ageing Dev.* 127, 830–839. doi: 10.1016/j.mad.2006.08.004

Wendt, I. R., and Chapman, J. B. (1976). Fluorometric studies of recovery metabolism of rat fast- and slow-twitch muscles. *Am. J. Physiol.* 230, 1644–1649

Zima, A. V., Copello, J. A., and Blatter, L. A. (2004). Effects of cytosolic $NADH/NAD^+$ levels on sarcoplasmic reticulum Ca^{2+} release in permeabilized rat ventricular myocytes. *J. Physiol.* 555, 727–741. doi: 10.1113/jphysiol.2003.055848

Zorov, D. B., Juhaszova, M., and Sollott, S. J. (2014). Mitochondrial reactive oxygen species (ROS) and ROS-induced ROS release. *Physiol. Rev.* 94, 909–950. doi: 10.1152/physrev.00026.2013

Conflict of Interest Statement: The authors declare that the research was conducted in the absence of any commercial or financial relationships that could be construed as a potential conflict of interest.

Received: 16 December 2014; accepted: 14 January 2015; published online: 04 February 2015.

Citation: Claflin DR, Jackson MJ and Brooks SV (2015) Age affects the contraction-induced mitochondrial redox response in skeletal muscle. Front. Physiol. ***6****:21. doi: 10.3389/fphys.2015.00021*

This article was submitted to Striated Muscle Physiology, a section of the journal Frontiers in Physiology.

frontiers in Physiology

ORIGINAL RESEARCH
published: 24 March 2015
doi: 10.3389/fphys.2015.00085

AMP-activated protein kinase controls exercise training- and AICAR-induced increases in SIRT3 and MnSOD

OPEN ACCESS

Edited by:
Brian McDonagh, University of Liverpool, UK

Reviewed by:
Han-Zhong Feng, Wayne State University School of Medicine, USA
Bruno Bastide, University of Lille Nord de France, University of Lille1, France
Qiang Tong, Baylor College of Medicine, USA

***Correspondence:**
Jonas T. Treebak, The Novo Nordisk Foundation Center for Basic Metabolic Research, Section of Integrative Physiology, University of Copenhagen, Blegdamsvej 3b, Building 6, 6th floor, DK2200 Copenhagen, Denmark
jttreebak@sund.ku.dk

†*These authors have contributed equally to this work.*

Specialty section:
This article was submitted to Striated Muscle Physiology, a section of the journal Frontiers in Physiology

Received: *29 November 2014*
Accepted: *04 March 2015*
Published: *24 March 2015*

Citation:
Brandauer J, Andersen MA, Kellezi H, Risis S, Frøsig C, Vienberg SG and Treebak JT (2015) AMP-activated protein kinase controls exercise training- and AICAR-induced increases in SIRT3 and MnSOD. Front. Physiol. 6:85. doi: 10.3389/fphys.2015.00085

***Josef Brandauer*[1,2†], *Marianne A. Andersen*[1†], *Holti Kellezi*[1], *Steve Risis*[1], *Christian Frøsig*[3], *Sara G. Vienberg*[1] *and Jonas T. Treebak*[1*]**

[1] *Section of Integrative Physiology, The Novo Nordisk Foundation Center for Basic Metabolic Research, University of Copenhagen, Copenhagen, Denmark,* [2] *Department of Health Sciences, Gettysburg College, Gettysburg, PA, USA,* [3] *Section of Molecular Physiology, Department of Nutrition, Exercise and Sports, The August Krogh Centre, University of Copenhagen, Copenhagen, Denmark*

The mitochondrial protein deacetylase sirtuin (SIRT) 3 may mediate exercise training-induced increases in mitochondrial biogenesis and improvements in reactive oxygen species (ROS) handling. We determined the requirement of AMP-activated protein kinase (AMPK) for exercise training-induced increases in skeletal muscle abundance of SIRT3 and other mitochondrial proteins. Exercise training for 6.5 weeks increased SIRT3 ($p < 0.01$) and superoxide dismutase 2 (MnSOD; $p < 0.05$) protein abundance in quadriceps muscle of wild-type (WT; $n = 13$–15), but not AMPK α2 kinase dead (KD; $n = 12$–13) mice. We also observed a strong trend for increased MnSOD abundance in exercise-trained skeletal muscle of healthy humans ($p = 0.051$; $n = 6$). To further elucidate a role for AMPK in mediating these effects, we treated WT ($n = 7$–8) and AMPK α2 KD ($n = 7$–9) mice with 5-amino-1-β-D-ribofuranosyl-imidazole-4-carboxamide (AICAR). Four weeks of daily AICAR injections (500 mg/kg) resulted in AMPK-dependent increases in SIRT3 ($p < 0.05$) and MnSOD ($p < 0.01$) in WT, but not AMPK α2 KD mice. We also tested the effect of repeated AICAR treatment on mitochondrial protein levels in mice lacking the transcriptional coactivator peroxisome proliferator-activated receptor γ-coactivator 1α (PGC-1α KO; $n = 9$–10). Skeletal muscle SIRT3 and MnSOD protein abundance was reduced in sedentary PGC-1α KO mice ($p < 0.01$) and AICAR-induced increases in SIRT3 and MnSOD protein abundance was only observed in WT mice ($p < 0.05$). Finally, the acetylation status of SIRT3 target lysine residues on MnSOD (K122) or oligomycin-sensitivity conferring protein (OSCP; K139) was not altered in either mouse or human skeletal muscle in response to acute exercise. We propose an important role for AMPK in regulating mitochondrial function and ROS handling in skeletal muscle in response to exercise training.

Keywords: AMPK, SIRT3, MnSOD, SOD2, ROS, OSCP, exercise training, mitochondrial biogenesis

Introduction

Mitochondrial density and capacity for oxidative ATP synthesis in skeletal muscle are tightly linked to cellular energetic demands (Spina et al., 1996; Egan and Zierath, 2013). Protein deacetylases such as sirtuins (SIRTs) are important modulators of gene expression and protein activity and are involved in mitochondrial biogenesis. SIRT1 is mainly located in the nucleus and deacetylates the transcriptional coactivator, peroxisome proliferator-activated receptor γ-coactivator 1α (PGC-1α) (Nemoto et al., 2005), thereby increasing mitochondrial biogenesis (Puigserver et al., 1998) and improving mitochondrial function (Gerhart-Hines et al., 2007). PGC-1α also induces gene expression of the mitochondrial sirtuin SIRT3 (Schwer et al., 2002) in muscle cells and hepatocytes (Kong et al., 2010).

SIRT3 modulates mitochondrial gene expression and function. SIRT3-driven processes occur via a general deacetylation of mitochondrial proteins (Lombard et al., 2007), including key elements of the citric acid cycle and proteins involved in oxidative phosphorylation (Hallows et al., 2006; Schwer et al., 2006; Wu et al., 2013; Vassilopoulos et al., 2014), or reactive oxygen species (ROS) handling (Someya et al., 2010; Tseng et al., 2013). Thus, SIRT1 may increase SIRT3 expression via PGC-1α deacetylation to facilitate an increase in mitochondrial function and/or density.

Exercise training and caloric restriction (CR) induce mitochondrial biogenesis, but SIRT1-mediated adaptations to exercise and CR are blunted in AMP-activated protein kinase (AMPK)-deficient skeletal muscle (Cantó et al., 2010). AMPK is a heterotrimeric protein consisting of multiple catalytic (α1, α2) and regulatory (β1, β2, γ1, γ2, γ3) subunits. AMPK functions as a major sensor of cellular energy status and can be activated pharmacologically and in response to muscle contraction and CR (Koh et al., 2008). Importantly, AMPK directly phosphorylates PGC-1α (Jäger et al., 2007) which may result in SIRT1-mediated deacetylation and activation of PGC-1α (Cantó et al., 2009) and thus link cellular energy status, mitochondrial biogenesis, and ROS handling.

AMPK activation via 5-amino-1-β-D-ribofuranosyl-imidazole-4-carboxamide (AICAR) increases SIRT3 mRNA level in hepatocytes (Buler et al., 2014). While SIRT3 reduces oxidative stress induced by CR (Someya et al., 2010), AMPK partly coordinates the cellular response to CR (Shinmura et al., 2007), supporting the hypothesis that AMPK may regulate SIRT3.

Exercise training increases ROS processing in skeletal muscle (Parise et al., 2005) via a mechanism that is incompletely understood. A potential mitochondrial signaling cascade response involving SIRT3 and FOXO3A-dependent transcription of catalase and MnSOD has been proposed (Jacobs et al., 2008), but the role of this cascade in exercise-training induced adaptations is unknown. MnSOD and catalase govern the conversion of superoxide to water and oxygen in sequential steps (Reid, 2001). Activation of MnSOD is enhanced by SIRT3-dependent deacetylation at K122, enabling the cell to scavenge ROS (Tao et al., 2010). Other regulatory acetylation sites have also been reported (Qiu et al., 2010; Chen et al., 2011), but the importance for each of these sites in relation to different stimuli remains elusive.

In summary, activation of AMPK via exercise or pharmacological treatment may phosphorylate PGC-1α, increase SIRT3 protein expression, and enhance the ability of skeletal muscle to better handle ROS via deacetylation and activation of MnSOD. Whether this pathway is redundant or exclusively dependent on AMPK is unknown. Given the functional connection between AMPK activators and PGC-1α-dependent increases of SIRT3 abundance and its downstream targets, we determined the effects of exercise training and pharmacological AMPK activation via AICAR in mouse models overexpressing a kinase dead version of the catalytic α2 AMPK subunit dominant in skeletal muscle as well as in skeletal muscle of PGC-1α deficient mice.

Materials and Methods

Exercise Training—Humans

Skeletal muscle samples were obtained from young male subjects previously described in an earlier study (Frøsig et al., 2004). The exercise training study was performed in compliance with the Helsinki II Declaration, with approval from the local ethics committee (#KF 01-070/96). Exercise training consisted of 15 sessions of one-legged knee extensor endurance training over the course of 3 weeks. The duration of the exercise sessions started at 1 h per session and was gradually increased to 2 h per session for the final 5 sessions. Needle biopsies were obtained under local anesthesia (2% lidocaine) from the right and left *vastus lateralis* muscles before training and 15 h ($n = 8$) after the final exercise bout.

Acute Exercise—Humans

Vastus lateralis muscle samples were obtained from healthy young men before and after an acute bout of one-legged knee-extensor exercise. Selected data from this experiment have been published previously (Treebak et al., 2014). This study was approved by the local ethics committee (#KF 1277313) and complied with the Helsinki II Declaration. Seven subjects volunteered to perform an acute bout of one-legged knee-extensor exercise at 80% of peak work load for 1 h during the morning after an overnight fast. In the 1-h exercise bout, peak work load was increased to 100% for 5 min intervals after 15 min and again after 35 min. Needle biopsies from the right and left *vastus lateralis* muscle were obtained before (Pre) and immediately after (Post) exercise cessation as described (Treebak et al., 2014).

Animal Experiments

All animal experiments complied with the European Convention for the protection of Vertebrate Animals used for Experiments and Other Scientific Purposes (Council of Europe 123, Strasbourg, France, 1985) and were approved by the Danish Animal Experimental Inspectorate (#2012-15-2934-26 and #2012-15-2934-307).

Exercise Training—Mice

Female mice (9–15 weeks of age) overexpressing a kinase dead (KD) α2 AMPK subunit in skeletal muscle (Mu et al., 2001)

or WT littermates underwent 6.5 weeks of endurance exercise training (n = 12–15/group). Selected data from these experiments have been published previously (Brandauer et al., 2013). Mice had free access to running wheels for voluntary running 7 days/week. Running distance was recorded using a cycle odometer (#BC1009, Sigma Sport®, Germany). WT and AMPK α2 KD mice performed similar amounts of voluntary running (Brandauer et al., 2013). In addition, mice were exercised 1 h/day at 16 m/min on a motorized treadmill (Exer-3/6, Columbus Instruments) on weekdays as described (Brandauer et al., 2013). The treadmill was horizontal the first week, and the incline was increased by 2.5° per week up to 10° where it remained for the duration of the study. The morning following the final exercise bout, mice were anesthetized by an intraperitoneal (i.p.) injection using Avertin (250 mg tribromoethanol/kg body weight). Quadriceps muscles were removed, snap-frozen in liquid nitrogen, and stored at −80°C until further analyses.

AICAR Treatment Studies

To determine whether AICAR-induced increases in SIRT3 and other mitochondrial proteins depend on AMPK, male AMPK α2 KD and WT mice (11–12 weeks of age) received a daily subcutaneous injection of 500 mg/kg body weight AICAR or 0.9% NaCl solution for 4 weeks (n = 7–8) as described (Brandauer et al., 2013). Mice were anesthetized via i.p. injection of Avertin (250 mg/kg body weight) 24 h following the last AICAR/vehicle treatment to avoid any confounding effects of the last AICAR/saline injection. Quadriceps muscle was obtained, snap-frozen in liquid N_2, and stored at −80°C. Samples from a previously published study of male and female whole-body PGC-1α KO and WT mice were also analyzed. The mice in this study were treated with AICAR under the same conditions as described above (Leick et al., 2009, 2010a). In order to determine the acute effect of a single injection of AICAR, we analyzed samples originating from a previous study (Leick et al., 2010a). Male and female PGC-1α KO mice and WT littermates (n = 6–8) were injected subcutaneously with a single dose of AICAR (500 mg/kg body weight) or saline. Quadriceps muscles were taken 4 h after the injection, snap-frozen in liquid N_2 and stored at −80°C.

Acute Exercise in Previously Trained or Untrained Mice

To assess the effects of acute exercise in trained and untrained mouse skeletal muscle, female C57BL/6JBom (Taconic, Denmark) mice (9–10 weeks of age) underwent 5.5 weeks of endurance exercise training (n = 26) or served as sedentary controls (n = 24). The training consisted of voluntary running with free access to wheel cages 7 days/week with running distance being recorded by a cycle odometer (#BC1009, Sigma Sport®, Germany). In addition, mice were exercised 1 h/day on weekdays with accelerating speeds from 8 to 18 m/min on a motorized treadmill (Exer-3/6, Columbus Instruments) or placed on a "mock" treadmill for the sedentary control group. The treadmill was horizontal the first week, and the incline was increased by 2.5° per week up to 10° at the final week to account for increased performance and to ensure a continuous training stimulus. Untrained control animals were acclimatized to treadmill running for 15–20 min with accelerating speeds from 8 to 18 m/min at a 5° incline for three consecutive days, with 1 day of rest prior to the acute exercise experiment. On the experimental day, both trained and sedentary control mice were divided into three groups: non-exercised controls (n = 8 sedentary, 9 trained), and mice performing either moderate-intensity (n = 8 sedentary, 8 trained) or high-intensity acute exercise (n = 7 sedentary, 8 trained), resulting in six experimental groups. Based on the recorded running distances of each mouse, mice were assigned to one of the three groups so that the average amount of training performed in the training period was similar between the three groups (i.e., 5.1 ± 0.6 km/day; mean ± SEM). Mice then performed an acute treadmill exercise bout for 1 h or served as sedentary controls. "Moderate intensity" was defined as 12 m/min at 0° incline, while "high intensity" was defined as 18 m/min with a 10° incline. Mice were euthanized by cervical dislocation immediately after the acute exercise bout. Quadriceps muscles were quickly removed, snap frozen in liquid nitrogen, and stored at –80° until further analysis.

Tissue Processing and Western Blot Analyses

All muscle samples were processed using steel bead homogenization (Tissue Lyser II, Qiagen) in ice-cold lysis buffer (pH 7.4; 10% glycerol; 1% IGEPAL; Hepes, 50 mM; NaCl, 150 mM; NaF, 10 mM; EDTA, 1 mM; EGTA, 1 mM; sodium pyrophosphate, 20 mM; sodium orthovanadate, 2 mM; sodium-pyrophosphate 1 mM; nicotinamide 5 mM; Thiamet G 4 μM and protease inhibitors (SigmaFast, Sigma Aldrich) according to manufacturer's instructions). Protein concentrations were determined using BCA assays (Thermo Scientific, #23223 and #23224). Equal amounts of protein were resolved by SDS-PAGE and transferred to polyvinylidene difluoride (PVDF) membranes (Millipore, Denmark) as described (Brandauer et al., 2013). Western blots were executed in a balanced design, with samples from all experimental conditions present on all gels, and identical internal control samples included on each blot. The internal control sample was prepared as a pool of all samples from a given experiment. All samples on individual gels were normalized to the internal control sample in order to permit comparison of samples resolved on separate gels. Following transfer, samples were subjected to immunoblot analysis to detect protein abundance using following antibodies against SIRT3 (Cell Signaling, #5490S), SIRT1 (Millipore, #07-131), MnSOD, (Millipore, #06-948), MnSOD K122 acetylation (kindly provided by Prof. David Gius, Northwestern University Feinberg School of Medicine, Chicago, Illinois; see Tao et al., 2010) and Catalase (R&D Systems, #AF3398). Protein abundance of the oxidative phosphorylation complexes was determined using antibodies against Complex I (NDUFB8, Invitrogen, #459210), Complex II (Fp subunit, Invitrogen, #459200), Complex III (Core subunit I, Invitrogen, #459140), Complex IV (Subunit I, Invitrogen, #459600), Complex V (i.e., F1F0 ATP synthase; oligomycin-sensitivity conferring protein [OSCP] subunit (Santa Cruz, #sc-74786), cytochrome C (BD Biosciences #556433) and OSCP K139 acetylation (kindly provided by Prof. David Gius). The specificity of the MnSOD K122 and OSCP K139 antibody used in this study has been verified (Tao et al., 2010; Vassilopoulos et al., 2014) and

was confirmed by "split-blot" analyses, where samples prepared from the same mouse quadriceps muscle or human *vastus lateralis* muscle was resolved in three adjacent wells. After transfer to PVDF, the membrane was cut through the center well and the membrane halves were probed with the total MnSOD/OSCP or MnSOD K122/OSCP K139 antibodies, respectively. Complete alignment of the bands was confirmed (**Figure 7**).

Quantitative Polymerase Chain Reaction (qPCR)

qPCR was performed as described (Brandauer et al., 2013). RNA from quadriceps muscles was extracted using Trizol (Invitrogen, #15596-018) and reverse transcription was performed using iScript cDNA synthesis kit (BioRad, #170-8891). Real-time qPCR was performed using 2 μl of template cDNA, 300 nM of sense and antisense oligonucleotides and SYBR Green PCR Master Mix (AH Diagnostic, #600882) in a final volume of 10 μl. Fluorescence measurements and data analysis were performed on the CFX96 real time system (BioRad). Gene expression was determined using primer sequences: SIRT3 forward primer: 5′-TACAGAAATCAGTGCCCCGA-3′ and reverse primer: 5′-GGTGGACACAAGAACTGCTG-3′; MnSOD forward primer: 5′-ACTGAAGTTCAATGGTGGGG- 3′ and reverse primer: 5′-GCTTGATAGCCTCCAGCAAC- 3′ and normalized by input cDNA (Qubit ssDNA assay kit, Invitrogen, #Q10212).

Statistics

Statistical analyses were performed by either 2 × 2 analysis of variance (ANOVA), by 2 × 3 ANOVA, or by 2 × 2 repeated-measures ANOVA as appropriate. The Tukey test was used *post-hoc*. If statistical interactions were borderline significant ($0.05 < p < 0.1$) and the observed power was low (<0.5), individual *t*-tests were performed as noted in the description of the results. As incomplete sample sets are excluded from statistical analyses in repeated-measures ANOVA, statistical analyses performed on data from the human training study were only performed on 6 sets of samples. Statistical significance was set at $p < 0.05$. All data are reported as mean ± SEM.

Results

Exercise Training in Mice Increases SIRT3 and MnSOD in an AMPK-Dependent Manner

To verify the potency of the exercise training program and to assess the importance of AMPK on exercise-induced mitochondrial adaptations in skeletal muscle, we performed Western blot analyses on mitochondrial Complex I through V (OSCP) and cytochrome C on samples from WT and AMPK α2 KD mice that had completed 6.5 weeks of endurance exercise training. WT and AMPK α2 KD mice performed similarly in average distance run (Brandauer et al., 2013), average duration of exercise/day (WT, 140 ± 16 min/day; KD, 168 ± 29 min/day; $p = 0.38$) and average running speed (WT, 1.39 ± 0.04 km/h; KD, 1.27 ± 0.07 km/h, $p = 0.15$).

We found no interaction effects in any of the data sets presented in **Figures 1A–F**, likely due to low statistical power. However, if individual *t*-tests were performed between control and trained mice, we found significant ($p < 0.05$) increases in Complexes I, II, and IV protein abundance in the WT mice only. Collectively, these data suggest a regulatory role for AMPK in mediating the effects of endurance exercise training on mitochondrial protein expression.

Endurance exercise training increased SIRT3 protein abundance in skeletal muscle from WT, but not AMPK α2 KD mice ($p < 0.01$; $n = 12$–15) (**Figure 2A**). On the other hand, no statistical differences in SIRT3 mRNA levels were observed between genotypes or in response to exercise training (**Figure 2B**). Exercise training tended to increase skeletal muscle MnSOD protein levels in WT relative to KD mice (WT, 49%; AMPK α2 KD, 11%; genotype × treatment interaction effect, $p = 0.079$; observed power 0.294; **Figure 2C**). A *t*-test showed an exercise-induced increase in skeletal muscle MnSOD protein level in WT ($p < 0.05$), but not AMPK α2 KD mice. MnSOD mRNA levels were unchanged in response to exercise training in both genotypes (**Figure 2D**). Endurance exercise did not alter SIRT1 (**Figure 2E**) or catalase protein levels (**Figure 2F**). Thus, AMPK is required for upregulation of SIRT3 and MnSOD protein levels in response to exercise training.

Skeletal Muscle MnSOD Protein Abundance is Increased Following Endurance Exercise Training in Human Skeletal Muscle

We employed a model of one-legged endurance exercise training to study SIRT3 and MnSOD protein abundance in trained and untrained human skeletal muscle. A repeated-measures ANOVA revealed no significant changes in SIRT3 protein content following exercise training in humans ($n = 6$; **Figure 3A**). When samples were analyzed to determine MnSOD content, a borderline significant interaction effect (leg × intervention; $p = 0.051$, $n = 6$; observed power; 0.471; **Figure 3B**) was observed. A *t*-test comparing the control leg to the trained leg after the exercise intervention revealed MnSOD protein was increased in trained skeletal muscle ($p < 0.05$). Collectively, our data indicate that protein content of MnSOD is upregulated in response to exercise training in human skeletal muscle.

Repeated AMPK Activation by AICAR Increases SIRT3 and MnSOD Protein in an AMPK- and PGC-1α-Dependent Manner

To more directly confirm a role for AMPK in the regulation of skeletal muscle SIRT3 and MnSOD protein abundance, we treated WT and AMPK α2 KD mice with AICAR, a pharmacological AMPK activator. We performed Western blot analyses for proteins involved in oxidative phosphorylation to determine the efficacy of the AICAR treatment. Similarly to the results observed in the exercise training studies, any AICAR-induced increase in skeletal muscle abundance of oxidative phosphorylation complex proteins was blunted in AMPK α2 KD mice (**Figures 4A–F**). However, no significant interaction effects were found for Complex I-V, most likely due to low statistical power. When individual *t*-tests were performed, significant increases in protein content were found in the WT group for Complexes I, IV, and V. Treatment with AICAR increased

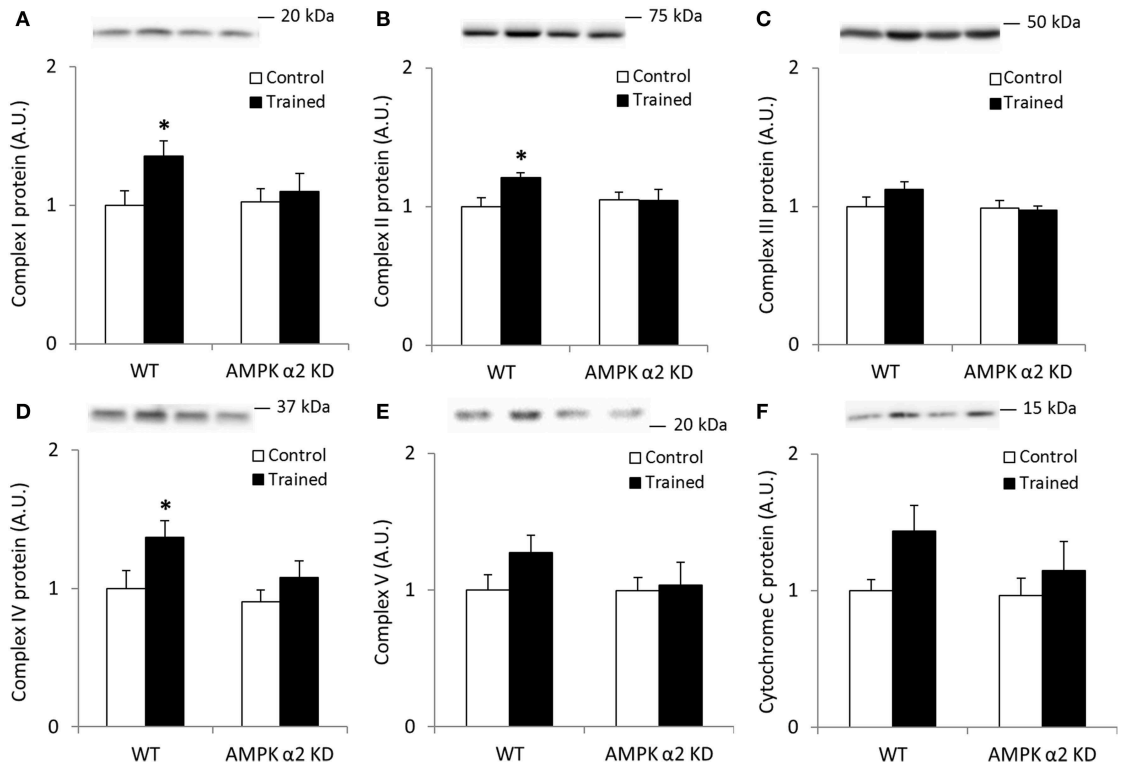

FIGURE 1 | Exercise training increase mitochondrial oxidative phosphorylation complexes in an AMPK α2-dependent manner. Protein levels of oxidative phosphorylation complexes, **(A)** Complex I, **(B)** Complex II, **(C)** Complex III, **(D)** Complex IV, **(E)** Complex V (oligomycin-sensitivity conferring protein subunit, OSCP), and **(F)** Cytochrome C were evaluated in quadriceps muscle of sedentary (control) or exercise trained female WT and AMPK α2 KD mice ($n = 13$–15). Values are mean ± SEM. *indicates vs. WT control ($p < 0.05$) analyzed by unpaired *t*-tests.

abundance of cytochrome C in the WT mice ($p < 0.01$) in an AMPK-dependent manner (treatment × genotype interaction effect $p < 0.05$), and protein levels were lower in AMPK α2 KD mice ($p < 0.01$; **Figure 4F**).

AICAR treatment resulted in AMPK α2-dependent increases in SIRT3 protein levels (treatment × genotype interaction effect $p < 0.05$; $n = 7$–8; **Figure 5A**) whereas mRNA expression increased independent of genotype ($p < 0.01$; **Figure 5B**). Likewise, MnSOD protein levels increased in an AMPK α2-dependent manner (treatment × genotype interaction effect $p < 0.05$; $n = 7$–8; **Figure 5C**) while MnSOD mRNA expression increased in response to AICAR independent of AMPK α2 ($p < 0.01$, $n = 6$–8; **Figure 5D**). Together, these data support the hypothesis that AMPK activation governs post-transcriptional regulation of SIRT3 and MnSOD protein levels. Repeated treatment with AICAR did not increase SIRT1 or catalase protein levels (**Figures 5E,F**).

We next assessed whether increases in SIRT3 and MnSOD following AICAR treatment depend on functional PGC-1α signaling. AICAR treatment increased skeletal muscle protein level of SIRT3 and MnSOD in WT, but not in PGC-1α KO mice (treatment × genotype interaction effect $p < 0.05$; $n = 9$–10; **Figures 6A,B**), and total protein of SIRT3 and MnSOD was generally reduced in control PGC-1α KO mice ($p < 0.01$; $n = 9$–10; **Figures 6A,B**). SIRT1 and catalase protein levels were similar in the WT and PGC-1α mice and remained unaltered in response to repeated AICAR treatment (**Figures 6C,D**). These data suggest that SIRT3 and MnSOD protein abundance is regulated in a signaling axis involving both AMPK and PGC-1α. In an attempt to establish indirect evidence that upregulation of SIRT3 and MnSOD protein with AICAR is mediated through transcriptional regulation of the SIRT3 and MnSOD genes by a PGC-1α-dependent mechanism, we measured mRNA levels of SIRT3 and MnSOD in PGC-1α KO animals treated repeatedly with AICAR over 4 weeks. Although mRNA levels of both SIRT3 and MnSOD were reduced in the PGC-1α KO animals, no increase with AICAR was detected in either genotype (**Figures 6E,F**). To determine whether an acute AICAR injection would increase mRNA levels of SIRT3 and MnSOD, we analyzed samples from PGC-1α KO and WT mice taken 4 h after a single injection of AICAR/saline (Leick et al., 2010a). As in the repeated-AICAR experiment, PGC-1α KO mice had lower mRNA levels of SIRT3 and MnSOD, but AICAR did not increase SIRT3 or MnSOD mRNA (**Figures 6G,H**).

Combined Effects of Endurance Exercise Training and Acute Exercise on Mitochondrial Protein Acetylation State in Mouse Quadriceps Muscle

SIRT3 is involved in the activation of MnSOD by deacetylating K122. Deacetylation of this residue would be expected

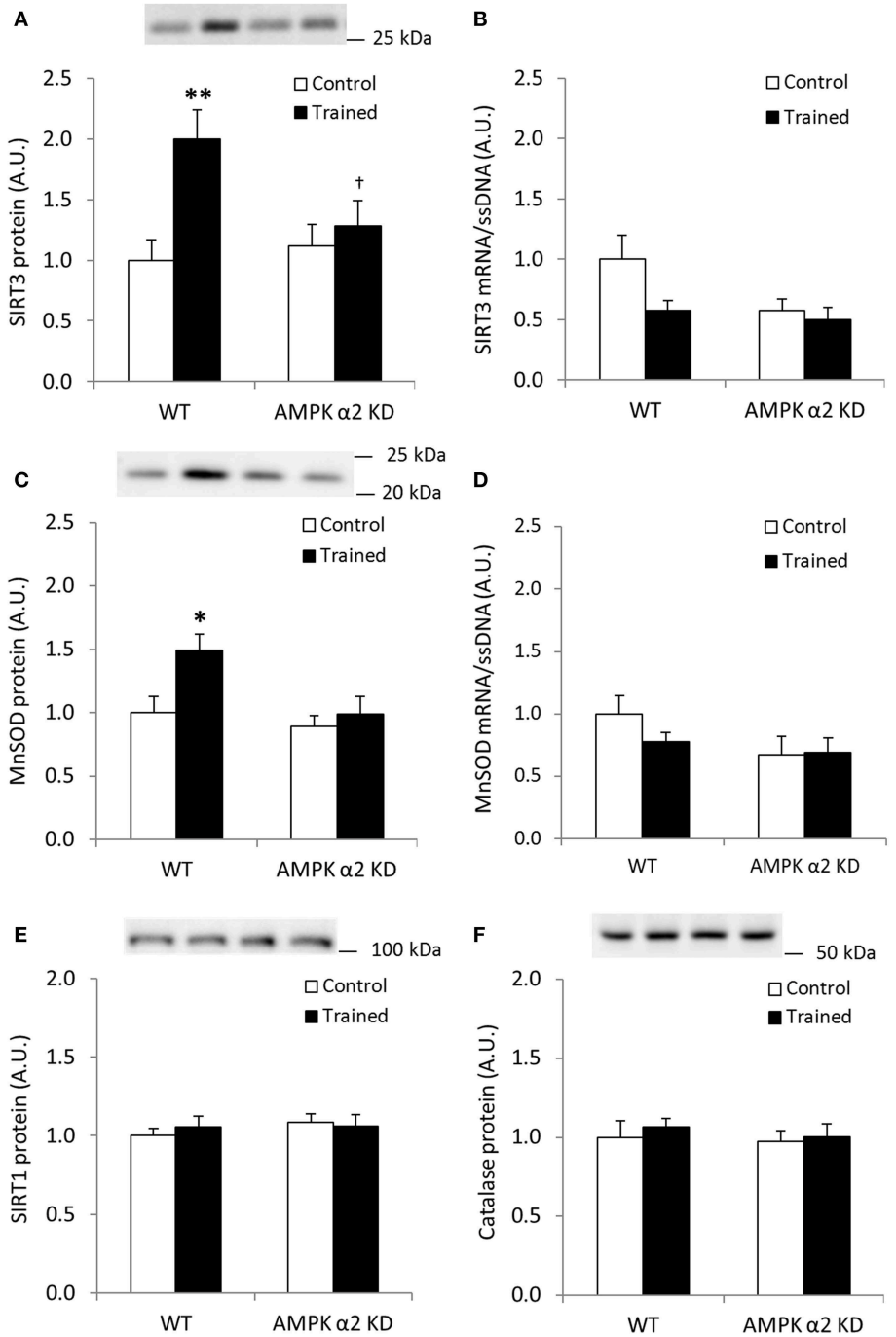

FIGURE 2 | Exercise training increases SIRT3 and MnSOD protein in mouse skeletal muscle in an AMPK α2-dependent manner. (A) SIRT3 protein, **(B)** SIRT3 mRNA ($n = 11$–14), **(C)** MnSOD protein, **(D)** MnSOD mRNA ($n = 11$–14), **(E)** SIRT1 protein, and **(F)** Catalase protein levels were measured in quadriceps muscle of control or exercised trained female WT and AMPK α2 KD mice ($n = 13$–15 for protein measurements). Quadriceps muscles were obtained the day after the final bout of exercise. Values are mean ± SEM. An interaction effect ($p < 0.05$; treatment × genotype) was present in **(A)**. * indicates vs. WT control ($p < 0.05$; analyzed by independent *t*-test), ** indicates vs. WT control ($p < 0.01$), and † indicates genotype effect within trained groups ($p < 0.05$).

to occur if superoxides are produced in mitochondria during exercise. To determine whether SIRT3-mediated deacetylation of mitochondrial proteins in skeletal muscle is dependent on training status, and whether acute exercise in sedentary and exercise trained muscle would lead to a differentiated acetylation response, C57BL/6JBom mice were exercise trained or

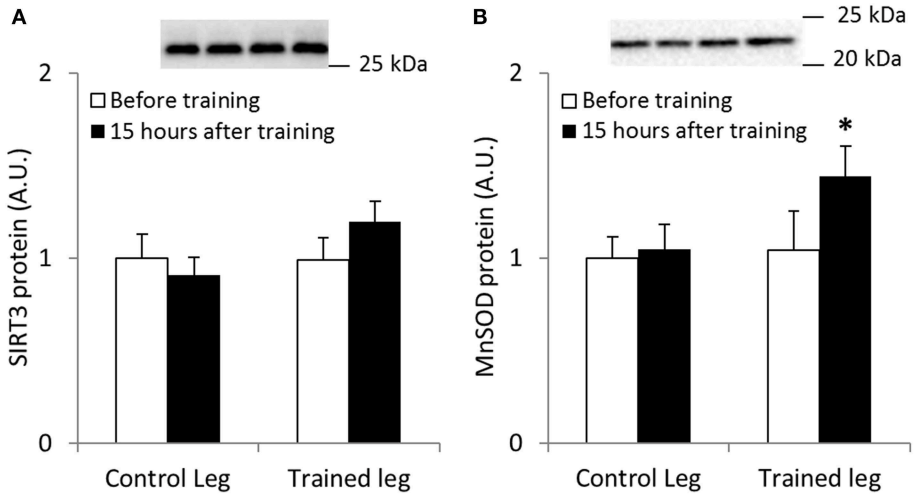

FIGURE 3 | One-legged knee-extensor endurance exercise training increases MnSOD protein levels in human *vastus lateralis* muscle. Male individuals performed 15 sessions of 1–2 h of one-legged knee extensor endurance exercise training over a period of 3 weeks. SIRT3 and MnSOD protein levels were measured from biopsies obtained before training and 15 h after the last bout of exercise ($n = 8$). **(A)** SIRT3 and **(B)** MnSOD protein levels. A borderline interaction effect of leg × intervention ($p = 0.051$) was found for MnSOD protein levels (observed power 0.471). * indicates vs. control leg after training ($p < 0.05$; paired t-test). Values are mean ± SEM. Statistical analyses were performed for $n = 6$ due to incomplete sample sets.

maintained as sedentary controls. On the day of tissue collection, mice were subjected to an acute 1-h bout of "moderate" or "high" intensity exercise or served as sedentary controls. Thus, using muscle samples from this experiment in addition to an antibody against acetylated K122 of MnSOD known to be important for MnSOD activity (Tao et al., 2010), the putative improved ability of trained muscle to handle ROS could be determined. To test the specificity of antibodies against total MnSOD and MnSOD K122 in skeletal muscle, we performed "split-blot" analyses and found bands from both antibodies to align in mouse and human skeletal muscle (**Figure 7A**). OSCP K139 antibody specificity has been previously validated (Vassilopoulos et al., 2014), and we further verified total OSCP and OSCP K139 specificity in skeletal muscle tissue by performing "split-blot" analyses and confirming that bands for OSCP and OSCP K139 align in human and mouse skeletal muscle (**Figure 7B**).

First, we confirmed that exercise training increases SIRT3 protein content in mouse quadriceps muscle (**Figure 8A**). Unexpectedly, 60 min of high-intensity acute exercise caused further increases in SIRT3 protein abundance in both previously sedentary and trained mice (**Figure 8A**). This increase in protein content was not accompanied by a parallel increase in SIRT3 mRNA in these samples relative to samples from any of the other groups (data not shown). Contrary to the AMPK α2 KD/WT exercise training study described above (**Figures 2E,F**), SIRT1 and catalase protein levels increased in response to exercise training. No additional change occurred in response to acute exercise (**Figures 8B,C**). Furthermore, MnSOD protein levels increased with exercise training (**Figure 8D**) to a similar degree as WT mice in the AMPK α2 KD/WT training study (**Figure 8D** vs. **Figure 2C**).

Although the importance of mitochondria as a source of superoxides during muscle contraction has been questioned (McArdle et al., 2004), we assessed acetylation level of MnSOD in response to exercise training and an acute bout of exercise. We detected increased acetylation of MnSOD K122 in the samples from exercise-trained animals, whereas acetylation levels were unaffected by acute exercise (**Figure 8E**). When MnSOD K122 acetylation status was normalized to total MnSOD protein abundance, acetylation status remained unchanged across conditions (**Figure 8F**).

We also tested the hypothesis that acetylation of OSCP on the K139 residue is a marker of cellular energy stress, and that exercised trained muscle would be less susceptible to exercise-induced changes in K139 acetylation. OSCP protein abundance increased with exercise training in mouse quadriceps muscle (**Figure 8G**), in addition to a pronounced increase in acetylation of OSCP K139 (**Figure 8H**). When OSCP acetylation level was normalized to total OSCP protein, K139 acetylation increased with exercise training (**Figure 8I**). Contrary to our hypothesis, OSCP K139 acetylation relative to total OSCP was unaffected by acute exercise (**Figures 8H,I**).

Acetylation Patterns in Human *Vastus Lateralis* with Acute Exercise

To compare the MnSOD and OSCP acetylation response obtained in exercised mouse quadriceps muscle with acutely exercised human skeletal muscle, we determined the acetylation level of these proteins in samples obtained from strenuously exercised *vastus lateralis* muscle of healthy young men. Acute exercise did not alter total protein abundance of either MnSOD or OSCP, nor did this intervention alter relative protein acetylation directly following exercise cessation (**Figures 9A–F**).

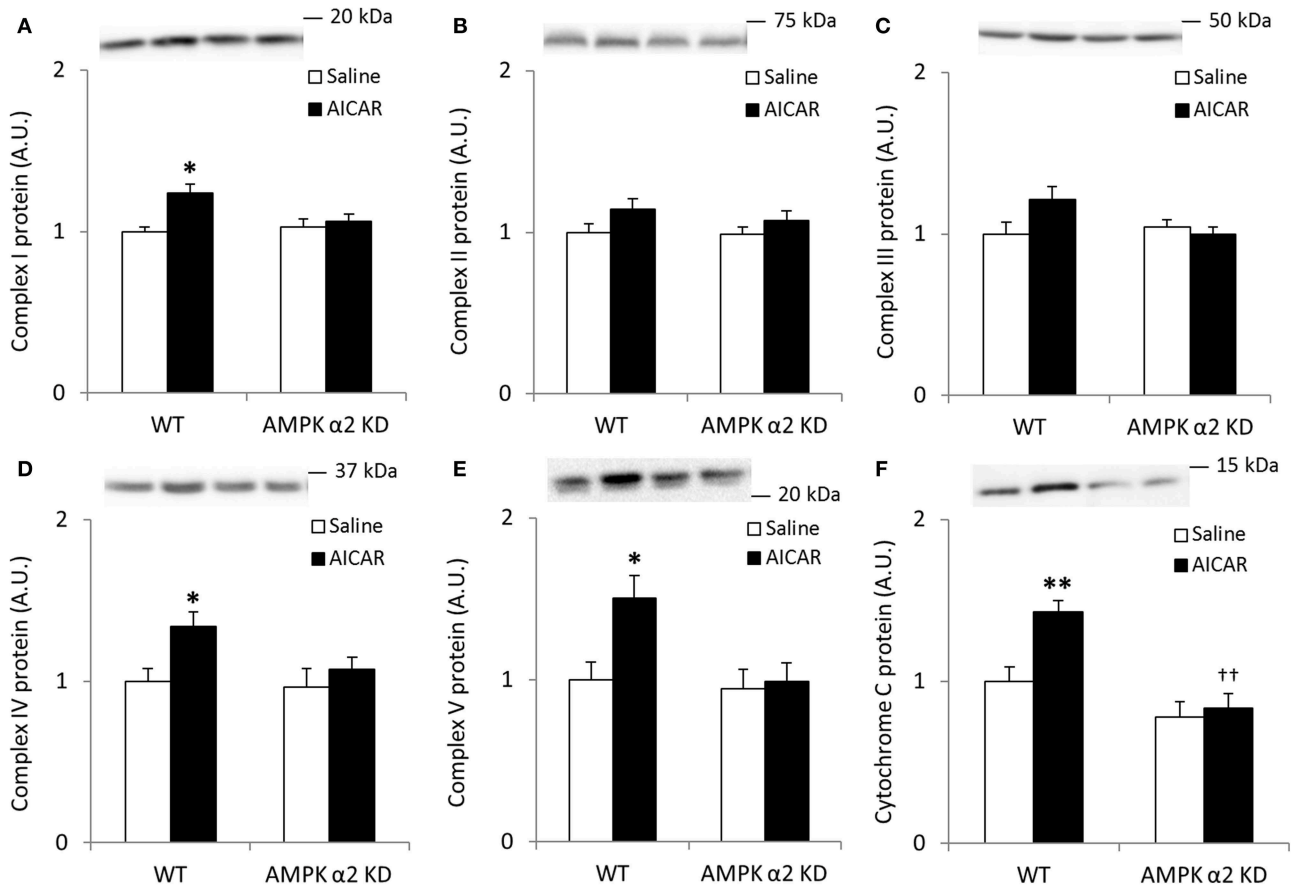

FIGURE 4 | Repeated treatment with AICAR increases abundance of mitochondrial electron transport chain proteins in an AMPK α2-dependent manner. WT and AMPK α2 KD male mice were given daily subcutaneous injections with AICAR (500 mg/kg body weight) or saline for 4 weeks. **(A–E)** Protein abundance of oxidative phosphorylation Complexes I–V and **(F)** Cytochrome C was measured in quadriceps muscle ($n = 7$–8). A significant interaction effect (treatment × genotype; $p < 0.05$) was observed for Cytochrome C. Values are mean ± SEM. * indicates vs. WT saline ($p < 0.05$) analyzed by *t*-tests, ** indicates vs. WT saline ($p < 0.01$), and †† indicates genotype effect within AICAR treated animals ($p < 0.01$).

Discussion

AMPK is a cellular "fuel gauge" that integrates and communicates disruptions in cellular energy charge to downstream targets (Hardie, 2011). One key signaling pathway by which AMPK exerts its effects is via the AMPK-PGC-1α-SIRT3 axis, which likely affects mitochondrial function and gene expression to adapt to metabolic changes (Hallows et al., 2006; Schwer et al., 2006; Someya et al., 2010; Tseng et al., 2013; Wu et al., 2013; Vassilopoulos et al., 2014). Here, we present evidence that AMPK is required for the increase in skeletal muscle SIRT3 and MnSOD protein abundance in addition to proteins in the mitochondrial respiratory complexes following exercise training and repeated AICAR treatment.

AMPK plays a critical role in mediating AICAR-induced increases in mitochondrial protein abundance (Jørgensen et al., 2007). The present study confirms these findings and provides additional evidence that AMPK is required to fully beget exercise training-induced increases in mitochondrial oxidative phosphorylation complexes. This observation is in line with recent data showing that exercise training-induced adaptations in skeletal muscle on mitochondrial Complexes I-V are dependent on the upstream AMPK kinase, LKB1 (Tanner et al., 2013). Other studies employing the same (Abbott and Turcotte, 2014) or similar mouse models of AMPK deficiency (Röckl et al., 2007) as in the present investigation did not detect AMPK-dependent defects in the ability to increase mitochondrial protein content. However, these studies only assessed citrate synthase activity and did not report the abundance of electron transport chain proteins.

The one-legged endurance exercise training model represents a well-controlled method to study contraction-mediated adaptations in *vastus lateralis* muscle in humans (Andersen et al., 1985; Frøsig et al., 2004). Despite a relatively small sample size, we found near-significant increases in skeletal muscle MnSOD protein level in the trained, but not untrained leg of healthy volunteers. Conversely, SIRT3 protein levels were not increased. This is in conflict with emerging evidence that SIRT3 expression is increased in exercise-trained human and rodent skeletal muscle (Lanza et al., 2008; Palacios et al., 2009). While an early cross-sectional study reported higher protein activity of MnSOD in

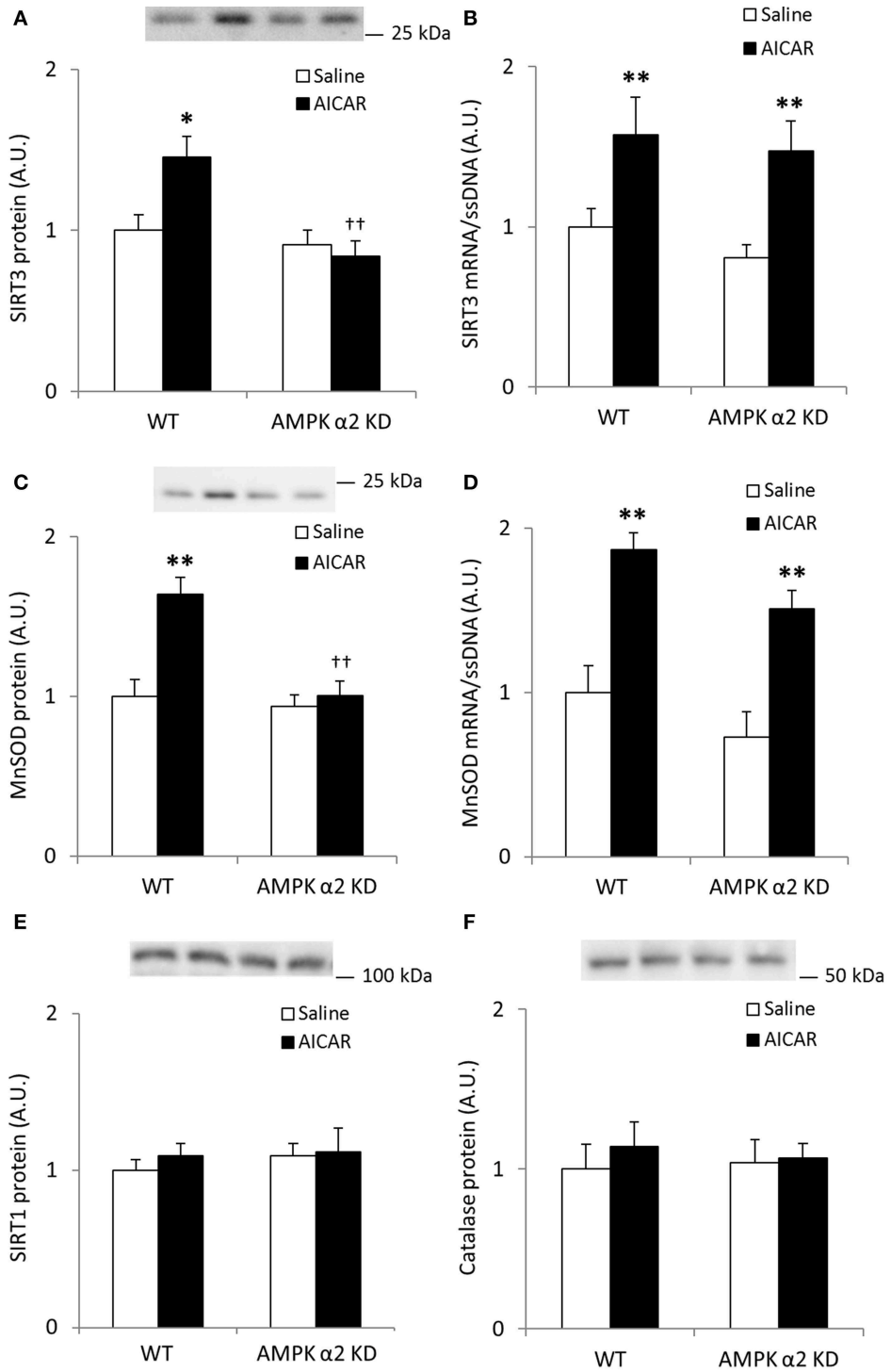

FIGURE 5 | Increases in quadriceps SIRT3 protein levels after repeated AICAR treatment are abolished in AMPK α2 KD mouse skeletal muscle. Levels of **(A)** SIRT3 protein, **(B)** SIRT3 mRNA, **(C)** MnSOD protein, **(D)** MnSOD mRNA, **(E)** SIRT1 protein, and **(F)** Catalase protein were determined in quadriceps muscle from WT and AMPK α2 KD male mice ($n = 7$–8) treated with daily subcutaneous injections of AICAR (500 mg/kg body weight) or saline for 4 weeks. Values are mean ± SEM. Interaction effects (treatment × genotype) were present in **(A)** ($p < 0.05$) and **(C)** ($p < 0.01$). * indicates vs. saline within genotype ($p < 0.05$), ** indicates vs. saline within genotype ($p < 0.01$), and †† indicates genotype effect within AICAR treated samples ($p < 0.01$).

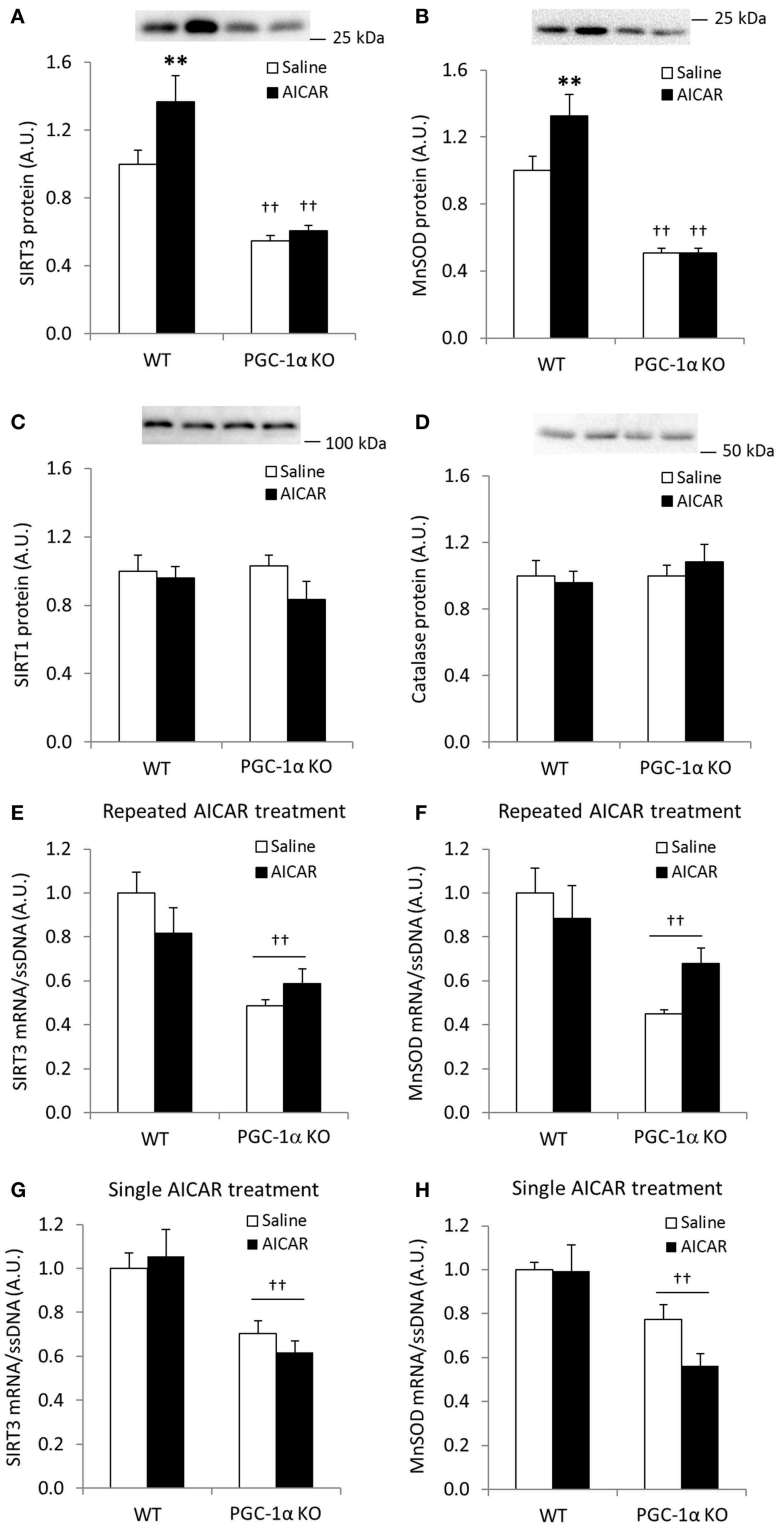

FIGURE 6 | AICAR-induced upregulation of SIRT3 and MnSOD protein in mouse skeletal muscle is dependent on PGC-1α. WT and PGC-1α KO mice received daily subcutaneous injection of AICAR (500 mg/kg body weight) or saline for 4 weeks. Quadriceps muscles were obtained the day after the last injection. **(A)** SIRT3 protein, **(B)** MnSOD protein, **(C)** SIRT1 protein, **(D)** Catalase protein, **(E)** SIRT3 mRNA, **(F)** MnSOD mRNA ($n = 9$–10). mRNA levels of **(G)** SIRT3 and **(H)** MnSOD were obtained from quadriceps muscles from WT and PGC-1α KO mice 4 h after a single injection of saline or AICAR (500 mg/kg body weight, $n = 6$–8). Values are mean ± SEM. Interaction effects (treatment × genotype) were present for data in **(A, C)** ($p < 0.05$), ** indicates vs. WT saline ($p < 0.01$), †† indicates genotype effect vs. WT ($p < 0.01$).

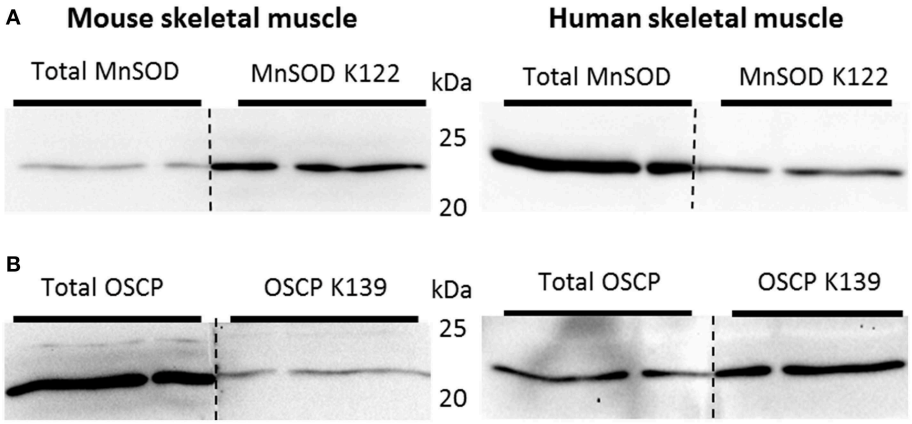

FIGURE 7 | Validation of antibodies targeting acetylated residues of MnSOD and OSCP. Validation of antibodies targeting **(A)** acetylated residue K122 of MnSOD and total MnSOD and **(B)** OSCP acetylation at residue K139 and total OSCP in mouse and human skeletal muscle by "split-blot" analysis.

skeletal muscle of individuals with high aerobic fitness (Jenkins et al., 1984), some longitudinal studies have called these findings into question (Tiidus et al., 1996; Tonkonogi et al., 2000).

In our study, SIRT3 or ROS defense protein abundance was unaltered by exercise training in AMPK α2 KD mice. These results are inconsistent with the notion that SIRT3 may be induced by exercise in an AMPK-independent manner (Gurd et al., 2012). While 7 days of chronic electrical stimulation increased SIRT3 level in rat hind limb muscles, AICAR treatment had no effect (Gurd et al., 2012). Apart from obvious species and protocol differences between the two studies, these findings could also suggest additional, possibly time-sensitive, regulatory mechanisms of SIRT3 protein levels.

Activation of SIRT1 via deletion of poly (ADP-ribose) polymerase-1 (PARP-1), a major NAD-consuming enzyme, increases mitochondrial content (Bai et al., 2011). In the present study, SIRT1 and catalase protein abundance was not consistently increased with exercise training, despite a substantive increase in skeletal muscle SIRT3 protein levels in WT mice. These findings corroborate earlier reports showing that SIRT1 expression is not strongly correlated with contraction-induced changes in mitochondrial protein abundance (Chabi et al., 2009; Ringholm et al., 2013). A proportionally larger increase in SIRT1 activity, rather than protein abundance, may explain the enhanced response to endurance training and AICAR in WT mice in our study. For example, high-intensity interval training increases overall SIRT1 activity, despite decreasing SIRT1 protein concentration in humans (Gurd et al., 2010). However, SIRT1 is an NAD-dependent sirtuin, and we have previously reported that AMPK α2 KD, PGC-1α KO, and corresponding WT littermates respond similarly in increasing protein abundance of nicotinamide phosphoribosyltransferase, the rate-limiting enzyme in NAD recycling, in response to exercise training (Brandauer et al., 2013). These data suggest that the differential response in mitochondrial protein abundance following exercise training is unrelated to SIRT1 activation via NAD. Interestingly, PARP-1 deletion leads to an activation of SIRT1, but not SIRT3, suggesting possible differences in sirtuin activation in different cellular compartments (Bai et al., 2011).

While SIRT3 and MnSOD protein abundance increased in response to exercise training in WT mice, SIRT3, and MnSOD mRNA levels were unaffected in both genotypes. On the other hand, repeated AICAR treatment increased SIRT3 and MnSOD protein levels in an AMPK α2-dependent manner, while mRNA levels of SIRT3 and MnSOD were increased in both WT and AMPK α2 KD mice. These data strongly suggest that AMPK is involved in post-transcriptional regulation of SIRT3 and MnSOD gene products with AICAR. Although previous studies have failed to demonstrate a role for AMPK α2 in regulating gene expression in mouse skeletal muscle after acute exercise (Jørgensen et al., 2005; Brandauer et al., 2013), we cannot rule out that AMPK could be important for promoting gene transcription of SIRT3 and MnSOD after exercise. Further studies are needed to clarify the differential effects of AICAR and exercise training on mRNA expression of these two genes.

We assessed the necessity of PGC-1α in mediating AICAR-induced increases in SIRT3 and MnSOD protein levels. While SIRT3 and MnSOD mRNA levels did not increase in WT or whole-body PGC-1α KO mice with either a single dose of AICAR or in response to repeated AICAR treatment, SIRT3 and MnSOD protein abundance with repeated AICAR treatment increased in WT mice but was abolished in PGC-1α KO mice. These mice also had drastically reduced SIRT3 and MnSOD protein abundance in untreated muscle, further underscoring the importance of PGC-1α in the maintenance of mitochondrial integrity. Although no data from exercise-trained PGC-1α KO muscle are presented here, exercise training restores muscle MnSOD concentration in a PGC-1α-independent manner in young mice (Geng et al., 2010), whereas the exercise training response on MnSOD protein levels has been found to be PGC-1α-dependent in old mice (Leick et al., 2010b; Olesen et al., 2013).

Our data on mitochondrial protein abundance should be interpreted in context with previously published literature on fiber type switching following exercise training or AICAR

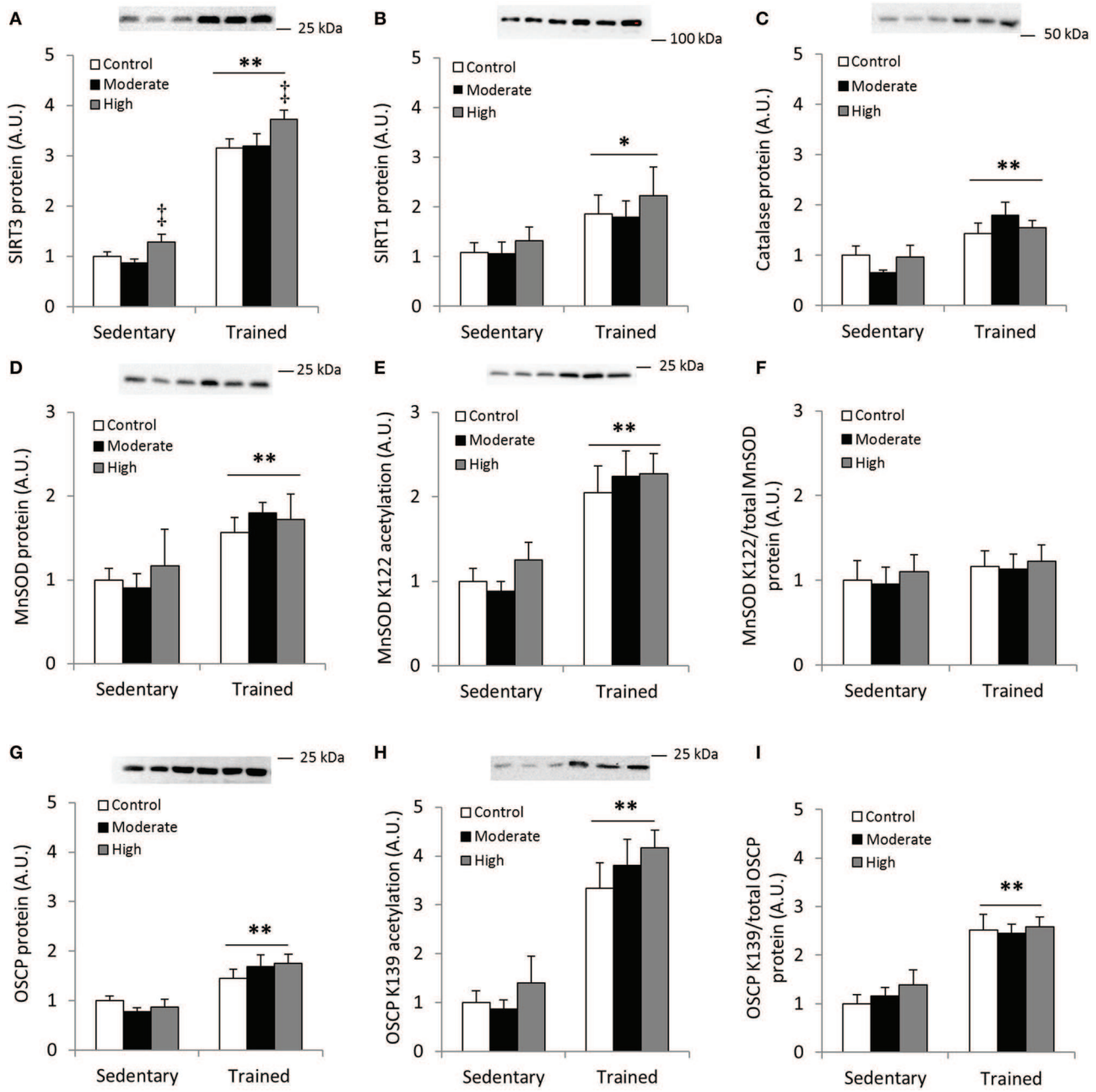

FIGURE 8 | Acute exercise does not result in deacetylation of MnSOD K122 or OSCP K139 in mouse skeletal muscle. C57BL/6JBom mice were exercise trained for 5.5 weeks ("Trained") or kept as sedentary controls ("Sedentary"). On the day of tissue collection, both groups were further divided into three groups that either rested ("Control") or performed 60 min of treadmill running at either 12 m/min (0° incline; "Moderate") or 18 m/min (10° incline; "High" intensity). **(A)** SIRT3, **(B)** SIRT1 and **(C)** Catalase protein abundance was measured in quadriceps muscles after 1 h of treadmill exercise. **(D)** Total MnSOD, **(E)** MnSOD K122 acetylation levels and **(F)** MnSOD K122 acetylation levels normalized to total MnSOD levels. **(G)** Protein levels of the Complex V subunit, F_1F_0 ATP synthase oligomycin-sensitivity conferring protein (OSCP), **(H)** OSCP K139 acetylation levels and **(I)** OSCP K139 acetylation/total OSCP. Values are mean ± SEM. $^{*/**}$ indicates main effect vs. sedentary ($p < 0.05/0.01$), ‡ main effect vs. control ($p < 0.01$), $n = 7$–9.

administration. AMPK and PGC-1α are vital regulators of cellular metabolic adaptations, and a functional AMPK α2 subunit appears to be required to fully realize training-induced IIb to IIa/x fiber type conversion (Röckl et al., 2007). Repeated AICAR treatment alone may be insufficient to change skeletal muscle fiber type (Bamford et al., 2003; Putman et al., 2003), although data from dystrophic mice indicates that AICAR may cause a phenotypic shift toward a more slow-twitch, oxidative

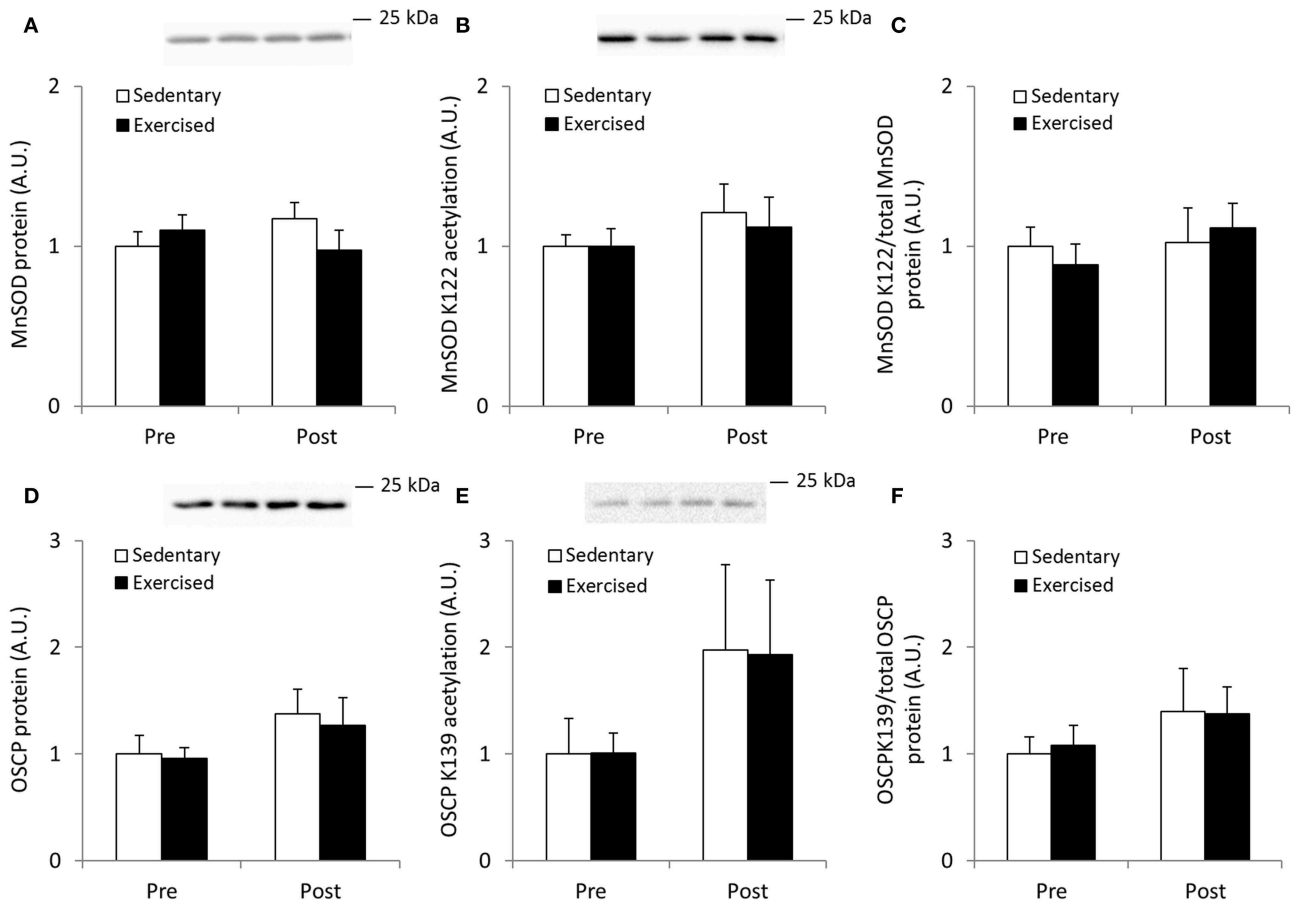

FIGURE 9 | Acetylation status of MnSOD K122 and OSCP K139 is unaffected by acute exercise in human skeletal muscle. Male subjects performed an acute bout (1 h) of one-legged extensor exercise at 80% peak work load after an over-night fast and *vastus lateralis* muscle biopsies from both legs were obtained before (Pre) and immediately after (Post) the exercise bout ($n = 7$). **(A)** MnSOD protein, **(B)** MnSOD K122 acetylation and **(C)** MnSOD K122 acetylation/MnSOD total protein abundance. **(D)** OSCP protein, **(E)** Acetylation status of OSCP K139 and **(F)** OSCP K139 normalized to total OSCP protein abundance. Values are mean ± SEM. No significant effects were observed.

fiber type under some circumstances (Ljubicic et al., 2011). PGC-1α is not only a major stimulator of mitochondrial biogenesis but also promotes type II to type I fiber type conversion (Lee et al., 2006), along with other factors such as calcineurin (Naya et al., 2000). Our data and these lines of evidence further support the notion that AMPK and PGC-1α are centrally important regulators of metabolic and contractile performance of mammalian skeletal muscle. However, the finding that AICAR treatment increases mitochondrial biogenesis, but may not necessarily change fiber type suggests that these processes may commonly occur in tandem but not be regulated by the same physiological stimuli.

SIRT3 is known to have deacetylase activity in the mitochondrion (Lombard et al., 2007). MnSOD activity is regulated through deacetylation via SIRT3 and plays an important role in handling and regulating ROS levels in mitochondria (Ahn et al., 2008; Tao et al., 2010). MnSOD has multiple acetylation sites (Rardin et al., 2013) where key lysine residues (e.g., K68 and K122) are deacetylated in response to exercise and cellular stress (Tao et al., 2010). To elucidate the interplay between aerobic fitness and stress induced by acute exercise, trained or untrained WT mice were subjected to an acute bout of "moderate" or "high"-intensity exercise, or assigned to a non-exercise control group. Despite the substantial increase in SIRT3 protein abundance, acetylation of regulatory lysine residue K122 of MnSOD or K139 of OSCP was not reduced in exercise-trained and/or acutely exercised mice at the various exercise intensities. Rather, when normalized to total protein levels, MnSOD K122 acetylation was unaltered between exercise trained and untrained mice, whereas acetylation status of K139 on OSCP was increased. This exercise training-induced increase in MnSOD implicates an enhanced cellular ROS handling capacity. However, our data on MnSOD and OSCP acetylation following acute exercise are not in obvious agreement with reported exercise-induced reductions in acetylation of these sites (Vassilopoulos et al., 2014). One difference between the two exercise protocols is that all mice in the present study completed the "moderate" and "high" intensity exercise bouts, while the exercise protocol in the previous

study (Vassilopoulos et al., 2014) was exhaustive. Exhaustive exercise may be required to detect an appreciable deacetylation of MnSOD and OSCP at these lysine residues. The lack of exercise-induced changes in MnSOD and OSCP acetylation was compared with human skeletal muscle samples obtained in conjunction with a one-legged exercise protocol. Under these conditions, we also failed to observe a differential regulation of MnSOD K122 and OSCP K139 between the exercised and sedentary legs. Thus, the effects of acute exercise on MnSOD and OSCP deacetylation may vary across different experimental models and organisms. Further studies are warranted to determine the exact factors regulating SIRT3-regulated protein deacetylation with acute exercise.

The substantial increase in K139 acetylation we found after exercise training in mice may seem counterintuitive. One explanation for this observed increased OSCP acetylation could be that total cellular mitochondrial content is enhanced. Exercise training may thus have resulted in an ATP-generating potential that surpasses the actual need for ATP, leading to ATP synthase inhibition via OSCP acetylation. Another possibility is that lysine residues other than K139 on OSCP or lysines on other subunits of the ATP synthase are important for ATP synthase activity, and that acetylation status of these is changed in response to training.

The fact that concentrations of the mitochondrial SIRT3 protein were more than 3-fold higher in exercise-trained compared with untrained mice presents an intriguing observation. Why increased deacetylase protein concentration would result in unchanged or even increased acetylation levels in MnSOD or OSCP, respectively, is not immediately clear. In this context, a previous study reported that SIRT3 reduces mitochondrial protein synthesis via deacetylation of the ribosomal protein MRPL10 (Yang et al., 2010). Such an adaptation would induce an ATP-"sparing" effect that would preserve ATP pools for cross-bridge cycling and maintaining calcium homeostasis. In short, an acute increase in SIRT3 protein or activity is consistent with an inhibition of protein synthesis and other energetically costly processes by AMPK activation (Jensen et al., 2009; Hardie, 2011; White and Schenk, 2012).

In conclusion, we provide evidence for both AMPK and PGC-1α in regulating protein abundance of SIRT3 and MnSOD. These proteins are important for the regulation of mitochondrial adaptation and the handling of ROS, respectively. The interactive effects of acute and chronic exercise on MnSOD and OSCP acetylation status constitute an unexplored avenue, with implications for intensity- and duration-dependent mitochondrial adaptations that warrant further investigation.

Author Contributions

Experiments and analyses of samples in the present manuscript were conducted in Section of Integrated Physiology at the Novo Nordisk Foundation Center for Basic Metabolic Research, University of Copenhagen.

1. Conception and design of the experiments: JB, MAA, SGV, JTT.
2. Collection, analysis and interpretation of data: JB, MAA, HK, SR, CF, SGV, JTT.
3. Drafting the manuscript: JB, MAA, JTT.
4. Edited, revised and approved the final version of the manuscript: All.

Financial Support

Support for this study was provided by the Novo Nordisk Foundation Center for Basic Metabolic Research and the Novo Nordisk Foundation (Excellence Project Award) to JTT. JB was supported by a Research and Professional Development Grant by Gettysburg College.

Acknowledgments

The authors wish to acknowledge the following people from Section of Molecular Physiology, Department of Nutrition, Exercise and Sports, University of Copenhagen for generous access to human skeletal muscle samples: Prof. Jørgen F. P. Wojtaszewski, Prof. Erik A. Richter, Prof. Bente Kiens, Dr. Jonas M. Kristensen, and Dr. Christian Pehmøller. Prof. Henriette Pilegaard and Dr. Lotte Leick, Molecular Integrative Physiology, Department of Biology, University of Copenhagen, and Mr. Joachim Fentz, Section of Molecular Physiology, Department of Nutrition, Exercise and Sports, University of Copenhagen are acknowledged for providing generous access to samples from PGC-1α knockout mice. Marianne M. Andersen, Betina Bolmgren, and Christine B. Janssens are acknowledged for skilled technical expertise. Prof. Morris J. Birnbaum (Howard Hughes Medical Institute and University of Pennsylvania School of Medicine) and Prof. Bruce Spiegelman (Dana-Farber Cancer Institute, Harvard Medical School) are acknowledged for providing founder AMPK α2 KD and PGC-1α KO mice, respectively. Prof. David Gius (Northwestern University Feinberg School of Medicine, Chicago, Illinois, USA) is acknowledged for kindly providing antibodies targeting acetylated K122 of MnSOD and K139 of OSCP. Finally, the authors wish to thank Prof. Juleen R. Zierath (Department of Molecular Medicine, Karolinska Institutet) for helpful discussions during the manuscript preparation.

References

Abbott, M. J., and Turcotte, L. P. (2014). AMPK-α2 is involved in exercise training-induced adaptations in insulin-stimulated metabolism in skeletal muscle following high-fat diet. *J. Appl. Physiol.* 117, 869–879. doi: 10.1152/japplphysiol.01380.2013

Ahn, B.-H., Kim, H.-S., Song, S., Lee, I. H., Liu, J., Vassilopoulos, A., et al. (2008). A role for the mitochondrial deacetylase Sirt3 in regulating energy homeostasis. *Proc. Natl. Acad. Sci. U.S.A.* 105, 14447–14452. doi: 10.1073/pnas.0803790105

Andersen, P., Adams, R. P., Sjogaard, G., Thorboe, A., and Saltin, B. (1985). Dynamic knee extension as model for study of isolated exercising muscle in humans. *J. Appl. Physiol.* 59, 1647–1653.

Bai, P., Cantó, C., Oudart, H., Brunyánszki, A., Cen, Y., Thomas, C., et al. (2011). PARP-1 inhibition increases mitochondrial metabolism through SIRT1 activation. *Cell Metab.* 13, 461–468. doi: 10.1016/j.cmet.2011.03.004

Bamford, J. A., Lopaschuk, G. D., MacLean, I. M., Reinhart, M. L., Dixon, W. T., and Putman, C. T. (2003). Effects of chronic AICAR administration on the metabolic and contractile phenotypes of rat slow- and fast-twitch skeletal muscles. *Can. J. Physiol. Pharmacol.* 81, 1072–1082. doi: 10.1139/y03-110

Brandauer, J., Vienberg, S. G., Andersen, M. A., Ringholm, S., Risis, S., Larsen, P. S., et al. (2013). AMP-activated protein kinase regulates nicotinamide phosphoribosyl transferase expression in skeletal muscle. *J. Physiol.* 591(Pt 20), 5207–5220. doi: 10.1113/jphysiol.2013.259515

Buler, M., Aatsinki, S.-M., Izzi, V., Uusimaa, J., and Hakkola, J. (2014). SIRT5 is under the control of PGC-1α and AMPK and is involved in regulation of mitochondrial energy metabolism. *FASEB J.* 28, 3225–3237. doi: 10.1096/fj.13-245241

Cantó, C., Gerhart-Hines, Z., Feige, J. N., Lagouge, M., Noriega, L., Milne, J. C., et al. (2009). AMPK regulates energy expenditure by modulating NAD+ metabolism and SIRT1 activity. *Nature* 458, 1056–1060. doi: 10.1038/nature07813

Cantó, C., Jiang, L. Q., Deshmukh, A. S., Mataki, C., Coste, A., Lagouge, M., et al. (2010). Interdependence of AMPK and SIRT1 for metabolic adaptation to fasting and exercise in skeletal muscle. *Cell Metab.* 11, 213–219. doi: 10.1016/j.cmet.2010.02.006

Chabi, B., Adhihetty, P. J., O'Leary, M. F. N., Menzies, K. J., and Hood, D. A. (2009). Relationship between Sirt1 expression and mitochondrial proteins during conditions of chronic muscle use and disuse. *J. Appl. Physiol.* 107, 1730–1735. doi: 10.1152/japplphysiol.91451.2008

Chen, Y., Zhang, J., Lin, Y., Lei, Q., Guan, K.-L., Zhao, S., et al. (2011). Tumour suppressor SIRT3 deacetylates and activates manganese superoxide dismutase to scavenge ROS. *EMBO Rep.* 12, 534–541. doi: 10.1038/embor.2011.65

Egan, B., and Zierath, J. R. (2013). Exercise metabolism and the molecular regulation of skeletal muscle adaptation. *Cell Metab.* 17, 162–184. doi: 10.1016/j.cmet.2012.12.012

Frøsig, C., Jørgensen, S. B., Hardie, D. G., Richter, E. A., and Wojtaszewski, J. F. P. (2004). 5′-AMP-activated protein kinase activity and protein expression are regulated by endurance training in human skeletal muscle. *Am. J. Physiol. Endocrinol. Metab.* 286, E411–E417. doi: 10.1152/ajpendo.00317.2003

Geng, T., Li, P., Okutsu, M., Yin, X., Kwek, J., Zhang, M., et al. (2010). PGC-1alpha plays a functional role in exercise-induced mitochondrial biogenesis and angiogenesis but not fiber-type transformation in mouse skeletal muscle. *Am. J. Physiol. Cell Physiol.* 298, C572–C579. doi: 10.1152/ajpcell.00481.2009

Gerhart-Hines, Z., Rodgers, J. T., Bare, O., Lerin, C., Kim, S.-H., Mostoslavsky, R., et al. (2007). Metabolic control of muscle mitochondrial function and fatty acid oxidation through SIRT1/PGC-1alpha. *EMBO J.* 26, 1913–1923. doi: 10.1038/sj.emboj.7601633

Gurd, B. J., Holloway, G. P., Yoshida, Y., and Bonen, A. (2012). In mammalian muscle, SIRT3 is present in mitochondria and not in the nucleus; and SIRT3 is upregulated by chronic muscle contraction in an adenosine monophosphate-activated protein kinase-independent manner. *Metab. Clin. Exp.* 61, 733–741. doi: 10.1016/j.metabol.2011.09.016

Gurd, B. J., Perry, C. G. R., Heigenhauser, G. J. F., Spriet, L. L., and Bonen, A. (2010). High-intensity interval training increases SIRT1 activity in human skeletal muscle. *Appl. Physiol. Nutr. Metab.* 35, 350–357. doi: 10.1139/H10-030

Hallows, W. C., Lee, S., and Denu, J. M. (2006). Sirtuins deacetylate and activate mammalian acetyl-CoA synthetases. *Proc. Natl. Acad. Sci. U.S.A.* 103, 10230–10235. doi: 10.1073/pnas.0604392103

Hardie, D. G. (2011). Energy sensing by the AMP-activated protein kinase and its effects on muscle metabolism. *Proc. Nutr. Soc.* 70, 92–99. doi: 10.1017/S0029665110003915

Jacobs, K. M., Pennington, J. D., Bisht, K. S., Aykin-Burns, N., Kim, H.-S., Mishra, M., et al. (2008). SIRT3 interacts with the daf-16 homolog FOXO3a in the mitochondria, as well as increases FOXO3a dependent gene expression. *Int. J. Biol. Sci.* 4, 291–299.

Jäger, S., Handschin, C., St-Pierre, J., and Spiegelman, B. M. (2007). AMP-activated protein kinase (AMPK) action in skeletal muscle via direct phosphorylation of PGC-1alpha. *Proc. Natl. Acad. Sci. U.S.A.* 104, 12017–12022. doi: 10.1073/pnas.0705070104

Jenkins, R. R., Friedland, R., and Howald, H. (1984). The relationship of oxygen uptake to superoxide dismutase and catalase activity in human skeletal muscle. *Int. J. Sports Med.* 5, 11–14. doi: 10.1055/s-2008-1025872

Jensen, T. E., Wojtaszewski, J. F. P., and Richter, E. A. (2009). AMP-activated protein kinase in contraction regulation of skeletal muscle metabolism: necessary and/or sufficient? *Acta Physiol. (Oxf).* 196, 155–174. doi: 10.1111/j.1748-1716.2009.01979.x

Jørgensen, S. B., Treebak, J. T., Viollet, B., Schjerling, P., Vaulont, S., Wojtaszewski, J. F. P., et al. (2007). Role of AMPKalpha2 in basal, training-, and AICAR-induced GLUT4, hexokinase II, and mitochondrial protein expression in mouse muscle. *Am. J. Physiol. Endocrinol. Metab.* 292, E331–E339. doi: 10.1152/ajpendo.00243.2006

Jørgensen, S. B., Wojtaszewski, J. F. P., Viollet, B., Andreelli, F., Birk, J. B., Hellsten, Y., et al. (2005). Effects of alpha-AMPK knockout on exercise-induced gene activation in mouse skeletal muscle. *FASEB J.* 19, 1146–1148. doi: 10.1096/fj.04-3144fje

Koh, H.-J., Brandauer, J., and Goodyear, L. J. (2008). LKB1 and AMPK and the regulation of skeletal muscle metabolism. *Curr. Opin. Clin. Nutr. Metab. Care* 11, 227–232. doi: 10.1097/MCO.0b013e3282fb7b76

Kong, X., Wang, R., Xue, Y., Liu, X., Zhang, H., Chen, Y., et al. (2010). Sirtuin 3, a new target of PGC-1alpha, plays an important role in the suppression of ROS and mitochondrial biogenesis. *PLoS ONE* 5:e11707. doi: 10.1371/journal.pone.0011707

Lanza, I. R., Short, D. K., Short, K. R., Raghavakaimal, S., Basu, R., Joyner, M. J., et al. (2008). Endurance exercise as a countermeasure for aging. *Diabetes* 57, 2933–2942. doi: 10.2337/db08-0349

Lee, W. J., Kim, M., Park, H.-S., Kim, H. S., Jeon, M. J., Oh, K. S., et al. (2006). AMPK activation increases fatty acid oxidation in skeletal muscle by activating PPARalpha and PGC-1. *Biochem. Biophys. Res. Commun.* 340, 291–295. doi: 10.1016/j.bbrc.2005.12.011

Leick, L., Fentz, J., Biensø, R. S., Knudsen, J. G., Jeppesen, J., Kiens, B., et al. (2010a). PGC-1{alpha} is required for AICAR-induced expression of GLUT4 and mitochondrial proteins in mouse skeletal muscle. *Am. J. Physiol. Endocrinol. Metab.* 299, E456–E465. doi: 10.1152/ajpendo.00648.2009

Leick, L., Hellsten, Y., Fentz, J., Lyngby, S. S., Wojtaszewski, J. F. P., Hidalgo, J., et al. (2009). PGC-1alpha mediates exercise-induced skeletal muscle VEGF expression in mice. *Am. J. Physiol. Endocrinol. Metab.* 297, E92–E103. doi: 10.1152/ajpendo.00076.2009

Leick, L., Lyngby, S. S., Wojtaszewski, J. F. P., Wojtasewski, J. F. P., and Pilegaard, H. (2010b). PGC-1alpha is required for training-induced prevention of age-associated decline in mitochondrial enzymes in mouse skeletal muscle. *Exp. Gerontol.* 45, 336–342. doi: 10.1016/j.exger.2010.01.011

Ljubicic, V., Miura, P., Burt, M., Boudreault, L., Khogali, S., Lunde, J. A., et al. (2011). Chronic AMPK activation evokes the slow, oxidative myogenic program and triggers beneficial adaptations in mdx mouse skeletal muscle. *Hum. Mol. Genet.* 20, 3478–3493. doi: 10.1093/hmg/ddr265

Lombard, D. B., Alt, F. W., Cheng, H.-L., Bunkenborg, J., Streeper, R. S., Mostoslavsky, R., et al. (2007). Mammalian Sir2 homolog SIRT3 regulates global mitochondrial lysine acetylation. *Mol. Cell. Biol.* 27, 8807–8814. doi: 10.1128/MCB.01636-07

McArdle, A., van der Meulen, J., Close, G. L., Pattwell, D., Van Remmen, H., Huang, T. T., et al. (2004). Role of mitochondrial superoxide dismutase in contraction-induced generation of reactive oxygen species in skeletal muscle extracellular space. *Am. J. Physiol. Cell Physiol.* 286, C1152–C1158. doi: 10.1152/ajpcell.00322.2003

Mu, J., Brozinick, J. T. Jr., Valladares, O., Bucan, M., and Birnbaum, M. J. (2001). A role for AMP-activated protein kinase in contraction- and hypoxia-regulated glucose transport in skeletal muscle. *Mol. Cell* 7, 1085–1094. doi: 10.1016/S1097-2765(01)00251-9

Naya, F. J., Mercer, B., Shelton, J., Richardson, J. A., Williams, R. S., and Olson, E. N. (2000). Stimulation of slow skeletal muscle fiber gene expression by calcineurin *in vivo*. *J. Biol. Chem.* 275, 4545–4548. doi: 10.1074/jbc.275.7.4545

Nemoto, S., Fergusson, M. M., and Finkel, T. (2005). SIRT1 functionally interacts with the metabolic regulator and transcriptional coactivator PGC-1{alpha}. *J. Biol. Chem.* 280, 16456–16460. doi: 10.1074/jbc.M501485200

Olesen, J., Ringholm, S., Nielsen, M. M., Brandt, C. T., Pedersen, J. T., Halling, J. F., et al. (2013). Role of PGC-1α in exercise training- and resveratrol-induced

prevention of age-associated inflammation. *Exp. Gerontol.* 48, 1274–1284. doi: 10.1016/j.exger.2013.07.015

Palacios, O. M., Carmona, J. J., Michan, S., Chen, K. Y., Manabe, Y. J. L. W. III., Goodyear, L. J., et al. (2009). Diet and exercise signals regulate SIRT3 and activate AMPK and PGC-1α in skeletal muscle. *Aging (Albany. NY)* 1, 771–783.

Parise, G., Phillips, S. M., Kaczor, J. J., and Tarnopolsky, M. A. (2005). Antioxidant enzyme activity is up-regulated after unilateral resistance exercise training in older adults. *Free Radic. Biol. Med.* 39, 289–295. doi: 10.1016/j.freeradbiomed.2005.03.024

Puigserver, P., Wu, Z., Park, C. W., Graves, R., Wright, M., and Spiegelman, B. M. (1998). A cold-inducible coactivator of nuclear receptors linked to adaptive thermogenesis. *Cell* 92, 829–839. doi: 10.1016/S0092-8674(00)81410-5

Putman, C. T., Kiricsi, M., Pearcey, J., MacLean, I. M., Bamford, J. A., Murdoch, G. K., et al. (2003). AMPK activation increases uncoupling protein-3 expression and mitochondrial enzyme activities in rat muscle without fibre type transitions. *J. Physiol.* 551, 169–178. doi: 10.1111/j.1469-7793.2003.00169.x

Qiu, X., Brown, K., Hirschey, M. D., Verdin, E., and Chen, D. (2010). Calorie restriction reduces oxidative stress by SIRT3-mediated SOD2 activation. *Cell Metab.* 12, 662–667. doi: 10.1016/j.cmet.2010.11.015

Rardin, M. J., Newman, J. C., Held, J. M., Cusack, M. P., Sorensen, D. J., Li, B., et al. (2013). Label-free quantitative proteomics of the lysine acetylome in mitochondria identifies substrates of SIRT3 in metabolic pathways. *Proc. Natl. Acad. Sci. U.S.A.* 110, 6601–6606. doi: 10.1073/pnas.1302961110

Reid, M. B. (2001). Invited review: redox modulation of skeletal muscle contraction: what we know and what we don't. *J. Appl. Physiol.* 90, 724–731.

Ringholm, S., Olesen, J., Pedersen, J. T., Brandt, C. T., Halling, J. F., Hellsten, Y., et al. (2013). Effect of lifelong resveratrol supplementation and exercise training on skeletal muscle oxidative capacity in aging mice; impact of PGC-1α. *Exp. Gerontol.* 48, 1311–1318. doi: 10.1016/j.exger.2013.08.012

Röckl, K. S. C., Hirshman, M. F., Brandauer, J., Fujii, N., Witters, L. A., and Goodyear, L. J. (2007). Skeletal muscle adaptation to exercise training: AMP-activated protein kinase mediates muscle fiber type shift. *Diabetes* 56, 2062–2069. doi: 10.2337/db07-0255

Schwer, B., Bunkenborg, J., Verdin, R. O., Andersen, J. S., and Verdin, E. (2006). Reversible lysine acetylation controls the activity of the mitochondrial enzyme acetyl-CoA synthetase 2. *Proc. Natl. Acad. Sci. U.S.A.* 103, 10224–10229. doi: 10.1073/pnas.0603968103

Schwer, B., North, B. J., Frye, R. A., Ott, M., and Verdin, E. (2002). The human silent information regulator (Sir)2 homologue hSIRT3 is a mitochondrial nicotinamide adenine dinucleotide-dependent deacetylase. *J. Cell Biol.* 158, 647–657. doi: 10.1083/jcb.200205057

Shinmura, K., Tamaki, K., Saito, K., Nakano, Y., Tobe, T., and Bolli, R. (2007). Cardioprotective effects of short-term caloric restriction are mediated by adiponectin via activation of AMP-activated protein kinase. *Circulation* 116, 2809–2817. doi: 10.1161/CIRCULATIONAHA.107.725697

Someya, S., Yu, W., Hallows, W. C., Xu, J., Vann, J. M., Leeuwenburgh, C., et al. (2010). Sirt3 mediates reduction of oxidative damage and prevention of age-related hearing loss under caloric restriction. *Cell* 143, 802–812. doi: 10.1016/j.cell.2010.10.002

Spina, R. J., Chi, M. M., Hopkins, M. G., Nemeth, P. M., Lowry, O. H., and Holloszy, J. O. (1996). Mitochondrial enzymes increase in muscle in response to 7-10 days of cycle exercise. *J Appl Physiol* 80, 2250–2254.

Tanner, C. B., Madsen, S. R., Hallowell, D. M., Goring, D. M. J., Moore, T. M., Hardman, S. E., et al. (2013). Mitochondrial and performance adaptations to exercise training in mice lacking skeletal muscle LKB1. *Am. J. Physiol. Endocrinol. Metab.* 305, E1018–E1029. doi: 10.1152/ajpendo.00227.2013

Tao, R., Coleman, M. C., Pennington, J. D., Ozden, O., Park, S.-H., Jiang, H., et al. (2010). Sirt3-mediated deacetylation of evolutionarily conserved lysine 122 regulates MnSOD activity in response to stress. *Mol. Cell* 40, 893–904. doi: 10.1016/j.molcel.2010.12.013

Tiidus, P. M., Pushkarenko, J., and Houston, M. E. (1996). Lack of antioxidant adaptation to short-term aerobic training in human muscle. *Am. J. Physiol. Regul. Integr. Comp. Physiol.* 271, R832–R836.

Tonkonogi, M., Walsh, B., Svensson, M., and Sahlin, K. (2000). Mitochondrial function and antioxidative defence in human muscle: effects of endurance training and oxidative stress. *J. Physiol.* 528, 379–388. doi: 10.1111/j.1469-7793.2000.00379.x

Treebak, J. T., Pehmøller, C., Kristensen, J. M., Kjøbsted, R., Birk, J. B., Schjerling, P., et al. (2014). Acute exercise and physiological insulin induce distinct phosphorylation signatures on TBC1D1 and TBC1D4 proteins in human skeletal muscle. *J. Physiol.* 592, 351–375. doi: 10.1113/jphysiol.2013.266338

Tseng, A. H. H., Shieh, S.-S., and Wang, D. L. (2013). SIRT3 deacetylates FOXO3 to protect mitochondria against oxidative damage. *Free Radic. Biol. Med.* 63, 222–234. doi: 10.1016/j.freeradbiomed.2013.05.002

Vassilopoulos, A., Pennington, J. D., Andresson, T., Rees, D. M., Bosley, A. D., Fearnley, I. M., et al. (2014). SIRT3 deacetylates ATP synthase F1 complex proteins in response to nutrient- and exercise-induced stress. *Antioxid. Redox Signal.* 21, 551–564. doi: 10.1089/ars.2013.5420

White, A. T., and Schenk, S. (2012). NAD+/NADH and skeletal muscle mitochondrial adaptations to exercise. *Am. J. Physiol. Endocrinol. Metab.* 303, E308–E321. doi: 10.1152/ajpendo.00054.2012

Wu, Y.-T., Lee, H.-C., Liao, C.-C., and Wei, Y.-H. (2013). Regulation of mitochondrial F(o)F(1)ATPase activity by Sirt3-catalyzed deacetylation and its deficiency in human cells harboring 4977bp deletion of mitochondrial DNA. *Biochim. Biophys. Acta* 1832, 216–227. doi: 10.1016/j.bbadis.2012.10.002

Yang, Y., Cimen, H., Han, M.-J., Shi, T., Deng, J.-H., Koc, H., et al. (2010). NAD+-dependent deacetylase SIRT3 regulates mitochondrial protein synthesis by deacetylation of the ribosomal protein MRPL10. *J. Biol. Chem.* 285, 7417–7429. doi: 10.1074/jbc.M109.053421

Conflict of Interest Statement: The authors declare that the research was conducted in the absence of any commercial or financial relationships that could be construed as a potential conflict of interest.

frontiers in Physiology

ORIGINAL RESEARCH
published: 10 April 2015
doi: 10.3389/fphys.2015.00105

Cholesterol removal from adult skeletal muscle impairs excitation–contraction coupling and aging reduces caveolin-3 and alters the expression of other triadic proteins

Genaro Barrientos[1†], Paola Llanos[2†], Jorge Hidalgo[1], Pura Bolaños[3], Carlo Caputo[3], Alexander Riquelme[4], Gina Sánchez[4,5,6], Andrew F. G. Quest[6,7,8] and Cecilia Hidalgo[1,4,6]*

[1] Physiology and Biophysics Program, Institute of Biomedical Sciences, School of Medicine, University of Chile, Santiago, Chile, [2] Institute for Research in Dental Sciences, Faculty of Dentistry, University of Chile, Santiago, Chile, [3] Centre of Biophysics and Biochemistry, Venezuelan Institute for Scientific Research, Caracas, Venezuela, [4] Biomedical Neuroscience Institute, School of Medicine, University of Chile, Santiago, Chile, [5] Pathophysiology Program, Institute of Biomedical Sciences, School of Medicine, University of Chile, Santiago, Chile, [6] Center for Molecular Studies of the Cell, School of Medicine, University of Chile, Santiago, Chile, [7] Laboratory of Cell Communication, Program in Cell and Molecular Biology, Institute of Biomedical Sciences, School of Medicine, University of Chile, Santiago, Chile, [8] Advanced Center for Chronic Diseases and Network for Metabolic Stress Signaling, University of Chile, Santiago, Chile

Cholesterol and caveolin are integral membrane components that modulate the function/location of many cellular proteins. Skeletal muscle fibers, which have unusually high cholesterol levels in transverse tubules, express the caveolin-3 isoform but its association with transverse tubules remains contentious. Cholesterol removal impairs excitation–contraction (E–C) coupling in amphibian and mammalian fetal skeletal muscle fibers. Here, we show that treating single muscle fibers from adult mice with the cholesterol removing agent methyl-β-cyclodextrin decreased fiber cholesterol by 26%, altered the location pattern of caveolin-3 and of the voltage dependent calcium channel Cav1.1, and suppressed or reduced electrically evoked Ca^{2+} transients without affecting membrane integrity or causing sarcoplasmic reticulum (SR) calcium depletion. We found that transverse tubules from adult muscle and triad fractions that contain ∼10% attached transverse tubules, but not SR membranes, contained caveolin-3 and Cav1.1; both proteins partitioned into detergent-resistant membrane fractions highly enriched in cholesterol. Aging entails significant deterioration of skeletal muscle function. We found that triad fractions from aged rats had similar cholesterol and RyR1 protein levels compared to triads from young rats, but had lower caveolin-3 and glyceraldehyde 3-phosphate dehydrogenase and increased Na^+/K^+-ATPase protein levels. Both triad fractions had comparable NADPH oxidase (NOX) activity and protein content of NOX2 subunits ($p47^{phox}$ and $gp91^{phox}$), implying that NOX activity does not increase during aging. These findings show that partial cholesterol removal impairs E–C coupling and alters caveolin-3 and Cav1.1 location pattern, and that aging reduces caveolin-3 protein

OPEN ACCESS

Edited by:
Brian McDonagh, University of Liverpool, UK

Reviewed by:
Nazareno Paolocci, Johns Hopkins University, USA
John James Mackrill, University College Cork, Ireland

***Correspondence:**
Cecilia Hidalgo, Facultad de Medicina, Center for Molecular Studies of the Cell and Physiology and Biophysics Program, Biomedical Neuroscience Institute, Instituto de Ciencias Biomédicas, Universidad de Chile, Independencia 1027, Santiago 8380453, Chile
chidalgo@med.uchile.cl

[†] These authors have contributed equally to this work.

Specialty section:
This article was submitted to Striated Muscle Physiology, a section of the journal Frontiers in Physiology

Received: *31 January 2015*
Accepted: *16 March 2015*
Published: *10 April 2015*

Citation:
Barrientos G, Llanos P, Hidalgo J, Bolaños P, Caputo C, Riquelme A, Sánchez G, Quest AFG and Hidalgo C (2015) Cholesterol removal from adult skeletal muscle impairs excitation–contraction coupling and aging reduces caveolin-3 and alters the expression of other triadic proteins. Front. Physiol. 6:105. doi: 10.3389/fphys.2015.00105

content and modifies the expression of other triadic proteins. We discuss the possible implications of these findings for skeletal muscle function in young and aged animals.

Keywords: transverse tubules, Ca^{2+} transients, RyR1, Cav1.1, GAPDH, NADPH oxidase, Na^+/K^+-ATPase

Introduction

In skeletal muscle, action potentials propagate into the fiber interior through the transverse tubule (T-tubule) system, an intracellular membrane network composed of narrow tubules around 40–85 nm in diameter that originate from deep invaginations of the surface plasma membrane (Melzer et al., 1995; Jayasinghe and Launikonis, 2013). The T-tubule network contains Cav1.1 voltage-dependent Ca^{2+} channels (Anderson et al., 1994)—also known as dihydropyridine receptors (DHPR)—which play a crucial role in skeletal muscle excitation–contraction (E–C) coupling. Skeletal muscle T-tubules form arrangements called triads with the two adjacent terminal cisternae of the sarcoplasmic reticulum (SR) (Franzini-Armstrong, 1972). At the triads, the T-tubule Cav1.1 channels physically interact with the type-1 ryanodine receptor (RyR1), Ca^{2+} release channels present in junctional SR (Marks et al., 1989; Zalk et al., 2007). Muscle depolarization triggers voltage-dependent Cav1.1 conformational changes (Rios et al., 1993; Minarovic and Meszaros, 1998) that elicit RyR1-mediated Ca^{2+} release (Anderson and Meissner, 1995; Fill and Copello, 2002); the ensuing increase in myoplasmic Ca^{2+} concentration ($[Ca^{2+}]$) triggers muscle contraction.

Reports regarding T-tubule lipid composition from vertebrate muscles have revealed some unusual features, characterized by high cholesterol and sphingolipid contents (Lau et al., 1979; Rosemblatt et al., 1981; Hidalgo et al., 1986), which endow T-tubule membranes with an unusually rigid lipid environment similar to that present in thermophilic bacteria (Hidalgo, 1985). The high cholesterol and sphingolipid levels of T-tubule membranes, which are significantly higher than those present in plasma membranes, are comparable to those reported in lipids rafts and caveolae (Smart et al., 1999). Previous studies indicate that treatment of cultured C2C12 muscle cells with the cholesterol-binding drug Amphotericin B considerably reduces the tubular elements connected to the surface (Carozzi et al., 2000). Similarly, treatment of fetal skeletal muscle cells from mice with the cholesterol-lowering agent MβCD decreases surface-connected tubular elements and disorganizes the T-tubule system (Pouvreau et al., 2004). Previous reports indicate that cholesterol removal impairs E–C coupling in amphibian (Launikonis and Stephenson, 2001) and skeletal muscles from fetal mice (Pouvreau et al., 2004). To test the hypothesis that T-tubule cholesterol content is important for E–C coupling in adult muscle, the first aim of the present work was to examine in single skeletal muscle fibers from adult mice the effects of partial cholesterol removal with MβCD on electrically evoked Ca^{2+} transients.

Caveolins are a particular class of membrane proteins that associate directly with cholesterol in lipid rafts and constitute structural components of caveolae. The scaffolding domain of caveolin participates in protein-protein interactions and the regulation of signal transduction events (Williams and Lisanti, 2004). Striated muscle tissue expresses mainly the caveolin-3 protein isoform (Song et al., 1996); yet, few studies have addressed the role of caveolin-3 in striated muscle function. In cardiac muscle cells, caveolin-3 associates with Cav1.2 (L-type) Ca^{2+} channels (Balijepalli et al., 2006). The expression levels of caveolin-3 in skeletal muscle modulate Ca^{2+} currents through Cav1.1 L-type calcium channels and caveolin-3 mutations reduce Cav1.1 currents without altering Cav1.1 expression levels (Weiss et al., 2008), suggesting a role for caveolin-3 in the E–C coupling process. Additionally, recent studies reported direct interaction of caveolin-3 with skeletal muscle RyR1 (Whiteley et al., 2012) and suggested inhibition of mechano-sensitive cation channels by caveolin-3 (Huang et al., 2013). The precise location of caveolin-3 in skeletal muscle fibers remains contentious. Previous studies reported that caveolin-3 is present in the sarcolemma (skeletal muscle surface plasma membrane) associated with the dystrophin complex (Song et al., 1996), and that during muscle differentiation caveolin-3 associates with developing T-tubules but is absent from mature T-tubules (Parton et al., 1997). A later study in soleus muscle from adult rats, however, reported that while caveolin-3 occurs at the highest density on the plasma membrane, it is also present in T-tubules (Ralston and Ploug, 1999). Caveolin-3 knockout mice present T-tubule system abnormalities (Galbiati et al., 2001), consistent with a T-tubule location, and also exhibit muscle degeneration (Hagiwara et al., 2000). A more recent study reported the presence of caveolin-3 in isolated SR vesicles (Li et al., 2006), albeit the low cholesterol content of these membranes (Lau et al., 1979; Rosemblatt et al., 1981) makes this location unlikely. Hence, to test the hypothesis that in adult muscle fibers caveolin-3 is present in the T-tubules, the second aim of this work was to study caveolin-3 location in adult mammalian skeletal muscle.

Aging entails significant deterioration of skeletal muscle function (Miller et al., 2014). Among other changes, a decreased intracellular Ca^{2+} peak associates with the reduction in muscle force observed during aging (Booth et al., 1994; Wang et al., 2000). Age-related changes in T-tubule protein and lipid composition might contribute to the observed defects in skeletal muscle function. In fact, previous work suggested that aged rats have uncoupled Cav1.1-RyR1 channels (Renganathan et al., 1997) and display a 60% reduction in Cav1.1 protein levels (O'connell et al., 2008). No information is available, however, on changes in T-tubule cholesterol and caveolin-3 levels during aging. Therefore, to test the hypothesis that aging brings about

Abbreviations: Cav1.1, Voltage-dependent Ca^{2+} channels; Ca^{2+}, Calcium; DHPR, Dihydropyridine receptor; DRM, Detergent resistant membranes; E–C coupling, excitation–contraction coupling; FDB, Flexor digitorium brevis; GAPDH, Glyceraldehyde 3-phosphate dehydrogenase; HRS, Heavy sarcoplasmic reticulum; LSR, Light reticulum; MβCD, Methyl-β-cyclodextrin; NOX, NADPH-oxidase; RyR1, Type-1 ryanodine receptor; SR, Sarcoplasmic reticulum; T-tubules, Transverse tubules.

changes in transverse tubule components, which might contribute to aged-related defective skeletal muscle function, the third aim of the present study was to investigate if aging modifies T-tubule cholesterol levels and to compare, in addition, the levels of key triadic proteins including caveolin-3 in young and aged rats. For this purpose, we used triad-enriched membrane fractions obtained from adult skeletal muscle that contain ∼10% attached T-tubules (Hidalgo et al., 1993), and which after isolation maintain the morphological features found in intact muscle (Wagenknecht et al., 2002). In particular, we investigated if caveolin-3 levels change in aged animals since alterations in the levels of this scaffolding protein may result in ion channel dysregulation, among other effects.

Our results show that partial cholesterol extraction from isolated single skeletal fibers impaired E–C coupling and altered Cav1.1 and caveolin-3 distribution. We also found caveolin-3 in T-tubules and T-tubule-containing triad fractions but not in SR membranes, and in cholesterol-enriched detergent-resistant membrane (DRM) fractions from T-tubules or triads. We observed significantly decreased caveolin-3 and glyceraldehyde 3-phosphate dehydrogenase (GAPDH) and increased Na^+/K^+-ATPase levels in triads from aged rats, but we did not detect changes in cholesterol and RyR1 protein levels. We discuss the possible implications of these findings for skeletal muscle E–C coupling in young and aged animals.

Materials and Methods

Animals

Male New Zealand white rabbits (6-month-old), Balb/C mice (8-week-old) and Sprague Dawley rats (3 or 24 months-old) were obtained from the Animal Facility at the Faculty of Medicine, Universidad de Chile. Room temperature was kept constant at 21°C, and light was maintained on a 12:12 h light-dark cycle. Mice were sacrificed by quick cervical dislocation. Rabbits and rats were euthanized by intraperitoneal overdose of sodium pentobarbital (100 mg/kg). All experiments were carried out following the guidelines provided by National Institutes of Health (USA) and the regulations for the Care and Use of Animals for Scientific Purposes; the Bioethics Committee of the Faculty of Medicine, Universidad de Chile approved all animal procedures performed in this work.

Materials

All reagents used were of analytical grade. Protease inhibitors (leupeptin, pepstatin A, benzamidine, and phenylmethylsulfonyl fluoride) were from Sigma-Aldrich (St. Louis, MO), MagFluo-4 AM and Fluo-4 AM were from Invitrogen (Carlsbad, CA), and Matrigel was from BD Biosciences (San Jose, CA). Paraformaldehyde was from Electron Microscopy Science (Hatfield, PA), Dulbecco's modified Eagle's medium supplemented with 10% fetal bovine serum was from Invitrogen (Carlsbad, CA) and was supplemented with 0.1 mg/ml penicillin–streptomycin from Sigma-Aldrich (St. Louis, MO). The BCA protein assay kit was from Pierce Biotechnology, Inc. (Rockford, IL), commercial BSA was from Sigma-Aldrich (St. Louis, MO) and Dako anti-fading reagent was from Dako (Denmark). Horseradish peroxidase-conjugated anti-IgG (anti-mouse or anti-rabbit) were from Santa Cruz Biotechnology, Inc. (Santa Cruz, CA). Antibodies against the α1s subunit of Cav1.1 were from Affinity BioReagents (Golden, CO; mouse monoclonal) or from Santa Cruz Biotechnology, Inc. (Santa Cruz, CA; rabbit polyclonal). Alexa Fluor-488 anti-mouse and Alexa Fluor-633 anti-rabbit antibodies were from Invitrogen (Carlsbad, CA). Caveolin-3 antibodies were from BD Biosciences (San Jose, CA) or Santa Cruz Biotechnology (Santa Cruz, CA), $gp91^{phox}$ and $p47^{phox}$ antibodies were from Santa Cruz Biotechnology (Santa Cruz, CA), GAPDH antibody was from Sigma-Aldrich (St. Louis, MO), RyR1 (34C) and Na^+/K^+-ATPase (α6F) antibodies were from Developmental Studies Hybridoma Bank http://dshb.biology.uiowa.edu/. The Amplex Red Cholesterol Assay kit was from Invitrogen (Carlsbad, CA), the total cholesterol assay kit was from Labtest (Sao Paulo, Brazil) and the ECL kit was from Thermo Fisher Scientific Inc. (Rockford, IL).

Fiber Isolation from Adult Skeletal Muscle

Flexor digitorum brevis (FDB) muscles were dissected from 8 week-old mice and single intact myofibers were isolated enzymatically as described (Carroll et al., 1995; Barrientos et al., 2009). Isolated fibers were plated on Matrigel-coated coverslips and maintained in Dulbecco's modified Eagle's medium supplemented with 10% fetal bovine serum and 0.1 mg/ml penicillin–streptomycin. Fibers were kept overnight in an incubator under 5% CO_2, and experiments were conducted within 12–24 h of plating.

Immunofluorescence

Dissociated single fibers from adult mice FDB muscles were plated on 35 mm coverslips coated with Matrigel. After washing with PBS, fibers were fixed by incubation for 10 min at room temperature with PBS supplemented with 4% paraformaldehyde. Next, fibers were rinsed with PBS, permeabilized with 0.1% TritonX-100 in PBS, rinsed with PBS and blocked for 1 h with PBS-1% BSA at room temperature. Fibers were incubated overnight with polyclonal rabbit antibodies against caveolin-3 (1:100, Santa Cruz Biotechnology; Santa Cruz, CA,) and Cav1.1 (1:100). Fibers were washed and incubated 1 h with Alexa Fluor-488 anti-mouse and Alexa Fluor-633 anti-rabbit antibodies. Samples treated with Dako anti-fading reagent were stored at 4°C until use.

Fluorescence Recording and Field Stimulation

All records were collected from single fibers bathed in mammalian Ringer solution (mM: 145 NaCl, 2.5 KCl, 1.0 $MgSO_4$, 2.5 $CaCl_2$, 10 glucose, 10 Hepes/Tris, pH 7.4). Fibers were incubated for 40 min at room temperature with 10 μM MagFluo-4 AM in mammalian Ringer solution containing 0.01% pluronic acid. Alternatively, fibers were loaded at room temperature for 40 min in mammalian Ringer plus 0.01% pluronic acid with the higher affinity Ca^{2+} dye Fluo-4 AM (10 μM). Fibers adhering spontaneously to the glass bottom of the experimental chamber were selected for fluorescence recording. The experimental chamber was mounted on the stage of an inverted Nikon Diaphot

TMD microscope equipped for epifluorescence. Fibers were illuminated with a xenon lamp (100 W) only during recording to avoid dye photobleaching. The characteristic wavelengths of filter combinations (excitation/dichroic/barrier) were (nm) 450–490/510/520. Light signals were collected from a spot of approximately 12 μm diameter, with a photomultiplier connected to a Nikon P1 amplifier. This procedure allowed recording from several fibers within the microscope field (Calderon et al., 2011).

Field stimulation leading to intracellular Ca^{2+} transients was elicited by applying supra-threshold rectangular current pulses (0.2–0.4 ms duration) through two platinum plate electrodes placed on either side along the experimental chamber. The amplifier output was connected to an Axon Instruments TL1 DMA interface. Data were acquired and analyzed using the Axon Instruments pCLAMP 6 software. Fluorescence values are expressed as $\Delta F/F_{rest}[(F - F_{rest})/F_{rest}]$, where F_{rest} correspond to the basal fluorescence recorded before stimulation (Capote et al., 2005).

Membrane Fractions

Triad-enriched fractions (hereafter referred to as triads) containing on average 10% attached T-tubules were isolated from rabbit or rat muscle as described previously (Hidalgo et al., 1993). T-tubule membranes, heavy sarcoplasmic reticulum (HRS) and light reticulum (LSR) from skeletal muscle were isolated as previously described (Rosemblatt et al., 1981), with some modifications. Briefly, 100 g of back muscles from rabbit or 15 g from the back and hind limb skeletal muscles from male rats were homogenized in four volumes of buffer A (mM: 100 KCl. 20 MOPS-Tris, pH 7.0). The suspension was centrifuged at 10,000 × g and the sediment was homogenized in buffer A, adjusted to 0.6 M KCl by solid salt addition and centrifuged for 1 h at 100,000 × g. The pellets were resuspended in buffer A containing a combination of protease inhibitors (1 μg/ml leupeptin, 1 μg/ml pepstatin, 0.4 mM benzamidine 1 mM phenylmethanesulfonylfluoride), and sedimented at 100,000 × g. The pellets were resuspended in sucrose buffer (buffer B; mM: 300 sucrose, 20 MOPS-Tris, pH 7.0, plus 1 μg/ml leupeptin, 1 μg/ml pepstatin, 0.4 mM benzamidine) and centrifuged at 100,000 × g. The resulting pellets were resuspended in buffer B, loaded on a discontinuous sucrose gradient (45, 35, 27.5, and 25% w/v) and centrifuged at 100,000 × g overnight. T-tubules were collected from the 25/27.5% interface. The HSR and LSR fractions were collected from the 35/45 and the 27.5/35% interfaces, respectively. Fractions were resuspended in buffer B, centrifuged for 30 min at 100,000 × g and the pellets were resuspended in a minimum volume of buffer B, frozen in liquid N_2 and stored at −80°C until use.

Junctional T-tubule fractions were prepared from triads as described (Horgan and Kuypers, 1987). Briefly, the triad fraction was loaded on top of an ion-free sucrose gradient (1.4–0.74 M) and centrifuged 16 h at 100,000 × g. This treatment separates the junctional T-tubule membranes from the triads and yields a light fraction containing junctional T-tubules. This fraction was collected, diluted in 20 mM MOPS/Tris, pH 7.2 supplemented with 1 μg/ml leupeptin, 1 μg/ml pepstatin, 0.4 mM benzamidine, and centrifuged for 1 h at 100,000 × g. The pellet, resuspended in a small volume of buffer B containing 1 μg/ml leupeptin, 1 μg/ml pepstatin, was stored at −80°C until use.

Detergent-resistant Membrane (DRM) Fractions

DRM fractions were prepared from triads and T-tubule membranes as described (Brown and Waneck, 1992; Sargiacomo et al., 1993) with minor modifications. Briefly, membrane fractions were resuspended and mixed in 2 ml (final volume) of Mes buffer saline (MBS, in mM: 150 NaCl, 25 Mes/NaOH, pH 6.5) containing 1% Triton X-100 and protease inhibitors (1 μg/ml leupeptin, 1 μg/ml pepstatin, 1 mM phenylmethanesulfonylfluoride, 0.4 mM benzamidine) and incubated for 15 min at 4°C. The suspensions, adjusted to 40% (w/v) sucrose by adding 2 ml of ice-cold 80% sucrose (w/v) in MBS, were placed at the bottom of an ultracentrifuge tube: two equal volume layers of 30 and 5% sucrose were added on top, and the gradients were centrifuged at 100,000 × g for 20 h. The light opalescent band confined to the 5–30% interface was collected, diluted three times with MBS and centrifuged at 100,000 × g for 1 h. The fractions thus obtained were resuspended in buffer B, frozen in liquid nitrogen and stored at −80°C until use.

SDS/PAGE and Western Blot Analysis

Membrane preparations were heat-denatured in SDS-containing sample buffer with reducing agents and loaded onto Tris-glycine 4–12% acrylamide gradient SDS-containing gels. Following electrophoresis at 100 V, proteins were transferred to nitrocellulose membranes at 100 V for 1 h. Membranes, blocked with 5% non-fat dry milk in Tris-saline buffer (mM: 140 NaCl, 20 Tris-HCl, pH 7.6) plus 0.2% Tween 20 were probed with specific antibodies directed against T-tubule or SR proteins. Horseradish peroxidase-conjugated anti-mouse or anti-rabbit IgG were used as secondary antibodies. Immunoblots were developed using an ECL kit and automated image capture was performed with the ChemiDoc system (Bio-Rad, Hercules, CA). All blot quantifications involved measuring band intensities; the amount of protein loaded in each lane was checked by Coomassie blue staining.

Other Procedures

NOX activity was determined as described previously (Sanchez et al., 2008). Protein concentration was determined by the BCA protein assay using commercial BSA as a standard. Cholesterol content was determined using the colorimetric total cholesterol kit or the fluorescence Amplex Red Cholesterol Assay kit, as detailed in the text. Electron microscopy (EM) analysis of DRM fractions was performed as described (Badizadegan et al., 2000).

Statistical Analysis

To detect significant differences between two groups, statistical analysis of data, presented as Mean ± SE, was determined with the Student's *t*-test (two-tailed); a value of $p < 0.05$ was considered statistically significant.

Results

Membrane Cholesterol Reduction Impairs Skeletal Muscle E–C Coupling

To study whether decreasing the high T-tubule cholesterol levels affects the E–C coupling process, we measured electrically induced Ca^{2+} transients in FDB fibers from adult mice before and after addition of the cholesterol-lowering agent MβCD. The

representative experiment illustrated in **Figure 1A** shows Ca^{2+} transients recorded in fibers loaded with the low-affinity Ca^{2+} probe MagFluo-4 before or 5, 20, and 25 min after perfusion with 1% MβCD, which abolished Ca^{2+} transients after 25 min. This treatment impaired Ca^{2+} transients in all fibers tested, isolated from six different animals. Of note, MβCD abolished Ca^{2+} transients in 26 of the 30 fibers tested and in the remaining 4 fibers it significantly reduced Ca^{2+} transient amplitude by 51.3 ± 27.6 (%).

To assay whether MβCD treatment modified resting myoplasmic free $[Ca^{2+}]$, which did not display apparent changes in fibers loaded with the low affinity Ca^{2+} probe MagFluo-4 (**Figure 1A**), we loaded fibers with Fluo-4, a high affinity fluorescent Ca^{2+} probe, and determined Ca^{2+} transients elicited by electrical field stimulation. The representative experiment illustrated in **Figure 1B** shows that initial stimulation at 20 Hz elicited significant Ca^{2+} transients in two fibers recorded in parallel. After perfusion with 1% MβCD, both fibers displayed for about 8 min Ca^{2+} transients of similar magnitudes in response to stimulation at 0.1 Hz, after which time the response declined abruptly and vanished within 2 min (**Figure 1B**). The same results were obtained in 26 fibers from five different mice treated with MβCD. In contrast, and in agreement with previous findings (Barrientos et al., 2009), control fibers (18 fibers from 5 mice) loaded with Fluo-4 AM in mammalian Ringer solution containing 0.01% pluronic acid, responded with Ca^{2+} transients of equal magnitude for at least 30 min when stimulated at 0.1 Hz (not shown).

Perfusion with 1% MβCD produced an increase in resting fluorescence coincident with the decline in Ca^{2+} transient amplitude, as evidenced from the parallel records from two fibers illustrated in **Figure 1B**; the Fluo-4 fluorescence increase reached a plateau 9–11 min after MβCD addition. Average fluorescence values recorded 20 min after MβCD addition showed a small but significant baseline fluorescence increase in MβCD-treated fibers ($n = 25$) relative to the controls ($n = 17$) (**Figure 1C**). This increase was observed at levels far from probe saturation, as indicated by the considerably higher fluorescence increase produced by the initial stimulation at 20 Hz. From this higher value and the K_d (345 μM) for Fluo-4, we estimate that the net increase in resting $[Ca^{2+}]$ was < 100 nM. Perfusion with 10 mM caffeine after MβCD removal, when resting $[Ca^{2+}]$ reached a plateau, produced a transient and significant increase in fluorescence (**Figure 1B**). The caffeine-stimulated fluorescence increase was observed in a large fraction (23/26) of MβCD-treated fibers and in all (18/18) control fibers.

These combined results indicate that perfusion with 1% MβCD, which decreases cholesterol levels by 26% in FDB fibers from adult muscle (**Table 1**), abolishes electrically evoked Ca^{2+} transients without significantly perturbing the membrane permeability barrier, as indicated by the lack of massive increase in myoplasmic $[Ca^{2+}]$. Additionally, the stimulatory effects of caffeine strongly suggest that the lack of response to electrical stimulation in MβCD-treated fibers is not due to SR depletion and presumably reflects impaired E–C coupling.

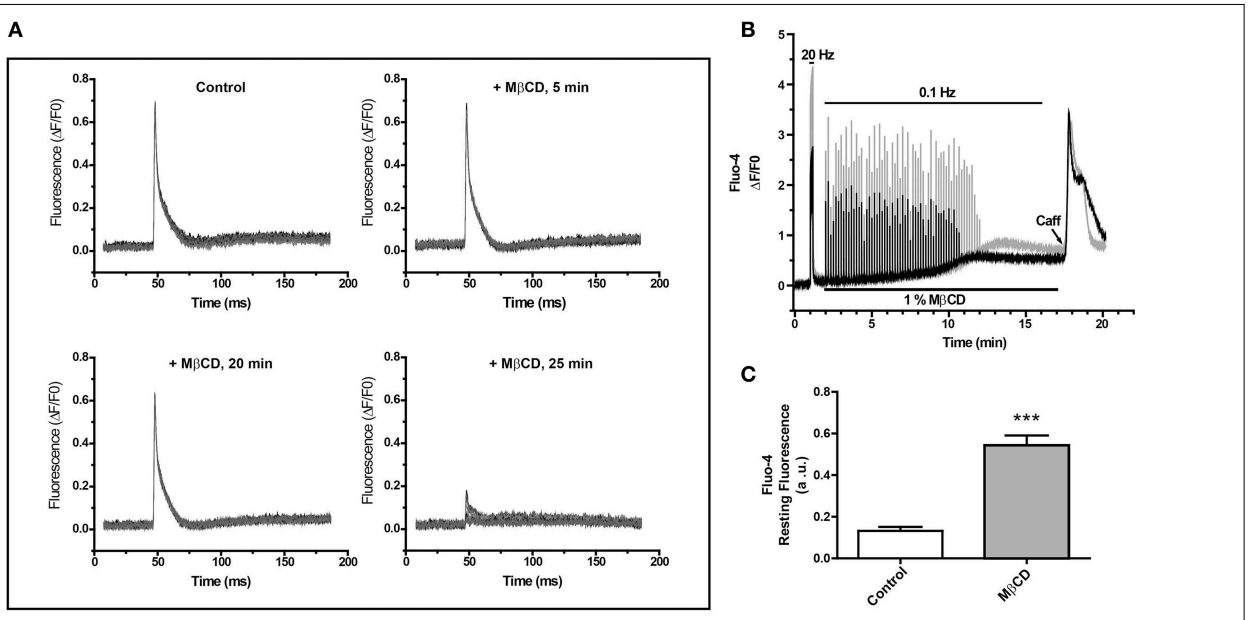

FIGURE 1 | Perfusion of single fibers from adult skeletal muscle with MβCD abolishes calcium transients and increases resting calcium levels. (A) FDB fibers were loaded with the low affinity Ca^{2+} sensor Mag-Fluo-4 and Ca^{2+} transients were elicited by electrical field stimulation. Fluorescence was evaluated before and after the addition of 1% MβCD. Each panel shows 10 transients, collected at 10 s intervals at the times indicated in the figure. **(B)** Ca^{2+} transients were elicited by electric field stimulation of FDB fibers loaded with Fluo-4, a high affinity Ca^{2+} probe. The traces show the fluorescence of two fibers and their responses to field stimulation at 20 or 0.1 Hz. The continuous line at the top represents the period of electric field stimulation, the lower continuous line indicates the period of perfusion with MβCD. The arrowhead indicates addition of 10 mM caffeine. **(C)** Average Fluo-4 resting fluorescence collected 20 min after initiation fluorescence recording in control ($n = 17$) or MβCD-treated ($n = 25$) fibers.

TABLE 1 | Cholesterol content in mice skeletal fibers and membrane fractions.

Assayed sample	Cholesterol (μg/mg protein)
SKELETAL FDB FIBERS	
A. Control	17.6 ± 1.2 (4)
B. MβCD-treated	13.1 ± 1.4 (4)
MEMBRANE FRACTIONS	
C. T-tubules (rabbit)	271.6 ± 14.8 (3)
D. DRM from T-tubules (rabbit)	1233.0 ± 69.55 (4)
Ratio D/C	4.5
E. Triads (rabbit)	41.5 ± 2.3 (4)
F. DRM from Triads (rabbit)	184.3 ± 4.9 (4)
Ratio F/E	4.4
G. Plasma membrane (Ortegren et al., 2004)	143
H. Caveolae (Ortegren et al., 2004)	400.5 ± 21
Ratio H/G	2.8

Total cholesterol content was measured, with the exception of the DRM fractions, with a commercial colorimetric kit; cholesterol content of DRM fractions was determined with the Amplex Red kit (for details see Materials and Methods). FDB cholesterol content was measured in sonicated whole fiber homogenates. Data represent Mean ± SE; the number of different preparation assayed is given in parenthesis.

Caveolin-3 Associates with T-tubule and Triad Membranes and is Absent from SR Fractions

Previous reports suggest a role for caveolin-3 in skeletal muscle E–C coupling (Weiss et al., 2008; Whiteley et al., 2012), which, as reported here, is sensitive to cholesterol removal from adult fibers. The caveolin proteins bind directly to cholesterol (Murata et al., 1995) and their presence in membranes correlates directly with membrane cholesterol levels (Toselli et al., 2005); however, the location of caveolin-3 in T-tubule membranes remains debatable. Accordingly, we tested here the location of caveolin-3 by immunohistochemistry of adult fibers from mice and by Western blot analysis of membrane fractions isolated from rabbit or rat skeletal muscle.

As illustrated in **Figure 2A**, caveolin-3 co-localizes with Cav1.1 in FDB fibers from adult mice skeletal muscle. Treatment of with 1% MβCD, which reduced cholesterol content by 26% (**Table 1**), produced a significant change in the distribution of both Cav1.1 (**Figure 2B**) and caveolin-3 (**Figure 2C**). After MβCD treatment, both proteins exhibited a decrease in the characteristic banding pattern displayed by control fibers, suggesting that partial reduction of fiber cholesterol content alters the typical array of Cav1.1 in the T-tubule membrane (**Figure 2B**) and reduces the association of caveolin-3 with T-tubules (**Figure 2C**). Similar results were obtained in 3–9 fiber preparations from each mouse, out of a total of four mice.

The representative Western blot illustrated in **Figure 3A** shows that caveolin-3 is present in T-tubules (lanes 1–2) and triads (lanes 5–6) isolated from rabbit skeletal muscle, but is absent from the LSR (lane 3) and HSR (lane 4) fractions, which are highly enriched in Ca^{2+}-ATPase and RyR1/calsequestrin, respectively (not shown). We obtained similar results in 3 independent preparations. The separate blots shown in **Figure 3B** confirm that T-tubule and triad fractions contain Cav1.1. These findings show unambiguously that caveolin-3 is present in T-tubules and T-tubule-containing triads but is absent from SR membranes. To further assay the specific association of caveolin-3 with T-tubule membranes, we dissociated triads isolated from rabbit muscle to generate a light fraction enriched in junctional T-tubule membranes (Horgan and Kuypers, 1987). The representative whole gel (stained with Coomassie blue) illustrated in **Figure 3C** (left) shows that the protein profile of T-tubules isolated from whole rabbit skeletal muscle (lane 1) is very similar to that of the junctional T-tubule fraction obtained from dissociated triads (lane 2). The respective Western blots shown at right in **Figure 3C** also indicate that both T-tubule fractions contain comparable caveolin-3 and Cav1.1 protein levels. Similar results were obtained in two different preparations. We also found caveolin-3 in triads from rat (**Figure 3D**, lane 2) that at equal protein loads migrated slightly faster but displayed similar band density as the caveolin-3 band present in triads from rabbit skeletal muscle (**Figure 3D**, lane 1). Junctional T-tubules isolated from rat triads also contained significant levels of caveolin-3 (data not shown).

Detergent Resistant Membranes (DRM) from Skeletal Muscle Contain High Cholesterol Levels, Caveolin-3 and Cav1.1

Incubation of T-tubules or triads with 1% Triton [X-100] (for details, see Experimental Procedures) yielded a light DRM fraction at the 5/30% sucrose interface. This fraction was visible to the naked eye, as illustrated in **Figure 4A** for the DRM fraction isolated from rabbit T-tubules; the representative electron micrograph of the DRM isolated from triads (rabbit) illustrated in **Figure 4B** revealed the presence of unilamellar vesicles (arrowheads) associated with electron-dense material.

DRM fractions isolated from triads migrated at a higher sucrose density (25–28% sucrose, w/v) than DRM fractions from T-tubules (16–18% sucrose, w/v). Both fractions had higher cholesterol contents than the corresponding initial fractions, albeit DRM fractions from triads had lower cholesterol levels than DRM fractions from T-tubules (**Table 1**). For comparison, the isolated caveolae and plasma membrane cholesterol levels (400 and 143 μg/mg protein, respectively) reported in the literature (Ortegren et al., 2004) yield a caveolae/plasma membrane cholesterol ratio of 2.8. Our results yield almost two-fold higher values for the ratios between the cholesterol contents of DRM from T-tubules or triads relative to the original membranes (**Table 1**). Immunoblot analysis (**Figure 4C**) revealed a significant enrichment in caveolin-3 in DRM fractions from triads (rabbit, lane 1; rat, lane 2) when compared to the original triad fractions (rat, lane 4; rabbit, lane 5) or to the junctional T-tubule membranes from rabbit (lane 3). As illustrated in **Figure 4D**, DRM fractions from triads (lanes 1–2) or T-tubules (lanes 3–4) also contained significant levels of the Cav1.1 protein.

To further test the association of caveolin-3 with cholesterol, we treated T-tubules or triads from rabbit with increasing concentrations of MβCD, centrifuged the fractions at 100,000 × g for 5 min and determined cholesterol and caveolin-3 protein contents in the resulting pellets and supernatants, respectively. As illustrated in **Figure 4E**, treatment with MβCD produced a

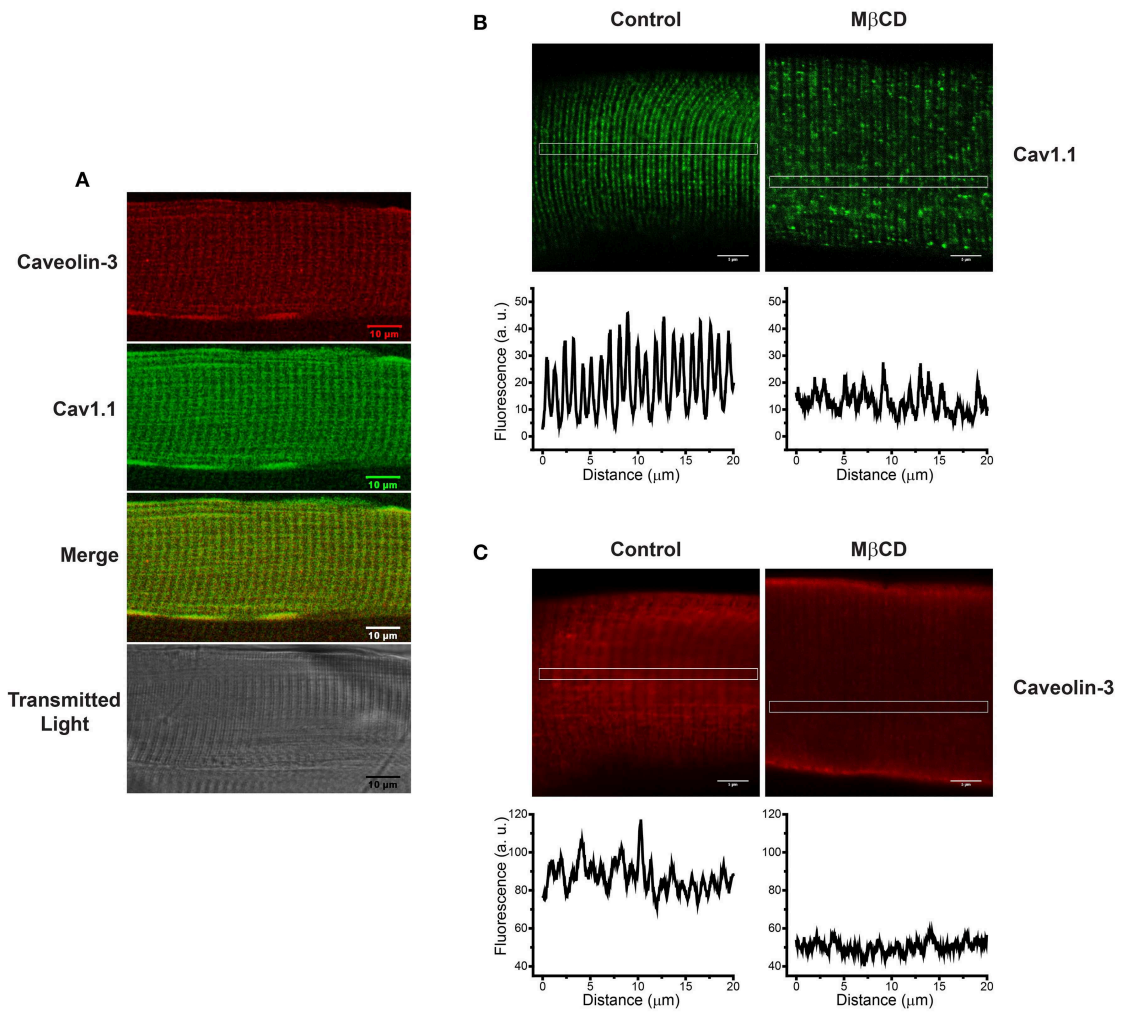

FIGURE 2 | Caveolin-3 is associated to T-tubules membranes in intact FDB fibers from adult skeletal muscle; treatment with MβCD alters the distribution of Cav1.1 and caveolin-3. (A) Immunohistochemistry of a single FDB fiber isolated from skeletal muscle of adult mice. The top panel shows caveolin-3 in red, the central panel shows Cav1.1 in green, the panel with the merged image shows the superposition of both fluorescence signals, and the lower panel shows the transmitted light image. **(B)** Distribution of Cav1.1 (green) in control (left panel) and fibers treated with 1% MβCD (right panel). The graphs under each image illustrate the horizontal fluorescence profiles collected from the rectangular region of interest (ROI) indicated in the images. **(C)** Distribution of caveolin-3 (red) in control (left panel) and MβCD-treated fibers (right panel). The graphs under each image illustrate the horizontal fluorescence profiles collected from the rectangular ROI indicated in each image. Scale bar: 5 μm.

concentration-dependent decrease in the cholesterol content of pellets from T-tubules (open circles) and triads (open squares). Analysis of caveolin-3 content in the respective supernatants of MβCD-treated fractions (**Figure 4F**) revealed that the soluble fractions from T-tubules contained caveolin-3 (lanes 1–4) whereas, the soluble fractions from triads lacked this protein (lanes 5–8).

Triads from Aged Rats Contain Decreased Protein Levels of Caveolin-3 and GAPDH

The representative Western blot illustrated in **Figure 5A** shows that triads from aged rats (24-month-old) contain significantly lower caveolin-3 protein contents than triads from young (3-month-old) rats. Likewise, triads from aged rats contain lower GAPDH levels (**Figure 5B**). Results from 6 aged and 6 young rats indicate both reductions are statistically significant (**Figures 5A,B**).

Triads from Aged Rats Contain Increased Na^+/K^+-ATPase α1 Subunit Protein Levels

The representative Western blot illustrated in **Figure 5C** indicates that triads from aged rats contain significant higher Na^+/K^+-ATPase α1 subunit levels than triads from young rats. Results from 6 aged and 6 young rats indicate that these differences are statistically significant (**Figure 5C**).

Triad RyR1 Protein Levels and Cholesterol Content Do Not Change with Age

Triads from young or aged rats contained comparable RyR1 protein levels, as shown in the representative Western blot

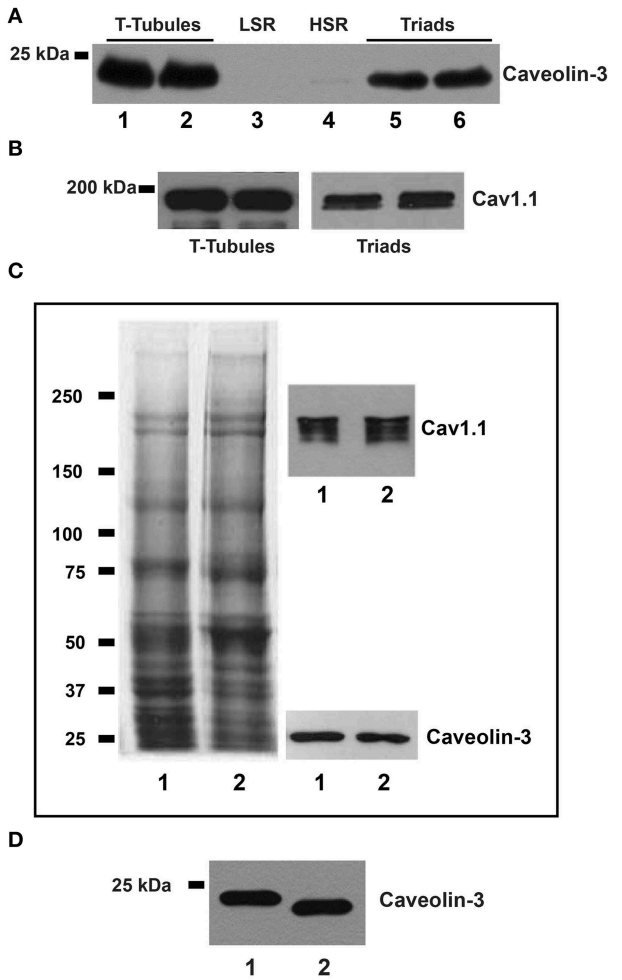

FIGURE 3 | Caveolin-3 is associated to T-tubules and triad fractions from adult skeletal muscle. (A) The representative upper blot shows membrane fractions from rabbit skeletal muscle, resolved by SDS/PAGE, transferred and tested with caveolin-3 or Cav1.1 antibodies. Each lane was loaded with 20 μg of protein. T-tubules, lanes 1 and 2; LSR, lane 3; HSR, lane 4; triads, lanes 5 and 6. **(B)** Separate blot showing that T-tubule and triad fractions contain Cav1.1. **(C)** The left panel shows a Coomassie blue stained gel; lane 1: T-tubules (20 μg), lane 2: junctional T-tubules (20 μg). The right panel shows the corresponding Western blots for caveolin-3 and Cav1.1, in the same samples loaded on the left panel. **(D)** Western blot of triad fractions; each lane was loaded with 20 μg of protein. Lane 1: triads from rabbit; lane 2: triads from rat.

illustrated in **Figure 5D** and by the average results from 6 young and 6 aged animals summarized in the graph shown in **Figure 5D**. We obtained inconclusive results regarding Cav1.1 protein levels. Triad fractions from four aged rats displayed similar Cav1.1 protein contents as young rats, but triads from two aged rats had significantly higher Cav1.1 protein levels. All six triad fractions assayed had comparable RyR1 and cholesterol contents (see below), presumably ruling out significant differences in T-tubule content among these fractions.

Triads from aged rats contain on average 51.3 ± 2.6 μg cholesterol/mg protein ($n = 6$; Mean ± SE); these values are not significantly different from the levels determined in triads from young rats: 53.2 ± 3.5 μg cholesterol/mg protein ($n = 6$; Mean ± SE).

Determination of NOX Subunits ($gp91^{phox}$ and $p47^{phox}$) Protein Contents and NOX Activity in Young and Aged Rats

As illustrated by the representative Western blot and the graph illustrated in **Figure 6A**, $gp91^{phox}$ protein levels did not change with age. The same observation applies to $p47^{phox}$ protein levels (**Figure 6B**); in this case, we observed a tendency toward a decrease with age, which was not statistically significant. In concordance with the lack of change of both $gp91^{phox}$ and $p47^{phox}$ protein levels, we found similar NOX activities in triads from young and aged rats (**Figure 6C**).

To summarize, the above results show that aging decreased caveolin-3 and GAPDH protein levels, increased the levels of the Na^+/K^+-ATPase protein, but did not modify either RyR1, $gp91^{phox}$ and $p47^{phox}$ protein levels or NOX activity.

Discussion

In this work, we addressed three related aspects. First, we tested the effects of the cholesterol-lowering agent MβCD on Ca^{2+} transients elicited by electrical field stimulation of skeletal fibers from adult mice, and found that MβCD reduced Ca^{2+} transients without disrupting fiber membrane integrity or emptying the SR of its Ca^{2+} content. Second, using several experimental strategies we determined unambiguously that caveolin-3, a cholesterol-associated protein, is present in T-tubules but not in HSR and LSR vesicles. Additionally, we found that treatment with MβCD altered the distribution of both Cav1.1 and caveolin-3 in FDB fibers from adult mice. Third, we found decreased caveolin-3 and GAPDH and increased Na^+/K^+-ATPase α1 subunit protein contents in triad fractions from aged rats, with no apparent age-related changes in cholesterol levels or RyR1, $gp91^{phox}$ and p47phox protein contents. We subsequently discuss the possible implications of these findings for skeletal muscle function in young and aged animals.

Treatment with MβCD Suppresses Depolarization-induced Ca^{2+} Transients

As reported previously, single skeletal muscle fibers from fetal mice treated with MβCD display defective E–C coupling but retain normal voltage dependence and exhibit similar action potentials as control fibers (Pouvreau et al., 2004). Our results in FDB fibers from adult mice indicate that MβCD partially removed cholesterol from these fibers, in agreement with our previous report (Llanos et al., 2015), suppressed Ca^{2+} transients in most fibers or significantly reduced their amplitude, and altered the distribution of both caveolin-3 and Cav1.1. Our determinations of Fluo-4 fluorescence suggest that MβCD treatment induced a moderate increase (≤2-fold) in myoplasmic resting [Ca^{2+}] and preserved caffeine-induced Ca^{2+} release. Altogether, results from previous studies combined with the

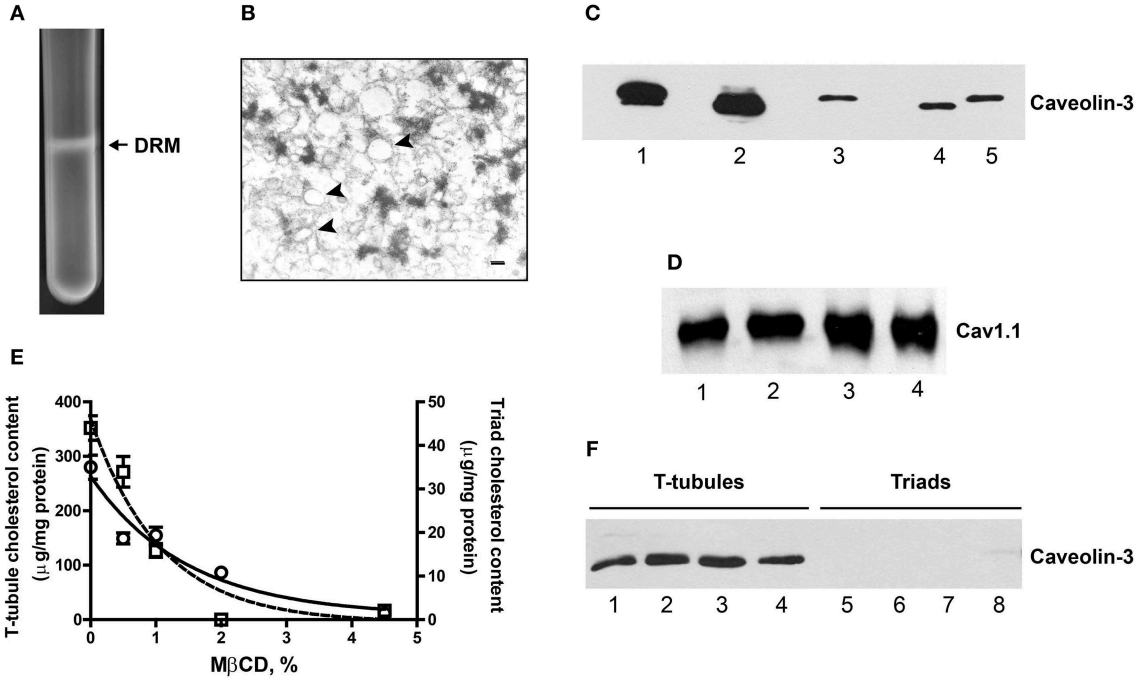

FIGURE 4 | DRM fractions from triads are enriched in caveolin-3 and contain Cav1.1. (A) Photograph of a centrifuge tube after 16 h of centrifugation of a sucrose gradient loaded with Triton X-100-treated triads, showing the appearance of an opalescent band containing the DRM fraction (for details, see the Experimental Procedures Section). **(B)** Representative EM photograph of a DRM fraction from triads. Unilamellar vesicles appear associated to electron dense material (arrows). Magnification: 150,000×; calibration bar, 20 nm. **(C)** Representative Western blot revealed with caveolin-3 antibodies. Lanes 1 and 2: 15 μg DRM isolated from triads from rabbit or rat, respectively. Lane 3: 15 μg of junctional T-tubules from triads from rabbit. Lanes 4 and 5: 20 μg, triads from rat or rabbit, respectively. Spaces between thes lanes correspond to empty lanes. **(D)** Western blot revealed with Cav1.1 antibodies. Lanes 1 and 2: 13 μg, DRM from triads from rabbit. Lanes 3 and 4: 6 μg, DRM from T-tubules from rabbit. **(E)** T-tubule and triads fractions from rabbit were treated with increasing MβCD concentrations, pelleted at 100,000 × g and the membrane cholesterol and soluble caveolin-3 were evaluated (for details, see Experimental Procedures Section). The graph shows the cholesterol content of MβCD-treated T-tubules (left y-axis) or triads (right y-axis). **(F)** Western blot showing caveolin-3 protein content in the supernatants of MβCD-treated T-tubules (lanes 1–4) or triads (lanes 5–8). Similar results were obtained in two different experiments.

present findings suggest that partial cholesterol removal affects T-tubule components, such as Cav1.1, which participate directly in the E–C coupling process. In fact, we found that MβCD treatment caused significant disarray in the regular pattern of Cav1.1 distribution. This alteration may underlie the selective and marked reduction in Cav1.1-mediated currents produced by MβCD, since a previous study indicates that membrane cholesterol removal from skeletal fibers from fetal mice specifically targets Cav1.1 channel function since T-type Ca^{2+} currents remain unaltered (Pouvreau et al., 2004). Of note, statin treatment to inhibit cholesterol synthesis (Istvan and Deisenhofer, 2001) produces T-tubule structural abnormalities in human patients (Voigt et al., 2013). A decrease in T-tubule cholesterol content may contribute to the skeletal muscle dysfunction described in patients undergoing statin therapy; in fact, as many as 25% of statin users who exercise may experience defective skeletal muscle function (Dirks and Jones, 2006). There is no information, however, regarding T-tubule cholesterol levels in these subjects. In addition, cholesterol removal may affect caveolin-3 distribution and function, in particular its role in E–C coupling, as discussed below.

Association of Caveolin-3 with T-tubules and DRM Fractions

Previous studies associated caveolin-3 with the T-tubule system only during development (Parton et al., 1997), and reported that in adult skeletal muscle caveolin-3 was exclusively present in association with the sarcolemmal membrane (Parton et al., 1997). Moreover, other studies described caveolin-3 in association with the SR membrane (Li et al., 2006). Our results in three different mammalian species—mice, rabbit and rat—show conclusively that in adult mammalian skeletal muscle this protein is associated to T-tubule and not to SR membranes, suggesting an evolutionary conserved role for caveolin-3 in T-tubule system development and preservation of structural integrity in adult muscle.

Here, we show that DRM fractions from either T-tubules or triads are highly enriched in cholesterol and caveolin-3 with respect to the original membrane fractions, and also contain Cav1.1. Our results complement previous studies showing the presence of both caveolin-3 and Cav1.2 in DRM obtained from cardiac tissue (Balijepalli et al., 2006). EM images of DRM obtained from triads revealed the presence of membrane-associated electron dense material, suggesting that in addition to

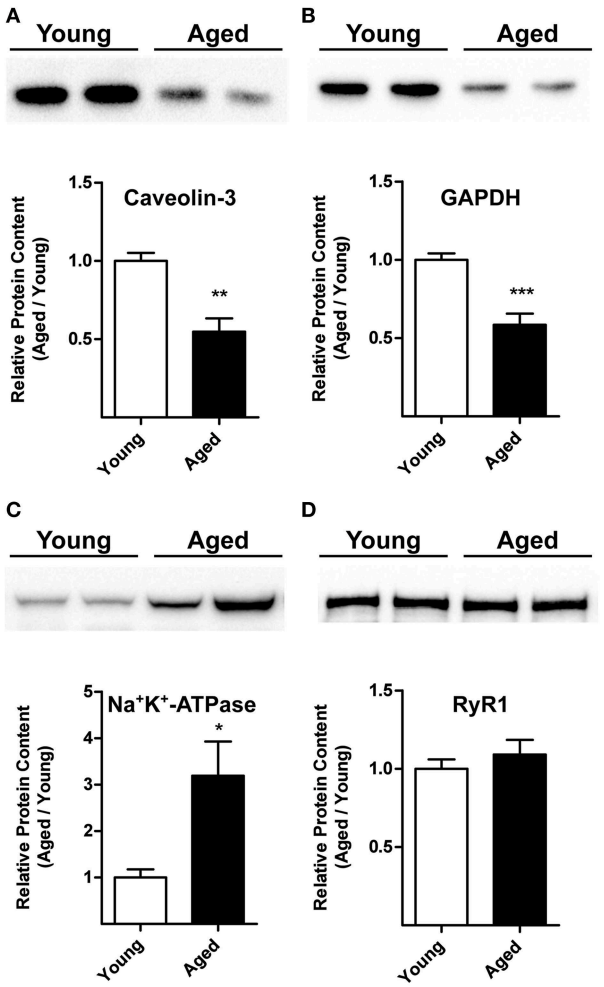

FIGURE 5 | Caveolin-3, GAPDH, Na^+/K^+-ATPase, and RyR1 protein contents in triads from young or aged rats. (A,B) The top panels illustrate representative Western blots. Each lane was loaded with 10 μg of protein assayed for caveolin-3 and GAPDH, respectively. **(C)** The top panel illustrates a representative Western blot for Na^+/K^+-ATPase; each lane was loaded with 30 μg of protein. **(D)** The top panel illustrates a representative Western blot for RyR1; each lane was loaded with 5 μg of protein. Each lane in the blots illustrated in **(A–D)** corresponds to triad fractions from different rats. The lower graphs in **(A–D)** present values (Mean ± SE) collected from triad fractions from 6 young and 6 aged rats. $^{*}p < 0.05$; $^{**}p < 0.01$; $^{***}p < 0.001$.

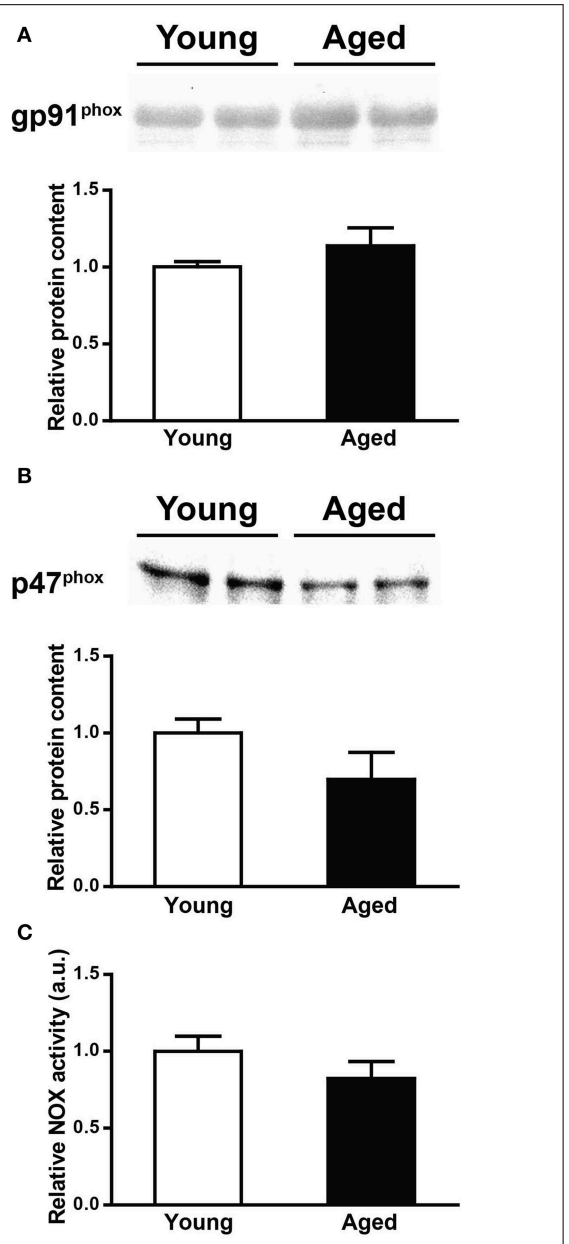

FIGURE 6 | $gp91^{phox}$ and $p47^{phox}$ protein levels and NOX activity in triads from young or aged rats. (A) The top panel illustrates a representative Western blot for $gp91^{phox}$; each lane was loaded with 40 μg of protein of triad fraction from different rats. **(B)** The top panel illustrates a representative Western blot for $p47^{phox}$; each lane was loaded with 15 μg of protein of triad fraction from different rats. The lower graphs in **(A,B)** summarize values (Mean ± SE) collected from triad fractions from 6 young and 6 aged rats. **(C)** NOX activity of triad fractions from young or aged rats; values (Mean ± SE) correspond to 6 young and 6 aged rats.

caveolin-3 and Cav1.1, other proteins of the E–C coupling complex remain associated with DRM fractions. In fact, we found that DRM fractions from triads migrated at higher sucrose densities than DRM from T-tubules, indicating higher protein to lipid ratios in the former fractions. Our results also reveal that cholesterol extraction from T-tubules and triads with MβCD produced concurrent caveolin-3 extraction to the supernatants only in isolated T-tubules. Previous work showed that caveolin-3 interacts both with Cav1.1 (Couchoux et al., 2011) and RyR1 (Whiteley et al., 2012); the persistence of this T-tubule/SR protein complex in triads may explain why removing cholesterol did not extract caveolin-3 from these fractions.

Caveolin-3 and Skeletal Muscle Function

The levels of caveolin-3 are critical for the correct functioning of skeletal muscle, because changes in the expression of this protein produce pathological phenomena (Galbiati et al., 2000; Hagiwara et al., 2000). Caveolin-3 reduction in skeletal

muscle myotubes from mice induces the opening of non-selective mechano-sensitive ion channels while caveolin-3 overexpression produces a small decrease in mechano-sensitive currents, suggesting that normal caveolin-3 expression contributes to protection of the sarcolemma from mechanical damage (Huang et al., 2013). Skeletal muscle also expresses caveolin-1 (Kawabe et al., 2001; Li et al., 2006); however, caveolin-1 does not restore completely the function of caveolin-3, since caveolin-3 knockout mice present T-tubule system abnormalities (Galbiati et al., 2001) and exhibit muscle degeneration (Hagiwara et al., 2000). Interestingly, mice null for caveolin-3 and caveolin-1 develop severe heart disease (Park et al., 2002), while caveolin-3 over expression induces a Duchenne-like phenotype in mice (Aravamudan et al., 2003). Furthermore, mice null for caveolin-3 and caveolin-1 display insulin resistance, glucose intolerance and decreased insulin-induced glucose uptake; re-expression of these proteins reverses these conditions (Capozza et al., 2005). The insulin receptor is unstable in caveolin-3 null mice; insulin binding induces its degradation suggesting that caveolin-3 stabilizes the insulin receptor (Capozza et al., 2005). Of note, caveolin-3 reduction in cardiac muscle cells produces severe alterations in cardiac function, characterized by considerable tissue degeneration, fibrosis, decreased cardiac function, and decreased activity of nitric oxide synthase (Aravamudan et al., 2003). Altogether, these reports suggest that alterations in caveolin-3 levels induce pathological conditions in skeletal and cardiac muscle.

Recent studies reported that caveolin-3 interacts with Cav1.1 (Couchoux et al., 2011) and RyR1 (Whiteley et al., 2012), suggesting that the two Ca^{2+} channels directly involved in E–C coupling establish functional links with caveolin-3. Cholesterol removal, which affects the distribution of both caveolin-3 and Cav1.1, may affect these functional connections giving rise to the defective E–C coupling responses reported in amphibian (Launikonis and Stephenson, 2001), fetal (Pouvreau et al., 2004) and adult rat skeletal muscle, where we found that partial cholesterol extraction inhibited Ca^{2+} transients. These effects are similar to the reported effects of aging on E–C coupling (Booth et al., 1994; Wang et al., 2000). Early studies indicated that rat skeletal muscle from 12-month-old rats had higher caveolin content than muscle from 3-month-old rats; however, whether this increase reflects augmented expression of caveolin-3, caveolin-1, or both was not evaluated (Munoz et al., 1996). Other early studies suggested that aging produces uncoupling between Cav1.1 and RyR1, with the consequent muscle weakness (Renganathan et al., 1997). Our results indicate that triad fractions from skeletal muscle of 24-month-old rats had 2-fold lower caveolin-3 protein levels than triads from young rats. As described above, caveolin-3 interacts with Cav1.1 and RyR1, forming a supra-molecular complex. Reduction in caveolin-3 protein levels during aging is likely to remodel or alter the integrity of this complex, causing E–C uncoupling. A decrease in caveolin-3 levels may also modify T-tubule architecture and T-tubule related signal transduction pathways, such as insulin-dependent glucose uptake.

Caveolin-3 binds directly to cholesterol (Murata et al., 1995) and sphingolipids (Haberkant et al., 2008). We found that DRM fraction from T-tubules or triads contained both caveolin-3 and Cav1.1; the possible association of these two proteins in cholesterol-enriched membrane regions supports the proposed role of caveolin-3 in regulating Cav1.1 function (Weiss et al., 2008). While we did not detect significant differences in cholesterol content between triads from young or aged rats, a marked reduction in caveolin-3 protein content during aging may affect the local cholesterol distribution in T-tubule membranes, altering the function of the caveolin-3-containing RyR1/Cav1.1 supramolecular complex, and hence E–C coupling. Accordingly, it would be of interest to investigate in future studies if restoring caveolin-3 levels in the skeletal muscle of aged animals improves their defective E–C coupling.

Changes in Other Triadic Proteins during Aging

RyR1 and Cav1.1

Our results in triads from skeletal muscle of 24-month-old rats confirm that RyR1 protein content does not change with rodent age (Russ et al., 2011). Previous reports suggest a drastic reduction of Cav1.1 and no significant change of RyR1 protein levels in total fractions from skeletal muscles of 30-month-old rats (O'connell et al., 2008). We obtained inconclusive results regarding changes in Cav1.1 protein levels with age, but we did not observe an age-related Cav1.1 reduction.

Na^+/K^+-ATPase

In rat skeletal muscle, aging causes muscle type-specific alterations in Na^+/K^+-ATPase activity and increases the expression of the enzyme α1 and β1-subunits, measured in total muscle homogenates (Sun et al., 1999). Immunohistochemistry analysis showed increased expression of the α1-subunit in white but not in red gastrocnemius muscle, which displays mainly a sarcolemmal pattern (Zhang et al., 2006). Increased expression of the Na^+/K^+-ATPase enzyme during aging, which we confirmed in triad fractions from aged muscle, may be relevant for muscle function during aging. Reduction of caveolin-3 content activates non-selective mechano-sensitive ion channels in skeletal muscle (Huang et al., 2013), whereas in cardiac muscle caveolin-3 regulates Kv1.5 potassium currents by modulating the number of functional channels in the membrane (Folco et al., 2004). Accordingly, decreased T-tubule caveolin-3 levels may result in increased Na^+ and K^+ fluxes via non-selective ion channels during aging, which if not compensated by active ion transport by the Na^+/K^+-ATPase would result in decreased excitability of skeletal muscle fibers, thereby contributing to contractile fatigue (Welle, 2002). Therefore, the increased Na^+/K^+-ATPase protein levels displayed by triads from aged rat muscle may reflect an adaptation mechanism to compensate for the increment of ionic T-tubule membrane permeability induced by the low caveolin-3 levels observed in aged muscle.

GAPDH

In addition to decreased caveolin-3 content, triads from aged rats displayed significant reductions in GAPDH protein content. Our results agree with previous reports showing that aged skeletal muscles display decreased levels of GAPDH mRNA

(Touchberry et al., 2006) and protein (Vigelso et al., 2015). In skeletal muscle, GAPDH binds to RyR1, Cav1.1 and the T-tubule membrane (Brandt et al., 1990), forming a complex that may functionally couple glycolysis with SERCA-mediated Ca^{2+} transport into the SR (Xu et al., 1995). SR-associated glycolytic enzymes may produce ATP locally, resulting in modifications of myoplasmic Ca^{2+} signals, either via SERCA-mediated Ca^{2+} uptake into the SR and/or via RyR1-mediated Ca^{2+} release, because ATP is a well-characterized physiological RyR agonist (Fill and Copello, 2002; Bull et al., 2007). The higher Na^+/K^+-ATPase levels displayed by triads from aged rats, combined with their reduced GAPDH content, suggest that aged muscle has a reduced capacity to generate ATP locally at the triads, which may result in inhibition of SR Ca^{2+} uptake and reduced RyR1 activity. We propose that these combined factors contribute to disrupt normal Ca^{2+} signaling, thereby reducing muscle contractility in aged skeletal muscle. Future studies should address this proposal.

NOX

Skeletal muscle activity increases ROS production (Reid et al., 1992; Borzone et al., 1994). In several tissues, the diverse NOX isoforms contribute to ROS generation (Bedard and Krause, 2007). Skeletal muscle expresses NOX4 mRNA as well as the mRNA for the $gp91^{phox}$ subunit of the NOX2 isoform (Cheng et al., 2001; Shiose et al., 2001), in addition to expressing proteins of the NOX2 complex (Javeshghani et al., 2002), but the role of NOX in activity–dependent ROS production in skeletal muscle remains inconclusive. For instance, NOX-mediated ROS production in diaphragm muscle does not contribute to the ROS increase produced by heat stress (Zuo et al., 2003). Nonetheless, skeletal muscle T-tubules express several NOX2 subunits and NOX2-generated ROS stimulate SR Ca^{2+} release, presumably as a result of NOX2-induced RyR1 redox modifications (Hidalgo et al., 2006). Recent studies using the ROS-sensitive probe rhoGFP indicate that contraction and stretching of skeletal muscle both activate NOX (Pal et al., 2013). We found that triads from young or aged rats contained similar $p47^{phox}$ and $gp91^{phox}$ protein levels and comparable NOX activities. Our results strongly suggest that NOX-generated ROS do not contribute to the increased resting ROS levels of aged muscle; however, we cannot rule out differential effects of exercise on NOX-dependent ROS production as a function of age. It has been proposed that mitochondrial and NOX are possible ROS sources in aged skeletal muscle (Bejma and Ji, 1999). Our results support a predominant mitochondrial origin for the reported increase in resting ROS production in skeletal muscle (Vasilaki et al., 2006; Umanskaya et al., 2014), which results in increased RyR1 oxidation (Andersson et al., 2011).

Concluding Remarks

In this work, we show that partial cholesterol extraction from single skeletal fibers isolated from mice adult skeletal muscle eliminated or significantly reduced electrically evoked Ca^{2+} transients, without affecting membrane permeability or causing SR calcium depletion. We propose that partial cholesterol removal impairs E–C coupling by modifying the interactions of the cholesterol-associated protein caveolin-3 with RyR1 and Cav1.1. In support of this proposal, we found caveolin-3 associated with the cholesterol-rich T-tubule membranes, but not with SR membranes; moreover, caveolin-3 is present together with Cav1.1 in cholesterol-enriched DRM fractions from T-tubules or triads. In addition, we observed significantly decreased caveolin-3 and GAPDH and increased Na^+/K^+-ATPase levels in triads from aged rats, but we did not detect changes in cholesterol or RyR1 protein levels. These findings suggest that age-related changes in triadic proteins, and in particular the decrease in caveolin-3 protein content, are likely to alter T-tubule related signal transduction pathways and to produce defective E–C coupling of aged skeletal muscle. Our results contribute to the field of muscle physiology by suggesting that cholesterol and caveolin-3 are important for the normal E–C coupling process, and that alterations in their levels contribute to the defective function of aged skeletal muscle.

Author Contributions

GB and PL performed experiments, analyzed data, and contributed to manuscript writing. PB, CC and AR performed experiments and analyzed data. GS performed experiments, analyzed data and critically reviewed the manuscript. JH analyzed data, contributed to the discussion of results and critically reviewed the manuscript. AQ and CH supervised the study, analyzed data and provided funding. CH wrote the manuscript and is the guarantor of this work and, as such, had full access to all the data in the study and takes responsibility for the integrity of the data and the accuracy of the data analysis.

Acknowledgments

This work was financed by FONDECYT (grants 1090071, 1140545, 1130250), FONDECYT-FONDAP (15130011), Millennium Science Initiative (BNI-P-09-015F), and CONICYT-Research Ring (ACT-1111). The funding agencies had no role in study design, data collection and analysis, decision to publish, or preparation of the manuscript. We thank L. Montecinos, M. Silva, F. Mieres, and S. Guzman for their skilled technical assistance.

References

Andersson, D. C., Betzenhauser, M. J., Reiken, S., Meli, A. C., Umanskaya, A., Xie, W., et al. (2011). Ryanodine receptor oxidation causes intracellular calcium leak and muscle weakness in aging. *Cell Metab.* 14, 196–207. doi: 10.1016/j.cmet.2011.05.014

Anderson, K., Cohn, A. H., and Meissner, G. (1994). High-affinity [3H]PN200-110 and [3H]ryanodine binding to rabbit and frog skeletal muscle. *Am. J. Physiol.* 266, C462–C466.

Anderson, K., and Meissner, G. (1995). T-tubule depolarization-induced SR Ca2+ release is controlled by dihydropyridine receptor- and Ca(2+)-dependent mechanisms in cell homogenates from rabbit

skeletal muscle. *J. Gen. Physiol.* 105, 363–383. doi: 10.1085/jgp.105.3.363

Aravamudan, B., Volonte, D., Ramani, R., Gursoy, E., Lisanti, M. P., London, B., et al. (2003). Transgenic overexpression of caveolin-3 in the heart induces a cardiomyopathic phenotype. *Hum. Mol. Genet.* 12, 2777–2788. doi: 10.1093/hmg/ddg313

Badizadegan, K., Dickinson, B. L., Wheeler, H. E., Blumberg, R. S., Holmes, R. K., and Lencer, W. I. (2000). Heterogeneity of detergent-insoluble membranes from human intestine containing caveolin-1 and ganglioside G(M1). *Am. J. Physiol. Gastrointest. Liver Physiol.* 278, G895–G904. doi: 10.1016/S0016-5085(00)84524-2

Balijepalli, R. C., Foell, J. D., Hall, D. D., Hell, J. W., and Kamp, T. J. (2006). Localization of cardiac L-type Ca(2+) channels to a caveolar macromolecular signaling complex is required for beta(2)-adrenergic regulation. *Proc. Natl. Acad. Sci. U.S.A.* 103, 7500–7505. doi: 10.1073/pnas.0503465103

Barrientos, G., Bose, D. D., Feng, W., Padilla, I., and Pessah, I. N. (2009). The Na+/Ca2+ exchange inhibitor 2-(2-(4-(4-nitrobenzyloxy)phenyl)ethyl)isothiourea methanesulfonate (KB-R7943) also blocks ryanodine receptors type 1 (RyR1) and type 2 (RyR2) channels. *Mol. Pharmacol.* 76, 560–568. doi: 10.1124/mol.109.057265

Bedard, K., and Krause, K. H. (2007). The NOX family of ROS-generating NADPH oxidases: physiology and pathophysiology. *Physiol. Rev.* 87, 245–313. doi: 10.1152/physrev.00044.2005

Bejma, J., and Ji, L. L. (1999). Aging and acute exercise enhance free radical generation in rat skeletal muscle. *J. Appl. Physiol.* 87, 465–470.

Booth, F. W., Weeden, S. H., and Tseng, B. S. (1994). Effect of aging on human skeletal muscle and motor function. *Med. Sci. Sports Exerc.* 26, 556–560. doi: 10.1249/00005768-199405000-00006

Borzone, G., Zhao, B., Merola, A. J., Berliner, L., and Clanton, T. L. (1994). Detection of free radicals by electron spin resonance in rat diaphragm after resistive loading. *J. Appl. Physiol.* 77, 812–818.

Brandt, N. R., Caswell, A. H., Wen, S. R., and Talvenheimo, J. A. (1990). Molecular interactions of the junctional foot protein and dihydropyridine receptor in skeletal muscle triads. *J. Membr. Biol.* 113, 237–251. doi: 10.1007/BF01870075

Brown, D., and Waneck, G. L. (1992). Glycosyl-phosphatidylinositol-anchored membrane proteins. *J. Am. Soc. Nephrol.* 3, 895–906.

Bull, R., Finkelstein, J. P., Humeres, A., Behrens, M. I., and Hidalgo, C. (2007). Effects of ATP, Mg2+, and redox agents on the Ca2+ dependence of RyR channels from rat brain cortex. *Am. J. Physiol. Cell Physiol.* 293, C162–C171. doi: 10.1152/ajpcell.00518.2006

Calderon, J. C., Bolanos, P., and Caputo, C. (2011). Kinetic changes in tetanic Ca(2)(+) transients in enzymatically dissociated muscle fibres under repetitive stimulation. *J. Physiol.* 589, 5269–5283. doi: 10.1113/jphysiol.2011.213314

Capote, J., Bolanos, P., Schuhmeier, R. P., Melzer, W., and Caputo, C. (2005). Calcium transients in developing mouse skeletal muscle fibres. *J. Physiol.* 564, 451–464. doi: 10.1113/jphysiol.2004.081034

Capozza, F., Combs, T. P., Cohen, A. W., Cho, Y. R., Park, S. Y., Schubert, W., et al. (2005). Caveolin-3 knockout mice show increased adiposity and whole body insulin resistance, with ligand-induced insulin receptor instability in skeletal muscle. *Am. J. Physiol. Cell Physiol.* 288, C1317–C1331. doi: 10.1152/ajpcell.00489.2004

Carozzi, A. J., Ikonen, E., Lindsay, M. R., and Parton, R. G. (2000). Role of cholesterol in developing T-tubules: analogous mechanisms for T-tubule and caveolae biogenesis. *Traffic* 1, 326–341. doi: 10.1034/j.1600-0854.2000.010406.x

Carroll, S. L., Klein, M. G., and Schneider, M. F. (1995). Calcium transients in intact rat skeletal muscle fibers in agarose gel. *Am. J. Physiol.* 269, C28–C34.

Cheng, G., Cao, Z., Xu, X., Van Meir, E. G., and Lambeth, J. D. (2001). Homologs of gp91phox: cloning and tissue expression of Nox3, Nox4, and Nox5. *Gene* 269, 131–140. doi: 10.1016/S0378-1119(01)00449-8

Couchoux, H., Bichraoui, H., Chouabe, C., Altafaj, X., Bonvallet, R., Allard, B., et al. (2011). Caveolin-3 is a direct molecular partner of the Cav1.1 subunit of the skeletal muscle L-type calcium channel. *Int. J. Biochem. Cell Biol.* 43, 713–720. doi: 10.1016/j.biocel.2011.01.011

Dirks, A. J., and Jones, K. M. (2006). Statin-induced apoptosis and skeletal myopathy. *Am. J. Physiol. Cell Physiol.* 291, C1208–C1212. doi: 10.1152/ajpcell.00226.2006

Fill, M., and Copello, J. A. (2002). Ryanodine receptor calcium release channels. *Physiol. Rev.* 82, 893–922. doi: 10.1152/physrev.00013.2002

Folco, E. J., Liu, G. X., and Koren, G. (2004). Caveolin-3 and SAP97 form a scaffolding protein complex that regulates the voltage-gated potassium channel Kv1.5. *Am. J. Physiol. Heart Circ. Physiol.* 287, H681–H690. doi: 10.1152/ajpheart.00152.2004

Franzini-Armstrong, C. (1972). Studies of the triad. 3. Structure of the junction in fast twitch fibers. *Tissue Cell* 4, 469–478. doi: 10.1016/S0040-8166(72)80023-5

Galbiati, F., Engelman, J. A., Volonte, D., Zhang, X. L., Minetti, C., Li, M., et al. (2001). Caveolin-3 null mice show a loss of caveolae, changes in the microdomain distribution of the dystrophin-glycoprotein complex, and t-tubule abnormalities. *J. Biol. Chem.* 276, 21425–21433. doi: 10.1074/jbc.M100828200

Galbiati, F., Volonte, D., Chu, J. B., Li, M., Fine, S. W., Fu, M., et al. (2000). Transgenic overexpression of caveolin-3 in skeletal muscle fibers induces a Duchenne-like muscular dystrophy phenotype. *Proc. Natl. Acad. Sci. U.S.A.* 97, 9689–9694. doi: 10.1073/pnas.160249097

Haberkant, P., Schmitt, O., Contreras, F. X., Thiele, C., Hanada, K., Sprong, H., et al. (2008). Protein-sphingolipid interactions within cellular membranes. *J. Lipid Res.* 49, 251–262. doi: 10.1194/jlr.D700023-JLR200

Hagiwara, Y., Sasaoka, T., Araishi, K., Imamura, M., Yorifuji, H., Nonaka, I., et al. (2000). Caveolin-3 deficiency causes muscle degeneration in mice. *Hum. Mol. Genet.* 9, 3047–3054. doi: 10.1093/hmg/9.20.3047

Hidalgo, C. (1985). Lipid phase of transverse tubule membranes from skeletal muscle. An electron paramagnetic resonance study. *Biophys. J.* 47, 757–764. doi: 10.1016/S0006-3495(85)83978-3

Hidalgo, C., Jorquera, J., Tapia, V., and Donoso, P. (1993). Triads and transverse tubules isolated from skeletal muscle contain high levels of inositol 1,4,5-trisphosphate. *J. Biol. Chem.* 268, 15111–15117.

Hidalgo, C., Parra, C., Riquelme, G., and Jaimovich, E. (1986). Transverse tubules from frog skeletal muscle. Purification and properties of vesicles sealed with the inside-out orientation. *Biochim. Biophys. Acta* 855, 79–88. doi: 10.1016/0005-2736(86)90191-4

Hidalgo, C., Sanchez, G., Barrientos, G., and Racena-Parks, P. (2006). A transverse tubule NADPH oxidase activity stimulates calcium release from isolated triads via ryanodine receptor type 1 s -glutathionylation. *J. Biol. Chem.* 281, 26473–26482. doi: 10.1074/jbc.M600451200

Horgan, D. J., and Kuypers, R. (1987). Isolation of transverse tubules by fractionation of sarcoplasmic reticulum preparations in ion-free sucrose density gradients. *Arch. Biochem. Biophys.* 253, 377–387. doi: 10.1016/0003-9861(87)90191-3

Huang, H., Bae, C., Sachs, F., and Suchyna, T. M. (2013). Caveolae regulation of mechanosensitive channel function in myotubes. *PLoS ONE* 8:e72894. doi: 10.1371/journal.pone.0072894

Istvan, E. S., and Deisenhofer, J. (2001). Structural mechanism for statin inhibition of HMG-CoA reductase. *Science* 292, 1160–1164. doi: 10.1126/science.1059344

Javeshghani, D., Magder, S. A., Barreiro, E., Quinn, M. T., and Hussain, S. N. (2002). Molecular characterization of a superoxide-generating NAD(P)H oxidase in the ventilatory muscles. *Am. J. Respir. Crit. Care Med.* 165, 412–418. doi: 10.1164/ajrccm.165.3.2103028

Jayasinghe, I. D., and Launikonis, B. S. (2013). Three-dimensional reconstruction and analysis of the tubular system of vertebrate skeletal muscle. *J. Cell Sci.* 126, 4048–4058. doi: 10.1242/jcs.131565

Kawabe, J. I., Grant, B. S., Yamamoto, M., Schwencke, C., Okumura, S., and Ishikawa, Y. (2001). Changes in caveolin subtype protein expression in aging rat organs. *Mol. Cell. Endocrinol.* 176, 91–95. doi: 10.1016/S0303-7207(01)00472-5

Lau, Y. H., Caswell, A. H., Brunschwig, J. P., Baerwald, R., and Garcia, M. (1979). Lipid analysis and freeze-fracture studies on isolated transverse tubules and sarcoplasmic reticulum subfractions of skeletal muscle. *J. Biol. Chem.* 254, 540–546.

Launikonis, B. S., and Stephenson, D. G. (2001). Effects of membrane cholesterol manipulation on excitation-contraction coupling in skeletal muscle of the toad. *J. Physiol.* 534, 71–85. doi: 10.1111/j.1469-7793.2001.00071.x

Li, C., Duan, W., Yang, F., and Zhang, X. (2006). Caveolin-3-anchored microdomains at the rabbit sarcoplasmic reticulum membranes. *Biochem. Biophys. Res. Commun.* 344, 1135–1140. doi: 10.1016/j.bbrc.2006.04.024

Llanos, P., Contreras-Ferrat, A., Georgiev, T., Osorio-Fuentealba, C., Espinosa, A., Hidalgo, J., et al. (2015). The cholesterol-lowering agent methyl-beta-cyclodextrin promotes glucose uptake via GLUT4 in adult muscle fibers and

reduces insulin resistance in obese mice. *Am. J. Physiol. Endocrinol. Metab.* 308, E294–E305. doi: 10.1152/ajpendo.00189.2014

Marks, A. R., Tempst, P., Hwang, K. S., Taubman, M. B., Inui, M., Chadwick, C., et al. (1989). Molecular cloning and characterization of the ryanodine receptor/junctional channel complex cDNA from skeletal muscle sarcoplasmic reticulum. *Proc. Natl. Acad. Sci. U.S.A.* 86, 8683–8687. doi: 10.1073/pnas.86.22.8683

Melzer, W., Herrmann-Frank, A., and Luttgau, H. C. (1995). The role of Ca2+ ions in excitation-contraction coupling of skeletal muscle fibres. *Biochim. Biophys. Acta* 1241, 59–116. doi: 10.1016/0304-4157(94)00014-5

Miller, M. S., Callahan, D. M., and Toth, M. J. (2014). Skeletal muscle myofilament adaptations to aging, disease, and disuse and their effects on whole muscle performance in older adult humans. *Front. Physiol.* 5:369. doi: 10.3389/fphys.2014.00369

Minarovic, I., and Meszaros, L. G. (1998). Fluorescent probing with felodipine of the dihydropyridine receptor and its interaction with the ryanodine receptor calcium release channel. *Biochem. Biophys. Res. Commun.* 244, 519–524. doi: 10.1006/bbrc.1998.8233

Munoz, P., Mora, S., Sevilla, L., Kaliman, P., Tomas, E., Guma, A., et al. (1996). Expression and insulin-regulated distribution of caveolin in skeletal muscle. Caveolin does not colocalize with GLUT4 in intracellular membranes. *J. Biol. Chem.* 271, 8133–8139. doi: 10.1074/jbc.271.14.8133

Murata, M., Peranen, J., Schreiner, R., Wieland, F., Kurzchalia, T. V., and Simons, K. (1995). VIP21/caveolin is a cholesterol-binding protein. *Proc. Natl. Acad. Sci. U.S.A.* 92, 10339–10343. doi: 10.1073/pnas.92.22.10339

O'connell, K., Gannon, J., Doran, P., and Ohlendieck, K. (2008). Reduced expression of sarcalumenin and related Ca2+ -regulatory proteins in aged rat skeletal muscle. *Exp. Gerontol.* 43, 958–961. doi: 10.1016/j.exger.2008.07.006

Ortegren, U., Karlsson, M., Blazic, N., Blomqvist, M., Nystrom, F. H., Gustavsson, J., et al. (2004). Lipids and glycosphingolipids in caveolae and surrounding plasma membrane of primary rat adipocytes. *Eur. J. Biochem.* 271, 2028–2036. doi: 10.1111/j.1432-1033.2004.04117.x

Pal, R., Basu Thakur, P., Li, S., Minard, C., and Rodney, G. G. (2013). Real-time imaging of NADPH oxidase activity in living cells using a novel fluorescent protein reporter. *PLoS ONE* 8:e63989. doi: 10.1371/journal.pone.0063989

Park, D. S., Woodman, S. E., Schubert, W., Cohen, A. W., Frank, P. G., Chandra, M., et al. (2002). Caveolin-1/3 double-knockout mice are viable, but lack both muscle and non-muscle caveolae, and develop a severe cardiomyopathic phenotype. *Am. J. Pathol.* 160, 2207–2217. doi: 10.1016/S0002-9440(10)61168-6

Parton, R. G., Way, M., Zorzi, N., and Stang, E. (1997). Caveolin-3 associates with developing T-tubules during muscle differentiation. *J. Cell Biol.* 136, 137–154. doi: 10.1083/jcb.136.1.137

Pouvreau, S., Berthier, C., Blaineau, S., Amsellem, J., Coronado, R., and Strube, C. (2004). Membrane cholesterol modulates dihydropyridine receptor function in mice fetal skeletal muscle cells. *J. Physiol.* 555, 365–381. doi: 10.1113/jphysiol.2003.055285

Ralston, E., and Ploug, T. (1999). Caveolin-3 is associated with the T-tubules of mature skeletal muscle fibers. *Exp. Cell Res.* 246, 510–515. doi: 10.1006/excr.1998.4305

Reid, M. B., Shoji, T., Moody, M. R., and Entman, M. L. (1992). Reactive oxygen in skeletal muscle. II. Extracellular release of free radicals. *J. Appl. Physiol.* 73, 1805–1809.

Renganathan, M., Messi, M. L., and Delbono, O. (1997). Dihydropyridine receptor-ryanodine receptor uncoupling in aged skeletal muscle. *J. Membr. Biol.* 157, 247–253. doi: 10.1007/s002329900233

Rios, E., Karhanek, M., Ma, J., and Gonzalez, A. (1993). An allosteric model of the molecular interactions of excitation-contraction coupling in skeletal muscle. *J. Gen. Physiol.* 102, 449–481. doi: 10.1085/jgp.102.3.449

Rosemblatt, M., Hidalgo, C., Vergara, C., and Ikemoto, N. (1981). Immunological and biochemical properties of transverse tubule membranes isolated from rabbit skeletal muscle. *J. Biol. Chem.* 256, 8140–8148.

Russ, D. W., Grandy, J. S., Toma, K., and Ward, C. W. (2011). Ageing, but not yet senescent, rats exhibit reduced muscle quality and sarcoplasmic reticulum function. *Acta Physiol.* 201, 391–403. doi: 10.1111/j.1748-1716.2010.02191.x

Sanchez, G., Escobar, M., Pedrozo, Z., Macho, P., Domenech, R., Hartel, S., et al. (2008). Exercise and tachycardia increase NADPH oxidase and ryanodine receptor-2 activity: possible role in cardioprotection. *Cardiovasc. Res.* 77, 380–386. doi: 10.1093/cvr/cvm011

Sargiacomo, M., Sudol, M., Tang, Z., and Lisanti, M. P. (1993). Signal transducing molecules and glycosyl-phosphatidylinositol-linked proteins form a caveolin-rich insoluble complex in MDCK cells. *J. Cell Biol.* 122, 789–807. doi: 10.1083/jcb.122.4.789

Shiose, A., Kuroda, J., Tsuruya, K., Hirai, M., Hirakata, H., Naito, S., et al. (2001). A novel superoxide-producing NAD(P)H oxidase in kidney. *J. Biol. Chem.* 276, 1417–1423. doi: 10.1074/jbc.M007597200

Smart, E. J., Graf, G. A., Mcniven, M. A., Sessa, W. C., Engelman, J. A., Scherer, P. E., et al. (1999). Caveolins, liquid-ordered domains, and signal transduction. *Mol. Cell. Biol.* 19, 7289–7304.

Song, K. S., Scherer, P. E., Tang, Z., Okamoto, T., Li, S., Chafel, M., et al. (1996). Expression of caveolin-3 in skeletal, cardiac, and smooth muscle cells. Caveolin-3 is a component of the sarcolemma and co-fractionates with dystrophin and dystrophin-associated glycoproteins. *J. Biol. Chem.* 271, 15160–15165. doi: 10.1074/jbc.271.25.15160

Sun, X., Nagarajan, M., Beesley, P. W., and Ng, Y. C. (1999). Age-associated differential expression of Na(+)-K(+)-ATPase subunit isoforms in skeletal muscles of F-344/BN rats. *J. Appl. Physiol.* 87, 1132–1140.

Toselli, M., Biella, G., Taglietti, V., Cazzaniga, E., and Parenti, M. (2005). Caveolin-1 expression and membrane cholesterol content modulate N-type calcium channel activity in NG108-15 cells. *Biophys. J.* 89, 2443–2457. doi: 10.1529/biophysj.105.065623

Touchberry, C. D., Wacker, M. J., Richmond, S. R., Whitman, S. A., and Godard, M. P. (2006). Age-related changes in relative expression of real-time PCR housekeeping genes in human skeletal muscle. *J. Biomol. Tech.* 17, 157–162.

Umanskaya, A., Santulli, G., Xie, W., Andersson, D. C., Reiken, S. R., and Marks, A. R. (2014). Genetically enhancing mitochondrial antioxidant activity improves muscle function in aging. *Proc. Natl. Acad. Sci. U.S.A.* 111, 15250–15255. doi: 10.1073/pnas.1412754111

Vasilaki, A., Mansouri, A., Van Remmen, H., Van Der Meulen, J. H., Larkin, L., Richardson, A. G., et al. (2006). Free radical generation by skeletal muscle of adult and old mice: effect of contractile activity. *Aging Cell* 5, 109–117. doi: 10.1111/j.1474-9726.2006.00198.x

Vigelso, A., Dybboe, R., Hansen, C. N., Dela, F., Helge, J. W., and Guadalupe-Grau, A. (2015). GAPDH and beta-actin protein decreases with aging making Stain-Free technology a superior loading control in Western Blotting of human skeletal muscle. *J. Appl. Physiol.* 118, 386–394. doi: 10.1152/japplphysiol.00840.2014

Voigt, T., Sebald, H. J., Schoenauer, R., Levano, S., Girard, T., Hoppeler, H. H., et al. (2013). Annexin A1 is a biomarker of T-tubular repair in skeletal muscle of nonmyopathic patients undergoing statin therapy. *FASEB J.* 27, 2156–2164. doi: 10.1096/fj.12-219345

Wagenknecht, T., Hsieh, C. E., Rath, B. K., Fleischer, S., and Marko, M. (2002). Electron tomography of frozen-hydrated isolated triad junctions. *Biophys. J.* 83, 2491–2501. doi: 10.1016/S0006-3495(02)75260-0

Wang, Z. M., Messi, M. L., and Delbono, O. (2000). L-Type Ca(2+) channel charge movement and intracellular Ca(2+) in skeletal muscle fibers from aging mice. *Biophys. J.* 78, 1947–1954. doi: 10.1016/S0006-3495(00)76742-7

Weiss, N., Couchoux, H., Legrand, C., Berthier, C., Allard, B., and Jacquemond, V. (2008). Expression of the muscular dystrophy-associated caveolin-3(P104L) mutant in adult mouse skeletal muscle specifically alters the Ca(2+) channel function of the dihydropyridine receptor. *Pflugers Arch.* 457, 361–375. doi: 10.1007/s00424-008-0528-z

Welle, S. (2002). Cellular and molecular basis of age-related sarcopenia. *Can. J. Appl. Physiol.* 27, 19–41. doi: 10.1139/h02-002

Whiteley, G., Collins, R. F., and Kitmitto, A. (2012). Characterization of the molecular architecture of human caveolin-3 and interaction with the skeletal muscle ryanodine receptor. *J. Biol. Chem.* 287, 40302–40316. doi: 10.1074/jbc.M112.377085

Williams, T. M., and Lisanti, M. P. (2004). The Caveolin genes: from cell biology to medicine. *Ann. Med.* 36, 584–595. doi: 10.1080/07853890410018899

Xu, K. Y., Zweier, J. L., and Becker, L. C. (1995). Functional coupling between glycolysis and sarcoplasmic reticulum Ca2+ transport. *Circ. Res.* 77, 88–97. doi: 10.1161/01.RES.77.1.88

Zalk, R., Lehnart, S. E., and Marks, A. R. (2007). Modulation of the ryanodine receptor and intracellular calcium. *Annu. Rev. Biochem.* 76, 367–385. doi: 10.1146/annurev.biochem.76.053105.094237

Zhang, L., Morris, K. J., and Ng, Y. C. (2006). Fiber type-specific immunostaining of the Na+,K+-ATPase subunit isoforms in skeletal muscle: age-associated differential changes. *Biochim. Biophys. Acta* 1762, 783–793. doi: 10.1016/j.bbadis.2006.08.006

Zuo, L., Pasniciuc, S., Wright, V. P., Merola, A. J., and Clanton, T. L. (2003). Sources for superoxide release: lessons from blockade of electron transport, NADPH oxidase, and anion channels in diaphragm. *Antioxid. Redox Signal.* 5, 667–675. doi: 10.1089/152308603770310347

Conflict of Interest Statement: The authors declare that the research was conducted in the absence of any commercial or financial relationships that could be construed as a potential conflict of interest.

frontiers in Physiology

ORIGINAL RESEARCH
published: 20 April 2015
doi: 10.3389/fphys.2015.00122

Chronic sustained hypoxia-induced redox remodeling causes contractile dysfunction in mouse sternohyoid muscle

Philip Lewis[1], *David Sheehan*[2], *Renata Soares*[3], *Ana Varela Coelho*[3] *and Ken D. O'Halloran*[1]*

[1] Department of Physiology, School of Medicine, University College Cork, Cork, Ireland, [2] School of Biochemistry and Cell Biology, University College Cork, Cork, Ireland, [3] Instituto de Tecnologia Química e Biológica António Xavier, New University of Lisbon, Lisbon, Portugal

OPEN ACCESS

Edited by:
Brian McDonagh,
University of Liverpool, UK

Reviewed by:
Leonardo F. Ferreira,
University of Florida, USA
Esther Barreiro,
Institut Hospital del Mar
d'Investigacions Mèdiques, Spain

***Correspondence:**
Ken D. O'Halloran,
Department of Physiology, School of Medicine, University College Cork,
3-079, Western Gateway Building,
Western Road, Cork, Ireland
k.ohalloran@ucc.ie

Specialty section:
This article was submitted to Striated Muscle Physiology, a section of the journal Frontiers in Physiology

Received: 16 January 2015
Accepted: 02 April 2015
Published: 20 April 2015

Citation:
Lewis P, Sheehan D, Soares R, Varela Coelho A and O'Halloran KD (2015) Chronic sustained hypoxia-induced redox remodeling causes contractile dysfunction in mouse sternohyoid muscle. Front. Physiol. 6:122. doi: 10.3389/fphys.2015.00122

Chronic sustained hypoxia (CH) induces structural and functional adaptations in respiratory muscles of animal models, however the underlying molecular mechanisms are unclear. This study explores the putative role of CH-induced redox remodeling in a translational mouse model, with a focus on the sternohyoid—a representative upper airway dilator muscle involved in the control of pharyngeal airway caliber. We hypothesized that exposure to CH induces redox disturbance in mouse sternohyoid muscle in a time-dependent manner affecting metabolic capacity and contractile performance. C57Bl6/J mice were exposed to normoxia or normobaric CH (FiO_2 = 0.1) for 1, 3, or 6 weeks. A second cohort of animals was exposed to CH for 6 weeks with and without antioxidant supplementation (tempol or N-acetyl cysteine in the drinking water). Following CH exposure, we performed 2D redox proteomics with mass spectrometry, metabolic enzyme activity assays, and cell-signaling assays. Additionally, we assessed isotonic contractile and endurance properties *ex vivo*. Temporal changes in protein oxidation and glycolytic enzyme activities were observed. Redox modulation of sternohyoid muscle proteins key to contraction, metabolism and cellular homeostasis was identified. There was no change in redox-sensitive proteasome activity or HIF-1α content, but CH decreased phospho-JNK content independent of antioxidant supplementation. CH was detrimental to sternohyoid force- and power-generating capacity and this was prevented by chronic antioxidant supplementation. We conclude that CH causes upper airway dilator muscle dysfunction due to redox modulation of proteins key to function and homeostasis. Such changes could serve to further disrupt respiratory homeostasis in diseases characterized by CH such as chronic obstructive pulmonary disease. Antioxidants may have potential use as an adjunctive therapy in hypoxic respiratory disease.

Keywords: hypoxia, oxidative stress, antioxidants, respiratory muscle, COPD

Introduction

The striated muscles of breathing are the final common effectors of the respiratory control system, critical in the maintenance of respiratory homeostasis. Pharyngeal dilator muscles are an important subset of the respiratory muscles serving to control the patency of the upper airway. Pharyngeal dilator muscle damage or dysfunction increases the risk of obstructive airway events. Upper airway muscle dysfunction is implicated in human obstructive sleep apnea (OSA), a common respiratory disorder characterized by repeated occlusions of the pharyngeal airway during sleep. Of note, OSA is prevalent in patients with chronic obstructive pulmonary disease (COPD), presenting as the "overlap syndrome" (Owens et al., 2008; McNicholas, 2009; Owens and Malhotra, 2010), but the reasons for the emergence of this co-morbidity are unclear.

Chronic sustained hypoxia (CH) is a dominant feature of respiratory diseases including COPD, but the putative role of CH in respiratory muscle remodeling and dysfunction is generally under-explored. Little is known about the effects of CH exposure on the respiratory muscles and there exists a general paucity of information concerning the pharyngeal dilator muscles despite the potential clinical relevance. Respiratory and limb muscle remodeling are features of COPD (Orozco-Levi, 2003; Doucet et al., 2004, 2010; Levine et al., 2013) and interestingly, exposure to CH elicits differential structural and functional adaptations in respiratory and limb muscles (El-Khoury et al., 2003, 2012; Faucher et al., 2005; McMorrow et al., 2011; Gamboa and Andrade, 2012; Carberry et al., 2014). We speculate that hypoxic remodeling of respiratory muscle has relevance to respiratory muscle plasticity in respiratory disease. Hypoxia-related remodeling of upper airway muscles may underpin poor upper airway control in COPD.

Pharyngeal dilator muscles are phasically active during inspiration and muscle activity is increased during hypoxic exposure (O'Halloran et al., 2002; Edge et al., 2014). Contractile activity increases reactive oxygen species (ROS) production which are pivotal for muscle adaptation to high altitude and respiratory diseases characterized by hypoxia (Zuo and Clanton, 2005; Marin-Corral et al., 2009; Murray, 2009; Chaudhary et al., 2012; El-Khoury et al., 2012; Levine et al., 2013; Puig-Vilanova et al., 2015). Thus, CH likely challenges respiratory muscles, including the pharyngeal dilator muscles, with enhanced ROS on two fronts—increased contractile activity during reflex hyperventilation and hypoxia *per se*. We postulated a role for ROS in eliciting CH-induced redox remodeling of key muscle proteins with resultant functional changes in the sternohyoid muscle—a representative pharyngeal dilator muscle. The supra- and infra-hyoid muscles of the upper airway control the position of the hyoid bone, displacing it anteriorly during inspiration to enlarge the caliber of the pharynx. Sternohyoid muscle length correlates to airway volume (Van Lunteren et al., 1987) and the muscle is recruited during increased respiratory drive (O'Halloran et al., 2002) and obstructive airway events (Edge et al., 2012). Sternohyoid muscle damage is reported in the English bulldog, an animal model of OSA (Petrof et al., 1994). We have extensively characterized sternohyoid muscle physiology (O'Halloran, 2006; Skelly et al., 2010; Shortt and O'Halloran, 2014; McDonald et al., 2015), including several studies in animal models of chronic hypoxia (Bradford et al., 2005; McMorrow et al., 2011; Skelly et al., 2011, 2012a,b, 2013; O'Connell et al., 2013; Carberry et al., 2014; McDonald et al., 2014). The sternohyoid muscle is suited to *ex vivo* study of contractile function due to ease of access, longitudinal arrangement of its fibers and the opportunity, employed in the present study, to keep bony origin and insertions intact in isolated preparations.

Given that ventilation, muscle contractile behavior, and the level of hypoxia experienced by the respiratory muscles, are likely temporally modified during the process of acclimatization to CH, we characterized protein carbonyl and free thiol content (the most common and most specific form of protein oxidation respectively (Dalle-Donne et al., 2006; El-Shafey et al., 2011) in the sternohyoid after 1, 3, or 6 weeks of CH exposure. In addition, we sought to identify redox-modified proteins in the sternohyoid muscle after 6 weeks of CH using 2D redox proteomics combined with mass spectrometry (Cole et al., 2014; Hu et al., 2014; Rainville et al., 2014) having reasoned that this information will aid the determination of how and where ROS exert their effects in muscle cells following CH exposure. We postulated that chymotrypsin-like activity of the 20S proteasome is increased in the sternohyoid after 6 weeks of CH given that proteasomal activity is highly sensitive to ROS (McClung et al., 2008; Aiken et al., 2011). Hypoxia through the hypoxia-inducible factor (HIF)-1α transcription factor promotes a more glycolytic phenotype in tissues to reduce the reliance on oxygen in ATP production (Howald et al., 1990; Murray, 2009; Wheaton and Chandel, 2011). HIF expression correlates with muscle fiber type and activity and is also modulated by ROS. Therefore, we reasoned that glyceraldehyde-3-phosphate dehydrogenase (GAPDH) and lactate dehydrogenase (LDH) activities would be temporally modified in the sternohyoid in response to CH exposure. We also assessed HIF-1α content, phospho-MAPK content (p38, JNK, ERK1/2), and sternohyoid isotonic contractile and endurance properties *ex vivo* after 6 weeks of CH in the presence or absence of chronic antioxidant supplementation with tempol or N-acetyl cysteine (NAC). We tested the hypothesis that CH causes aberrant redox modulation of sternohyoid muscle function which is reversible by antioxidant supplementation.

Materials and Methods

Ethical Approval

All protocols involving animals described in this study were approved by local ethics committee and were performed under license from the Irish Government Department of Health and Children in accordance with EU legislation.

Animal Model

In the first series of experiments, 48 adult male C576Bl/J mice (Charles River Laboratories, UK) were exposed to 1, 3, or 6 weeks of CH ($FiO_2 = 0.1$) or normoxia (6 groups: $n = 8$ per group, matched for age and weight) in environmental chambers (OxyCycler Model A84, BioSpherix Ltd, USA) with precise control of ambient oxygen concentration. All mice were housed at room

temperature on a 12:12-h light–dark cycle. Food and water were available *ad libitum*, and the chambers were opened briefly once a week for cleaning. In a second series, 32 adult male C576Bl/J mice were exposed to normoxia or CH with or without antioxidant supplementation with tempol or NAC for 6 weeks (4 groups: $n = 8$ per group, matched for age and weight). At the end of the gas treatment periods, animals were anesthetized by 5% isoflurane inhalation in oxygen and euthanized by cervical dislocation. Blood samples were taken in capillary tubes for hematocrit determination.

Molecular Studies

Tissue Preparation for Molecular Studies

Sternohyoid muscles were excised, snap frozen in liquid nitrogen and stored at −80°C. Frozen muscle samples were homogenized in 10% w/v modified radioimmunoprecipitation (RIPA) assay buffer (1X RIPA, 200 mM sodium fluoride, 1 mM phenylmethylsulfonyl fluoride, protease inhibitor cocktail, phosphatase inhibitor cocktail (Fisher Scientific, Ireland) and centrifuged at 13,000 *g* for 15 min to separate the insoluble fraction from crude protein homogenate. Protein concentrations were evaluated using a bicinchoninic assay (Pierce Biotechnology (Fisher Scientific), Ireland) against bovine serum albumin standards. Two additional muscles, the soleus and extensor digitorum longus (EDL), slow and fast fiber type limb muscles respectively, were also prepared in this manner for determination of total protein carbonyl and free thiol content for comparison to sternohyoid.

Total Protein Carbonyl and Free Thiol Content

As previously described (Cole et al., 2014; Hu et al., 2014; Rainville et al., 2014), muscle homogenates were incubated with either 2 mM fluorescein-thiosemicarbazide (FTSC) or 2 mM iodoacetamidofluorescein (IAF) (Sigma-Aldrich Co., Ireland) for 2 h in the dark on ice for detection of free protein carbonyl and thiol groups respectively. Samples were then precipitated with 20% trichloroacetic acid (TCA) in acetone, followed by centrifugation at 11,000 *g* for 3 min. Protein pellets were then washed with ice-cold excess 1:1 ethylacetate/ethanol or acetone (for FTSC and IAF respectively) to remove excess TCA, interfering salts and non-protein contaminants. Samples were dried, re-suspended in sample buffer containing 5% beta-mercaptoethanol and heated at 95°C for 5 min before electrophoretic separation on a 12% polyacrylamide gel (1D). Fluorescent images of the gels were captured on a Typhoon Trio+ Variable-Mode Imager (GE Healthcare, UK). Protein bands were visualized by colloidal coomassie staining (Dyballa and Metzger, 2009) and images were captured on a calibrating image densitometer (GS-800, Bio-Rad, USA).

2D Redox Proteomics

As previously described (Cole et al., 2014; Hu et al., 2014; Rainville et al., 2014), this method separates proteins according to their isoelectric point and molecular mass such that they appear as spots when stained on polyacrylamide gels; protein spots can be analyzed independently. Briefly, sternohyoid muscle samples were treated as described above for 1D preparation until re-suspension in sample buffer. Samples were instead re-suspended in rehydration buffer (7 M urea, 2 M thiourea, 2% (w/v) 3-[(3-Cholamidopropyl)dimethylammonio]-1-propanesulfonate, 4% (v/v) ampholytes (Pharmalyte 3–10, Amersham, UK), 1% (v/v) destreak reagent (Amersham) and a trace amount of bromophenol blue) and loaded onto 70 mm pH 3–10 non-linear immobilized pH gradient (IPG) strips (GE Healthcare) overnight. IPG strips were focused on a Protean isoelectric focusing (IEF) cell (BioRad) with linear voltage increases: 250 V for 15min; 4000 V for 2 h; then up to 20,000 V. Following IEF, strips were equilibrated (20 min) in equilibration buffer (6 M urea, 0.375 M Tris, pH 8.8, 2% (w/v) sodium-dodecyl sulfate, and 20% (v/v) glycerol) containing 2% (w/v) dithiothreitol, and then for 20 min in equilibration buffer containing 2.5% (w/v) iodoacetamide. Equilibrated strips were then subjected to gel electrophoresis. Fluorescent and colloidal coomassie stained gel images were captured as described above.

Image Analysis

Quantity One image analysis software (Bio-Rad) was used to subtract background and quantify optical density for total protein carbonyl and free thiol content. For each sample, intensity of fluorescence was normalized to intensity of coomassie staining. For 2D separations, alignment of gels, spot matching, and quantification of spot volumes was carried out using Progenesis SameSpots image analysis software (Version 4.5; Non-linear Dynamics, USA).

Protein Digestion and Identification

Gel spots were used for in-gel protein digestion with trypsin. The extracted peptides were loaded onto a R2 micro column (RP-C18 equivalent) where they were desalted, concentrated and eluted directly onto a MALDI plate using α-cyano-4-hydroxycinnamic acid (5 mg/ml) as matrix solution in 50% (v/v) acetonitrile and 5% (v/v) formic acid. Mass spectra of the peptides were acquired with positive reflectron mass spectrometry (MS) and MS/MS modes using MALDI-TOF/TOF MS instrument (4800 *plus* MALDI TOF/TOF analyzer). The collected MS and MS/MS spectra were analyzed in combined mode using Mascot (version 2.2; Matrix Science, Boston, MA) search engine and SwissProt (release 02_2013, 539,165 entries) database restricted to 50 ppm peptide mass tolerance for the parent ions, an error of 0.3 Da for the fragments, one missed cleavage in peptide masses, and carbamidomethylation of Cys and oxidation of Met as fixed and variable amino acid modifications, respectively. No taxonomy restrictions were applied. The identified proteins were only considered if a MASCOT score above 95% confidence was obtained ($p < 0.05$) and at least one peptide was identified with a score above 95% confidence ($p < 0.05$). This analysis was conducted by the Analytical Services Unit, Instituto de Tecnologia Química e Biológica (ITQB), New University of Lisbon, Lisbon, Portugal.

Chymotrypsin-like Proteasome Activity

Chymotrypsin-like activity of the 20S proteasome was measured fluorometrically in accordance with the manufacturer's instructions (Abcam, UK).

Glycolytic Enzyme Activities

For GAPDH activity measurement, samples were added to 13.5 mM sodium pyrophosphate buffer (pH 8.5) containing 30 mM sodium arsenate, 0.25 mM NAD with 3.325 mM DTT. Samples were incubated at 25°C for 10 min to achieve temperature equilibration and to establish a blank rate, if any. 0.5 mM DL-glyceraldehdye-3-phosphate was added and absorbance was recorded for 10 min at 339 nm. Measured rates were corrected by measuring the blank rate of the reaction. One unit is defined as 1 μmol NADH generated/minute/mg protein. Similarly, total LDH activity was calculated as rate of absorbance at 339 nm produced by oxidation of NADH at 25°C and pH 7.3 in 0.2 M Tris-HCL buffer containing 1 mM sodium pyruvate and 0.22 mM NADH.

HIF-1α and Phospho-MAPK Content

HIF-1α content and phospho-(p)-p38, p-JNK, p-ERK1/2 content were assayed by an immuno-linked luminescence assay in accordance with manufacturer's instructions (Mesoscale Discovery, Gaithersburg, USA). HeLa cells treated with and without cobalt chloride for 16 h provided positive and negative controls respectively for the HIF-1α assay. Lysate from Jurkat cells treated with 1 mol rapamycin for 3 h to activate MAPK phosphatase 1 was used as negative control for the MAPK assay. Lysate from Jurkat cells treated with 50 nM calyculin A and 200 nM PMA for 15 min to stimulate phosphorylation of MAPK proteins was used as a positive control (Mesoscale Discovery).

Isotonic Muscle Function

Ex Vivo Muscle Preparation

Animals were anesthetized by 5% isoflurane inhalation in air and euthanized by cervical dislocation. Sternohyoid muscles were excised and placed in a bath of Krebs solution (NaCl 120 mM, KCl 5 mM, Ca^{2+} gluconate 2.5 mM, $MgSO_4$ 1.2 mM, NaH_2PO_4 1.2 mM, $NaHCO_3$ 25 mM, glucose 11.5 mM, and 25 μM d-tubocurarine) at room temperature and gassed with carbogen (95% O_2/5% CO_2) before mounting in the test bath for assessment of muscle contractile and endurance performance. Whole intact mouse sternohyoid muscle bundles were arranged between the electrodes with the sternum anchored at a fixed base and hyoid bone connected by a non-elastic string to a dual-mode lever force transducer (Aurora Scientific, Canada) such that fibers were orientated vertically. Upon placement in the test bath, bundles were incubated at 35°C in Krebs solution gassed with carbogen (95% O_2/5% CO_2). Muscle performance has previously been shown (Skelly et al., 2010) to be optimal under hyperoxic conditions (95% O_2) compared to normoxic conditions (21% O_2). Bundles were equilibrated for 5 min in gassed Krebs solution prior to initiating the experimental protocol.

Protocol

Bundles were set to optimum length (Lo—length at which peak twitch force occurs) by adjusting the position of the force transducer with a micro-positioner and stimulating with repeated single pulses whilst adjusting muscle length until peak twitch force was reached. Contractile kinetics [time to peak (TTP) and half-relaxation time (T50)] were measured from the peak twitch force recordings. After 5 min of equilibration, the lever of the force transducer was set to maximum rigidity (∼500 mN; >100% load) and a tetanic contraction was elicited by stimulating the bundle with supra-maximal voltage at 100 Hz for 300 ms. The peak isometric force (F*max*) was established allowing determination of 100% load for isotonic assessments. Shortening contractions were elicited in incremental steps ranging from 0 to 100% load with 1 min rest between each step. Peak shortening velocity (V*max*) was determined during the initial 30 ms of shortening (see **Figure 1**) as this is when velocity is greatest (Watchko et al., 1997; Van Lunteren et al., 2007; Van Lunteren and Pollarine, 2010). Power was determined at each step as the product of force/cross-sectional area (CSA) *x* shortening velocity/Lo. Peak specific work (W*max*) was calculated as force/CSA *x* shortening (L/Lo) at the load where the product of these variables was greatest.

Isotonic Function Data Analysis

Muscle cross-sectional area (CSA) was calculated as the blotted dry muscle bundle weight divided by the product of Lo and the specific density which was assumed to be 1.056 g/cm^3. Specific force was calculated as N/cm^2. Specific shortening velocity was calculated as Lo/s. Specific power was calculated as Watts/cm^2. W*max* was calculated as Joules/cm^3.

Statistical Analyses

Statistical comparisons of the total mean fluorescence intensity for 1D preparations and FTSC/IAF- and coomassie-labeled spot volumes (2D) were measured using Student *t*-tests, Mann-Whitney *U*-tests, or One-Way ANOVA as appropriate after testing for normality and equal variance in the data sets. Student *t*-test or Mann-Whitney *U*-test was used as appropriate to compare control and CH groups for chymotrypsin-like activity of the 20S proteasome, and GAPDH and LDH activities. Tissue limitations restricted the measurement of all molecular components at all three time points of CH exposure. HIF-1α content and p-MAPK contents were compared between groups by One-Way

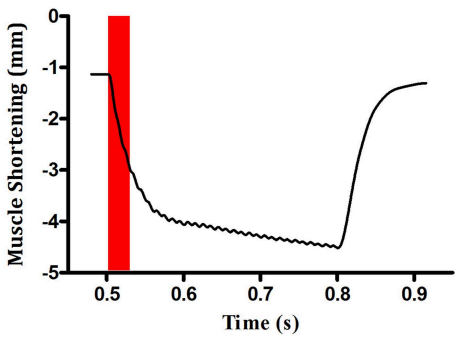

FIGURE 1 | Representative profile of sternohyoid peak shortening velocity. An original record illustrating a representative contraction at 0% load. Maximum velocity of shortening was calculated during the first 30 ms of the contraction.

ANOVA followed by Tukey's multiple comparison *post-hoc* test, or the Kruskal-Wallis test followed by Dunn's multiple comparison *post-hoc* test as appropriate, after testing for normality and equal variance in the data sets. Statistical comparisons were performed between groups for sternohyoid contractile and endurance performance using One-Way ANOVA followed by Tukey's multiple comparison *post-hoc* tests. Power-load relationship was assessed by Two-Way ANOVA followed by Bonferroni's *post-hoc* multiple comparison tests. Linear regression analysis was performed to assess the relationship between oxidative stress markers (protein free thiol and carbonyl groups) and sternohyoid muscle power. $P < 0.05$ was the criterion for statistical significance in all tests.

Results

Animal Model

Hematocrit was significantly ($p < 0.001$) increased by CH exposure (**Table 1**). Antioxidant supplementation in animals exposed to 6 weeks of CH had no effect on hematocrit compared to CH alone. Animals drank equivalent volumes of water (with or without antioxidant) per day. Body mass decreased after 1 week of CH exposure but all hypoxic animals returned to a growth curve equivalent to the control animals for weeks two through to six of the gas treatments (data not shown).

Total Protein Carbonyl and Free Thiol Content

Significant increases in sternohyoid carbonyl content were observed after 3 ($p < 0.001$) and 6 ($p < 0.001$) weeks of CH (**Figure 2A**)—indicative of increased sternohyoid protein oxidation. Sternohyoid protein free thiol content changes were bi-phasic (**Figure 2B**). There was a significant increase in sternohyoid protein free thiol content after 1 ($p < 0.05$) and 3 ($p < 0.01$) weeks of CH; however free thiol content was significantly lower than control after 6 weeks of CH ($p < 0.001$). For comparison, two limb muscles, namely soleus, and extensor digitorum longus (EDL) were also studied. Unlike the sternohyoid, there were no significant changes to the carbonyl content of the EDL proteome after CH exposure (**Figure 3A**). There was, however, significant increases in EDL free thiol content after 1 ($p < 0.01$), 3 ($p < 0.001$), and 6 ($p < 0.001$) weeks of CH—though the magnitude of the increase is seen to decrease over time (**Figure 3B**). Similar to the sternohyoid muscle, but unlike the EDL, significant increases in soleus protein carbonyl content were observed after 3 ($p < 0.05$), and 6 ($p < 0.01$) weeks of CH (**Figure 4A**). Soleus protein free thiol content was significantly increased after 1 ($p < 0.001$), 3 ($p < 0.01$), and 6 ($p < 0.001$) weeks of CH compared to controls (**Figure 4B**). Consistent with EDL, there was a decline in increased free thiol content in the soleus with progressive CH.

TABLE 1 | Hematocrit values after 1, 3, or 6 weeks of normoxia or chronic sustained hypoxia (CH).

	Normoxia	CH	*P*-value[a]
HEMATOCRIT (%)			
One Week	34 ± 2	52 ± 2	$P < 0.001$
Three Weeks	38 ± 1	65 ± 1	$P < 0.001$
Six Weeks	32 ± 1	62 ± 1	$P < 0.001$

Data are presented as mean ± SEM; n = 8 per group. [a]Student unpaired t-test.

2D Redox Proteomics

In the sternohyoid, 498, 264, and 996 resolved spots were matched in FTSC-, IAF-labeled and coomassie-stained separations respectively. A significant relative volume difference was observed in 87 FTSC, 51 IAF, and 156 coomassie spots comparing control and CH groups ($p < 0.05$). Proteins were selected for mass spectrometry analysis based on separation, resolution, abundance, and overlap in fluorescence-stain and muscle separations. Protein smears and gel defects were excluded. Results for protein remodeling are presented in **Table 2** with proteins grouped according to cellular location and/or function. Selected spots can be visualized on the representative coomassie stained gel shown in **Figure 5**. A change in FTSC and IAF fluorescence

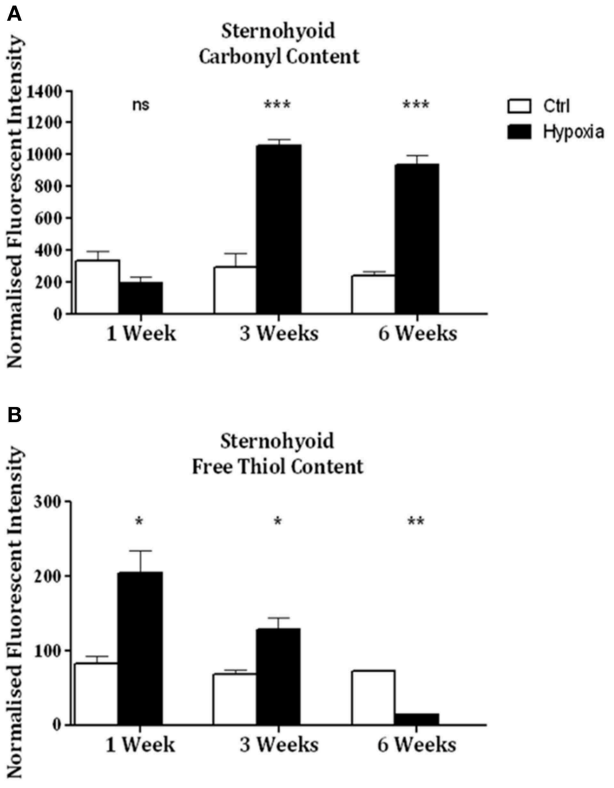

FIGURE 2 | Sternohyoid protein carbonyl and free thiol content after 1, 3, and 6 weeks of sustained hypoxia compared to normoxic controls. **(A)** Sternohyoid protein carbonyl content (mean ± SEM) after 1, 3, and 6 weeks of normoxia or sustained hypoxia expressed as normalized fluorescence intensity; $n = 5$–8 per group; **(B)** Sternohyoid protein free thiol content (mean ± SEM) after 1, 3, and 6 weeks of normoxia or sustained hypoxia expressed as normalized fluorescence intensity; $n = 7$–8 per group; $^{*}p < 0.05$, $^{**}p < 0.01$, $^{***}p < 0.001$, ns, not significant; Student *t*-test or Mann-Whitney test as appropriate. Ctrl, normoxic control; Hypoxia, sustained hypoxia ($FiO_2 = 0.1$).

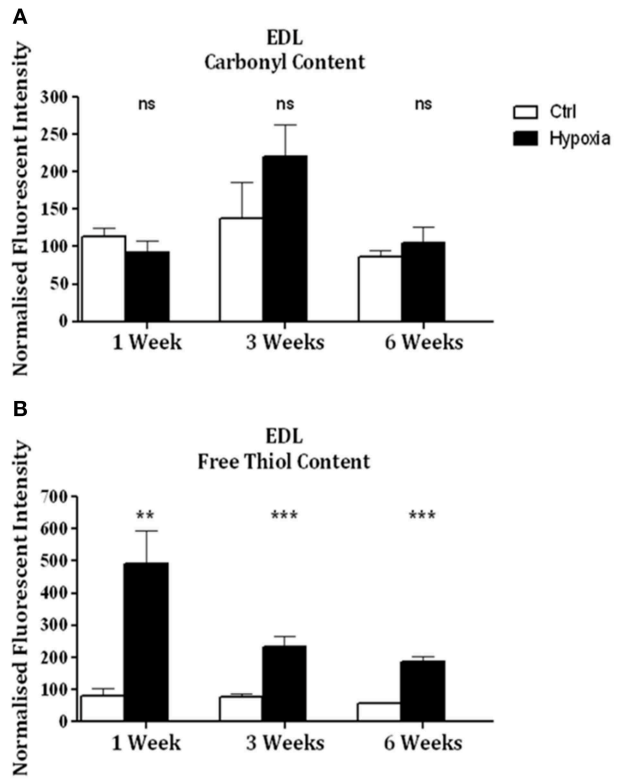

FIGURE 3 | EDL protein carbonyl and free thiol content after 1, 3, and 6 weeks of sustained hypoxia compared to normoxic controls. (A) EDL protein carbonyl content (mean ± SEM) after 1, 3, and 6 weeks of sustained hypoxia expressed as normalized fluorescence intensity; $n = 4$–8 per group; **(B)** EDL protein free thiol content (mean ± SEM) after 1, 3, and 6 weeks of sustained hypoxia expressed as normalized fluorescence intensity; $n = 6$–8 per group; $^{**}p < 0.01$, $^{***}p < 0.001$, ns, not significant; Student *t*-test or Mann-Whitney test as appropriate; Ctrl, normoxic control; Hypoxia, sustained hypoxia ($FiO_2 = 0.1$).

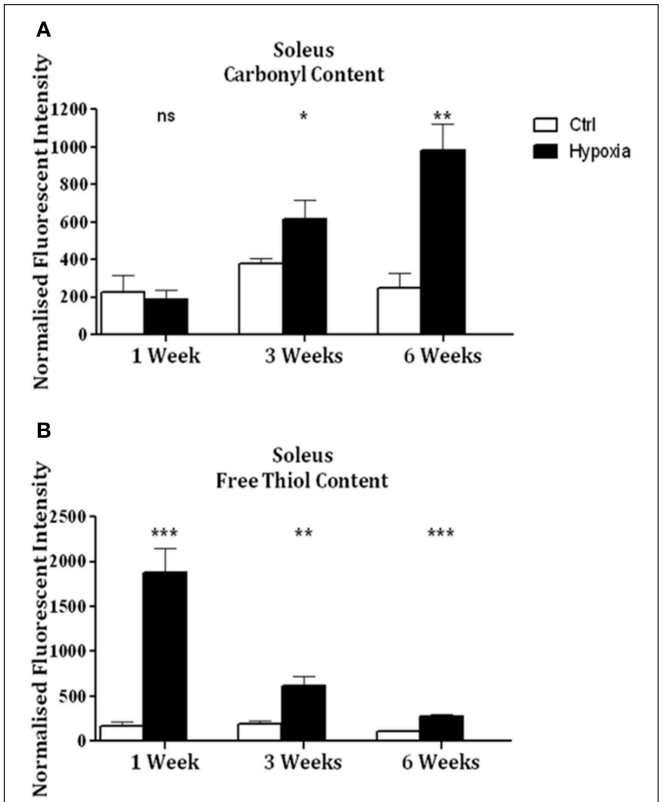

FIGURE 4 | Soleus protein carbonyl and free thiol content after 1, 3, and 6 weeks of sustained hypoxia compared to normoxic controls. (A) Soleus protein carbonyl content (mean ± SEM) after 1, 3, and 6 weeks of sustained hypoxia expressed as normalized fluorescence intensity; $n = 4$–8 per group; **(B)** Soleus protein free thiol content (mean ± SEM) after 1, 3, and 6 weeks of sustained hypoxia expressed as normalized fluorescence intensity; $n = 8$ per group; $^{*}p < 0.05$, $^{**}p < 0.01$, $^{***}p < 0.001$, ns, not significant; Student *t*-test or Mann-Whitney test as appropriate; Ctrl, normoxic control; Hypoxia, sustained hypoxia ($FiO_2 = 0.1$).

intensity signal independent of, or differential to, coomassie signal is indicative of protein redox remodeling.

Sternohyoid Glycolytic Enzyme Activities

Sternohyoid GAPDH activity was significantly increased after 1 week of CH ($p < 0.05$) but significantly decreased after 3 weeks of CH ($p < 0.01$) (data not shown). LDH activity in the sternohyoid (data not shown) was significantly increased after 1 week of CH ($p < 0.05$).

Sternohyoid Chymotrypsin-like Proteasome Activity

Chymotrypsin-like proteasome activity was unchanged in the sternohyoid after 6 weeks of CH (data not shown).

Sternohyoid HIF-1α Content

There was no change in sternohyoid HIF-1α content following 6 weeks of CH with or without antioxidant supplementation (data not shown).

Sternohyoid Phospho-MAPK Content

There was no change in sternohyoid p-p38 content following 6 weeks of CH with or without antioxidant supplementation (**Figure 6A**). However, 6 weeks of CH significantly decreased sternohyoid p-JNK content compared to control (One-Way ANOVA ($p < 0.01$) followed by Tukey's multiple comparison test ($p < 0.05$); chronic antioxidant supplementation with either tempol or NAC did not prevent this (**Figure 6B**). A similar effect was observed for sternohyoid p-ERK1/2 content. A Kruskal-Wallis test revealed a significant difference in the mean values of the groups. However, Dunn's multiple comparisons test revealed no significant differences between pairs (**Figure 6C**).

Sternohyoid Protein Carbonyl and Free Thiol Content after Antioxidant Treatment

In the second cohort of animals, significant increases in sternohyoid protein carbonyl content were again observed after 6 weeks of CH ($p < 0.001$). Chronic antioxidant supplementation with either Tempol ($p < 0.001$) or NAC ($p < 0.001$) significantly ameliorated the CH-induced increase in protein carbonyl content

TABLE 2 | Identifications by mass spectrometry of proteins undergoing significant redox remodeling in the sternohyoid muscle after 6 weeks of sustained hypoxia.

Spot #	Protein	Mw (Da)	GI number	Mascot score	Matched peptides	Sequence coverage	Carbonyl *p*-value, fold	Free thiol *p*-value, fold	Expression *p*-value, fold
ELECTRON TRANSPORT CHAIN									
1	Cytochrome bc - 1 complex subunit 1	52,819	341941780	430	6	26%	-	<0.01, −1.4	<0.001, −2
2	ATP Synthase subunit α	59,716	416677	997	6	53%	-	-	<0.01, +1.5
TCA CYCLE									
3	Aconitase hydratase	85,410	60391212	1210	11	41%	<0.01, +1.4	<0.001, −2	<0.01, −2.6
4	2-oxo-glutarate dehydrogenase, mt	116,375	146345472	477	4	22%	-	<0.01, −2.4	<0.01, +2.8
GLYCOLYSIS									
5	Fructose bis-phosphate aldolase A	39,331	113607	588	3	70%	-	<0.01, −2.9	-
6	Glyceraldehyde-3-phosphate dehydrogenase	35,787	120702	531	4	48%	-	<0.01, −1.6	<0.001, −2
7	Phosphoglycerate kinase 1	44,534	1730519	534	4	45%	-	-	<0.01,+1.7
8	Phosphoglycerate mutase 2	28,809	6093745	1010	9	57%	-	-	<0.01, +1.7
9	Pyruvate kinase isozymes M1/M2	57,305	146345448	837	6	53%	<0.01, −1.2	-	<0.01, +1.3
PHOSPHAGEN AND LIPID METABOLISM									
10	Glycerol-3-phosphate dehydrogenase [NAD(+)]	37,548	121557	412	3	48%	-	<0.01, −2	<0.01, −2.6
11	Creatine kinase m-type	43,014	124056470	784	7	42%	<0.01, +1.2	-	<0.01, −1.2
STRESS RESPONSE AND IRON HOMEOSTASIS									
12	Glycogen phosphorylase	97,225	14916635	1450	13	47%	<0.01, −1.3	-	<0.01, +4.1
13	90kDa heat shock protein	83,229	341941065	742	6	31%	-	-	<0.01, −1.3
14	Alpha crystallin B chain	20,056	6166129	761	7	65%	<0.01, +1.2	-	-
15	Myoglobin	17,059	127676	923	7	43%	-	-	<0.01, −1.7
16	Serotransferrin	76,674	21363012	121	1	17%	<0.01, −1.4	<0.01, +1.8	-
17	Carbonic anhydrase III	29,348	30581036	966	8	71%	<0.01, +1.2	<0.01, -2.7	<0.01, +1.9
18	Albumin	68,648	5915682	1340	11	53%	-	-	<0.01, −1.8
CROSS-BRIDGE AND SARCOPLASMIC RETICULUM									
19	Calsequestrin	46,420	341940315	543	4	19%	<0.01, −1.5	-	<0.01, −2.3

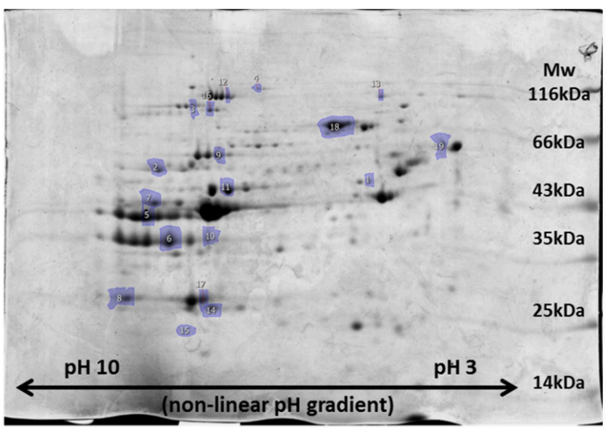

FIGURE 5 | Representative image of 2D-PAGE sternohyoid muscle protein profile after coomassie staining of proteins. A molecular mass marker ranging from 14 to 116 kDa is shown for size reference and isoelectric point is indicated along the range pH 10-3. Spot numbers match those presented in **Table 2**.

(**Figure 7A**). Similarly, sternohyoid protein free thiol content was significantly lower than control after 6 weeks of CH ($p < 0.01$) and antioxidant treatment with Tempol ($p < 0.001$) and NAC ($p < 0.05$) ameliorated this effect (**Figure 7B**).

Sternohyoid Muscle Function

There are no significant differences observed across groups for contractile kinetics, twitch force, V*max*, W*max*, or isotonic fatigue index (**Table 3**) as determined by One-Way ANOVA or Kruskal-Wallis test; however, CH exposure increased the contraction time, and decreased endurance (**Table 3**). NAC supplementation in CH increased peak twitch force, V*max*, W*max*, and endurance (**Table 3**). Fmax is significantly different across groups; decreased in CH compared to control and significantly increased by NAC supplementation in CH compared to CH alone as revealed by Tukey's multiple comparison *post-hoc* test (**Table 3**).

Sternohyoid muscle isotonic contractile function (power) was significantly depressed by CH exposure (**Figure 8**; Two-Way ANOVA: gas treatment: $p < 0.001$). Significant correlations were observed for oxidative stress markers and sternohyoid muscle function (**Figure 9**). The deleterious effects of CH exposure on sternohyoid function were prevented with antioxidant supplementation in CH using either tempol or NAC (**Figure 8**).

Discussion

This is the first study to identify proteins in an upper airway muscle undergoing redox remodeling following exposure to CH. CH decreased sternohyoid force- and power-generating

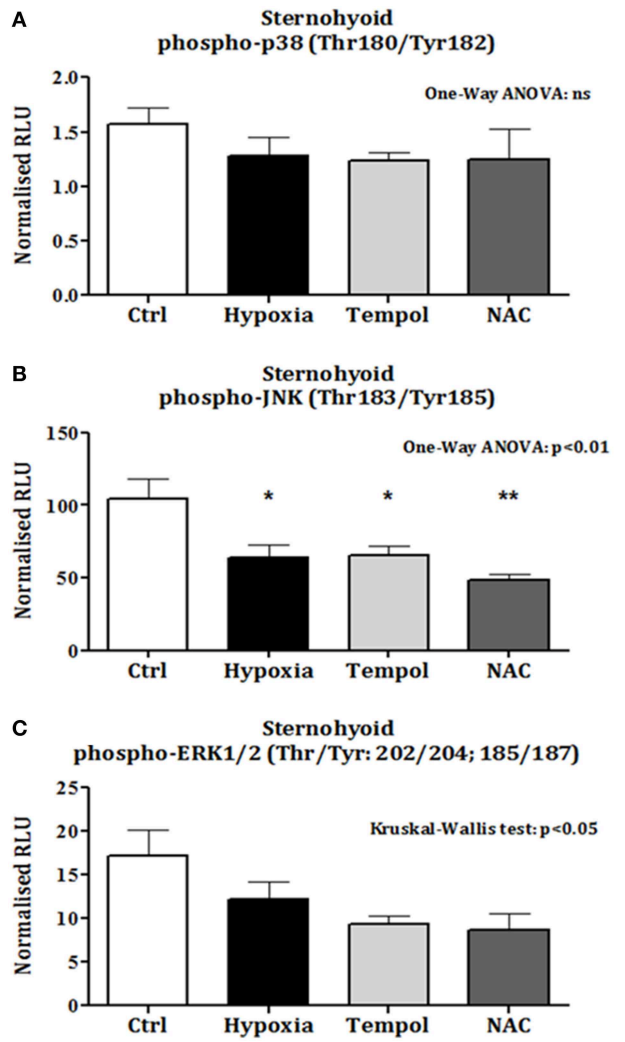

FIGURE 6 | Sternohyoid phospho-MAPK contents after 6 weeks of normoxia and sustained hypoxia ± chronic antioxidant supplementation. (A) Sternohyoid phospho-p38 content (mean ± SEM) expressed as normalized relative luminescence units; $n = 5$–7 per group; **(B)** Sternohyoid phospho-JNK content (mean ± SEM expressed as normalized relative luminescence units; $n = 5$–7 per group; **(C)** Sternohyoid phospho-ERK 1/2 content (mean ± SEM) expressed as normalized relative luminescence units; $n = 5$–7 per group; $^{*}p < 0.05$ and $^{**}p < 0.01$ vs. control, Tukey's multiple comparison test; Ctrl, normoxic control; Hypoxia, sustained hypoxia ($FiO_2 = 0.1$); Tempol, tempol + sustained hypoxia; NAC, NAC + sustained hypoxia; RLU, relative luminescence units.

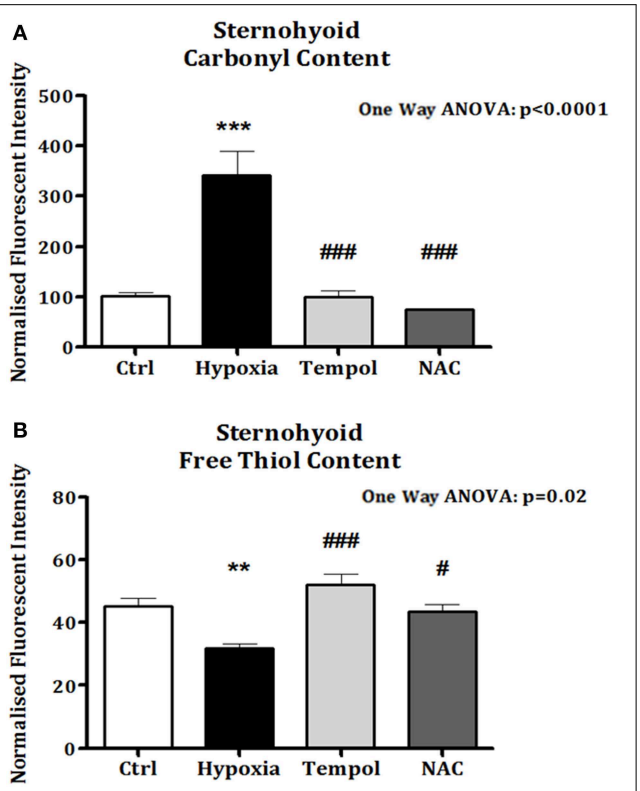

FIGURE 7 | Sternohyoid protein carbonyl and free thiol content following 6 weeks of normoxia and sustained hypoxia ± chronic antioxidant supplementation. (A) Sternohyoid protein carbonyl content (mean ± SEM) expressed as normalized fluorescence intensity; $n = 5$–7 per group; **(B)** Sternohyoid protein free thiol content (mean ± SEM) expressed as normalized fluorescence intensity; $n = 5$–7 per group; $^{**}p < 0.05$ and $^{***}p < 0.001$ vs. control, $^{\#}p < 0.05$ and $^{\#\#\#}p < 0.001$ vs. hypoxia, Tukey's multiple comparison test; Ctrl, normoxic control; Hypoxia, sustained hypoxia ($FiO_2 = 0.1$); Tempol, tempol + sustained hypoxia; NAC, NAC + sustained hypoxia.

capacity. Antioxidant supplementation prevented CH-induced sternohyoid dysfunction. The main findings of this study are: (1) CH induces temporal changes in protein carbonylation and free thiol oxidation in the sternohyoid, responses different to that seen in limb muscles; (2) Proteins key to muscle contraction, metabolism, and homeostasis are redox-modified in the sternohyoid following 6 weeks of CH; (3) Glycolytic enzyme activities are temporally affected in the sternohyoid following progressive CH exposure; (4) CH has no effect on sternohyoid HIF-1α content; (5) CH decreases p-JNK in sternohyoid independent of antioxidant status; (6) CH causes sternohyoid muscle dysfunction; (7) Oxidative stress markers and muscle function were significantly correlated; (8) Both protein oxidation and contractile impairment following CH are fully reversed by chronic antioxidant supplementation.

Muscle Redox Status

In skeletal muscle adaptation to high altitude and respiratory diseases featuring hypoxia, ROS have been shown to cause protein redox remodeling and to modify protein function with resultant changes in metabolic processes, homeostasis and contractile performance (Zuo and Clanton, 2005; Marin-Corral et al., 2009; Murray, 2009; Chaudhary et al., 2012; Levine et al., 2013; Puig-Vilanova et al., 2015). However, the cause and motive for increased ROS production is unclear and may differ in skeletal muscles given their varied functional roles. In the present study, we observed time-dependent increases in protein oxidation (both increased carbonyl content and decreased free thiol content) in CH-exposed sternohyoid muscle (differential to responses in limb muscles, which is likely pivotal for time-dependent and

TABLE 3 | Sternohyoid muscle contractile properties after 6 weeks of normoxia and sustained hypoxia ± chronic antioxidant supplementation.

	Normoxia	Hypoxia	Tempol	NAC	*P*-Value[a]
TTP (ms)	9 ± 0	10 ± 0	11 ± 1	10 ± 0	ns
T50 (ms)	11 ± 1	11 ± 1	14 ± 3	12 ± 2	ns
Pt (N/cm^2)	2.5 ± 0.4	1.6 ± 0.2	1.9 ± 0.2	3.0 ± 0.9	ns
Fmax (N/cm^2)	12.3 ± 1.5	8.0 ± 0.6*	11.0 ± 0.3	16.0 ± 2.3##	<0.01
Vmax (Lo/s)	5.4 ± 0.7	5.2 ± 0.9	6.1 ± 0.7	6.1 ± 0.4	ns
Wmax (J/cm^3)	0.6 ± 0.1	0.6 ± 0.1	0.8 ± 0.1	0.9 ± 0.1	ns
Fatigue Index (% of initial power)	63 ± 14	36 ± 7	33 ± 11	46 ± 12	ns

*Data are presented as mean ± SEM; n = 5–8 per group; [a]One Way ANOVA, *p < 0.05 vs. Normoxia and ##p 0.01 vs. Hypoxia, Tukey's post-hoc multiple comparison test; ns, not significant; Hypoxia, 6 weeks of sustained hypoxia (FiO_2 = 0.1); Tempol, tempol + hypoxia; NAC, NAC + hypoxia.*

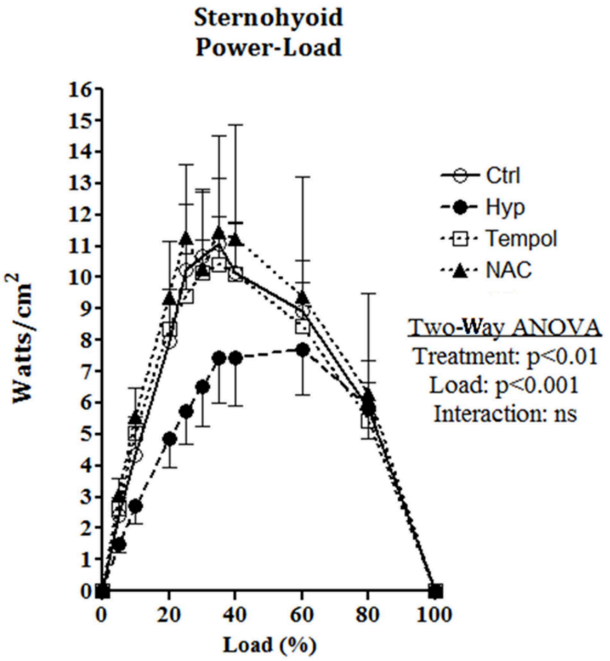

FIGURE 8 | Sternohyoid power-load relationship following 6 weeks of normoxia and sustained hypoxia ± chronic antioxidant supplementation. Sternohyoid specific power (mean ± SEM) expressed as Watts/CSA (cm^2) as a function of load expressed as a percentage of peak force (force/peak force*100); *n* = 5–7 per group; Ctrl, normoxic control; Hyp, sustained hypoxia (FiO_2 = 0.1); Tempol, tempol + sustained hypoxia; NAC, NAC + sustained hypoxia. *P*-values shown for two factor (treatment × load) analysis of variance highlighting a significant effect of 6 weeks of sustained hypoxia on sternohyoid power-load relationship. Antioxidant supplementation reversed the effects of hypoxia.

differential structural and functional remodeling reported in previous studies (El-Khoury et al., 2003, 2012; Faucher et al., 2005; Gamboa and Andrade, 2010, 2012; McMorrow et al., 2011; Carberry et al., 2014). This, in turn, may be of clinical significance given that CH is potentially implicated in the progression of respiratory diseases.

Clearly there is differential muscle protein redox remodeling which appears unrelated to fiber type *per se* given the similarities between the EDL and sternohyoid muscles, and unrelated to respiratory vs. limb muscle differences *per se* given the differences observed in the EDL compared with the soleus. As the soleus is a postural muscle, it exhibits greater contractile activity than the EDL which is used for more powerful movements of the limbs. The combination of activity and hypoxic exposure is potentially synergistic in driving protein oxidation, with reflex hyperventilation and hypoxia combining to drive protein oxidation in the sternohyoid. Furthermore, a comparison of basal carbonyl signals from sternohyoid and limb muscle proteomes suggests that basal workload of a given muscle is more important in determining carbonylation of proteins than fiber type *per se*.

2D redox proteomic profiling of the sternohyoid muscle after 6 weeks of CH exposure reveals key proteins in muscle that are targeted by ROS, many of which are redox modified in COPD muscle (Marin-Corral et al., 2009). It is clear from **Table 2** that extensive remodeling occurs to mitochondrial, metabolic, and associated proteins, suggesting that the mitochondria are the primary source of remodeling stress. Reflex hyperventilation increases metabolic demand and subsequent metabolic substrate flux to the respiratory chain. With hypoxia, stockpiling of electrons occurs, increasing electron leak and subsequent ROS formation. This is supported by the findings of decreased muscle mitochondrial density and mitochondrial remodeling in hypoxia, high altitude, and respiratory-related diseases (Hoppeler et al., 1990, 2003; Gosker et al., 2000; Wijnhoven et al., 2006; Viganò et al., 2008; Gamboa and Andrade, 2010, 2012). The fold change in free thiol content following 1 week of CH is greatest in soleus>EDL>sternohyoid suggesting that fiber type, more so than contractile activity, is key to this change.

EDL free thiol content remains elevated above control whereas carbonyl content was unchanged after 6 weeks of CH; however the pattern of change is similar to the sternohyoid and soleus muscles. It is likely to be a combination of hypoxia, muscle fiber composition, and workload in hypoxia that accounts for the differential changes in respiratory and limb muscle protein oxidation and functional changes. In keeping with the notion of muscle specific effects of CH, other studies have reported differential effects of oxidation, based on carbonyl and thiol measurements as well as other indicators of altered cellular oxidative/reductive state which are proposed to depend on the activity and/or local cellular environment of the relevant protein (Haycock et al., 1998; Kadiiska et al., 2005; El-Shafey et al., 2011). See additional discussion in the supplementary file.

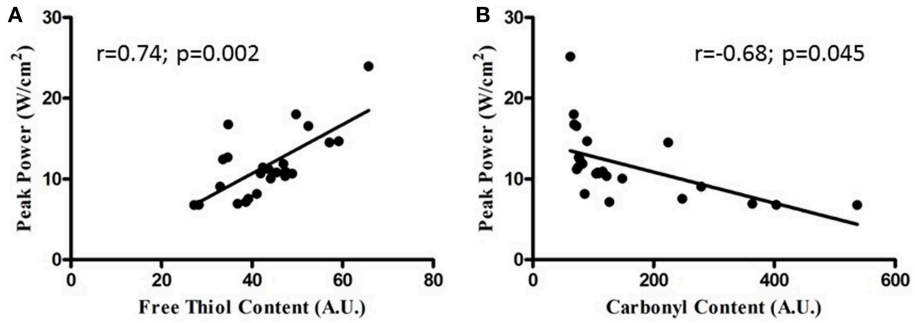

FIGURE 9 | Relationship between sternohyoid power and oxidative stress markers. Relationship between sternohyoid specific peak power and muscle oxidative stress markers [protein free thiol content **(A)** and carbonyl content **(B)**] plotting data from all animals in the second cohort of studies; $n = 24$. Note the correlation coefficients and statistically significant relationships.

Muscle Redox Signaling

Decreased sternohyoid GAPDH activity with progressive hypoxia is consistent with the decreased expression measured by proteomic profiling after 6 weeks of CH. CH-induced changes in LDH activity in the sternohyoid follow a similar pattern to GAPDH. As muscle function and metabolism are intrinsically interlinked through HIF signaling (Semenza et al., 1994; Vogt et al., 2001; Kim et al., 2006), one might have expected a CH-induced increase in HIF-1α content. However, decreased GAPDH expression and decreased GAPDH and LDH activities observed in the sternohyoid muscle of our mouse model are suggestive of decreased HIF-1α content. Interestingly, after 6 weeks of CH exposure we observed that there was no change in sternohyoid HIF-1α content. It is plausible that the degree of hypoxia experienced by the sternohyoid may change temporally with acclimatization to hypoxia such that HIF-1α may have been activated earlier in the exposure. Of note, for example, GAPDH activity is increased in sternohyoid muscle after 1 but not 3 weeks of CH. Protein carbonylation is elevated in CH sternohyoid after 6 weeks suggesting that although ROS are presumably elevated in the muscle there is no ROS-dependent HIF-1α activation. Moreover, antioxidant supplementation did not affect HIF-1α content in CH sternohyoid. Thus, our results suggest that redox modulation of sternohyoid metabolism and function is HIF-1α independent.

The MAPK proteins are involved in a diverse array of cellular signaling events and are vital to muscle growth and homeostasis. p38 activity in muscle is strongly associated with promoting atrophy in COPD limb muscle (Lemire et al., 2012) and is potentially required for hypoxia signaling of HIF via mitochondrial ROS production (Emerling et al., 2005). However, neither HIF-1α content nor chymotrypsin-like 20S proteasome activity changed in the sternohyoid muscle following CH. Indeed, hypertrophy of fast fibers in the sternohyoid is reported following CH exposure in the rat (McMorrow et al., 2011) suggesting enhanced protein synthesis. This is especially interesting, as the present study has established for the first time, that the CH sternohyoid has decreased (not increased) power-generating capacity, highlighting a potent redox-dependent inhibitory effect of CH on the contractile machinery of the airway dilator muscle, rather than CH-induced muscle atrophy.

p-JNK content is decreased in the sternohyoid following CH exposure. Differential regulation of p38 and JNK occurs at the MAP2K level and is potentially influenced by contractile activity and mechanical stress (Sawada et al., 2001). The combination of hypoxic/redox stress, muscle fiber type combination, and mechanical activity of the sternohyoid is likely important in determining the stress kinase response to CH exposure. A ROS/p-JNK-dependent mechanism is implicated in CH-induced sternohyoid dysfunction but it is important to note that antioxidant supplementation did not prevent the CH-induced decrease in p-JNK (or p-ERK1/2), whereas antioxidants prevented sternohyoid redox stress and contractile dysfunction following CH exposure.

Sternohyoid Isotonic Performance

The sternohyoid force- and power-generating capacity was significantly depressed by CH exposure. Muscle oxidative stress markers and contractile power were significantly correlated; moreover, antioxidant supplementation during CH exposure prevented both protein redox stress and contractile dysfunction. Therefore, we posit that CH-induced redox remodeling of key proteins in metabolism and the contractile apparatus is central to CH-induced sternohyoid muscle dysfunction. Concerning the potential clinical relevance of our findings, sternohyoid dysfunction could serve to increase obstructive airway events *in vivo*—further disrupting respiratory homeostasis in diseases characterized by hypoxic stress. We speculate that CH-induced redox remodeling and functional deficit in pharyngeal dilator muscles potentially underpins the higher prevalence of OSA observed in COPD patients (the overlap syndrome) (Owens and Malhotra, 2010).

Summary and Conclusions

This study highlights the application of a redox proteomics approach to a translational animal model of hypoxia. CH exposure causes progressive redox remodeling in the sternohyoid (upper airway dilator) muscle with differential responses to limb muscles. CH results in metabolic protein structural remodeling

with resultant changes in enzyme activity. Redox and expression changes were shown to occur to various protein chaperones including those important to cross-bridge maintenance. Ultimately, it appears that CH-induced redox changes result in functional deficit in the sternohyoid, given that antioxidant supplementation during CH exposure prevents both protein stress and functional impairment. We hypothesize a pivotal role for ROS in pharyngeal dilator muscle structural and functional (mal)adaptations to CH. The putative role of hypoxia in driving respiratory muscle remodeling in human respiratory disease warrants investigation.

Author Contributions

The study was conceived and designed by PL and KO. Experiments and data analyses were performed by PL in the laboratories of KO and DS. Mass spectrometry experiments were performed and analyzed by RS in the laboratory of AV. The manuscript was written by PL and KO with contributions from the other authors.

Acknowledgments

This project was funded by The Health Research Board (Ireland), and by the Strategic Research Fund, University College Cork, Ireland.

Supplementary Material

The Supplementary Material for this article can be found online at: http://journal.frontiersin.org/article/10.3389/fphys.2015.00122/abstract

References

Aiken, C. T., Kaake, R. M., Wang, X., and Huang, L. (2011). Oxidative stress-mediated regulation of proteasome complexes. *Mol. Cell. Proteomics* 10, R110.006924. doi: 10.1074/mcp.R110.006924

Bradford, A., McGuire, M., and O'Halloran, K. D. (2005). Does episodic hypoxia affect upper airway dilator muscle function? Implications for the pathophysiology of obstructive sleep apnoea. *Respir. Physiol. Neurobiol.* 147, 223–234. doi: 10.1016/j.resp.2005.04.001

Carberry, J. C., McMorrow, C., Bradford, A., Jones, J. F. X., and O'Halloran, K. D. (2014). Effects of sustained hypoxia on sternohyoid and diaphragm muscle during development. *Eur. Respir. J.* 43, 1149–1158. doi: 10.1183/09031936.00139512

Chaudhary, P., Suryakumar, G., Prasad, R., Singh, S. N., Ali, S., and Ilavazhagan, G. (2012). Chronic hypobaric hypoxia mediated skeletal muscle atrophy: role of ubiquitin-proteasome pathway and calpains. *Mol. Cell. Biochem.* 364, 101–113. doi: 10.1007/s11010-011-1210-x

Cole, C., Coelho, A. V., James, R. H., Connelly, D., and Sheehan, D. (2014). Proteomic responses to metal-induced oxidative stress in hydrothermal vent-living mussels, Bathymodiolus sp., on the Southwest Indian Ridge. *Mar. Env. Res.* 96, 29–37. doi: 10.1016/j.marenvres.2013.09.003

Dalle-Donne, I., Aldini, G., Carini, M., Colombo, R., Rossi, R., and Milzani, A. (2006). Protein carbonylation, cellular dysfunction, and disease progression. *J. Cell. Mol. Med.* 10, 389–406. doi: 10.1111/j.1582-4934.2006.tb00407.x

Doucet, M., Debigaré, R., Joanisse, D. R., Côté, C., Leblanc, P., Grégoire, J., et al. (2004). Adaptation of the diaphragm and the vastus lateralis in mild-to-moderate COPD. *Eur. Respir. J.* 24, 971–979. doi: 10.1183/09031936.04.00020204

Doucet, M., Dubé, A., Joanisse, D. R., Debigaré, R., Michaud, A., Paré, M.-È., et al. (2010). Atrophy and hypertrophy signalling of the quadriceps and diaphragm in COPD. *Thorax* 65, 963–970. doi: 10.1136/thx.2009.133827

Dyballa, N., and Metzger, S. (2009). Fast and sensitive colloidal coomassie G-250 staining for proteins in polyacrylamide gels. *J. Vis. Exp.* 30:e1431. doi: 10.3791/1431

Edge, D., Jones, J. F. X., Bradford, A., and O'Halloran, K. D. (2012). Effect of chronic intermittent hypoxia on reflex recruitment of sternohyoid EMG during airway obstruction in the anaesthetised rat. *Proc Physiol Soc* 27, PC223.

Edge, D., McDonald, F. B., Jones, J. F. X., Bradford, A., and O'Halloran, K. D. (2014). Effect of chronic intermittent hypoxia on the reflex recruitment of the genioglossus during airway obstruction in the anesthetized rat. *Prog. Brain Res.* 209, 147–168. doi: 10.1016/B978-0-444-63274-6.00008-4

El-Khoury, R., Bradford, A., and O'Halloran, K. D. (2012). Chronic hypobaric hypoxia increases isolated rat fast-twitch and slow-twitch limb muscle force and fatigue. *Physiol. Res.* 61, 195–201.

El-Khoury, R., O'Halloran, K. D., and Bradford, A. (2003). Effects of chronic hypobaric hypoxia on contractile properties of rat sternohyoid and diaphragm muscles. *Clin. Exp. Pharmacol. Physiol.* 30, 551–554. doi: 10.1046/j.1440-1681.2003.03874.x

El-Shafey, A. F., Armstrong, A. E., Terrill, J. R., Grounds, M. D., and Arthur, P. G. (2011). Screening for increased protein thiol oxidation in oxidatively stressed muscle tissue. *Free Radic. Res.* 45, 991–999. doi: 10.3109/10715762.2011.590136

Emerling, B. M., Platanias, L. C., Black, E., Nebreda, A. R., Davis, R. J., and Chandel, N. S. (2005). Mitochondrial reactive oxygen species activation of p38 mitogen-activated protein kinase is required for hypoxia signaling. *Mol. Cell. Biol.* 25, 4853–4862. doi: 10.1128/MCB.25.12.4853-4862.2005

Faucher, M., Guillot, C., Marqueste, T., Kipson, N., Mayet-Sornay, M.-H., Desplanches, D., et al. (2005). Matched adaptations of electrophysiological, physiological, and histological properties of skeletal muscles in response to chronic hypoxia. *Pflügers Arch.* 450, 45–52. doi: 10.1007/s00424-004-1370-6

Gamboa, J. L., and Andrade, F. H. (2010). Mitochondrial content and distribution changes specific to mouse diaphragm after chronic normobaric hypoxia. *Am. J. Physiol. Regul. Integr. Comp. Physiol.* 298, R575–R583. doi: 10.1152/ajpregu.00320.2009

Gamboa, J. L., and Andrade, F. H. (2012). Muscle endurance and mitochondrial function after chronic normobaric hypoxia: contrast of respiratory and limb muscles. *Pflügers Arch.* 463, 327–338. doi: 10.1007/s00424-011-1057-8

Gosker, H. R., Wouters, E. F., van der Vusse, G. J., and Scholsa, M. (2000). Skeletal muscle dysfunction in chronic obstructive pulmonary disease and chronic heart failure: underlying mechanisms and therapy perspectives. *Am. J. Clin. Nutr.* 71, 1033–1047.

Haycock, J. W., Mac Neil, S., and Mantle, D. (1998). Differential protein oxidation in Duchenne and Becker muscular dystrophy. *Neuroreport* 9, 2201–2207. doi: 10.1097/00001756-199807130-00010

Hoppeler, H., Howald, H., and Cerretelli, P. (1990). Human muscle structure after exposure to extreme altitude. *Experientia* 46, 1185–1187. doi: 10.1007/BF01936933

Hoppeler, H., Vogt, M., Weibel, E. R., and Flück, M. (2003). Response of skeletal muscle mitochondria to hypoxia. *Exp. Physiol.* 88, 109–119. doi: 10.1113/eph8802513

Howald, H., Pette, D., Simoneau, J. A., Uber, A., Hoppeler, H., and Cerretelli, P. (1990). Effect of chronic hypoxia on muscle enzyme activities. *Int. J. Sport. Med.* 11(Suppl. 1), S10–S14. doi: 10.1055/s-2007-1024847

Hu, W., Culloty, S., Darmody, G., Lynch, S., Davenport, J., Ramirez-Garcia, S., et al. (2014). Toxicity of copper oxide nanoparticles in the blue mussel, Mytilus edulis: a redox proteomic investigation. *Chemosphere* 108, 289–299. doi: 10.1016/j.chemosphere.2014.01.054

Kadiiska, M. B., Gladen, B. C., Baird, D. D., Germolec, D., Graham, L. B., Parker, C. E., et al. (2005). Biomarkers of oxidative stress study II: are oxidation products of lipids, proteins, and DNA markers of CCl4 poisoning? *Free Radic. Biol. Med.* 38, 698–710. doi: 10.1016/j.freeradbiomed.2004.09.017

Kim, J., Tchernyshyov, I., Semenza, G. L., and Dang, C. V. (2006). HIF-1-mediated expression of pyruvate dehydrogenase kinase: a metabolic switch

required for cellular adaptation to hypoxia. *Cell Metab.* 3, 177–185. doi: 10.1016/j.cmet.2006.02.002

Lemire, B. B., Debigaré, R., Dubé, A., Thériault, M.-E., Côté, C. H., and Maltais, F. (2012). MAPK signaling in the quadriceps of patients with chronic obstructive pulmonary disease. *J. Appl. Physiol.* 113, 159–166. doi: 10.1152/japplphysiol.01518.2011

Levine, S., Bashir, M. H., Clanton, T. L., Powers, S. K., and Singhal, S. (2013). COPD elicits remodeling of the diaphragm and vastus lateralis muscles in humans. *J. Appl. Physiol.* 114, 1235–1245. doi: 10.1152/japplphysiol.01121.2012

Marin-Corral, J., Minguella, J., Ramírez-Sarmiento, A. L., Hussain, S. N. A., Gea, J., and Barreiro, E. (2009). Oxidised proteins and superoxide anion production in the diaphragm of severe COPD patients. *Eur. Respir. J.* 33, 1309–1319. doi: 10.1183/09031936.00072008

McClung, J. M., Whidden, M. A., Kavazis, A. N., Falk, D. J., Deruisseau, K. C., and Powers, S. K. (2008). Redox regulation of diaphragm proteolysis during mechanical ventilation. *Am. J. Physiol. Regul. Integr. Comp. Physiol.* 294, R1608–R1617. doi: 10.1152/ajpregu.00044.2008

McDonald, F. B., Edge, D., and O'Halloran, K. D. (2014). Chronic nitric oxide synthase inhibition does not impair upper airway muscle adaptation to chronic intermittent hypoxia in the rat. *Prog. Brain Res.* 212, 237–251. doi: 10.1016/B978-0-444-63488-7.00012-4

McDonald, F. B., Skelly, J. R., and O'Halloran, K. D. (2015). The β_2-adrenoceptor agonist terbutaline recovers rat pharyngeal dilator muscle force decline during severe hypoxia. *Oral Dis.* 21, e121–e127. doi: 10.1111/odi.12247

McMorrow, C., Fredsted, A., Carberry, J., O'Connell, R. A., Bradford, A., Jones, J. F. X., et al. (2011). Chronic hypoxia increases rat diaphragm muscle endurance and sodium-potassium ATPase pump content. *Eur. Respir. J.* 37, 1474–1481. doi: 10.1183/09031936.00079810

McNicholas, W. T. (2009). Chronic obstructive pulmonary disease and obstructive sleep apnea: overlaps in pathophysiology, systemic inflammation, and cardiovascular disease. *Am. J. Respir. Crit. Care Med.* 180, 692–700. doi: 10.1164/rccm.200903-0347PP

Murray, A. J. (2009). Metabolic adaptation of skeletal muscle to high altitude hypoxia: how new technologies could resolve the controversies. *Genome Med.* 1:117. doi: 10.1186/gm117

O'Halloran, K. D., McGuire, M., O'Hare, T., and Bradford, A. (2002). Chronic intermittent asphyxia impairs rat upper airway muscle responses to acute hypoxia and asphyxia. *Chest* 122, 269–275. doi: 10.1378/chest.122.1.269

O'Connell, R. A., Carberry, J., and O'Halloran, K. D. (2013). Sternohyoid and diaphragm muscle form and function during postnatal development in the rat. *Exp. Physiol.* 98, 1386–1400. doi: 10.1113/expphysiol.2013.073346

O'Halloran, K. D. (2006). Effects of nicotine on rat sternohyoid muscle contractile properties. *Respir. Physiol. Neurobiol.* 150, 200–210. doi: 10.1016/j.resp.2005.05.018

Orozco-Levi, M. (2003). Structure and function of the respiratory muscles in patients with COPD: impairment or adaptation? *Eur. Respir. J. Suppl.* 46, 41s–51s. doi: 10.1183/09031936.03.00004607

Owens, R. L., Eckert, D. J., Yeh, S. Y., and Malhotra, A. (2008). Upper airway function in the pathogenesis of obstructive sleep apnea: a review of the current literature. *Curr. Opin. Pulm. Med.* 14, 519–524. doi: 10.1097/MCP.0b013e3283130f66

Owens, R. L., and Malhotra, A. (2010). Sleep-disordered breathing and COPD: the overlap syndrome. *Respir Care* 55, 1333–1344; discussion: 1344–1346.

Petrof, B. J., Pack, A. I., Kelly, A. M., Eby, J., and Hendricks, J. C. (1994). Pharyngeal myopathy of loaded upper airway in dogs with sleep apnea. *J. Appl. Physiol.* 76, 1746–1752.

Puig-Vilanova, E., Rodriguez, D. A., Lloreta, J., Ausin, P., Pascual-Guardia, S., Broquetas, J., et al. (2015). Oxidative stress, redox signaling pathways, and autophagy in cachectic muscles of male patients with advanced COPD and lung cancer. *Free Radic. Biol. Med.* 79, 91–108. doi: 10.1016/j.freeradbiomed.2014.11.006

Rainville, L.-C., Carolan, D., Varela, A. C., Doyle, H., and Sheehan, D. (2014). Proteomic evaluation of citrate-coated silver nanoparticles toxicity in Daphnia magna. *Analyst* 139, 1678–1686. doi: 10.1039/c3an02160b

Sawada, Y., Nakamura, K., Doi, K., Takeda, K., Tobiume, K., Saitoh, M., et al. (2001). Rap1 is involved in cell stretching modulation of p38 but not ERK or JNK MAP kinase. *J. Cell Sci.* 114, 1221–1227.

Semenza, G. L., Roth, P. H., Fang, H. M., and Wang, G. L. (1994). Transcriptional regulation of genes encoding glycolytic enzymes by hypoxia-inducible factor 1. *J. Biol. Chem.* 269, 23757–23763.

Shortt, C. M., and O'Halloran, K. D. (2014). Hydrogen peroxide alters sternohyoid muscle function. *Oral Dis.* 20, 162–170. doi: 10.1111/odi.12084

Skelly, J. R., Bradford, A., Jones, J. F., and O'Halloran, K. D. (2010). Superoxide scavengers improve rat pharyngeal dilator muscle performance. *Am. J. Respir. Cell Mol. Biol.* 42, 725–731. doi: 10.1165/rcmb.2009-0160OC

Skelly, J. R., Edge, D., Shortt, C. M., Jones, J. F., Bradford, A., and O'Halloran, K. D. (2012a). Respiratory control and sternohyoid muscle structure and function in aged male rats: decreased susceptibility to chronic intermittent hypoxia. *Respir. Physiol. Neurobiol.* 180, 175–182. doi: 10.1016/j.resp.2011.11.004

Skelly, J. R., Edge, D., Shortt, C. M., Jones, J. F., Bradford, A., and O'Halloran, K. D. (2012b). Tempol ameliorates pharyngeal dilator muscle dysfunction in a rodent model of chronic intermittent hypoxia. *Am. J. Respir. Cell Mol. Biol.* 46, 139–148. doi: 10.1165/rcmb.2011-0084OC

Skelly, J. R., O'Connell, R. A., Jones, J. F., and O'Halloran, K. D. (2011). Structural and functional properties of an upper airway dilator muscle in aged obese male rats. *Respiration* 82, 539–549. doi: 10.1159/000332348

Skelly, J. R., Rowan, S. C., Jones, J. F., and O'Halloran, K. D. (2013). Upper airway dilator muscle weakness following intermittent and sustained hypoxia in the rat: effects of a superoxide scavenger. *Physiol. Res.* 16, 187–196.

Van Lunteren, E., Haxhiu, M. A., and Cherniack, N. S. (1987). Relation between upper airway volume and hyoid muscle length. *J. Appl. Physiol.* 63, 1443–1449.

Van Lunteren, E., and Pollarine, J. (2010). Improvement of diaphragm and limb muscle isotonic contractile performance by K+ channel blockade. *J. Neuroeng. Rehabil.* 7:1. doi: 10.1186/1743-0003-7-1

Van Lunteren, E., Pollarine, J., and Moyer, M. (2007). Isotonic contractile impairment due to genetic CLC-1 chloride channel deficiency in myotonic mouse diaphragm muscle. *Exp. Physiol.* 92, 717–729. doi: 10.1113/expphysiol.2007.038190

Viganò, A., Ripamonti, M., De Palma, S., Capitanio, D., Vasso, M., Wait, R., et al. (2008). Proteins modulation in human skeletal muscle in the early phase of adaptation to hypobaric hypoxia. *Proteomics* 8, 4668–4679. doi: 10.1002/pmic.200800232

Vogt, M., Puntschart, A., Geiser, J., Zuleger, C., Billeter, R., and Hoppeler, H. (2001). Molecular adaptations in human skeletal muscle to endurance training under simulated hypoxic conditions. *J. Appl. Physiol.* 91, 173–182.

Watchko, J. F., Daood, M. J., Sieck, G. C., LaBella, J. J., Ameredes, B. T., Koretsky, A. P. et al. (1997). Combined myofibrillar and mitochondrial creatine kinase deficiency impairs mouse diaphragm isotonic function. *J. Appl. Physiol.* 82, 1416–1423.

Wheaton, W. W., and Chandel, N. S. (2011). Hypoxia. 2. Hypoxia regulates cellular metabolism. *Am. J. Physiol. Cell Physiol.* 300, C385–C393. doi: 10.1152/ajpcell.00485.2010

Wijnhoven, J. H., Janssen, J. M., van Kuppevelt, T. H., Rodenburg, R. J. T., and Dekhuijzen, P. N. R. (2006). Metabolic capacity of the diaphragm in patients with COPD. *Respir. Med.* 100. 1064–1071. doi: 10.1016/j.rmed.2005.09.029

Zuo, L., and Clanton, T. L. (2005). Reactive oxygen species formation in the transition to hypoxia in skeletal muscle. *Am. J. Physiol. Cell Physiol.* 289, C207–C216. doi: 10.1152/ajpcell.00449.2004

Conflict of Interest Statement: The authors declare that the research was conducted in the absence of any commercial or financial relationships that could be construed as a potential conflict of interest.

frontiers in PHYSIOLOGY

ORIGINAL RESEARCH ARTICLE
published: 30 January 2015
doi: 10.3389/fphys.2015.00015

Chronic intermittent hypoxia increases rat sternohyoid muscle NADPH oxidase expression with attendant modest oxidative stress

Robert Williams[1], Paul Lemaire[1], Philip Lewis[1], Fiona B. McDonald[2], Eric Lucking[2], Sean Hogan[1], David Sheehan[3], Vincent Healy[1] and Ken D. O'Halloran[1]*

[1] Department of Physiology, School of Medicine, University College Cork, Cork, Ireland
[2] School of Medicine and Medical Science, University College Dublin, Dublin, Ireland
[3] School of Biochemistry and Cell Biology, University College Cork, Cork, Ireland

Edited by:
Brian McDonagh, University of Liverpool, UK

Reviewed by:
Nazareno Paolocci, Johns Hopkins University, USA
Cecilia Hidalgo, Universidad de Chile, Chile

***Correspondence:**
Ken D. O'Halloran, Department of Physiology, School of Medicine, University College Cork, 3-079, Western Gateway Building, Western Road, Cork, Ireland
e-mail: k.ohalloran@ucc.ie

Chronic intermittent hypoxia (CIH) causes upper airway muscle dysfunction. We hypothesized that the superoxide generating NADPH oxidase (NOX) is upregulated in CIH-exposed muscle causing oxidative stress. Adult male Wistar rats were exposed to intermittent hypoxia (5% O_2 at the nadir for 90 s followed by 210 s of normoxia), for 8 h per day for 14 days. The effect of CIH exposure on the expression of NOX subunits, total myosin and 4-hydroxynonenal (4-HNE) protein adducts in sternohyoid muscle was determined by western blotting and densitometry. Sternohyoid protein free thiol and carbonyl group contents were determined by 1D electrophoresis using specific fluorophore probes. Aconitase and glutathione reductase activities were measured as indices of oxidative stress. HIF-1α content and key oxidative and glycolytic enzyme activities were determined. Contractile properties of sternohyoid muscle were determined *ex vivo* in the absence and presence of apocynin (putative NOX inhibitor). We observed an increase in NOX 2 and p47 phox expression in CIH-exposed sternohyoid muscle with decreased aconitase and glutathione reductase activities. There was no evidence, however, of increased lipid peroxidation or protein oxidation in CIH-exposed muscle. CIH exposure did not affect sternohyoid HIF-1α content or aldolase, lactate dehydrogenase, or glyceraldehyde-3-phosphate dehydrogenase activities. Citrate synthase activity was also unaffected by CIH exposure. Apocynin significantly increased sternohyoid force and power. We conclude that CIH exposure upregulates NOX expression in rat sternohyoid muscle with concomitant modest oxidative stress but it does not result in a HIF-1α-dependent increase in glycolytic enzyme activity. Constitutive NOX activity decreases sternohyoid force and power. Our results implicate NOX-dependent reactive oxygen species in CIH-induced upper airway muscle dysfunction which likely relates to redox modulation of key regulatory proteins in excitation-contraction coupling.

Keywords: apocynin, intermittent hypoxia, NADPH oxidase, oxidative stress, respiratory muscle, sternohyoid, sleep apnea, upper airway

INTRODUCTION

Obstructive sleep apnea syndrome (OSAS) is a debilitating oxidative stress disorder (Lavie, 2003) which is very common. OSAS is associated with a wide spectrum of co-morbidities including cardiovascular, metabolic and neurocognitive dysfunction (Verstraeten, 2007; Lévy et al., 2009). Chronic intermittent hypoxia (CIH) is a central dominant feature of OSAS, and there is now convincing evidence from animal models that CIH recapitulates many of the hallmark features of the disorder. Upper airway (UA) muscle dysfunction is implicated in the pathophysiology of OSAS. OSAS patients (Carrera et al., 1999) and the English bulldog (Petrof et al., 1994), an animal model of OSAS, show signs of UA dilator muscle remodeling, dysfunction and damage. CIH alters UA muscle function (McGuire et al., 2002; Liu et al., 2005; Pae et al., 2005; Dunleavy et al., 2008; Ding and Liu, 2011; Skelly et al., 2012a) and induces UA muscle structural remodeling in some (McGuire et al., 2002; Pae et al., 2005) but not all (Ray et al., 2007; Skelly et al., 2012a) studies.

CIH exposure is typically associated with an increased production of reactive oxygen species (ROS) (Prabhakar, 2001; Peng and Prabhakar, 2003; Yuan et al., 2004; Shan et al., 2007; Dunleavy et al., 2008; Dutta et al., 2008; Raghuraman et al., 2009; Sharma et al., 2009; Khan et al., 2011) which can contribute to the development of skeletal muscle dysfunction (Dunleavy et al., 2008; Dutta et al., 2008; Jackson, 2008; Ding and Liu, 2011; Skelly et al., 2012a; Shortt et al., 2014). Pro-oxidants exacerbate (Dunleavy et al., 2008), while antioxidant strategies ameliorate (Dunleavy et al., 2008; Skelly et al.,

2012a; Shortt et al., 2014) CIH-induced respiratory muscle dysfunction. Moreover, superoxide scavengers increase sternohyoid muscle force (Skelly et al., 2010, 2012b) highlighting that basal ROS production is inhibitory to UA muscle function. These observations highlight that ROS are important modulators of respiratory muscle performance under physiological and pathophysiological conditions. Although it is well established that CIH increases ROS production, the source of ROS is less clear. CIH-induced oxidative stress in the liver (Jun et al., 2008), cardiovascular system (Nisbet et al., 2009), and brain (Hui-guo et al., 2010) is ameliorated by the inhibition of NADPH oxidase (NOX) activity suggesting that this membrane-bound superoxide generating enzyme is a major source of CIH-induced ROS. In skeletal muscle fibers, NOXs are localized to the sarcoplasmic reticulum (Xia et al., 2003), transverse tubules (Hidalgo et al., 2006), and plasma membranes (Javesghani et al., 2002); inhibition of NOXs in skeletal muscle reduces the levels of superoxide (Javesghani et al., 2002; Patwell et al., 2004). We recently reported that CIH-induced diaphragm dysfunction in the rat is blocked by chronic supplementation with the putative NOX inhibitor—apocynin (Shortt et al., 2014). Together, these studies implicate a role for NOX-derived ROS in skeletal muscle (dys) function.

We sought to determine the effects of CIH on the expression levels of NOX proteins in rat sternohyoid muscle (a representative UA dilator critical in the control of airway caliber) and to establish whether or not CIH alters the redox status of the sternohyoid. In functional studies of sternohyoid muscle *ex vivo*, we explored the effects of apocynin on isometric and isotonic contractile properties. We postulated that CIH upregulates NOX expression in rat sternohyoid muscle resulting in oxidative stress and that NOX-dependent ROS exert an inhibitory effect on sternohyoid force- and power-generating capacity.

MATERIALS AND METHODS

ETHICAL APPROVAL

All procedures involving animals were performed under license from the Irish Government Department of Health and Children and were carried out in accordance with National and European guidelines, following approval from University College Dublin Animal Research Ethics Committee.

CHRONIC INTERMITTENT HYPOXIA

Adult male Wistar rats were exposed to sham or chronic intermittent hypoxia (CIH) exposure. Rats were housed as normal in standard cages placed within commercially designed environmental chambers (Oxycyler™, Biospherix, USA) for daily gas treatments. Ambient oxygen was servo-controlled to generate intermittent hypoxia: 90 s hypoxia (5% O_2 at the nadir) and 210 s normoxia (21% O_2), 12 cycles per hour, 8 h per day for 14 consecutive days. A rodent pulse oximeter (Mouse Ox™ Starr Life Sciences Corp., USA) was used to determine the resulting arterial oxygen saturation (SaO_2) during CIH exposure; SaO_2 decreased to ∼70–80% at the nadir of the recurrent hypoxic events. On the day following gas treatments, animals were euthanized humanely (cervical spinal transection under 5% isoflurane anesthesia) and the sternohyoid muscles were excised.

TISSUE PREPARATION

Muscles were homogenized (GLH Homogeniser Omni International) in RIPA lysis buffer (25 mM Tris-HCl pH 7.6, 150 mM sodium chloride, 1% NP-40, 1% sodium deoxycholate, 0.1% SDS) supplemented with protease inhibitor cocktail (1 mM AEBSF, 800 μM aprotinin, 40 μM bestatin, 14 μM E-64, 20 μM leupeptin, 15 μM pepstatin A; Sigma Aldrich, Ireland) and phosphatase inhibitors 10 mM sodium fluoride, 1 mM sodium orthovanadate, using a 10% w/v ratio. Samples were homogenized using 8 × 10 s bursts and left on ice for 20 min. Homogenates were then centrifuged for 15 min at 11,000 g and the supernatants were stored at −80°C. Protein concentration was determined using a bicinchoninic (BCA) assay (Thermo Scientific, Ireland) as described in the manufacturer's protocol with absorbances measured at 562 nm using a SpectraMax-M3 spectrophotometer (Molecular Devices, USA).

WESTERN BLOTTING

Protein samples were mixed with an equal volume of 2x laemmli buffer (4% sodium dodecyl sulfate (SDS), 10% β-mercaptoethanol, 20% glycerol, 0.004% bromophenol blue, 0.125 M Tris-HCl, pH 6.8) and 15 μg of protein from each sample was resolved on 7.5 and 12.5% SDS-polyacrylamide gels depending on the protein. Resolved proteins were then electrophoretically transferred onto nitrocellulose membranes (Bio-Rad, Hercules, CA). Membranes were incubated in 0.1% (w/v) Ponceau S in 5% acetic acid to reversibly stain the transferred proteins to assess equal protein loading and transfer, and were digitally photographed for densitometric analysis. The membranes were blocked for 1 h in TBST (20 mM Tris-HCl, pH 7.6, 150 mM NaCl, 0.1% Tween) containing 5% non-fat dried milk and were incubated overnight with the primary antibody specific for the protein of interest as follows: anti-NOX 2 and anti-p47 phox, 1:1000 (BD Biosciences, UK); anti-p22 phox, 1:1000 (Santa Cruz, USA); anti-4-HNE, 1:2000 (Millipore, Ireland).

Membranes were incubated for 1 h at room temperature with a 1:2000 dilution of HRP-linked anti-rabbit or anti-mouse secondary antibody (Cell Signaling Technology, USA) in 5% non-fat dried milk/TBST depending on the primary antibody of interest. Bands were visualized using enhanced chemiluminescence (ECL Plus, GE Healthcare, UK) and exposure to chemiluminescent sensitive film (Kodak, USA). Films were developed, digitally photographed and densitometric analysis of bands of interest was performed (QuantityOne, Biorad). Band intensities of proteins of interest were normalized to the intensities of the corresponding Ponceau S staining proteins which were also measured by densitometric analysis to adjust for protein loading, allowing comparative analysis between sham and CIH-exposed muscles.

PROTEIN FREE THIOL AND CARBONYL GROUP CONTENT

Muscle homogenates were incubated with either 2 mM iodoacetamidofluorescein (IAF) or 2 mM fluorescein-thiosemicarbazide (FTSC) (Sigma-Aldrich Co., Ireland) for 2 h in the dark on ice for detection of protein free thiol and carbonyl groups, respectively. Samples were then precipitated with 20% trichloroacetic acid (TCA) in acetone, followed by centrifugation at 11,000 g at 4°C for 3 min. Protein pellets were then washed with ice-cold

excess 1:1 ethylacetate/ethanol or acetone (for FTSC and IAF respectively) to remove excess TCA, interfering salts and non-protein contaminants. Samples were dried, re-suspended in sample buffer containing 5% β-mercaptoethanol and heated at 95°C for 5 min before 1D electrophoretic separation on a 12% polyacrylamide gel. Fluorescent images of the gels were captured on a Typhoon Trio+ Variable-Mode Imager (GE Healthcare, UK). Protein bands were visualized by colloidal coomassie staining and images were captured on a calibrating image densitometer (GS-800, Bio-Rad, USA).

HIF-1α AND METABOLIC ENZYME ACTIVITIES

Sternohyoid HIF-1α content was assayed by an immuno-linked luminescence assay in accordance with manufacturer's instructions (Mesoscale Discovery, Gaithersburg, USA). HeLa cells treated with and without cobalt chloride for 16 h provided positive and negative controls respectively for the HIF-1α assay. Aconitase activity was measured using a colorimetric reaction in accordance with the manufacturer's instructions (Abcam, Cambridge, UK). Aconitase is a TCA cycle enzyme that catalyzes the isomerisation of citrate to isocitrate. Isocitrate, in this assay, undergoes further biochemical reaction resulting in a product that converts a nearly colorless probe into an intensely colored form with a peak absorbance at 450 nm. Samples were incubated in an activating solution containing cysteine-HCl and $(NH_4)_2Fe(SO_4)_2$on ice for 1 h before addition to a 96-well plate in duplicate along with isocitrate standards. One half of the duplicate wells received the sample reaction mixture (containing assay buffer, enzyme mix and substrate) and the other half the background mixture (containing assay buffer and enzyme mix only) and samples were incubated for 60 min at 25°C. Developer was then added to each well and samples were incubated for a further 10 min. Absorbance was measured at 450 nm and background was subtracted from the test sample. One unit of aconitase activity is the amount of enzyme that will isomerize 1 mmoles of isocitrate per minute at pH 7.4 and 25°C. Fructose-1, 6-bisphosphate Aldolase A (aldolase) is the isoform of the enzyme found predominantly in skeletal muscle. It is the 4th enzyme of the glycolysis pathway which catalyzes the conversion of fructose-1-6-bisphosphate into both 3-phosphoglyceraldehyde and dihydroxyacetone phosphate. We developed an assay based upon Boyer's modification of the hydrazine assay where 3-phosphoglyceraldehyde reacts with hydrazine to form a hydrazone which absorbs at 240 nm. 4 mM fructose-1,6-bisphosphate (pH 7.5) (25% v/v), 0.03 mM EDTA pH 7.5 (25% v/v), and 2.3 mM hydrazine sulfate (25% v/v) were added to a 96-well plate and absorbance was recorded for 10 min. Samples and a dH_2O blank (25% v/v) were then added to the plate and absorbance was recorded for another 10 min. Using the linear portions of the curve, the A_{240}/min of the blank was subtracted from the A_{240}/min of the test. One unit is described as a change in absorbance of 1.00 per minute at 25°C and pH 7.5. For GAPDH activity measurement, samples were added to 13.5 mM sodium pyrophosphate buffer (pH 8.5) containing 30 mM sodium arsenate, 0.25 mM NAD with 3.325 mM DTT. Samples were incubated at 25°C for 10 min to achieve temperature equilibration and to establish a blank rate, if any. 0.5 mM DL-glyceraldehdye-3-phosphate was added and absorbance was recorded for 10 min at 339 nm. Measured rates were corrected by measuring the blank rate of the reaction. One unit is defined as 1 μmol NADH generated per minute. Citrate synthase activity was determined using a commercial kit (Sigma) as per manufacturer's instructions. Citrate synthase catalyzes the reaction between acetyl coenzyme A (acetyl CoA) and oxaloacetic acid (OAA) to form citric acid and CoA with a thiol group which reacts with DTNB in the reaction mixture to form 5-thio-nitrobemzoic acid (TNB) which is absorbed at 412 nm. One unit causes the synthesis of one micromole of citrate per minute per mg protein at 25°C and pH 7.5.

MUSCLE PHYSIOLOGY

Adult male Wistar rats were anesthetized with 5% isoflurane by inhalation in oxygen and killed by cervical spinal transection. Sternohyoid muscles were excised and longitudinal bundles were suspended vertically with fine (non-elastic) string; one end of each strip was mounted to tissue holders, while the other end was tied firmly to a hook, which sat on a dual-mode force transducer allowing assessment of isometric and isotonic properties. The muscle fiber bundles affixed to the tissue holders were then suspended in standard water-jacketed tissue baths. The tissue baths were filled with Krebs salt solution, maintained at 35°C and bubbled with 95% O_2 and 5% CO_2. The Krebs solution contained: 120 mM NaCl, 25 mM $NaHCO_3$, 12 mM $MgSO_4$, 1.2 mM NaH_2PO4, 2.5 mM CaGluconate, 5 mM KCl, and 11.5 mM Glucose. D-tubocurarine (25 μM) was used in all experiments to exclude any potential involvement of excitation of intramuscular nerve branches. The muscles were stimulated using supramaximal square wave constant current stimulators delivered via two platinum electrodes which flanked the tissue in the bath. The change in tension was transduced, amplified and converted from an analog-to-digital signal where it was displayed and recorded on a computer for later analysis. Optimum muscle length (L_o) was determined by repeated twitch stimulation while adjusting the length of the muscle with the micropositioner. The muscle preparations remained at L_o for the duration of the study. Studies were conducted in the absence and presence of the putative NOX inhibitor, apocynin (2 mM). Muscle preparations were allowed to equilibrate for 10 min before starting the experimental protocol.

Protocol

Isometric twitch force and kinetics (contraction time and half-relaxation time) were determined with the lever arm of the force transducer set to maximum rigidity (∼500 mN; >100% load). Next, an isometric tetanic contraction (F*max*) was elicited by stimulating at 100 Hz for 300 ms (O'Halloran, 2006; Skelly et al., 2010, 2012a,b; Shortt et al., 2014). Following a 5 min rest period, concentric contractions were elicited in incremental steps with varying load (0.1, 1, 5, 10, 15, 20%; % of F*max*) with 1 min rest between each contraction. Muscle length returned to L_o following each contraction. Shortening (S*max*) was determined as the maximum distance shortened during contraction. Peak shortening velocity (V*max*) was determined as distance shortened during the

initial 30 ms of shortening, when velocity is greatest at 0% load. Mechanical power was determined at each step of the incremental load step test as the product of force x shortening velocity.

DATA ANALYSIS

Peak specific force (F*max*) was calculated in N/cm^2 of muscle cross-sectional area. Cross-sectional area was calculated as follows: mass (g)/(Lo (cm) × muscle density (g/cm^3); muscle density was estimated to be 1.056 g/cm^3. Maximum shortening (S*max*) was calculated as length shortened per optimal length (L/L$_o$). Peak shortening velocity (V*max*) was calculated as L$_o$/s. Peak mechanical power (P*max*) was calculated as Watts/cm^2.

STATISTICAL ANALYSIS

Data are expressed as mean ± SEM. Statistical comparisons were performed between groups using Student unpaired *t*-tests, Mann Whitney *U*-tests, or Two-Way ANOVA with Bonferroni *post-hoc* tests as appropriate using Graph Pad Prism. $P < 0.05$ was the criterion for statistical significance in all tests.

RESULTS

EFFECT OF CIH ON STERNOHYOID NOX SUBUNIT AND MYOSIN EXPRESSION

We postulated that CIH would increase sternohyoid NOX subunit expression. Western blots are shown in **Figures 1A,B**. CIH significantly increased NOX 2 (**Figures 1A,C**) and p47 phox (**Figures 1B,E**)—but not p22 phox (**Figures 1A,D**)—expression in rat sternohyoid muscle. Total myosin protein content was unaffected by CIH exposure (not shown).

EFFECT OF CIH ON STERNOHYOID 4-HNE PROTEIN ADDUCT LEVELS AND PROTEIN FREE THIOL AND CARBONYL GROUP CONTENT

We postulated that CIH would increase lipid peroxidation and protein oxidation. Western blot with respective Ponceau S stained gel is shown in **Figure 2A**. CIH exposure did not affect sternohyoid 4-HNE protein adduct levels (**Figure 2B**). Representative fluorescent 1D gels tagging protein free thiols (**Figure 2C**) and protein carbonyls (**Figure 2E**) are shown with respective coomassie stained gels. CIH exposure did not affect protein free thiol (**Figure 2D**) or carbonyl group (**Figure 2F**) content.

EFFECT OF CIH ON STERNOHYOID MUSCLE ACONITASE AND GLUTATHIONE REDUCTASE ACTIVITIES

We postulated that CIH would decrease aconitase and glutathione reductase activities indicative of oxidative stress. CIH exposure significantly decreased aconitase (**Figure 3A**) and glutathione reductase (**Figure 3B**) activities.

EFFECT OF CIH ON STERNOHYOID MUSCLE HIF-1α CONTENT AND OXIDATIVE AND GLYCOLYTIC ENZYME ACTIVITIES

We postulated that CIH would increase HIF-1α content and cause a shift from oxidative-to-glycolytic metabolism. CIH exposure

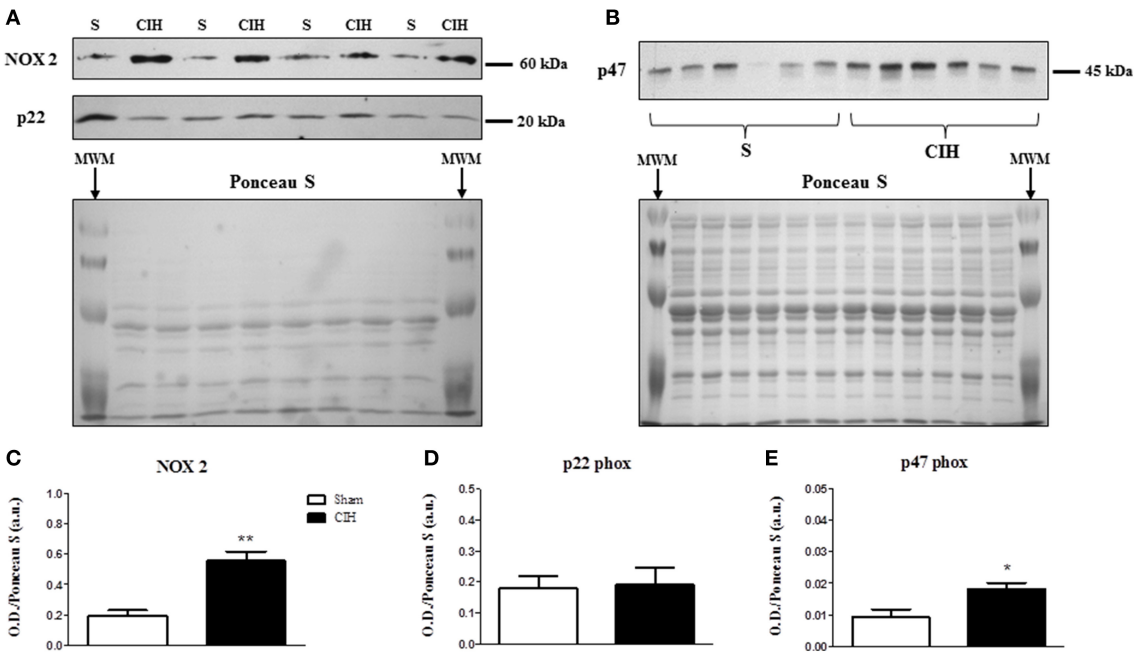

FIGURE 1 | Western blot of NOX subunit expression in the sternohyoid muscle from sham (S) and chronic intermittent hypoxia (CIH)-exposed rats. (A) Expression of the catalytic superoxide-generating NOX 2 subunit and the co-anchoring p22 phox subunit with the corresponding Ponceau S stained membrane used to normalize protein loading and electro-transfer. MWM = pre-stained molecular weight markers. **(B)** Expression of the organizer subunit, p47 phox with corresponding Ponceau S stained membrane. Densitometric analysis of NOX subunit band intensities normalized by densitometric intensities of corresponding Ponceau-S stained proteins expressed in arbitrary units (a.u.) are shown in **(C–E)**. **(C)** A near 3-fold increase in NOX 2 expression was observed in the CIH-exposed group compared to sham control (** $P = 0.002$; Student unpaired *t*-test, $n = 4$ per group). **(D)** No change in the p22 phox subunit expression was observed ($P = 0.884$, $n = 4$ per group). **(E)** A near 2-fold increase in the p47 phox subunit expression was observed in the CIH-exposed group compared to sham control (* $P = 0.014$, $n = 6$ per group). Values are mean ± SEM.

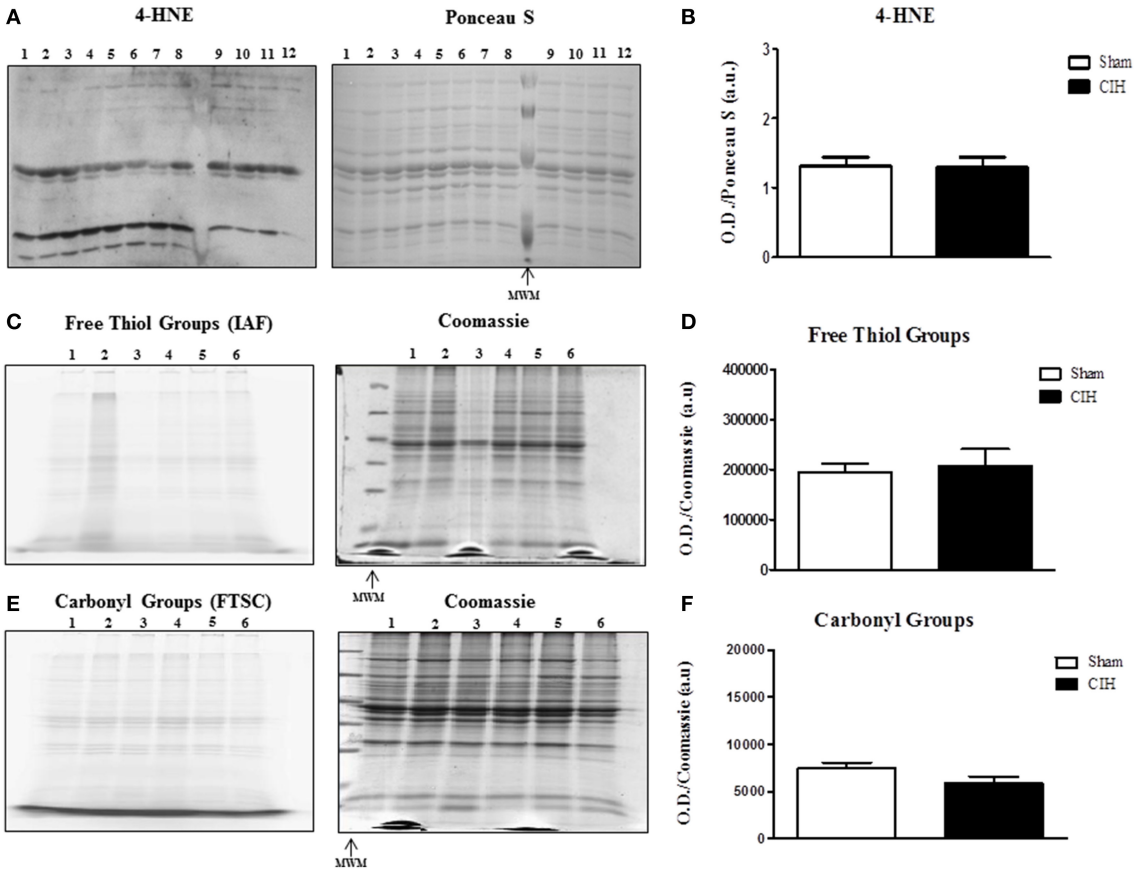

FIGURE 2 | Western blot of 4-HNE protein adducts and 1D electrophoresis to determine free thiol and carbonyl group content in the sternohyoid muscle from sham and chronic intermittent hypoxia (CIH)-exposed rats. Sham and CIH samples were loaded in alternate lanes (numbered in the figure). **(A)** Sternohyoid 4-HNE content together with Ponceau S stained membrane. **(B)** Densitometric analysis of 4-HNE protein adduct band intensities normalized by densitometric intensities of corresponding Ponceau S stained proteins expressed in arbitrary units (a.u.) from sham and CIH-exposed rats. No significant difference was observed in 4-HNE protein adduct content ($P = 0.9372$; Student unpaired *t*-test) comparing sham and CIH-exposed sternohyoid muscles. Representative images of sternohyoid iodoacetamidofluorescein (IAF)-tagged protein free thiol groups **(C)** and fluorescein-thiosemicarbazide (FTSC)-tagged carbonyl groups **(E)** with corresponding coomassie stained membranes used to normalize protein loading and electrotransfer. Densitometric analysis of protein free thiol group **(D)** and carbonyl group **(F)** contents normalized by densitometric intensities of corresponding coomassie stained proteins expressed in arbitrary units (a.u.) from sham and CIH-exposed rats. Protein free thiol and carbonyl group content of the sternohyoid muscle was not significantly different in sham and CIH-exposed rats ($P = 0.699$ and $P = 0.180$ respectively; Student unpaired *t*-tests). Values are mean ± SEM; $n = 6$ per group.

did not affect sternohyoid HIF-1α content (not shown). Similarly, CIH exposure did not affect citrate synthase (0.23 ± 0.01 vs. 0.22 ± 0.01, mean±SEM, units/mg protein; Student unpaired *t*-test: $p = 0.518$), aldolase (1.90 ± 0.06 vs. 2.00 ± 0.11 units/mg protein; $p = 0.425$), lactate dehydrogenase (0.45 ± 0.08 vs. 0.42 ± 0.08 units/mg protein; $p = 0.805$) or glyceraldehyde-3-phosphate dehydrogenase (0.56 ± 0.12 vs. 0.53 ± 0.09 units/mg protein; $p = 0.845$) activities.

EFFECT OF APOCYNIN ON STERNOHYOID MUSCLE CONTRACTILE PROPERTIES

We postulated that the putative NOX inhibitor—apocynin—would increase force- and power-generating capacity of the sternohyoid muscle. Data for sternohyoid muscle contractile properties are shown in **Table 1**. Contractile kinetics and twitch force determined during isometric contractions were unaffected by apocynin. There was an increase in the maximum velocity of shortening (V*max*) in apocynin-treated preparations during isotonic contractions but this did not achieve statistical significance ($p = 0.095$). Maximum muscle shortening during isometric contractions (S*max*) was unaffected by apocynin. Conversely, apocynin significantly increased sternohyoid muscle peak tetanic force (F*max*; **Figure 4A**) determined under isometric conditions and increased muscle power (force x velocity of shortening; **Figure 4B**) over a range of loads (10–20% of F*max*) during concentric contractions.

DISCUSSION

The key findings of this study are: (1) CIH significantly increased NOX 2 and p47 phox—but not p22 phox—subunit expression in rat sternohyoid muscle; (2) CIH did not increase the levels of sternohyoid 4-HNE protein adducts; (3) CIH did not

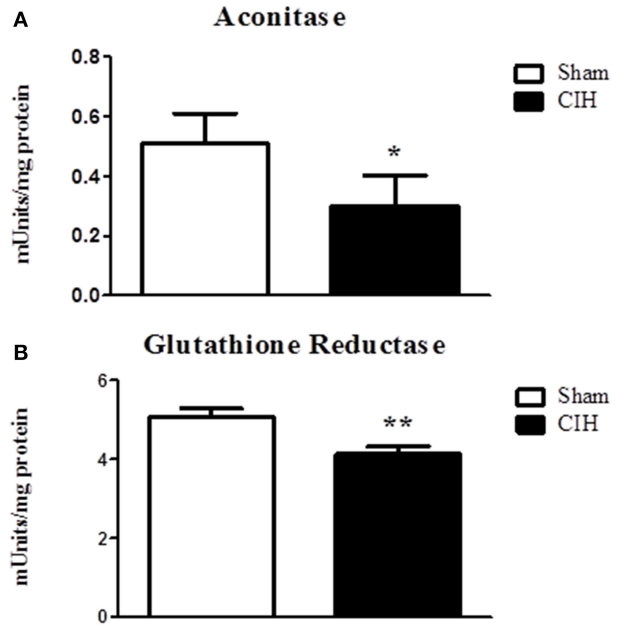

FIGURE 3 | Sternohyoid muscle aconitase and glutathione reductase enzyme activities in sham and chronic intermittent hypoxia (CIH)-exposed rats. Aconitase **(A)** and glutathione reductase **(B)** activities were significantly decreased in CIH-exposed sternohyoid muscles compared to sham controls: $^{*}P = 0329$ and $^{**}P = 0.0046$; Student unpaired *t*-tests. Values are mean ± SEM; $n = 8$ per group.

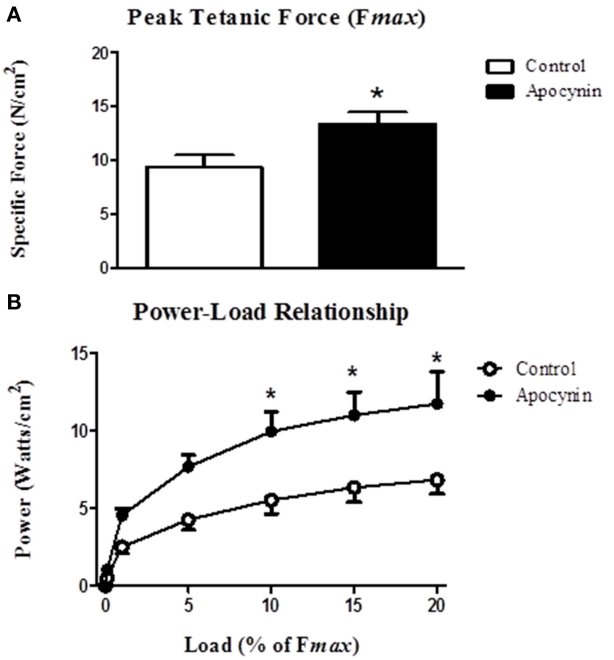

FIGURE 4 | Sternohyoid muscle isometric and isotonic contractile properties in the absence and presence of apocynin. (A) Sternohyoid peak tetanic force (F*max*) determined *ex vivo* in the absence or presence of 2 mM apocynin (putative NOX inhibitor). F*max* was significantly increased in apocynin-treated muscle preparations ($^{*}P = 0.03$; Student unpaired *t*-test). **(B)** Power-load relationship of sternohyoid muscle determined *ex vivo* in the absence or presence of 2 mM apocynin. Power (force x velocity of shortening) was significantly increased in apocynin-treated preparations ($P = 0.023$ (drug); Two Way repeated measures ANOVA; $^{*}P < 0.01$ Bonferroni *post-hoc* test). Values are mean ± SEM; $n = 5$ per group.

Table 1 | Sternohyoid muscle contractile properties in the absence and presence of 2 mM apocynin.

	Control	Apocynin	*P*-value
CT (ms)	15 ± 1	17 ± 2	0.407[a]
½RT (ms)	12 ± 1	12 ± 2	0.647[a]
Pt (N/cm^2)	2.5 ± 0.6	2.6 ± 0.2	0.922[b]
V*max* (Lo/s)	6.5 ± 0.8	8.9 ± 0.7	0.095[c]
S*max* (L/Lo)	0.29 ± 0.02	0.34 ± 0.03	0.129[a]

Values are mean ± SEM; n = 5 for both groups. CT, isometric contraction time; ½RT, isometric half-relaxation time; Pt, isometric twitch force; Vmax, maximum shortening velocity under isotonic conditions of zero load normalized to optimum length (Lo); Smax, peak shortening normalized to Lo. Data were compared using [a] Student unpaired t-test, [b] Student unpaired t-test with Welch's correction or [c] Mann Whitney U-test as appropriate following tests for normality and equal variances in the data sets.

affect protein free thiol or carbonyl group content in sternohyoid muscle; (4) CIH decreased aconitase and glutathione reductase activities indicative of modest oxidative stress; (5) CIH did not affect HIF-1α content or the activities of citrate synthase, aldolase, lactate dehydrogenase or glyceraldehyde-3-phosphate dehydrogenase; (6) The putative NOX inhibitor—apocynin—significantly increased sternohyoid force and power.

It is well established in various animal models that CIH impairs respiratory muscle function (Dunleavy et al., 2008; Skelly et al., 2010, 2012a; Shortt et al., 2014). We have previously reported sternohyoid muscle weakness in adult male Wistar rats, an effect that was ameliorated by chronic tempol (a superoxide scavenger) supplementation (Skelly et al., 2012a) implicating ROS in CIH-induced muscle dysfunction. A variety of sources of ROS have been described but the major contributing source in CIH-induced UA muscle dysfunction has yet to be determined. A number of models have identified the NOX complex as a potential source of ROS contributing to redox modulation and/or oxidative injury (Pigeolet et al., 1990; Berry et al., 2000; Ozaki et al., 2000; Javesghani et al., 2002; Hidalgo et al., 2006; Nair et al., 2011; Shortt et al., 2014). Xia et al. (2003) identified a much higher rate of superoxide production per milligram of protein in the sarcoplasmic reticulum compared to the mitochondria in muscle. In view of these studies and our previous work (Skelly et al., 2010, 2012a,b), we sought to investigate NOX as a potential source of ROS in CIH-exposed UA muscle.

The present study shows that CIH exposure increased key NOX subunits in sternohyoid muscle. We observed a near 3-fold increase in the catalytic subunit—NOX 2—and a near 2-fold increase in the organizer subunit—p47 phox. There is a body of research that implicates hypoxia as a driving force underpinning enhanced NOX expression and activity in various tissues. Acute repetitive hypoxia was shown to increase NOX activity ∼12-fold in the carotid body (Peng et al., 2009). This increase in activity was

associated with an increase in NOX mRNA and protein expression. CIH was also shown to increase NOX 2 protein and mRNA expression in PC12 pheochromocytoma cells as well as mouse embryonic fibroblasts mediated through hypoxia inducible factor 1 (HIF-1) (Yuan et al., 2011). Similarly, Souvannakitti et al. (2010) showed that CIH increases NOX 2 activity and mRNA expression in adrenal medullae of neonatal rats. Recent work by Zhou et al. (2012) examined the effects of different CIH paradigms, reporting time- and intensity-dependent increases in rat myocardial p22 phox mRNA expression. Extending this line of enquiry, ours is the first study to our knowledge to report an increase in NOX 2 and p47 phox protein subunits in CIH-exposed UA respiratory muscle and this appears to be independent of HIF-1α activation. We acknowledge, however, that the exact site(s) of NOX subunit upregulation is not known and it could extend to the muscle vasculature; this is a limitation of the experimental approach taken in the present study.

Animal models of CIH most often report evidence of increased oxidative stress in various tissues, consistent with the observation that human OSAS is an oxidative stress disorder (Lavie, 2003). Despite reporting a significant increase in NOX subunit expression in CIH-exposed sternohyoid muscle, we did not detect overt oxidative stress in the tissue, assessed by measurement of protein free thiol and carbonyl group content. This was further corroborated by assessment of the levels of 4-HNE (a highly reactive lipid peroxidation product and initiator of oxidative stress) which was unchanged in the CIH-exposed airway dilator muscle. On the face of it, the apparent lack of oxidative stress following CIH is surprising given our previous findings that antioxidant supplementation ameliorates or prevents CIH-induced respiratory muscle dysfunction (Dunleavy et al., 2008; Skelly et al., 2012a; Shortt et al., 2014). Of note however, CIH-induced sternohyoid muscle dysfunction is reversible by acute antioxidant treatment following CIH exposure (Skelly et al., 2012a). The latter observation strongly suggests that CIH exposure does not cause irreversible oxidative modification (damage) to muscle, consistent with the lack of evidence of increased protein carbonylation in CIH-exposed muscle reported in the present study. Rather, CIH-induced sternohyoid muscle weakness (Skelly et al., 2012a) appears to be a dynamic ROS-dependent process that is entirely reversible, which is important in the context of potential antioxidant pharmacotherapy for human OSAS. Of note, CIH was associated with significant decreases in aconitase and glutathione reductase activities highlighting the development of a modest oxidative stress in CIH-exposed muscle.

In view of the collective data described above, we speculate that CIH-induced sternohyoid dysfunction (Skelly et al., 2012a) is mediated by altered redox signaling, perhaps within microdomains of the muscle, evidently with no widespread cellular stress. A number of groups have reported localization of the NOX subunit complex, or at least some components, to areas near the sarcoplasmic reticulum and transverse tubules of muscle (Xia et al., 2003; Hidalgo et al., 2006; Sun et al., 2011). Oxidation of redox-sensitive cysteine residues in these microdomains affects calcium release through ryanodine receptor channels (Hidalgo et al., 2006; Sun et al., 2011); Ca^{2+} release is promoted during low level ROS turnover but is inhibited during high level ROS production (Geiszt et al., 1997; Kawakami and Okabe, 1998; Reid, 2001). Thus, it is plausible to suggest that CIH-induced NOX-dependent elevated ROS might impair muscle force-generating capacity without concomitant widespread oxidative stress/injury. CIH-induced oxidative damage has been observed in skeletal muscle (Dutta et al., 2008) and other tissues (Veasey et al., 2004; Raghuraman et al., 2009; Khan et al., 2011). It appears that the detrimental effects of CIH manifest in a "dose"-dependent manner and the effects of oxidative stress may be organ-specific (Shan et al., 2007; Jun et al., 2008). It is worth noting that the experimental paradigm of CIH used in our studies is relatively modest and based on the observations of Raghuraman et al. (2009), that short bouts of IH (15 s hypoxia; 5 min normoxia) produce higher levels of ROS compared to 90 s hypoxic/normoxic cycles, our paradigm might not be expected to produce severe oxidative stress *per se*.

To explore the potential for NOX-dependent ROS to modulate sternohyoid muscle performance, we examined the effects of apocynin on sternohyoid muscle contractile properties. Apocynin significantly increased isometric sternohyoid peak force revealing that basal NOX-derived ROS exert a powerful inhibitory influence on sternohyoid contractile performance. This finding is consistent with a previous study by our group highlighting that superoxide scavengers are powerful inotropic agents (Skelly et al., 2010, 2012a), extending this work to suggest that NOX is an important source of basal ROS production in rat sternohyoid muscle. Of note, apocynin did not affect isometric contractile kinetics although an increase in the maximum velocity of shortening under isotonic conditions was observed. This failed to achieve statistical significance but the increase likely contributed to the increase in power-generating capacity observed in apocynin-treated preparations. The greater power-generating capacity of the sternohyoid over physiological loads (predominantly due to increased force-generating capacity) translates *in vivo* to a greater capacity to preserve and maintain UA caliber, given that the sternohyoid is a recognized UA dilator muscle. Our data highlight that ROS are powerful inhibitors of sternohyoid force and power, and by extension we posit that increased ROS associated with CIH (or other stimuli including enhanced muscle activity) impairs sternohyoid muscle function. The significance of our findings, in concert with our previous study (Skelly et al., 2012a), is that CIH exposure—a dominant feature of human sleep-disordered breathing—is detrimental to the control of UA caliber, potentially increasing the risk of obstructive airway events. In this regard, CIH exposure could establish an inescapable cycle serving to exacerbate and perpetuate respiratory morbidity in human OSAS.

It is plausible to suggest that NOX-derived ROS could affect contractile function through actions at one or more sites critical in the excitation-contraction coupling mechanism (Geiszt et al., 1997; Kawakami and Okabe, 1998; Reid, 2001; Hidalgo et al., 2006; van der Poel et al., 2007; Lamb and Westerblad, 2011; Sun et al., 2011). It is likely that ROS downstream of superoxide, such as hydrogen peroxide, affect sternohyoid muscle performance (Shortt and O'Halloran, 2014). We speculate that the inotropic effects of apocynin relate to redox modulation of calcium sensitivity of the contractile filaments (Edwards et al., 2007; Murphy et al., 2008). Collectively, the data are consistent with the

widely held view that ROS are important signaling molecules in the context of skeletal muscle function. By extension, we postulate that increased NOX-derived ROS production following CIH exposure is likely responsible for sternohyoid muscle weakness (Skelly et al., 2012a), given that ROS are inhibitory to sternohyoid force (this study; Skelly et al., 2010, 2012a,b).

In summary, we have previously shown that CIH exposure causes upper airway dilator muscle weakness, an effect which is blocked by chronic antioxidant supplementation. Here we report that CIH exposure results in increased sternohyoid muscle NOX 2 and p47 phox subunit expression with attendant modest oxidative stress. Apocynin significantly enhanced sternohyoid muscle force- and power-generating capacity. Our results implicate NOX as a potential source of ROS which exert substantial inhibitory effects on sternohyoid muscle performance. We speculate that CIH-induced muscle dysfunction relates to NOX-dependent redox modulation within specific myocellular microdomains relevant to contractile function. The results are further supportive of our previous contention that antioxidant treatment may serve as a useful adjunctive therapy in human OSAS.

AUTHOR CONTRIBUTIONS

Fiona B. McDonald and Eric Lucking generated the animal model; Robert Williams and Vincent Healy performed electrophoresis and densitometry; Paul Lemaire and Philip Lewis performed enzyme assays; Sean Hogan and Philip Lewis performed muscle physiology experiments; David Sheehan provided advice and expertise on 1D electrophoresis experiments which were performed in his laboratory; all authors contributed to interpretation of the data sets; Ken D. O'Halloran conceived the idea of the study and designed the experiments; Robert Williams drafted the original manuscript; critical revision was provided by David Sheehan, Vincent Healy and Ken D. O'Halloran; all authors approved the final version of the manuscript.

ACKNOWLEDGMENTS

Funded by the Health Research Board (Ireland) and the Department of Physiology, School of Medicine, University College Cork, Ireland.

REFERENCES

Berry, C., Hamilton, C. A., Brosnan, M. J., Magill, F. G., Berg, G. A., McMurray, J. J. V., et al. (2000). Investigation into the sources of superoxide in human blood vessels: angiotensin II increases superoxide production in human internal mammary arteries. *Circulation* 101, 2206–2212. doi: 10.1161/01.CIR.101.18.2206

Carrera, M., Barbe, F., Sauleda, J., Tomas, M., Gomez, C., and Agusti, A. G. (1999). Patients with obstructive sleep apnea exhibit genioglossus dysfunction that is normalized after treatment with continuous positive airway pressure. *Am. J. Respir. Crit. Care Med.* 159, 1960–1966. doi: 10.1164/ajrccm.159.6.9809052

Ding, W. H., and Liu, Y. H. (2011). Genistein attenuates genioglossus muscle fatigue under chronic intermittent hypoxia by down-regulation of oxidative stress level and up-regulation of antioxidant enzyme activity through ERK1/2 signaling pathway. *Oral Dis.* 17, 677–684. doi: 10.1111/j.1601-0825.2011.01822.x

Dunleavy, M., Bradford, A., and O'Halloran, K. D. (2008). Oxidative stress impairs upper airway muscle endurance in an animal model of sleep-disordered breathing. *Adv. Exp. Med. Biol.* 605, 458–462. doi: 10.1007/978-0-387-73693-8_80

Dutta, A., Ray, K., Singh, V. K., Vats, P., Singh, S. N., and Singh, S. B. (2008). L-carnitine supplementation attenuates intermittent hypoxia-induced oxidative stress and delays muscle fatigue in rats. *Exp. Physiol.* 93, 1139–1146. doi: 10.1113/expphysiol.2008.042465

Edwards, J. N., Macdonald, W. A., van der Poel, C., and Stephenson, D. G. (2007). O2- production at 37 degrees C plays a critical role in depressing tetanic force of isolated rat and mouse skeletal muscle. *Am. J. Physiol. Cell Physiol.* 293, C650–C660. doi: 10.1152/ajpcell.00037.2007

Geiszt, M., Kapus, A., Németh, K., Farkas, L., and Ligeti, E. (1997). Regulation of capacitative Ca^{2+} influx in human neutrophil granulocytes: alterations in chronic granulomatous disease. *J. Biol. Chem.* 272, 26471–26478. doi: 10.1074/jbc.272.42.26471

Hidalgo, C., Sánchez, G., Barrientos, G., and Aracena-Parks, P. (2006). A transverse tubule NADPH oxidase activity stimulates calcium release from isolated triads via ryanodine receptor type 1 S-glutathionylation. *J. Biol. Chem.* 281, 26473–26482. doi: 10.1074/jbc.M600451200

Hui-guo, L., Kui, L., Yan-ning, Z., and Yong-jian, X. (2010). Apocynin attenuate spatial learning deficits and oxidative responses to intermittent hypoxia. *Sleep Med.* 11, 205–212. doi: 10.1016/j.sleep.2009.05.015

Jackson, M. J. (2008). Free radicals generated by contracting muscle: by-products of metabolism or key regulators of muscle function? *Free Rad. Biol. Med.* 44, 132–141. doi: 10.1016/j.freeradbiomed.2007.06.003

Javesghani, D., Magder, S. A., Barreiro, E., Quinn, M. T., and Hussain, S. N. A. (2002). Molecular characterization of a superoxide-generating NAD(P)H oxidase in the ventilatory muscles. *Am. J. Respir. Crit. Care Med.* 165, 412–418. doi: 10.1164/ajrccm.165.3.2103028

Jun, J., Savransky, V., Nanayakkara, A., Bevans, S., Li, J., Smith, P. L., et al. (2008). Intermittent hypoxia has organ-specific effects on oxidative stress. *Am. J. Physiol. Regul. Integr. Comp. Physiol.* 295, R1274–R1281. doi: 10.1152/ajpregu.90346.2008

Kawakami, M., and Okabe, E. (1998). Superoxide anion radical-triggered Ca^{2+} release from cardiac sarcoplasmic reticulum through ryanodine receptor Ca^{2+} channel. *Mol. Pharmacol.* 53, 497–503.

Khan, S. A., Nanduri, J., Yuan, G., Kinsman, B., Kumar, G. K., Joseph, J., et al. (2011). NADPH oxidase 2 mediates intermittent hypoxia-induced mitochondrial complex I inhibition: relevance to blood pressure changes in rats. *Antiox. Redox Signal.* 14, 533–542. doi: 10.1089/ars.2010.3213

Lamb, G. D., and Westerblad, H. (2011). Acute effects of reactive oxygen and nitrogen species on the contractile function of skeletal muscle. *J. Physiol.* 589, 2119–2127. doi: 10.1113/jphysiol.2010.199059

Lavie, L. (2003). Obstructive sleep apnoea syndrome- an oxidative stress disorder. *Sleep Med. Rev.* 7, 35–51. doi: 10.1053/smrv.2002.0261

Lévy, P., Bonsignore, M. R., and Eckel, J. (2009). Sleep, sleep-disordered breathing and metabolic consequences. *Eur. Respir. J.* 34, 243–260. doi: 10.1183/09031936.00166808

Liu, S. S., Liu, H. G., Xiong, S. D., Niu, R. J., Xu, Y. J., and Zhang, Z. X. (2005). Effects of Shen-Mai injection on sternohyoid contractile properties in chronic intermittent hypoxia rat. *Zhonghua Jie He He Hu Xi Za Zhi* 28, 611–614.

McGuire, M., MacDermott, M., and Bradford, A. (2002). Effects of chronic episodic hypoxia on rat upper airway muscle contractile properties and fiber-type distribution. *Chest* 122, 1012–1017. doi: 10.1378/chest.122.3.1012

Murphy, R. M., Dutka, T. L., and Lamb, G. D. (2008). Hydroxyl radical and glutathione interactions alter calcium sensitivity and maximum force of the contractile apparatus in rat skeletal mscle fibres. *J. Physiol.* 586, 2203–2216. doi: 10.1113/jphysiol.2007.150516

Nair, D., Dayyat, E. A., Zhang, S. X., Wang, Y., and Gozal, D. (2011). Intermittent hypoxia-induced cognitive deficits are mediated by NADPH oxidase activity in a murine model of sleep apnea. *PLoS ONE* 6:e19847. doi: 10.1371/journal.pone.0019847

Nisbet, R. E., Graves, A. S., Kleinhenz, D. J., Rupnow, H. L., Reed, A. L., Fan, T.-H. M., et al. (2009). The role of NADPH oxidase in chronic intermittent hypoxia-induced pulmonary hypertension in mice. *Am. J. Respir. Cell Mol. Biol.* 40, 601–609. doi: 10.1165/2008-0145OC

O'Halloran, K. D. (2006). Effects of nicotine on rat sternohyoid muscle contratile properties. *Respir. Physiol. Neurobiol.* 150, 200–210. doi: 10.1016/j.resp.2005.05.018

Ozaki, M., Deshpande, S. S., Angkeow, P., Bellan, J., Lowenstein, C. J., Dinauer, M. C., et al. (2000). Inhibition of the Rac1 GTPase protects against nonlethal ischemia/reperfusion-induced necrosis and apoptosis *in vivo*. *FASEB J.* 14, 418–429.

Pae, E.-K., Wu, J., Nguyen, D., Monti, R., and Harper, R. M. (2005). Geniohyoid muscle properties and myosin heavy chain composition are altered after

short-term intermittent hypoxic exposure. *J. Appl. Physiol.* 98, 889–894. doi: 10.1152/japplphysiol.00978.2004

Patwell, D. M., McArdle, A., Morgan, J. E., Patridge, T. A., and Jackson, M. J. (2004). Release of reactive oxygen and nitrogen species from contracting skeletal muscle cells. *Free Rad. Biol. Med.* 37, 1064–1072. doi: 10.1016/j.freeradbiomed.2004.06.026

Peng, Y.-J., Nanduri, J., Yuan, G., Wang, N., Deneris, E., Pendyala, S., et al. (2009). NADPH oxidase is required for the sensory plasticity of the carotid body by chronic intermittent hypoxia. *J. Neurosci.* 29, 4903–4910. doi: 10.1523/JNEUROSCI.4768-08.2009

Peng, Y. J., and Prabhakar, N. R. (2003). Reactive oxygen species in the plasticity of respiratory behavior elicited by chronic intermittent hypoxia. *J. Appl. Physiol.* 94, 2342–2349.

Petrof, B. J., Pack, A. I., Kelly, A. M., Eby, J., and Hendricks, J. C. (1994). Pharyngeal myopathy of loaded upper airway in dogs with sleep apnea. *J. Appl. Physiol.* 76, 1746–1752.

Pigeolet, E., C. P., Houbion, A., Lambert, D., Michiels, C., Raes, M., Zachary, M. D., et al. (1990). Glutathione peroxidase, superoxide dismutase, and catalase inactivation by peroxides and oxygen derived free radicals. *Mech. Ageing Dev.* 51, 283–297. doi: 10.1016/0047-6374(90)90078-T

Prabhakar, N. R. (2001). Oxygen sensing during intermittent hypoxia: cellular and molecular mechanisms. *J. Appl. Physiol.* 90, 1986–1994.

Raghuraman, G., Rai, V., Peng, Y. J., Prabhakar, N. R., and Kumar, G. K. (2009). Pattern-specific sustained activation of tyrosine hydroxylase by intermittent hypoxia: role of reactive oxygen species-dependent downregulation of protein phosphatase 2A and upregulation of protein kinases. *Antiox. Redox Signal.* 11, 1777–1789. doi: 10.1089/ars.2008.2368

Ray, A. D., Magalang, U. J., Michlin, C. P., Ogasa, T., Krasney, J. A., Gosselin, L. E., et al. (2007). Intermittent hypoxia reduces upper airway stability in lean but not obese Zucker rats. *Am. J. Physiol. Regu. Integr. Comp. Physiol.* 293, R372–R378. doi: 10.1152/ajpregu.00038.2007

Reid, M. B. (2001). Plasticity in skeletal, cardiac, and smooth muscle: invited review: redox modulation of skeletal muscle contraction: what we know and what we don't. *J. Appl. Physiol.* 90, 724–731.

Shan, X., Chi, L., Ke, Y., Luo, C., Qian, S., Gozal, D., et al. (2007). Manganese superoxide dismutase protects mouse cortical neurons from chronic intermittent hypoxia-mediated oxidative damage. *Neurobiol. Dis.* 28, 206–215. doi: 10.1016/j.nbd.2007.07.013

Sharma, S. D., Raghuraman, G., Lee, M. S., Prabhakar, N. R., and Kumar, G. K. (2009). Intermittent hypoxia activates peptidylglycine alpha-amidating monooxygenase in rat brain stem via reactive oxygen species-mediated proteolytic processing. *J. Appl. Physiol.* 106, 12–19. doi: 10.1152/japplphysiol.90702.2008

Shortt, C. M., Fredsted, A., Chow, H. B., Williams, R., Skelly, J. R., Edge, D., et al. (2014). Reactive oxygen species mediated diaphragm fatigue in a rat model of chronic intermittent hypoxia. *Exp. Physiol.* 99, 688–700. doi: 10.1113/expphysiol.2013.076828

Shortt, C. M., and O'Halloran, K. D. (2014). Hydrogen peroxide alters sternohyoid muscle function. *Oral Dis.* 20, 162–170. doi: 10.1111/odi.12084

Skelly, J. R., Bradford, A., Jones, J. F., and O'Halloran, K. D. (2010). Superoxide scavengers improve rat pharyngeal dilator muscle performance. *Am. J. Respir. Cell Mol. Biol.* 42, 725–731. doi: 10.1165/rcmb.2009-0160OC

Skelly, J. R., Edge, D., Shortt, C. M., Jones, J. F. X., Bradford, A., and O'Halloran, K. D. (2012a). Tempol ameliorates pharyngeal dilator muscle dysfunction in a rodent model of chronic intermittent hypoxia. *Am. J. Respir. Cell Mol. Biol.* 46, 139–148. doi: 10.1165/rcmb.2011-0084OC

Skelly, J. R., Rowan, S. C., Jones, J. F., and O'Halloran, K. D. (2012b). Upper airway dilator muscle weakness following intermittent and sustained hypoxia in the rat: effects of a superoxide scavenger. *Physiol. Res.* 62, 187–196.

Souvannakitti, D., Nanduri, J., Yuan, G., Kumar, G. K., Fox, A. P., and Prabhakar, N. R. (2010). NADPH oxidase-dependent regulation of T-Type Ca^{2+} channels and ryanodine receptors mediate the augmented exocytosis of catecholamines from intermittent hypoxia-treated neonatal rat chromaffin cells. *J. Neurosci.* 30, 10763–10772. doi: 10.1523/JNEUROSCI.2307-10.2010

Sun, Q.-A., Hess, D. T., Nogueira, L., Yong, S., Bowles, D. E., Eu, J., et al. (2011). Oxygen-coupled redox regulation of the skeletal muscle ryanodine receptor-Ca^{2+} release channel by NADPH oxidase 4. *Proc. Natl. Acad. Sci. U.S.A.* 108, 16098–16103. doi: 10.1073/pnas.1109546108

van der Poel, C., Edwards, J. N., Macdonald, W. A., and Stephenson, D. G. (2007). Mitochondrial superoxide production in skeletal muscle fibers in the rat and decreased fiber excitability. *Am. J. Physiol. Cell Physiol.* 292, C1353–C1360. doi: 10.1152/ajpcell.00469.2006

Veasey, S. C., Zhan, G., Fenik, P., and Pratico, D. (2004). Long-term intermittent hypoxia: reduced excitatory hypoglossal nerve output. *Am. J. Respir. Crit. Care Med.* 170, 665–672. doi: 10.1164/rccm.200403-261OC

Verstraeten, E. (2007). Neurocognitive effects of obstructive sleep apnea syndrome. *Curr. Neurol. Neurosci. Rep.* 7, 161–166. doi: 10.1007/s11910-007-0012-8

Xia, R., Webb, J. A., Gnall, L. L., Cutler, K., and Abramson, J. J. (2003). Skeletal muscle sarcoplasmic reticulum contains a NADH-dependent oxidase that generates superoxide. *Am. J. Physiol. Cell Physiol.* 285, C215–C221. doi: 10.1152/ajpcell.00034.2002

Yuan, G., Adhikary, G., McCormick, A. A., Holcroft, J. J., Kumar, G. K., and Prabhakar, N. R. (2004). Role of oxidative stress in intermittent hypoxia-induced immediate early gene activation in rat PC12 cells. *J. Physiol.* 557, 773–783. doi: 10.1113/jphysiol.2003.058503

Yuan, G., Khan, S. A., Luo, W., Nanduri, J., Semenza, G. L., and Prabhakar, N. R. (2011). Hypoxia-inducible factor 1 mediates increased expression of NADPH oxidase-2 in response to intermittent hypoxia. *J. Cell. Physiol.* 226, 2925–2933. doi: 10.1002/jcp.22640

Zhou, W. E. I., Li, S., Wan, N., Zhang, Z., Guo, R. U. N., and Chen, B. (2012). Effects of various degrees of oxidative stress induced by intermittent hypoxia in rat myocardial tissues. *Respirology* 17, 821–829. doi: 10.1111/j.1440-1843.2012.02157.x

Conflict of Interest Statement: The authors declare that the research was conducted in the absence of any commercial or financial relationships that could be construed as a potential conflict of interest.

Received: 27 November 2014; accepted: 10 January 2015; published online: 30 January 2015.

Citation: Williams R, Lemaire P, Lewis P, McDonald FB, Lucking E, Hogan S, Sheehan D, Healy V and O'Halloran KD (2015) Chronic intermittent hypoxia increases rat sternohyoid muscle NADPH oxidase expression with attendant modest oxidative stress. Front. Physiol. ***6****:15. doi: 10.3389/fphys.2015.00015*

This article was submitted to Striated Muscle Physiology, a section of the journal Frontiers in Physiology.

frontiers in Physiology

MINI REVIEW
published: 01 September 2015
doi: 10.3389/fphys.2015.00239

Potential molecular mechanisms underlying muscle fatigue mediated by reactive oxygen and nitrogen species

Edward P. Debold *

Department of Kinesiology, University of Massachusetts, Amherst, MA, USA

Intense contractile activity causes a dramatic decline in the force and velocity generating capacity of skeletal muscle within a few minutes, a phenomenon that characterizes fatigue. Much of the research effort has focused on how elevated levels of the metabolites of ATP hydrolysis might inhibit the function of the contractile proteins. However, there is now growing evidence that elevated levels of reactive oxygen and nitrogen species (ROS/RNS), which also accumulate in the myoplasm during fatigue, also play a causative role in this type of fatigue. The most compelling evidence comes from observations demonstrating that pre-treatment of intact muscle with a ROS scavenger can significantly attenuate the development of fatigue. A clear advantage of this line of inquiry is that the molecular targets and protein modifications of some of the ROS scavengers are well-characterized enabling researchers to begin to identify potential regions and even specific amino acid residues modified during fatigue. Combining this knowledge with assessments of contractile properties from the whole muscle level down to the dynamic motions within specific contractile proteins enable the linking of the structural modifications to the functional impacts, using advanced chemical and biophysical techniques. Based on this approach at least two areas are beginning emerge as potentially important sites, the regulatory protein troponin and the actin binding region of myosin. This review highlights some of these recent efforts which have the potential to offer uniquely precise information on the underlying molecular basis of fatigue. This work may also have implications beyond muscle fatigue as ROS/RNS mediated protein modifications are also thought to play a role in the loss of muscle function with aging and in some acute pathologies like cardiac arrest and ischemia.

Keywords: muscle, fatigue, reactive oxygen species, myosin, troponin, tropomyosin

OPEN ACCESS

Edited by:
Brian McDonagh, University of Liverpool, UK

Reviewed by:
Leonardo F. Ferreira, University of Florida, USA
D. George Stephenson, La Trobe University, Australia
James Nathan Cobley, Abertay University, UK

***Correspondence:**
Edward P. Debold, Department of Kinesiology, University of Massachusetts, 158 Totman Bldg., 30 Eastman Lane, Amherst, MA 01003, USA
edebold@kin.umass.edu

Specialty section:
This article was submitted to Striated Muscle Physiology, a section of the journal Frontiers in Physiology

Received: *21 May 2015*
Accepted: *07 August 2015*
Published: *01 September 2015*

Citation:
Debold EP (2015) Potential molecular mechanisms underlying muscle fatigue mediated by reactive oxygen and nitrogen species. Front. Physiol. 6:239. doi: 10.3389/fphys.2015.00239

Introduction

Intense exercise can be sustained for only a few minutes before the force and motion generating capacity of skeletal muscle is severely compromised; a phenomenon which defines fatigue (Westerblad et al., 1991; Fitts, 1994; Allen, 2009). Understanding the mechanisms through which this occurs is important to our basic understanding of muscle but also for the development of therapies to improve the physical function of the elderly and chronically ill, so debilitated by fatigue. The extent and rate of fatigue from intense exercise is dependent on numerous factors

including the intensity of contraction as well as the rate and duration of stimulation (Fitts, 1994). In humans there are many potential sites of failure and many transient intracellular biochemical changes, including the accumulation of metabolites of ATP hydrolysis (Fitts, 1994). The role of accumulating metabolites has been particularly well-studied, detailed in other reviews (Westerblad et al., 1991; Fitts, 1994, 1996; Cooke, 2007; Enoka and Duchateau, 2007; Allen et al., 2008; Allen, 2009; Debold, 2012). Although less well-studied, there is growing evidence that elevated levels of reactive oxygen and nitrogen species (ROS/RNS) accumulate during intense contractile activity and play a causative role in the fatigue process (Westerblad and Allen, 2011).

Some of the most compelling evidence comes from the observation that pre-treatment with exogenous ROS scavengers attenuates the rate and extent of fatigue in intact muscle (see **Figure 1**). While this is most pronounced in isolated muscle preparations (Shindoh et al., 1990; Moopanar and Allen, 2005, 2006) where the *ex vivo* nature of the preparations might augment the level of ROS (Halliwell, 2014), it has also been observed in exercising humans (Reid et al., 1994; Medved et al., 2004; Ferreira et al., 2011; Slattery et al., 2014). The preventative effect of ROS scavengers is most obvious in humans when fatigue is induced with low stimulation frequencies (Reid et al., 1994), but it is also dependent on the variant of ROS scavenger (Hernández et al., 2012). Thus, there is evidence that ROS/RNS scavengers can delay fatigue and that the accumulation of ROS is linked to the onset and extent of fatigue, which provide compelling support for a causative role. The molecular mechanisms underlying these effects remain unclear but in the last 5–10 years several research groups have made significant advances that have identified specific contractile proteins modified by ROS/RNS and their impact on molecular function (Callahan et al., 2001; Moopanar and Allen, 2005, 2006; Prochniewicz et al., 2008; Dutka et al., 2011; Klein et al., 2011; Mollica et al., 2012; Moen et al., 2014b; Cheng et al., 2015). This review focuses on these recent efforts that highlight the potential molecular mechanism of ROS/RNS mediated fatigue.

What are ROS/RNS and How Do They Affect Muscle Function?

ROS/RNS are chemically reactive molecules making them capable of transiently or permanently damaging cell membranes

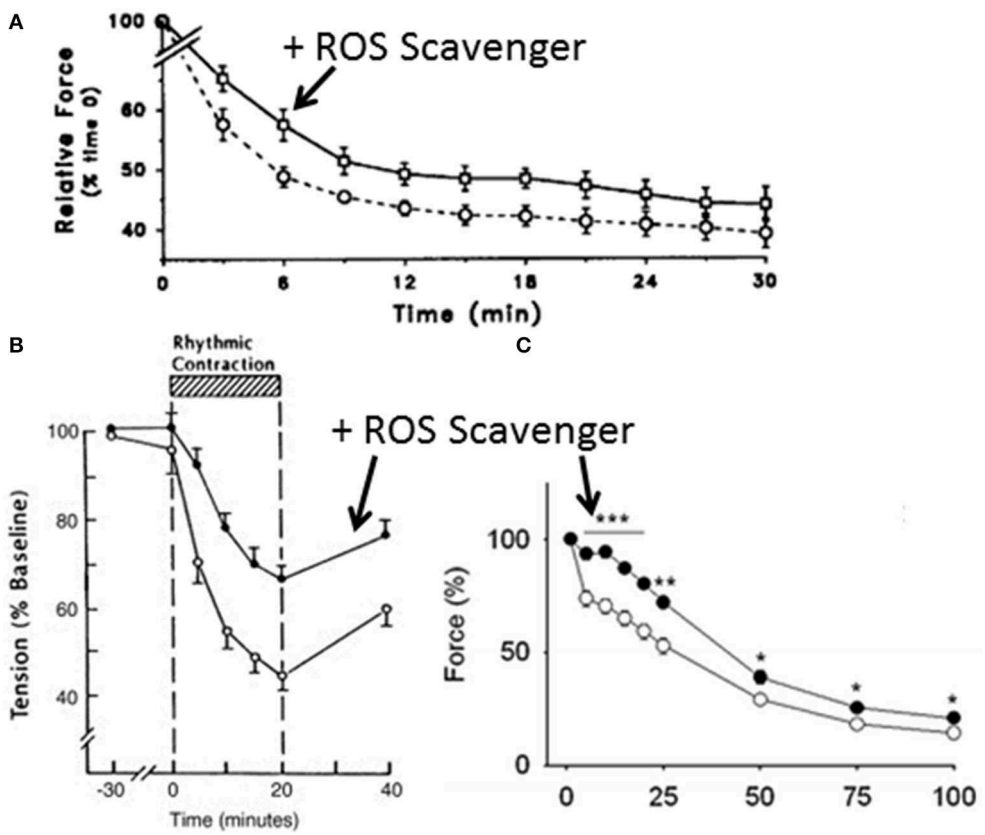

FIGURE 1 | Effect of reactive oxygen species scavengers on fatigue. (A) Effect of pretreatment with ROS scavenger, *N*-acetylcysteine (circles) vs. control (squares) on the fatigue profile of the tibialis anterior muscle in humans stimulated at 10 Hz with a surface electrode. The drop in force was significant under both conditions but the force was greater with *N*-acetylcysteine treatment. Reprinted from Reid et al. (1994) with rights and permission from American Society for Clinical Investigation. **(B)** Effect of the *N*-acetylcysteine on the development of diaphragm fatigue in an anesthetized intact rabbit preparation. Reprinted from Shindoh et al. (1990) with permission. **(C)** Effect of *N*-acetylcysteine on the development of fatigue in isolated mouse extensor digitorum longus muscle. Reprinted from Katz et al. (2014) with permission. *, ** and *** indicate significantly different from corresponding control value (open circles) at $p < 0.05$, $p < 0.01$, and $p < 0.001$ respectively.

and proteins (Moen et al., 2014b). The most important species of ROS/RNS for muscle contraction appear to be hydrogen peroxide (H_2O_2), superoxide ($O_2^{-\cdot}$) as well as nitric oxide which is a precursor to the RNS peroxynitrite ($ONOO^-$), and involved in the S-Nitrosylation of proteins (Reid, 2001a). ROS were originally thought to be primarily generated in the mitochondria as a by-product of oxidative phosphorylation, however more recent findings suggest that the amount generated in the mitochondria is likely quite low, with an upper estimate of ∼0.15% (St-Pierre et al., 2002). Instead newer measurements suggest that the primary source of ROS in the cytosol is generated by membrane bound NADPH oxidases (Sakellariou et al., 2011, 2013). For a detailed description of ROS/RNS generating reactions the reader is directed to several excellent reviews (Reid, 2001b; Allen et al., 2008; Powers et al., 2011). Regardless of the source, free radicals are continually produced in muscle cells. At rest, low levels are generated and thought to play an important role in maintaining normal muscle function (Reid, 2001b). In fact, when levels of ROS are low, as might occur at rest or even in the early stages of fatigue, they appear to enhance not inhibit force production (Reid, 2001b) and may even help to delay the onset of fatigue (Mollica et al., 2012). However, as contraction intensifies and/or becomes prolonged, ROS/RNS become elevated and are thought to inhibit proper function of muscle proteins (Reid, 2001a). Consistent with this idea, at higher concentrations, certain ROS inhibit contractile function in isolated muscle fibers (Andrade et al., 1998). When excessively elevated, the reactive nature of ROS/RNS mean that they can induce structural modifications to contractile proteins at cysteine and methionine residues, including for example the formation of disulfide bridges between neighboring cysteine residues either within or between proteins. These modifications may be benign or could depress the function of key contractile proteins. Therefore, goal of much of the recent research in this area has focused on linking loss of contractile protein function to a specific structural alteration; recent advances in biochemical and biophysical techniques are making this a tractable problem.

Skeletal muscle fatigue from intense contractile activity could result from the failure anywhere along the muscle activation pathway, from the firing of neurons in the motor cortex to the generation of force and motion by an actomyosin cross-bridge. A wealth of evidence suggests that this type of fatigue is primarily due to a failure that is distal to the central nervous system (Merton, 1954; Cady et al., 1989; Westerblad et al., 1991). Thus, it is thought that the mechanisms that underlie the role for ROS/RNS in fatigue are also mediated distal to the neuromuscular junction (Westerblad and Allen, 2011). Based on the idea that fatigue originates peripherally there are four key sites at which ROS/RNS mediated fatigue could potentially develop (Westerblad and Allen, 2011): (1) compromised ability to depolarize the sarcolemma; (2) reduction in the amount of Ca^{++} released from the sarcoplasmic reticulum (SR); (3) a decrease in the Ca^{++}-sensitivity of the thin filament; and (4) a direct effect on myosin's ability to bind to and translocate an actin filament.

Do ROS Contribute to Fatigue by Affecting Membrane Excitability and/or Ca^{++} Release from the SR?

A decrease in membrane excitability is one potential mechanism, and based on observations in intact fibers this is believed to occur during fatigue (Juel, 1988), with the effect most pronounced deep within the t-tubules (Balog et al., 1994). Presumably this results from the inability to restore the Na^+/K^+ balance with repeated contractions (Juel, 1988) due to ROS modifications of the Na^+/K^+ pump acting to inhibit its function (McKenna et al., 2006). Interestingly, pretreatment of humans with *N*-acetylcysteine (NAC) (a thiol containing compound (Ferreira and Reid, 2008) that spurs the resynthesize glutathione, a major endogenous antioxidant) increased time to fatigue at 92% of VO_2 peak by ∼25% (McKenna et al., 2006). Subsequent biochemical analysis of muscle biopsies revealed that NAC attenuated the decline Na^+/K^+ pump activity, suggesting that this type of fatigue may involve ROS/RNS modification of proteins responsible for maintaining membrane excitability.

However, a distinctly different conclusion was reached by authors using intact fibers that were exposed to elevated levels of exogenous H_2O_2. These findings consistently show that elevated H_2O_2 decreases isometric force but not the intracellular [Ca^{++}] (Andrade et al., 1998, 2001), suggesting that the signal to the SR to release Ca^{++} and thus membrane excitability is not compromised by ROS in these preparations. Part of the discrepancy in the findings may be due to different stimulation rates employed since the experiments on isolated preparations typically show little or no effect on intracellular Ca^{++}-levels with fatigue typically stimulate the muscle at 40 Hz or greater, a rate at which ROS scavengers have little effect on fatigue (Ferreira and Reid, 2008). Another issue may be the timing of the exposure to the oxidants as it has been shown that different regions of the contractile proteins are accessible based on the level of Ca^{++}-activation (Gross and Lehman, 2013). Or the discrepancy may be related to the use of exogenous H_2O_2, which has been hypothesized to exert different effects than those generated endogenously (Forman, 2007).

If membrane excitability were compromised by fatigue it should translate into a weaker signal activating the voltage sensitive receptors of the t-tubules (DHPR) and in turn less release of Ca^{++} by the ryanodine receptors (RyR), causing less activation of the thin filament and thus less cross-bridge formation and force generation (Balog and Fitts, 1996). Support for this notion comes from observations in mechanically skinned fibers in which fatigue, accelerated by higher temperatures, was mitigated by the superoxide scavenger Tiron (van der Poel and Stephenson, 2007). Consistent with this observation studies utilizing vesicles with RYR channels have demonstrated that this channel can be oxidized and that this can affect its ability to release Ca^{++} by increasing their sensitivity to Ca^{++}-induced-Ca^{++}-release (CICR) (Marengo et al., 1998). Likewise, exposure of skinned muscle fibers to H_2O_2 can also increase CICR. Furthermore, NO has been shown to exert regulatory effects on the RYR channels in skeletal muscle (Sun et al., 2001, 2003).

Despite these modifications, exposure of isolated intact muscle preparations to exogenous ROS have generally demonstrated insignificant effects on Ca^{++} released from the SR in response to an action potential (Lamb and Posterino, 2003; Posterino et al., 2003), even at higher temperatures(Place et al., 2009). This suggests that Ca^{++} release is not susceptible to ROS when activated via the nerve whereas it is when stimulated artificially in skinned fibers. Further support for this notion comes from observations showing that the ROS scavenger, Tiron, significantly attenuates the development of fatigue in intact fibers without altering the intracellular [Ca^{++}] (Moopanar and Allen, 2005). Therefore, despite the findings in skinned muscle fibers most current evidence in intact preparations suggests that ROS/RNS mediated fatigue is not due to a loss of membrane excitability or an inability to release Ca^{++} but rather to an effect downstream of Ca^{++} release (Westerblad and Allen, 2011).

Does ROS Contribute to Fatigue by Decreasing Myofilament Ca^{++}-Sensitivity?

During normal muscle activation Ca^{++} release from the SR is followed by a series of complex molecular events that ultimately lead to tropomyosin moving over the surface of actin to reveal the myosin binding sites (Gordon et al., 2000). During fatigue disruption of any one of these steps would disrupt thin filament activation leading a decrease in Ca^{++}-sensitivity. These steps include the binding of Ca^{++} to the calcium binding subunit of troponin (TnC), which triggers the c-terminal domain of the inhibitory subunit of Tn (TnI) to retract from its binding site on actin (Takeda et al., 2003), that allows tropomyosin (Tm) to move further into the groove in actin making the myosin binding sites more accessible (Gordon et al., 2000). In the most widely accepted model of thin filament activation Tm is believed be in a dynamic equilibrium among three positions on actin (Galinska-Rakoczy et al., 2008) with the filament only fully activated when a myosin molecule is strongly bound to actin (McKillop and Geeves, 1993). This is required because the strong-binding of myosin moves Tm a further distance away from the myosin binding sites allowing for neighboring myosins to strongly bind to the filament (Galinska-Rakoczy et al., 2008). Therefore, ROS/RNS could elicit fatigue by either altering Tn's ability to bind Ca^{++} and communicate this signal to its other subunits and Tm, and/or by disrupting myosin's ability to strongly bind to actin. This effect may be particularly relevant because in the latter stages of fatigue, through mechanisms independent of ROS, Ca^{++} release from the SR is compromised (Lee et al., 1991) resulting in a lower intracellular level of Ca^{++} with any given level of stimulation.

Some of the earliest efforts, in chemically skinned cardiac muscle fibers, found that exposure to elevated levels of superoxide had a large effect on maximal force but did not reduce Ca^{++}-sensitivity (MacFarlane and Miller, 1992). Similarly, exposure of rabbit diaphragm fibers to superoxide reduced maximal force but did not change the concentration of Ca^{++} required to reach half maximal force (pCa_{50}) (Darnley et al., 2001). Skinned single skeletal muscle fibers to respond similarly to elevated ROS, seeing a decrease in maximal isometric force with no change in Ca^{++}-sensitivity (van der Poel and Stephenson, 2002). Although this study was focused on determining the effects of elevated temperatures on contractile function, the findings are relevant to the role of ROS in muscle fatigue because they indicated that the depression in function at higher temperatures was due to elevated levels of superoxide. Consistent with this idea, the depression in maximal isometric force could be reversed by the disulphide reducing agent dithiotheritol (DTT) (van der Poel and Stephenson, 2002), which is similar to what is seen with fatigue (Moopanar and Allen, 2005). Collectively these findings suggest that ROS have a pronounced, depressive effect on maximal isometric force and little impact on Ca^{++}-sensitivity. Thus, these findings point toward ROS potentially having a direct effect on actomyosin and not the regulatory proteins troponin and tropomyosin.

However, these findings stand in stark contrast to the results from intact muscle preparations which have consistently observed that ROS decreases Ca^{++}-sensitivity while exerting minimal effects on maximal isometric force (Andrade et al., 1998, 2001; Moopanar and Allen, 2005, 2006). For example, elevated levels of H_2O_2 produced a pronounced rightward shift in the force-calcium relation in intact muscle fibers without affecting the intracellular Ca^{++} concentration (**Figure 2**), suggesting that the H_2O_2 decreased the Ca^{++}-sensitivity of the myofilaments (Andrade et al., 1998). This work was confirmed and extended in a more recent where intact muscle was fatigued in the presence of DTT (Moopanar and Allen, 2006). In this study living mouse fast muscle fibers were stimulated to fatigue while simultaneously measuring isometric force and intracellular levels of Ca^{++}, enabling the ability to directly determine the

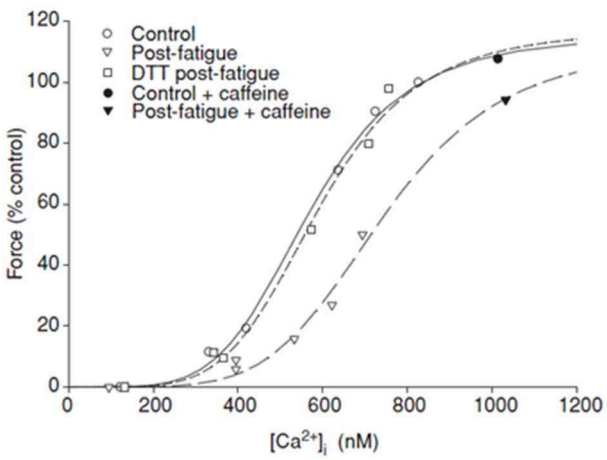

FIGURE 2 | ROS mediated fatigue and Ca^{++}-sensitivity. Force-calcium relation plotted during fatigue of intact mouse flexor brevis muscle fibers stimulated at 100 Hz, at 37°C. Force expressed relative to rested value under control conditions. Fatigue under control conditions produced a strong rightward shift in the relation and depressed maximal force. Maximal force but not Ca^{++}-sensitivity was restored with caffeine. Treatment with dithiothreitol (DTT) restored Ca^{++}-sensitivity. Reprinted from Moopanar and Allen (2006) with permission from John Wiley and Sons publishing company.

force-calcium relationship in an intact fiber during fatigue. Consistent with prior experiments in intact muscle, Ca^{++} release was compromised by fatigue but this was not reversed by DTT, indicating no role for ROS. Ca^{++}-sensitivity however was depressed and was fully reversed by DTT. While subsequent findings suggested that iron leeching off the stimulating electrode in these experiments likely drove the ROS concentration higher than originally reported (Reardon and Allen, 2009a,b) it remains clear that elevated levels of ROS mediated the depressive effects on force. Therefore, these findings suggest that elevated levels of ROS decrease the Ca^{++}-sensitivity of the myofilaments and that this may be the primary mechanism through which ROS induces fatigue in intact muscle.

It is not clear why the results from skinned muscle fibers differ so strongly from those using intact muscle fibers. While it can be argued that intact fibers, which can be exposed to a fatiguing protocol, represent the more physiologically relevant findings, a careful delineation of the differences between these findings may provide key insights into the mechanisms underlying ROS induced muscle fatigue. Along this line of thought, a recent report focused on prolonged low-frequency force depression observed that both the SR Ca^{++}-release and myofilament sensitivity can be altered by fatiguing stimulation in intact fibers (Cheng et al., 2015). To explain these findings they suggested a model where the mechanism of ROS mediated fatigue is dependent on the stimulation protocol, with one type of protocol superoxide is generated in the mitochondria and owing to its proximity and possible physical connections to the SR (Boncompagni et al., 2009) directly affects the DHP and RyR channels, and as a result reduces Ca^{++} release, but has no effect on Ca^{++}-sensitivity. In contrast, other types of fatigue protocols, and exposures to exogenous ROS/RNS, result in a more broad cytosolic elevation of ROS (e.g., exogenous H_2O_2 exposure) that modifies the thick and thin filaments of the sarcomere, leading to a decrease in Ca^{++}-sensitivity.

Since DTT targets disulphide linkages the findings of Moopanar and Allen (2006) suggest that these types of modifications are driving the ROS mediated fatigue, but it is unclear which of the contractile proteins involved determining the Ca^{++}-sensitivity are modified by the ROS. However, related work in diaphragm muscle fatigued under hypoxic conditions may offer insight (de Paula Brotto et al., 2001). In response to fatiguing stimulation there was evidence of TnI and TnC degradation, both of which are integral to proper thin filament activation. The loss in force during fatigue was attributed to the cleavage of these subunits of Tn which the authors speculated resulted from ROS modification that targeted them for proteolysis (de Paula Brotto et al., 2001). The authors also speculated that although hypoxia might generate a greater and more diverse pool of ROS that the same ROS might also appear during physiological fatigue because muscle is thought to become hypoxic to some extent during fatigue even under normoxic conditions (Babcock et al., 1995).

Alternatively fatigue may not lead to cleavage of TnI but rather might induce post-translational modifications of Tn/Tm. In support of this notion a recent study focused on identifying the mechanisms of the increased Ca^{++}-sensitivity following a treatment that oxidizes cysteine residues (disulphide 2,2′-dithiodipyridine or DTDP) found that the effects could be attributed to the addition of a glutathione to a specific cysteine residue (Cys133) in TnI (Mollica et al., 2012). This residue is in a crucial mobile region of TnI that switches between being bound to actin (low Ca^{++}) and bound to a hydrophobic patch on the N-lobe of TnC (High Ca^{++}) (Takeda et al., 2003). Therefore, this modification likely would lead to this region more readily associating with TnC and therefore could explain the increased Ca^{++}-sensitivity under the conditions tested. This effect appears to increase with exercise and thus the authors suggested it may help delay the onset of, rather than contribute to, fatigue. Thus, this effect is the opposite of the depressive effects described above but highlights that the regulatory proteins can be post-translationally modified in response to exercise. It would be interesting to determine if the modification is lost as fatigue becomes more severe or if other alterations that lead to depressed Ca^{++}-sensitivity appear in the same crucial region of TnI.

Yet another possible explanation for these observations would be the oxidation-induced dissociation of TnC from the troponin complex and thus the thin filament. This notion is supported by evidence showing that oxidation of the Cys 98 residue of the D/E helix of TnC reduces its affinity for the thin filament and the effect is readily reversed by exposure to DTT (Pinto et al., 2011). It will be informative to understand the mechanisms underlying this event in more detail and how it might impact fatigue in future work.

Overall these data demonstrate strong evidence that the ROS/RNS mediated fatigue could involve alterations in the structure and function of the muscle regulatory proteins that is consistent with the observed decrease in Ca^{++} sensitivity.

Is Myosin's Function Affected by ROS/RNS During Fatigue?

The skinned fibers studies demonstrating that elevated levels of ROS/RNS decrease maximal isometric force but not Ca^{++}sensitivity suggest that under these conditions ROS/RNS may act by modifying myosin and/or actin. Such targets and modifications have yet to be thoroughly investigated but some recent work focused on understanding the broad effects of oxidative stress on muscle have highlighted that myosin may have redox sensitive residues in the actomyosin interface (Prochniewicz et al., 2008; Klein et al., 2011; Moen et al., 2014a,b) that affect its function. Consistent with others, this group has shown that non-physiological concentrations of H_2O_2 (5–50 mM) can reduce the maximal isometric force, maximal ATPase rate and Ca^{++} -sensitivity of chemically skinned skeletal muscle fibers (Prochniewicz et al., 2008). Electron paramagnetic resonance labeling experiments revealed that the treatment increases the fraction of myosin heads in the strongly bound state in relaxed conditions (i.e., low Ca^{++}). With more heads in a strongly bound state at rest, less heads will be able to go through the weak-to-strong force generating transition upon activation, and thus this may explain the decrease in maximal isometric force in the muscle fibers in response to H_2O_2. Further, analysis

using mass spectrometry showed the addition of multiple oxygen atoms on both myosin's heavy and light chains, which occurred exclusively at methionine residues. This provides a link between the loss of force generation with a modification to a specific residue on myosin. In a follow up study, using myosin expressed in *Dictyostelium Discoideum* (*Dicty*), the authors demonstrated that most of H_2O_2's effects on myosin function can be attributed to oxidation at a single methionine residue (M394) in the actin-binding interface (Klein et al., 2011). This hypothesis is further supported by more recent work demonstrating that the depressive effects of oxidation at this site can be completely reversed by exposure to methionine sulfoxide reductase targeting the M394 site (Moen et al., 2014a). Interestingly in human skeletal muscle myosin this residue is a Cys not a Met, but the effects of oxidation at this residue when it is changed to a Cys in the *Dicty* construct are nearly identical to those when M394 is oxidized (Moen et al., 2014a). Thus, this is an interesting line of experiments and highlights that myosin can be modified by ROS species which are elevated during fatigue, and that the functional differences are attributable to the modification at a single residue in the actomyosin interface. It will be important to determine if the modification also happens in human skeletal muscle during fatigue and to demonstrate that it contributes to the depressive effects seen during fatigue. This would be particularly exciting because presumably it could be readily reversed.

Acknowledgments

EPD is funded by the American Heart Association (GIA#14GRNT20450002).

References

Allen, D. G. (2009). Fatigue in working muscles. *J. Appl. Physiol.* 106, 358–359. doi: 10.1152/japplphysiol.91599.2008

Allen, D. G., Lamb, G. D., and Westerblad, H. (2008). Skeletal muscle fatigue: cellular mechanisms. *Physiol. Rev*. 88, 287–332. doi: 10.1152/physrev.00015.2007

Andrade, F. H., Reid, M. B., Allen, D. G., and Westerblad, H. (1998). Effect of hydrogen peroxide and dithiothreitol on contractile function of single skeletal muscle fibres from the mouse. *J. Physiol.* 509(Pt 2), 565–575. doi: 10.1111/j.1469-7793.1998.565bn.x

Andrade, F. H., Reid, M. B., and Westerblad, H. (2001). Contractile response of skeletal muscle to low peroxide concentrations: myofibrillar calcium sensitivity as a likely target for redox-modulation. *FASEB J*. 15, 309–311. doi: 10.1096/fj.00-0507fje

Babcock, M. A., Johnson, B. D., Pegelow, D. F., Suman, O. E., Griffin, D., and Dempsey, J. A. (1995). Hypoxic effects on exercise-induced diaphragmatic fatigue in normal healthy humans. *J. Appl. Physiol. (1985)* 78, 82–92.

Balog, E. M., and Fitts, R. H. (1996). Effects of fatiguing stimulation on intracellular Na+ and K+ in frog skeletal muscle. *J. Appl. Physiol. (1985)* 81, 679–685.

Balog, E. M., Thompson, L. V., and Fitts, R. H. (1994). Role of sarcolemma action potentials and excitability in muscle fatigue. *J. Appl. Physiol. (1985)* 76, 2157–2162.

Boncompagni, S., Rossi, A. E., Micaroni, M., Hamilton, S. L., Dirksen, R. T., Franzini-Armstrong, C., et al. (2009). Characterization and temporal development of cores in a mouse model of malignant hyperthermia. *Proc. Natl. Acad. Sci. U.S.A.* 106, 21996–22001. doi: 10.1073/pnas.0911496106

Cady, E. B., Jones, D. A., Lynn, J., and Newham, D. J. (1989). Changes in force and intracellular metabolites during fatigue of human skeletal muscle. *J. Physiol.* 418, 311–325. doi: 10.1113/jphysiol.1989.sp017842

Callahan, L. A., She, Z. W., and Nosek, T. M. (2001). Superoxide, hydroxyl radical, and hydrogen peroxide effects on single-diaphragm fiber contractile apparatus. *J. Appl. Physiol. (1985)* 90, 45–54.

Cheng, A. J., Bruton, J. D., Lanner, J. T., and Westerblad, H. (2015). Antioxidant treatments do not improve force recovery after fatiguing stimulation of mouse skeletal muscle fibres. *J. Physiol.* 593, 457–472. doi: 10.1113/jphysiol.2014.279398

Cooke, R. (2007). Modulation of the actomyosin interaction during fatigue of skeletal muscle. *Muscle Nerve* 36, 756–777. doi: 10.1002/mus.20891

Darnley, G. M., Duke, A. M., Steele, D. S., and MacFarlane, N. G. (2001). Effects of reactive oxygen species on aspects of excitation-contraction coupling in chemically skinned rabbit diaphragm muscle fibres. *Exp. Physiol.* 86, 161–168. doi: 10.1113/eph8602109

Debold, E. P. (2012). Recent insights into the molecular basis of muscular fatigue. *Med. Sci. Sports Exerc*. 44, 1440–1452. doi: 10.1249/mss.0b013e31824cfd26

de Paula Brotto, M., van Leyen, S. A., Brotto, L. S., Jin, J. P., Nosek, C. M., and Nosek, T. M. (2001). Hypoxia/fatigue-induced degradation of troponin I and troponin C: new insights into physiologic muscle fatigue. *Pflugers Arch*. 442, 738–744. doi: 10.1007/s004240100587

Dutka, T. L., Mollica, J. P., and Lamb, G. D. (2011). Differential effects of peroxynitrite on contractile protein properties in fast- and slow-twitch skeletal muscle fibers of rat. *J. Appl. Physiol. (1985)* 110, 705–716. doi: 10.1152/japplphysiol.00739.2010

Enoka, R. M., and Duchateau, J. (2007). Muscle fatigue: what, why and how it influences muscle function. *J. Physiol.* 586, 11–23. doi: 10.1113/jphysiol.2007.139477

Ferreira, L. F., Campbell, K. S., and Reid, M. B. (2011). Effectiveness of sulfur-containing antioxidants in delaying skeletal muscle fatigue. *Med. Sci. Sports Exerc*. 43, 1025–1031. doi: 10.1249/MSS.0b013e3182019a78

Ferreira, L. F., and Reid, M. B. (2008). Muscle-derived ROS and thiol regulation in muscle fatigue. *J. Appl. Physiol. (1985)* 104, 853–860. doi: 10.1152/japplphysiol.00953.2007

Fitts, R. H. (1994). Cellular mechanisms of muscle fatigue. *Physiol. Rev*. 74, 49–94.

Fitts, R. H. (1996). Muscle fatigue: the cellular aspects. *Am. J. Sports Med*. 24, S9–S13.

Forman, H. J. (2007). Use and abuse of exogenous H2O2 in studies of signal transduction. *Free Radic. Biol. Med*. 42, 926–932. doi: 10.1016/j.freeradbiomed.2007.01.011

Galinska-Rakoczy, A., Engel, P., Xu, C., Jung, H., Craig, R., Tobacman, L. S., et al. (2008). Structural basis for the regulation of muscle contraction by troponin and tropomyosin. *J. Mol. Biol*. 379, 929–935. doi: 10.1016/j.jmb.2008.04.062

Gordon, A. M., Homsher, E., and Regnier, M. (2000). Regulation of contraction in striated muscle. *Physiol. Rev*. 80, 853–924.

Gross, S. M., and Lehman, S. L. (2013). Accessibility of myofilament cysteines and effects on ATPase depend on the activation state during exposure to oxidants. *PLoS ONE* 8:e69110. doi: 10.1371/journal.pone.0069110

Halliwell, B. (2014).Cell culture, oxidative stress, and antioxidants: avoiding pitfalls. *Biomed. J*. 37, 99–105. doi: 10.4103/2319-4170.128725

Hernández, A., Cheng, A., and Westerblad, H. (2012). Antioxidants and skeletal muscle performance: "common knowledge" vs. experimental evidence. *Front. Physiol.* 3:46. doi: 10.3389/fphys.2012.00046

Juel, C. (1988). Muscle action potential propagation velocity changes during activity. *Muscle Nerve* 11, 714–719. doi: 10.1002/mus.880110707

Katz, A., Hernández, A., Caballero, D. M., Briceno, J. F., Amezquita, L. V., Kosterina, N., et al. (2014). Effects of N-acetylcysteine on isolated mouse skeletal muscle: contractile properties, temperature dependence, and metabolism. *Pflugers Arch*. 466, 577–585. doi: 10.1007/s00424-013-1331-z

Klein, J. C., Moen, R. J., Smith, E. A., Titus, M. A., and Thomas, D. D. (2011). Structural and functional impact of site-directed methionine oxidation in myosin. *Biochemistry* 50, 10318–10327. doi: 10.1021/bi201279u

Lamb, G. D., and Posterino, G. S. (2003). Effects of oxidation and reduction on contractile function in skeletal muscle fibres of the rat. *J. Physiol.* 546, 149–163. doi: 10.1113/jphysiol.2002.027896

Lee, J. A., Westerblad, H., and Allen, D. G. (1991). Changes in tetanic and resting [Ca2+]i during fatigue and recovery of single muscle fibres from *Xenopus laevis*. *J. Physiol.* 433, 307–326. doi: 10.1113/jphysiol.1991.sp018427

MacFarlane, N. G., and Miller, D. J. (1992). Depression of peak force without altering calcium sensitivity by the superoxide anion in chemically skinned cardiac muscle of rat. *Circ. Res.* 70, 1217–1224. doi: 10.1161/01.RES.70.6.1217

Marengo, J. J., Hidalgo, C., and Bull, R. (1998). Sulfhydryl oxidation modifies the calcium dependence of ryanodine-sensitive calcium channels of excitable cells. *Biophys. J.* 74, 1263–1277. doi: 10.1016/S0006-3495(98)77840-3

McKenna, M. J., Medved, I., Goodman, C. A., Brown, M. J., Bjorksten, A. R., Murphy, K. T., et al. (2006). N-acetylcysteine attenuates the decline in muscle Na+,K+-pump activity and delays fatigue during prolonged exercise in humans. *J. Physiol.* 576, 279–288. doi: 10.1113/jphysiol.2006.115352

McKillop, D. F., and Geeves, M. A. (1993). Regulation of the interaction between actin and myosin subfragment 1: evidence for three states of the thin filament. *Biophys. J.* 65, 693–701. doi: 10.1016/S0006-3495(93)81110-X

Medved, I., Brown, M. J., Bjorksten, A. R., Murphy, K. T., Petersen, A. C., Sostaric, S., et al. (2004). N-acetylcysteine enhances muscle cysteine and glutathione availability and attenuates fatigue during prolonged exercise in endurance-trained individuals. *J. Appl. Physiol (1985)* 97, 1477–1485. doi: 10.1152/japplphysiol.00371.2004

Merton, P. A. (1954). Voluntary strength and fatigue. *J. Physiol.* 123, 553–564. doi: 10.1113/jphysiol.1954.sp005070

Moen, R. J., Cornea, S., Oseid, D. E., Binder, B. P., Klein, J. C., and Thomas, D. D. (2014a). Redox-sensitive residue in the actin-binding interface of myosin. *Biochem. Biophys. Res. Commun.* 453, 345–349. doi: 10.1016/j.bbrc.2014.09.072

Moen, R. J., Klein, J. C., and Thomas, D. D. (2014b). Electron paramagnetic resonance resolves effects of oxidative stress on muscle proteins. *Exerc. Sport Sci. Rev.* 42, 30–36. doi: 10.1249/JES.0000000000000004

Mollica, J. P., Dutka, T. L., Merry, T. L., Lamboley, C. R., McConell, G. K., McKenna, M. J., et al. (2012). S-glutathionylation of troponin I (fast) increases contractile apparatus Ca2+ sensitivity in fast-twitch muscle fibres of rats and humans. *J. Physiol.* 590, 1443–1463. doi: 10.1113/jphysiol.2011.224535

Moopanar, T. R., and Allen, D. G. (2005). Reactive oxygen species reduce myofibrillar Ca2+ sensitivity in fatiguing mouse skeletal muscle at 37 degrees C. *J. Physiol.* 564, 189–199. doi: 10.1113/jphysiol.2005.083519

Moopanar, T. R., and Allen, D. G. (2006). The activity-induced reduction of myofibrillar Ca2+ sensitivity in mouse skeletal muscle is reversed by dithiothreitol. *J. Physiol.* 571, 191–200. doi: 10.1113/jphysiol.2005.101105

Pinto, J. R., de Sousa, V. P., and Sorenson, M. M. (2011). Redox state of troponin C cysteine in the D/E helix alters the C-domain affinity for the thin filament of vertebrate striated muscle. *Biochim. Biophys. Acta* 1810, 391–397. doi: 10.1016/j.bbagen.2010.11.008

Place, N., Yamada, T., Zhang, S. J., Westerblad, H., and Bruton, J. D. (2009). High temperature does not alter fatigability in intact mouse skeletal muscle fibres. *J. Physiol.* 587, 4717–4724. doi: 10.1113/jphysiol.2009.176883

Posterino, G. S., Cellini, M. A., and Lamb, G. D. (2003). Effects of oxidation and cytosolic redox conditions on excitation-contraction coupling in rat skeletal muscle. *J. Physiol.* 547, 807–823. doi: 10.1113/jphysiol.2002.035204

Powers, S. K., Nelson, W. B., and Hudson, M. B. (2011). Exercise-induced oxidative stress in humans: cause and consequences. *Free Radic. Biol. Med.* 51, 942–950. doi: 10.1016/j.freeradbiomed.2010.12.009

Prochniewicz, E., Spakowicz, D., and Thomas, D. D. (2008). Changes in actin structural transitions associated with oxidative inhibition of muscle contraction. *Biochemistry* 47, 11811–11817. doi: 10.1021/bi801080x

Reardon, T. F., and Allen, D. G. (2009a). Iron injections in mice increase skeletal muscle iron content, induce oxidative stress and reduce exercise performance. *Exp. Physiol.* 94, 720–730. doi: 10.1113/expphysiol.2008.046045

Reardon, T. F., and Allen, D. G. (2009b). Time to fatigue is increased in mouse muscle at 37 degrees C; the role of iron and reactive oxygen species. *J. Physiol.* 587, 4705–4716. doi: 10.1113/jphysiol.2009.173005

Reid, M. B. (2001a). Invited Review: redox modulation of skeletal muscle contraction: what we know and what we don't. *J. Appl. Physiol. (1985)* 90, 724–731.

Reid, M. B. (2001b). Nitric oxide, reactive oxygen species, and skeletal muscle contraction. *Med. Sci. Sports Exerc.* 33, 371–376. doi: 10.1097/00005768-200103000-00006

Reid, M. B., Stokic, D. S., Koch, S. M., Khawli, F. A., and Leis, A. A. (1994). N-acetylcysteine inhibits muscle fatigue in humans. *J. Clin. Invest.* 94, 2468–2474. doi: 10.1172/JCI117615

Sakellariou, G. K., Pye, D., Vasilaki, A., Zibrik, L., Palomero, J., Kabayo, T., et al. (2011). Role of superoxide-nitric oxide interactions in the accelerated age-related loss of muscle mass in mice lacking Cu,Zn superoxide dismutase. *Aging Cell* 10, 749–760. doi: 10.1111/j.1474-9726.2011.00709.x

Sakellariou, G. K., Vasilaki, A., Palomero, J., Kayani, A., Zibrik, L., McArdle, A., et al. (2013). Studies of mitochondrial and nonmitochondrial sources implicate nicotinamide adenine dinucleotide phosphate oxidase(s) in the increased skeletal muscle superoxide generation that occurs during contractile activity. *Antioxid. Redox. Signal.* 18, 603–621. doi: 10.1089/ars.2012.4623

Shindoh, C., DiMarco, A., Thomas, A., Manubay, P., and Supinski, G. (1990). Effect of N-acetylcysteine on diaphragm fatigue. *J. Appl. Physiol. (1985)* 68, 2107–2113.

Slattery, K. M., Dascombe, B., Wallace, L. K., Bentley, D. J., and Coutts, A. J. (2014). Effect of N-acetylcysteine on cycling performance after intensified training. *Med. Sci. Sports Exerc.* 46, 1114–1123. doi: 10.1249/MSS.0000000000000222

St-Pierre, J., Buckingham, J. A., Roebuck, S. J., and Brand, M. D. (2002). Topology of superoxide production from different sites in the mitochondrial electron transport chain. *J. Biol. Chem.* 277, 44784–44790. doi: 10.1074/jbc.M207217200

Sun, J., Xin, C., Eu, J. P., Stamler, J. S., and Meissner, G. (2001). Cysteine-3635 is responsible for skeletal muscle ryanodine receptor modulation by NO. *Proc. Natl. Acad. Sci.U.S.A.* 98, 11158–11162. doi: 10.1073/pnas.201289098

Sun, J., Xu, L., Eu, J. P., Stamler, J. S., and Meissner, G. (2003). Nitric oxide, NOC-12, and S-nitrosoglutathione modulate the skeletal muscle calcium release channel/ryanodine receptor by different mechanisms. An allosteric function for O2 in S-nitrosylation of the channel. *J. Biol. Chem.* 278, 8184–8189. doi: 10.1074/jbc.M211940200

Takeda, S., Yamashita, A., Maeda, K., and Maéda, Y. (2003). Structure of the core domain of human cardiac troponin in the $Ca^{(2+)}$-saturated form. *Nature* 424, 35–41. doi: 10.1038/nature01780

van der Poel, C., and Stephenson, D. G. (2002). Reversible changes in $Ca^{(2+)}$-activation properties of rat skeletal muscle exposed to elevated physiological temperatures. *J. Physiol.* 544, 765–776. doi: 10.1113/jphysiol.2002.024968

van der Poel, C., and Stephenson, D. G. (2007). Effects of elevated physiological temperatures on sarcoplasmic reticulum function in mechanically skinned muscle fibers of the rat. *Am. J. Physiol. Cell Physiol.* 293, C133–C141. doi: 10.1152/ajpcell.00052.2007

Westerblad, H., and Allen, D. G. (2011). Emerging roles of ROS/RNS in muscle function and fatigue. *Antioxid. Redox. Signal.* 15, 2487–2499. doi: 10.1089/ars.2011.3909

Westerblad, H., Lee, J. A., Lannergren, J., and Allen, D. G. (1991). Cellular mechanisms of fatigue in skeletal muscle. *Am. J. Physiol.* 261, C195–C209.

Conflict of Interest Statement: The author declares that the research was conducted in the absence of any commercial or financial relationships that could be construed as a potential conflict of interest.

frontiers in Physiology

REVIEW
published: 11 March 2015
doi: 10.3389/fphys.2015.00063

Can endurance exercise preconditioning prevention disuse muscle atrophy?

Michael P. Wiggs *

Department of Applied Physiology and Kinesiology, Center for Exercise Science, University of Florida, Gainesville, FL, USA

Emerging evidence suggests that exercise training can provide a level of protection against disuse muscle atrophy. Endurance exercise training imposes oxidative, metabolic, and heat stress on skeletal muscle which activates a variety of cellular signaling pathways that ultimately leads to the increased expression of proteins that have been demonstrated to protect muscle from inactivity –induced atrophy. This review will highlight the effect of exercise-induced oxidative stress on endogenous enzymatic antioxidant capacity (i.e., superoxide dismutase, glutathione peroxidase, and catalase), the role of oxidative and metabolic stress on PGC1-α, and finally highlight the effect heat stress and HSP70 induction. Finally, this review will discuss the supporting scientific evidence that these proteins can attenuate muscle atrophy through exercise preconditioning.

Keywords: bed rest, unloading, immobilization, superoxide dismutase, HSP70, PGC1-α, mitophagy, oxidative stress

OPEN ACCESS

Edited by:
Brian McDonagh,
University of Liverpool, UK

Reviewed by:
Nazareno Paolocci,
Johns Hopkins University, USA
Daniela Caporossi,
University of Rome Foro Italico, Italy

***Correspondence:**
Michael P. Wiggs,
Department of Applied Physiology and Kinesiology,
Center for Exercise Science,
University of Florida,
Room 25 Florida Gym, Gainesville,
FL 32611, USA
mwiggs@ufl.edu

Specialty section:
This article was submitted to Striated Muscle Physiology, a section of the journal Frontiers in Physiology

Received: *11 December 2014*
Accepted: *17 February 2015*
Published: *11 March 2015*

Citation:
Wiggs MP (2015) Can endurance exercise preconditioning prevention disuse muscle atrophy? Front. Physiol. 6:63. doi: 10.3389/fphys.2015.00063

Introduction

Prolonged periods of inactivity results in a loss of muscle protein, fiber atrophy, and impaired muscle function. It is widely recognized that maintaining skeletal muscle structure and function is important in promoting health and quality of life (Wolfe, 2006). A loss of muscle mass can impair the ability to perform activities of daily living, prolong periods of rehabilitation and be a major risk factor for chronic disease. Therefore, it is important to find ways to attenuate rapid muscle atrophy during periods of prolonged disuse.

Common disuse atrophy conditions include prolonged bed rest, limb immobilization/casting, and prolonged exposure to microgravity. The rapid decrease in muscle size observed during disuse is due to both a reduction in muscle protein synthesis and an increase in protein degradation. Therefore, countermeasures to prevent muscle wasting generally target these pathways. In this regard, it is well established that exercise training is able to increase muscle protein synthesis and has been used as a counter-measure to disuse muscle atrophy in many of these conditions (reviewed in Glover and Phillips, 2010). Indeed, both resistance and endurance exercise have been shown to attenuate muscle disuse muscle atrophy in both human and animal models of muscle atrophy and this has been termed "exercise preconditioning."

However, not all disuse atrophy conditions allow for exercise training during the period of muscle inactivity. For example, during casting and limb immobilization, it is physically impossible to exercise the affected muscles. Another example is mechanical ventilation induced-diaphragm atrophy. This is caused by inactivity of the diaphragm during mechanical ventilation (MV), which causes rapid (e.g., within 12 h) atrophy of the diaphragm (Powers et al., 2013). Recently

our lab demonstrated that endurance exercise training prior to MV protected the diaphragm from muscle atrophy (Smuder et al., 2012a). To date, this is one of the few studies to examine the protective effects of exercise preconditioning against disuse muscle atrophy. Therefore, this review will highlight several potential cytoprotective proteins that are altered with exercise training that may be critical in protecting against disuse muscle atrophy. The review will begin with a brief discussion the regulation of muscle size, followed by the pertinent adaptations related to mitochondria, since mitochondrial health plays a key role in maintaining muscle size and function, and finaly the potential cytoprotective proteins induced by exercise will be discussed.

Overview of the Regulation of Muscle Size

Muscle atrophy results from decrease in protein synthesis and an increase in protein degradation that ultimately leads to a decrease in myofiber size due to loss of contractile proteins, organelles, nuclei, and cytoplasm (Thomason and Booth, 1990). Indeed, animal studies have demonstrated that an increase in protein degradation and a decrease in protein synthesis contribute to disuse atrophy. This section will briefly describe the molecular basis for these processes (detailed review by Schiaffino et al., 2013).

Skeletal Muscle Proteolysis

In regards to proteolysis, skeletal muscle utilizes four complementary pathways to remove damaged, misfolded, or unnecessary proteins (**Figure 1**). These pathways include calpain, caspase-3, ubiquitin proteasome pathway, and autophagy (reviewed in Jackman and Kandarian, 2004). The calpain family of proteins is calcium dependent proteases that are important in the initiation of the breakdown of actin, myosin, and other structural proteins. Indeed, target pharmacological inhibition of calpain protects against disuse muscle atrophy (Tischler et al., 1990; Goll et al., 2003; Maes et al., 2007; Nelson et al., 2012; Talbert et al., 2013a). Caspase-3 is a member of the cysteine-aspartic acid protease family. Caspase-3 is most often defined by its central role in the removal of nuclei by myonuclear apoptosis; however, recent info also demonstrates the caspase-3 can work in concert with calpain in the cleavage of myofibrillar proteins (Du et al., 2004; Dupont-Versteegden, 2006; Smuder et al., 2010). Similar to calpain, inhibition or genetic knockdown of caspase-3 is sufficient to attenuate disuse muscle atrophy (McClung et al., 2007; Nelson et al., 2012; Talbert et al., 2013a; Zhu et al., 2013). Together, it is believed that calpain and caspase-3 are required for disuse atrophy because they begin the initial breakdown of the contractile apparatus of the muscle (Jackman and Kandarian, 2004). Further breakdown of these proteins is accomplished by the ubiquitin-proteasome pathway (Lecker et al., 1999). The proteasome pathway is also important in the degradation of misfolded, smaller polypeptides, and unnecessary proteins. Presently, the role of autophagy in disuse atrophy remains unclear. Early studies suggested that pharmacological inhibition of autophagy had minimal effects on muscle atrophy (Tischler et al., 1990); however, recent evidence suggests that autophagy may play an important role in disuse atrophy, specifically in the ability to selectively degrade organelles such as mitochondria (i.e., mitophagy) (Sandri, 2013). This will be discussed in greater detail in later sections.

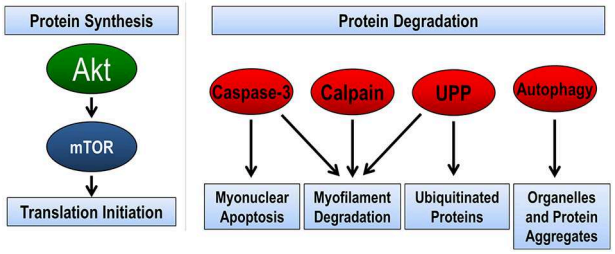

FIGURE 1 | Pathways regulating skeletal muscle size. The balance between protein synthesis and protein degradation determines muscle size. Muscle protein synthesis is regulated through the Akt/mTOR pathway. There are four pathways of protein degradation to degrade cellular components, caspase-3 removes nuclei (apoptosis) and along with the calpain family of proteins can breakdown the contractile proteins (myofilaments) in muscle into smaller polypeptides. The ubiquitin-proteasome pathway (UPP) breaks down the small peptides and any other protein targeted by ubiquitination for degradation. Finally, autophagy breaks down organelles, such as mitochondria and endoplasmic reticulum, and large protein aggregates.

Skeletal Muscle Protein Synthesis

Protein synthesis in cells is accomplished by a tightly controlled and structured scheme of signaling pathways, which culminate in the translation of messenger RNA (mRNA) into a specific protein. Within hours of disuse, muscle protein synthesis is rapidly depressed roughly 25–50% of control and reaches a new baseline level that persists throughout the period of inactivity (De Boer et al., 2007; Kortebein et al., 2008; Symons et al., 2009; Ferrando et al., 2010) The Akt/mTOR pathway is a crucial regulator of muscle mass by controlling formation of translation initiation machinery, the rate limiting step in protein synthesis (Bodine et al., 2001). Disuse atrophy results in decrease in this signaling pathway by decrease the phosphorylation of Akt and its downstream target mTOR. This ultimately leads to a decreased formation of the translation initiation complex and therefore, muscle protein synthesis.

In summary, it is believed that increased protein degradation and decreased protein synthesis contribute to disuse muscle atrophy. Of note, the increase in protein degradation persists only for a few days, while the decrease in protein synthesis happens within hours and remains depressed for the duration of disuse.

Endurance Exercise Training-Induced Adaptive Response in Skeletal Muscle

Classic studies elegantly demonstrate that prolonged endurance exercise training results in beneficial adaptations to skeletal muscle (Saltin et al., 1977; Holloszy and Coyle, 1984). Note that resistance exercise may also have positive effects in skeletal muscle. Unless otherwise stated, exercise training will specifically reference prolonged moderate to high intensity endurance exercise training. One of the fundamental principles of endurance training is a beneficial changes that with mitochondria in skeletal

muscle. Given than exercise intensity and duration are sufficient to elicit a response, mitochondrial alterations are two-fold. First, there is an increase in mitochondrial turnover that is due to both an increase in new mitochondrion being made and slight increase in old mitochondria being removed. The end result is that exercise creates a larger population of mitochondria within skeletal muscle. In addition, increase in mitochondrial content improves the control of energy metabolism, and results in the oxidation of more fatty acids and less glycogen for ATP production. Indeed, these alterations are important because they are in contrast of many of the changes that occur with disuse atrophy, and will be discussed in detail later in this review.

Many of the adaptations that occur with exercise training occur due to an adaptive response. In other words, acute intense exercise training imposes a brief physiological stress on skeletal muscle. Examples of these stresses include oxidative, thermal, mechanical, metabolic, and cytokine production. In response to these stressors, signaling pathways are activated in order to increase the protein content of stress response proteins. This review will focus on several proteins that may play a role in cytoprotection, which are increased in response to acute exercise training due to oxidative, metabolic, and thermal stress.

The notion that exercise training can be cytoprotective against disuse muscle atrophy originates from the idea that repeated bouts of the exercise over a prolonged period of time results in an accumulation of these cytoprotective proteins, and therefore allows the skeletal muscle to be more resistant to the stress. It is important to note that many of the signaling pathways and proteins that are increased following endurance exercise are also found to be increased in disease states. Disuse muscle atrophy or disease states are associated with chronic exposure to stressors, and therefore the alterations in signaling pathways and protein expression are required for maintenance of cell homeostasis. In contrast, exercise-induced cellular stress is acute, lasting at most a few hours. Rest periods following exercise allows the skeletal muscle to handle the stressor and ultimately adapt. In theory exercise training may protect muscle from disuse atrophy by providing a "reserve" of cytoprotective proteins and increases the cell's ability to resist stress.

Role of Mitochondria and Oxidative Stress in Disuse Muscle Atrophy

Disuse muscle atrophy offers a different model of atrophy as opposed to many other models of atrophy because it is not associated with an increase in markers of inflammation. Therefore, the signals that promote atrophy are derived intracellularly. Evidence suggests that the major source of these intracellular signals arise in the mitochondria (Powers et al., 2012b).

Mitochondrial Morphology and Function are Altered During Disuse

The first studies to demonstrate that muscle inactivity was associated with alterations in mitochondria were completed in the early 1960s. These studies demonstrated that muscles subjected to denervation had mitochondria that were irregularly shaped and swollen (Aloisi et al., 1960; Carafoli et al., 1964; Muscatello and Patriarca, 1968) and had impaired mitochondrial coupling. Since these initial investigations, it has become well accepted that disuse muscle atrophy results in altered mitochondrial morphology and mitochondrial dysfunction (Powers et al., 2012b). Indeed, disuse atrophy disrupts the functioning of the oxidative phosphorylation system (i.e., electron transport chain), which results in the generation of superoxide (O_2^-). The O_2^- is dismutated to hydrogen peroxide and can then diffuse from the mitochondrion into the cytoplasm and negatively affect cell signaling pathways.

The Dual Role of Oxidative Stress in Disuse Muscle Atrophy and Exercise-Induced Adaptations in Skeletal Muscle

Several studies have demonstrated that disuse atrophy promotes an increase in reactive oxygen species (ROS) production in skeletal muscle (Adhihetty et al., 2007b; Muller et al., 2007; Kavazis et al., 2009). This increase is accompanied by a decreased expression of mitochondrial proteins and decreased mitochondrial respiration (i.e., ATP production). Increased ROS production alters redox signaling in muscle fibers that can increase proteolysis and decrease protein synthesis (reviewed in Powers, 2014). To further compound these effects, disuse muscle atrophy is associated with an overall decrease in antioxidant capacity in skeletal muscle (Lawler et al., 2003; Falk et al., 2006; Kavazis et al., 2009; Min et al., 2011). This decrease in antioxidant capacity is likely due to decreased antioxidant scavenging ability and not a decrease in antioxidant enzyme content (Kondo et al., 1993; Lawler et al., 2003).

Paradoxically, it is well established that endurance exercise increases oxidative stress in skeletal muscle. The first report of exercise-induced ROS in skeletal muscle was first reported over 30 years ago by Davies et al. (1982). Since that seminal report, many studies have confirmed that muscle contraction markedly increases the amount of ROS production compared to resting skeletal muscle (Powers and Jackson, 2008). An increase in ROS production has been demonstrated to be a powerful signaling molecule in activating signaling pathways. Importantly, increased ROS production acts as a powerful signal for the activation of transcription factors that increase endogenous antioxidant proteins (Powers et al., 2011). Indeed, evidence now suggests that the transient oxidative stress that occurs with exercise may be required for skeletal muscle adaptation to occur. Studies in animals (Gomez-Cabrera et al., 2005, 2008a) and humans (Ristow et al., 2009) have demonstrated that preventing exercise-induced oxidative stress blunted an increase in markers of mitochondrial biogenesis and endogenous antioxidants with training. Therefore, it appears that exercise-induced oxidative stress is required for the adaptive response of antioxidants.

The key difference between exercise-induced oxidative stress and oxidative stress associated with disuse atrophy is the duration of the exposure. Oxidative stress following exercise is transient in nature, while disuse atrophy results in chronic exposure to elevated ROS. Therefore the next section will briefly discuss endogenous antioxidants that are important in maintaining homeostasis in skeletal muscle and will discuss which of these antioxidants may confer protection due to exercise preconditioning.

The Role of Endogenous Antioxidants in Protection Against Disuse Atrophy

Skeletal muscle maintains a tightly controlled network of antioxidant defense mechanisms to reduce the potential for oxidative damage during periods of increased oxidative stress. Indeed, prolonged muscle inactivity is associated with a decrease in antioxidant capacity as well as an increase in ROS production and emission from mitochondria (Lawler et al., 2003; Falk et al., 2006; Kavazis et al., 2009; Min et al., 2011). In this section, we will provide a brief overview of three primary antioxidant enzymes in muscle: superoxide dismutase, glutathione peroxidase, and catalase and three accessory antioxidant enzymes: thioredoxin, glutaredoxin, and peroxiredoxin.

Superoxide Dismutase

Three isoforms of superoxide dismutase (SOD) are present in skeletal muscle. All three isoforms convert superoxide radicals into hydrogen peroxide and oxygen using a transition metal. SOD1 primarily is located within the cytosol and the mitochondrial intermembrane space and requires copper-zinc (Cu,-Zn-SOD) as a cofactor. SOD2 uses manganese (Mn-SOD) and is located only in the mitochondrial matrix. SOD3 also uses copper-zinc as a cofactor and is distributed in the extracellular space.

The general consensus in the literature is that chronic exercise training results in an overall increase in total SOD activity (reviewed in Powers et al., 2011). However, which specific isoform(s) are primarily responsible for the increase in activity is less clear. To further complicate matters, some studies have shown different responses in mRNA, protein content, and enzyme activity following exercise. For example, Strobel et al. demonstrated that 14 weeks of exercise training in mice resulted in no change in SOD2 mRNA, an increase in SOD2 protein content, and an unexplained decrease in SOD2 activity in skeletal muscle (Strobel et al., 2011). The variability in responses can likely be explained by experimental differences, such as differences in exercise protocols, muscle groups studied (i.e., fiber type), timing of tissue sampling, and under-powered studies. Nonetheless, generalizations can be made for each isoform.

SOD1 and SOD2 are the primary isoforms that have been studied to date. In regard to SOD1, numerous studies have shown an increase in either mRNA expression, protein content, or enzymatic activity (Oh-Ishi et al., 1996, 1997; Gore et al., 1998; Gomez-Cabrera et al., 2008a,b; Ristow et al., 2009; Meier et al., 2013). However, a similar number of studies can be found that have reported no change in at least one of these markers (Oh-Ishi et al., 1996; Lambertucci et al., 2007; Brooks et al., 2008). Therefore, since evidence exists both for and against, it is difficult to determine if an increase in SOD1 following exercise can be protective. There is a similar body of literature for SOD2; however, the majority of studies demonstrate at least one marker of SOD2 (i.e., mRNA expression, protein content, or enzymatic activity) is increased with exercise training (Oh-Ishi et al., 1997; Gore et al., 1998; Lambertucci et al., 2007; Gomez-Cabrera et al., 2008a; Ristow et al., 2009). To date, little is known about the response of SOD3 to exercise training.

Glutathione Peroxidase and Catalase

Hydrogen peroxide generated by the SOD family of antioxidants remains a reactive compound that can generate free radicals and is considered cytotoxic. Both glutathione peroxidase (GPX) and catalase are important antioxidants because they catalyze reactions that reduce hydrogen peroxide (reviewed in Powers and Jackson, 2008). In muscle cells, GPX expression is sensitive to oxidative stress (Zhou et al., 2001) and the majority of the literature suggests that GPX activity is increased following acute and chronic exercise (Laughlin et al., 1990; Criswell et al., 1993; Powers et al., 1994; Gore et al., 1998; Itoh et al., 2004; Lambertucci et al., 2007; Ristow et al., 2009; Smuder et al., 2011; Mangner et al., 2013). In contrast, changes in catalase expression following exercise is less clear, however the consensus is that catalase activity is not increased following training (Oh-Ishi et al., 1997; Smuder et al., 2011; Mangner et al., 2013).

Thioredoxin, Glutaredoxin, and Peroxiredoxin

In addition to the previously discussed antioxidant enzymes, skeletal muscle also contains several accessory enzymes that contribute directly or indirectly as antioxidants. The most important accessory antioxidant enzymes include thioredoxin, glutaredoxin, and peroxiredoxin.

The thioredoxin enzyme system is composed of both thioredoxin (Txn) and thioredoxin reductase (TxnRd). There are two isoforms of thioredoxin that are delineated from each other based on the cellular compartment in which they are found. Txn1 located in the cytosol and Txn2 found in the mitochondrial matrix (Arnér and Holmgren, 2000). Txn is an important disulfide reductase in the cell and therefore is important in maintaining proteins in their reduced state (Holmgren, 1989). Furthermore, it has recently been suggested that Txn2, in conjunction with glutathione (GSH), is an important regulator of hydrogen peroxide emission from mitochondria (Aon et al., 2012). Importantly, Txn protein content is decreased with hindlimb unloading (Matsushima et al., 2006). Unfortunately, there is a little evidence on the response of Txn1 or 2 following exercise training. However, recent reports suggest that TxnRd2, a necessary component in the system needed to catalyze the reduction (e.g., recycling) of Txn2, is increased in skeletal muscle following training (Fisher-Wellman et al., 2013).

Similar to Txn, glutaredoxin (Grx) is a thiodisulfide oxidoreductase that protects and repairs protein thiols during periods of oxidant stress (Holmgren, 1989). Grx protects protein thiols by the transfer of electrons from NADPH; this catalytic response is coupled with GSH and glutathione reductase. Three Grx isoforms are found in skeletal muscle. Grx1 is located in the cytosol and Grx2 and Grx5 are found in the mitochondria (Holmgren, 1989).

Peroxiredoxin (Prdx) is a peroxidase capable of reducing hydrogen peroxide and other hydroperoxides and peroxynitrate using electrons provided by thiol compounds (e.g., Txn) (Yin et al., 2012). There are six isoforms of Prdx; PrdxI, Prdx2, and Prdx6 are located in the cytosol whereas Prdx3 is located in the mitochondria (Yin et al., 2012). Prdx5 is located in both the cytosol and mitochondria whereas Prdx4 is found in the extracellular space (Yin et al., 2012).

The paucity of data on the response of accessory antioxidant enzymes to exercise training in skeletal muscle makes it difficult to make concrete statements on their role in the prevention of oxidative stress in skeletal muscle; however a few general conclusions can be reached. The Prdx isoforms are the most commonly studied group of enzymes following exercise training. Unfortunately, a clear pattern of expression following exercise or disuse does not exist. In general, Prdx expression is decreased with unloading in skeletal muscle; however exercise training does not consistently increase expression of any of the isoforms.

The Txn system is of interesting note because it has recently been reported that Txn2, in conjunction with glutathione (GSH), is an important regulator of hydrogen peroxide emission from mitochondria (Stanley et al., 2011; Aon et al., 2012). Importantly, Txn protein content is decreased with hindlimb unloading (Matsushima et al., 2006). Unfortunately, there is a little evidence on the response of Txn1 or 2 following exercise training. However, recent reports suggest that TxnRd2, a necessary component in the system needed to catalyze the reduction (e.g., recycling) of Txn2, is increased in skeletal muscle following training (Fisher-Wellman et al., 2013). Therefore, it stands to reason that exercise may prevent disuse atrophy-induced oxidative stress by increasing the buffering capacity of H_20_2 in mitochondria.

In summary, endurance exercise training improves muscle antioxidant capacity as evidenced by several studies demonstrating less oxidative stress in trained muscles following a bout of intense exercise. The current body of literature suggests that the improvement in antioxidant capacity is due in part to increased activity of SOD2 and GPX, with the possibility that SOD1 may play a contributory role. Additional work is needed to clarify the importance and physiological roles that accessory antioxidant systems in regards to exercise training adaptations and disuse muscle atrophy, however promising new experiments suggest that these antioxidant systems may provide a novel approach to preventing disuse atrophy.

Can Increased Antioxidants Protect Against Disuse Muscle Atrophy?

It has been difficult to determine cause and effect for the hypothesis that increased antioxidant capacity can prevent disuse muscle atrophy. One reason for this is the lack of ability to use genetic knockout mice to determine gain or loss of function. SOD1 genetic knockout mice ($SOD1^{-/-}$) display increased markers of oxidative stress and marked muscle atrophy compared to wild type controls (Muller et al., 2006). Overexpression of SOD1 results in motor neuron disease and gross atrophy of skeletal muscle (Gurney et al., 1994; Rando et al., 1998; Zhang et al., 2013). It is believed that this sensitization of muscle to increased SOD1 activity is due to an imbalance between hydrogen peroxide generated by SOD1 without a concomitant increase in the enzymes that convert hydrogen peroxide to water and oxygen. Moreover, disruption of the SOD2 gene is lethal in mice due to neurodegeneration and cardiac dysfunction (Lebovitz et al., 1996). Therefore, it is difficult to conclude that increased expression of SOD1 or SOD2 can protect against oxidative stress during periods of disuse.

Without the ability to use transgenic animals, a common experimental design to determine the effect of antioxidant capacity on disuse muscle atrophy has been to provide exogenous antioxidant supplements. Examples of these supplements include vitamin C, vitamin E, trolox, N-acetylcysterine, and mitochondrial targeted antioxidants. Unfortunately, definitive proof that antioxidant supplementation protects against disuse atrophy does not exist because there is data for and against the idea that antioxidants can prevent disuse atrophy. For example, several studies using a variety of antioxidants in various disuse atrophy models suggest that antioxidant supplementation may provide protection against disuse atrophy (Kondo et al., 1991, 1992; Appell et al., 1997; Betters et al., 2004; Servais et al., 2007; Agten et al., 2011; Min et al., 2011; Talbert et al., 2013b), while several other papers provide evidence that antioxidant supplementation is not protective (Koesterer et al., 2002; Farid et al., 2005; Brocca et al., 2010; Desaphy et al., 2010). Indeed, these studies have spurred debates if oxidative stress is a cause of muscle atrophy or purely a consequence (Brocca et al., 2010; Powers et al., 2012a); compelling arguments for each side can be made. It is clear that more research is needed in this area, with a particular focus to address this issue in humans.

The Role of Mitochondria and PGC1-α in Disuse Muscle Atrophy

As previously mentioned, exercise training and disuse have opposite effects on skeletal muscle mitochondria. Prolonged exercise training results in an increase in mitochondrial turnover. However, because mitochondrial biogenesis is increased at a greater rate than removal of mitochondria, exercise training results in an increase in an overall increase in mitochondrial content. A potent activator of mitochondrial biogenesis is peroxisome proliferative activated receptor-γ coactivator 1α (PGC1-α) (**Figure 2**). Thus, the first part of this section will focus on PGC1-α's role

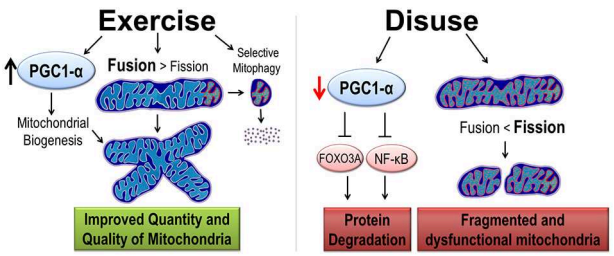

FIGURE 2 | Exercise and disuse effects on mitochondrial quality and quantity. Exercise training promotes cytoprotective effects by the induction of PGC1-α protein, considered the master regulator of mitochondrial biogenesis. Exercise improves quality in two ways. First, mitochondrial dynamics are shifted such that fusion is greater than fission resulting in larger mitochondrial network. Second, increased selective mitophagy removes old and dysfunctional mitochondria (denoted with red and orange organelles). In contrast, disuse decreases PGC1-α, removing its inhibition of protein degradation pathways. Furthermore, mitochondrial dynamics are shifted toward fission causing a small, fragmented, and dysfunctional mitochondria.

in mitochondrial turnover followed by a discussion on PGC1-α regulation of protein degradation.

PGC1–α Increases Mitochondrial Content is Skeletal Muscle

PGC1-α was first discovered in the lab of Bruce Spiegelman while studying adaptive thermogenesis in adipose tissue and skeletal muscle (Puigserver et al., 1998). This study speculated that increased expression of PGC1-α was an important modulator of mitochondrial biogenesis. Indeed, follow-up studies in skeletal muscle demonstrated that PGC1-α acts as co-activator by docking with transcription factors and aiding in the recruitment of regulatory protein complexes that increase gene transcription of proteins involved in mitochondrial biogenesis, rates of cellular respiration, and glucose uptake/utilization (Puigserver et al., 1998, 1999; Wu et al., 1999; St-Pierre et al., 2003).

In skeletal muscle, PGC1-α is frequently considered a "master regulator" of mitochondrial biogenesis because of its powerful role as a transcription co-factor. Indeed, PGC-1α interacts with and co-activates numerous transcription factors and nuclear receptors, including estrogen-related receptor-α (ERRα), nuclear respiratory factor-1 (NRF-1) and 2, myocyte enhancer factor 2 (MEF2), and mitochondrial transcription factor A (Tfam) (Spiegelman, 2007). All of these transcription factors directly regulate the expression of important nuclear-encoded mitochondrial genes necessary metabolic adaptations in skeletal muscle. Furthermore, overexpression of PGC1-α drives skeletal muscle fiber types to much more oxidative phenotype (Lin et al., 2002).

Mitochondrial and Metabolic Alteration with Disuse and Exercise

Prolonged disuse muscle atrophy is associated with impaired oxidative metabolism and an increase in glycolysis. This is due in part to a decrease in mitochondrial biogenesis, mitochondrial content, and electron transport chain components (Lecker et al., 2004; Kang and Ji, 2013). The onset of mitochondrial dysfunction is rapid and results in an increase in ROS production and metabolic stress due to increased reliance on glycolysis, decreased fat oxidation, and substrate accumulation, which ultimately leads to inefficient ATP production (Stein and Wade, 2005). The opposite is true for exercise trained muscle, which demonstrates an increase in oxidative metabolism, increased utilization of fat, and increased mitochondrial biogenesis (Holloszy and Coyle, 1984). It is becoming increasingly apparent that PGC1-α is an important mediator of these exercise-induced effects and may be an important mediator of exercise induced-cytoprotection. Because PGC1- α is such a power inducer of fuel intake and β-oxidation, it follows that the metabolic changes that occur with exercise-induced PGC1- α expression can protect against metabolic deficits seen with disuse atrophy.

PGC1- α Activity Regulates Protein Degradation Pathways

Although it is well established that the decrease in protein synthesis contributes to disuse atrophy; to date, there has been no data suggesting that PGC1-α signaling is directly mediates the protein synthesis pathways (Brault et al., 2010). However, PGC1-α transcriptional activity has been shown to prevent muscle protein degradation. This was first demonstrated by Sandri et al., who showed that over-expression of PGC1-α in mice prevented denervation-induced muscle atrophy by preventing the expression of key genes in the ubiquitin proteasome pathway and autophagy (Sandri et al., 2006). Furthermore, this study demonstrated that elevated PGC1-α content prevented transcriptional activity of FoxO3a. Upon activation, FoxO3a moves from the sarcoplasm into the nucleus where it acts as a potent translational activator of proteins in the ubiquitin-proteasome (i.e., atrogin-1 and MAFbx), autophagy, and apoptosis pathways. Additionally, a recent study suggests that PGC1-α can inhibit the NF-κB signaling pathway (Eisele et al., 2013), which is another important pathway in muscle protein degradation (reviewed in Jackman and Kandarian, 2004). Therefore, we conclude that PGC1-α is an important modulator of protein degradation pathways in disuse muscle atrophy and thus helps mediated the exercise preconditioning effect (**Figure 2**).

The rationale that PGC1-α mediates exercise-induced cytoprotection is two-fold. First, disuse muscle atrophy is associated with a decreased expression of PGC1-α content, as demonstrated in both animal and human models (Sandri et al., 2006; Sacheck et al., 2007; Kang and Ji, 2013). Therefore, it stands to reason, that preventing a decrease below basal levels of PGC1-α may prevent muscle atrophy. In this regard, PGC1-α expression is highly inducible with high intensity endurance exercise (Baar et al., 2002; Pilegaard et al., 2003; Smuder et al., 2012a) and importantly protein expression accumulates in skeletal muscle after training (Russell et al., 2003; Taylor et al., 2005). Thus, it follows that exercise training, prior to disuse muscle atrophy, can increase PGC1-α protein content such that the inactivity-induced decrease is mitigated or it only reaches the level of the basal untrained state. Indeed, expression of PGC1-α in fast-twitch muscles of mice, to levels commonly seen with exercise training, were able to attenuate disuse muscle atrophy (Sandri et al., 2006); thus, making PGC1-α a potentially important mediator of disuse atrophy protein degradation.

Endurance Exercise Improves Mitochondrial Quality

As previously mentioned, exercise training is a potent stimulus for mitochondrial biogenesis; however, recent evidence suggests that endurance training may also improve mitochondrial quality through two mutually exclusive pathways: alterations in mitochondrial dynamics and selective autophagic degradation of mitochondria (i.e., mitophagy).

Mitochondrial Dynamics

Isolated mitochondria are often represented as spherical shaped individual organelles, however, *in vitro* they form a complex interconnected network. The shape of the mitochondrial network is said to be dynamic because segments of mitochondria frequently divide (i.e., fission) and join (i.e., fusion). Mitochondrial dynamics are controlled by a family of mitochondrial shaping proteins (Dimmer and Scorrano, 2006; Iqbal and Hood, 2014). Key proteins that promote mitochondrial fission include

Dynamin-related protein-1 (Drp1) and Fission 1 (Fis1), whereas proteins regulating mitochondrial fusion include optic atrophy 1 (Opa1) and mitofusion 1 and 2 (Mfn1/2) (reviewed in Westermann, 2010; Chan, 2012). The role of fusion and fission in cells is complex, but it is believed that increased fusion of mitochondria is associated with improved function, while fission is a mechanism by which damaged portions of mitochondria are sectioned off the reticulum and targeted for degradation by autophagy (i.e., mitophagy).

Mitophagy

As previously discussed, autophagy is the degradation pathway that allows cells to degrade organelles and macromolecules. There are two classifications of autophagy, selective or non-selective (i.e., macroautophagy). Selective autophagy is defined by the autophagasome directly targeting an organelle that has been selected by the cell to be degraded. Often, selective autophagy refers to degradation of mitochondria or endoplasmic reticulum. Non-selective autophagy indiscriminately degrades organells and macromolecules. The process of autophagy consists of cytosolic components to be degraded that are sequestered into double membrane vesicles called autophagosomes. These autophagosomes fuse with lysosomes containing hydrolytic enzymes that break down cellular components (He and Klionsky, 2009). Although autophagy plays a prominent role in protein degradation during disuse, it also appears to have a housekeeping role by turning over organelles and degrading protein aggregates. Mice with genetic ablation of rate limiting proteins in the autophagic machinery display marked muscle atrophy and weakness (Masiero et al., 2009; Chang et al., 2012).

Mitophagy denotes the degradation of mitochondria through autophagy and is regulated independently of macroautophagy (Kanki and Klionsky, 2008). Following damage, the mitochondrial phosphatase and tensin homolog-induced kinase-1 (PINK1) becomes stabilized on the outer mitochondrial membrane (Vincow et al., 2013). PINK1 then recruits the protein Parkin, an e3 ubiquitin ligase, which tags several outer mitochondrial membrane proteins with ubiquitin and results in the fragmentation and isolation of impaired mitochondria (Narendra et al., 2010). Currently, little is known about the proteins that interact between the autophagasome and PINK1 and Parkin on the mitochondria. Briefly, several candidate proteins have been identified. For example BCL-2, a key anti-apoptotic factor, binds to proteins related to phagasome development (Liang et al., 1999). BNIP3 (Bcl-2 and 19 kD interacting protein-37) and BNIP3-like protein (BNIP3L) have also been identified as proteins than can pair autophagasomes with uqiquintated mitochondrial protein (Zhang and Ney, 2009). Finally, autophagy related gene 32 (Atg32) is another protein recently to confers selectivity of the autophagosome to mitochodnria (Kanki et al., 2009). The field of mitophagy is an active area of research that is rapidly evolving and complex field of study, and therefore the specifics are beyond the scope of this review. Please see the following references for in depth review (Twig and Shirihai, 2011; Youle and Narendra, 2011; Feng et al., 2013).

Mitochondrial Dynamics and Mitophagy in Exercise and Disuse

Mitochondrial dynamics and mitophagy are both altered with exercise training (**Figure 2**). In regard to mitochondrial dynamics, George Brooks' lab in the late 1980s was the first to demonstrate that the mitochondria reticulum became more expansive following chronic exercise training (Kirkwood et al., 1987). This suggested exercise training shifted the expression of fission and fusion machinery toward that of enhanced fusion. Improvements in biochemical and imaging techniques have provided evidence to support this theory. Exercise training is sufficient to increase expression of MFN1/2 and increases interactions between mitochondria (Ding et al., 2010; Picard et al., 2013; Iqbal and Hood, 2014). A primary pathway that drives the expression following exercise is PGC1 (Cartoni et al., 2005; Zechner et al., 2010) Concomitantly, fission protein expression is reduced with training (Perry et al., 2010; Iqbal and Hood, 2014). So what is the role of increased fusion of mitochondria? It is believed that the physiological relevance of increased fusion is mixing of mitochondrial content such as metabolic substrates, mitochondrial DNA, and proteins. Therefore, content mixing allows for a homogenous population of mitochondria, which in theory allows healthy mitochondria to positively affect damaged mitochondria.

Disuse atrophy is associated with a fragmented mitochondrial reticulum that is remodeled through autophagy (Romanello et al., 2010) (**Figure 2**). Note, mitochondria often appear enlarged in skeletal muscle atrophy (Powers et al., 2012b). This is not to be confused with a smaller, disorganized network. Instead, these mitochondria are enlarged due to swelling. Disuse atrophy results in an imbalance between fission and fusion events with an overall shift in the direction of fusion. Based on protein expression levels, disuse atrophy results in a down regulation of fusion machinery while fission events remain relatively constant (Iqbal and Hood, 2014; Cannavino et al., 2015). However, it is prudent to not exclude an increase in fission proteins with only a few data points. Indeed, expression of fission machinery is sufficient to cause muscle atrophy in mice (Romanello et al., 2010). Nonetheless, it is clear that disuse atrophy shifts the balance between fusion and fission results in small, fragmented mitochondria with a reduced capacity of ATP re-synthesis and increase in ROS emission (Twig et al., 2008).

It has recently been demonstrated that exercise training induces mitophagy, which is required for some of the exercise induced adaptations of skeletal muscle (Grumati et al., 2011; Lira et al., 2013). Although slightly counter intuitive, increased mitophagy following exercise is beneficial by improving overall mitochondrial quality through the selective removal of damaged or dysfunctional mitochondria (Safdar et al., 2011). Combined with evidence that exercise training or chronic stimulation of muscle results in a mitochondrial phenotype that resists oxidative stress and mitochondrial mediated apoptosis (Adhihetty et al., 2007a; O'leary and Hood, 2008), these data suggest that exercise training induced global changes in mitochondria may be cytoprotective by increasing quantity and improving quality of skeletal muscle mitochondria (**Figure 2**).

As previously discussed, disuse atrophy causes a decrease in mitochondrial number through targeted degradation.

Mitochondria are segregated by fission and then selectively targeted for degradation via mitophagy. This process is to remove damaged mitochondria and decrease mitochondrial number to match metabolic demands. Therefore, mitophagy, *per se*, is not a direct contributor to disuse atrophy.

In summary, it appears that a basal level of mitophagy is necessary to maintain cellular homeostasis. The function of mitophagy is to remove damaged and/or old organelles so that these can be replaced by newer, healthier organelles. Exercise training is the excellent example of mitophagy improving overall mitochondrial quality by increasing following exercise training and remodeling of the mitochondrial phenotype.

The Role of Heat Shock Protein 70 in Prevention of Muscle Atrophy

The heat shock family of proteins is known as molecular chaperone proteins that have been demonstrated to increase following exercise. In general, their role is three-fold: (1) facilitate folding of de novo synthesized proteins; (2) assist in the re-folding of misfolded proteins and denatured proteins, and (3) aid in the transport of those proteins to their correct cellular compartments (Feder and Hofmann, 1999). Heat shock proteins (HSPs) can be classified into a number of families that are traditionally named for their molecular mass. These include small HSPs (between 8 and 27 kDa), HSP60 (i.e., 60 kDa), HSP 70, and HSP90. Of these, HSP70 is the most studied and will be the focus of the following section.

HSP70 is Induced by Cell Stress and Exercise

HSP70, also commonly referred to as HSP72, is a highly conserved protein whose expression is increased following stress, hence why HSP70 is termed a stress-inducible member of the HSP family of proteins. Its expression is responsive to thermal stress, oxidative stress, mechanical stress, metabolic stress, and cytokines. Importantly, exercise training promotes these stressors and it is clear that exercise is a powerful inducer of HSP70 protein content.

The first evidence that exercise increased HSP70 protein content was generated in 1990 when Locke et al. postulated that exercising skeletal muscle from mice increased protein synthesis of stress protein similar to that of a protein produced during heat stress (Locke et al., 1990). Shortly thereafter, it was confirmed that exercise training increased HSP70 mRNA in both rodent (Salo et al., 1991) and human skeletal muscle (Puntschart et al., 1996). Since these original studies, it is now well accepted that a single bout of exercise is sufficient to increase HSP70 mRNA and protein expression in animals and humans in an intensity dependent manner (Milne and Noble, 2002; Morton et al., 2009). Importantly, prolonged exercise training increases baseline levels of HSP70 (Liu et al., 1999; Ecochard et al., 2000; González et al., 2000; Atalay et al., 2004; Kayani et al., 2008; Smuder et al., 2012b). It is important to note that mechanical unloading has the opposite effect of exercise on HSP70 content in muscle. Disuse atrophy is associated with a rapid decrease in HSP70 protein content (Lawler et al., 2006; Senf et al., 2008; Moriggi et al., 2010; Lomonosova et al., 2012).

Increased HSP70 Content Protects Against Disuse Muscle Atrophy

Early studies demonstrated that exposing mice to a non-lethal heat stress provides the animal with protection against a subsequent typically lethal heat exposure. These protective findings were attributed to a family of proteins that were induced by heat stress and these findings were soon translated to skeletal muscle (Garramone et al., 1994).In the study by Garramone et al., prior exposure to heat stress (i.e., greater than 41°C) conferred protection against ischemic injury in rat skeletal muscle (Garramone et al., 1994).

In regards to disuse muscle atrophy, there are several lines of evidence that induction of HSP70 content can protect against the negative biochemical and structural changes associated with muscle atrophy. First, prior exposure to heat stress demonstrates protection against atrophy in hind limb unloading, immobilization, and mechanical ventilation (Naito et al., 2000; Selsby and Dodd, 2005; Ichinoseki-Sekine et al., 2014). However, because heat stress may cause other adaptive responses independent of HSP70, these studies do not prove cause and effect. Direct evidence in support of this hypothesis comes from muscle-specific overexpression of HSP70. For example, Senf et al., demonstrated that HSP70 overexpression attenuated 4 days of immobilization-induced muscle atrophy (Senf et al., 2008). However, conversely, another study using whole body overexpression was unable to prevent 7 days of unloading-induced atrophy (Miyabara et al., 2012). Several possibilities exist for this discrepancy including species differences (rat/mice), duration of immobilization (4 day/7 days), and method of overexpression (single muscle electroporation/whole body overexpression). It important to note that the global (i.e., whole body) HSP70 overexpressing mice had significantly smaller muscles compared to their wild type littermates, suggesting altered physiology in these animals (Miyabara et al., 2012). Nonetheless, it appears that HSP70 is an important stress response protein that has the potential to protect against disuse muscle atrophy.

Mechanisms by which HSP70 Protects Against Muscle Atrophy

HSP70 is localized in many different subcellular locations including mitochondria, nucleus, ribosomes, and in the cytoplasm. Therefore, it is no surprise that HSP70 may protect against muscle atrophy through a multitude of different mechanisms (**Figure 3**). First, HSP70 is most well-known for its ability to serve as a chaperone and prevent dysfunction and/or targeted proteolysis of oxidized proteins by binding to and assisting in their re-folding. An important example of this mechanism is demonstrated by the ability of HSP70 to protect against damaging increases in intracellular calcium during muscle atrophy by binding to oxidized sarcoplasmic/endoplasmic reticulum Ca^{2+}-ATPase (SERCA) to preserve its function (Gehrig et al., 2012). Second, the chaperone function of HSP70 can maintain mitochondrial integrity by protecting mitochondria against apoptotic stimuli and contribute to the repair of damaged proteins (Kang et al., 1990; Mosser et al., 2000). Third, HSP72 can prevent disuse atrophy induced-proteolysis by inhibiting activation of FoxO3a

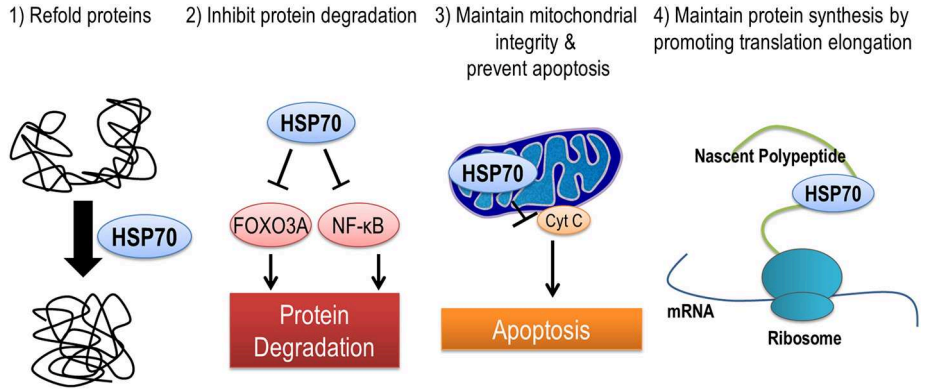

FIGURE 3 | HSP70 is an inducible chaperone protein that can be provide protection against muscle atrophy in several ways. (1) Refolding of misfolded or unfolded proteins, (2) inhibiting select pathways of protein degradation, (3) maintaining mitochondrial integrity and reducing apoptosis by preventing the release of cytochrome C from mitochondria, and (4) improving translation elongation and promoting protein synthesis.

and NF-κB signaling pathways (Senf et al., 2008, 2010). And finally, expression of HSP72 may prevent an atrophy induced decrease in muscle protein synthesis by maintaining the rate of translation elongation of nascent polypeptides (Nelson et al., 1992; Ku et al., 1995).

Conclusions

The idea that lifelong endurance training can be protective against disuse muscle atrophy has yet to be definitively proven in scientific literature, however the theory remains valid. An acute bout of exercise training results in a small stimulus that brings about an adaptive response. Prolonged exercise training results in an accumulation of these adaptive responses. Therefore, it follows that when skeletal muscle has adapted to small repeated stresses, it is much better suited to handle the stress brought on by disuse muscle atrophy. These adaptations include, but are not limited to, limiting oxidative stress during disuse atrophy by increased antioxidant systems to buffer increased ROS production or by having newer, healthier mitochondria that produce less ROS when inactive. There is also the possibility of increased proteins such as PGC1-α and HSP70 that can prevent activation of key protein degradation pathways, protect against mitochondrial dysfunction, maintain muscle protein synthesis, and assist in the refolding of damaged proteins. Furthermore, there are likely numerous other proteins that could be cytoprotective and therefore more work in this area needs to be done.

Acknowledgments

I would like to thank Dr. Scott Powers for his mentorship, encouragement and countless discussions that facilitated the scientific evidence and rationale behind this review.

References

Adhihetty, P. J., Ljubicic, V., and Hood, D. A. (2007a). Effect of chronic contractile activity on SS and IMF mitochondrial apoptotic susceptibility in skeletal muscle. *Am. J. Physiol. Endocrinol. Metab.* 292, E748–E755. doi: 10.1152/ajpendo.00311.2006

Adhihetty, P. J., O'leary, M. F., Chabi, B., Wicks, K. L., and Hood, D. A. (2007b). Effect of denervation on mitochondrially mediated apoptosis in skeletal muscle. *J. Appl. Physiol.* 102, 1143–1151. doi: 10.1152/japplphysiol.00768.2006

Agten, A., Maes, K., Smuder, A., Powers, S. K., Decramer, M., and Gayan-Ramirez, G. (2011). N-Acetylcysteine protects the rat diaphragm from the decreased contractility associated with controlled mechanical ventilation. *Crit. Care Med.* 39, 777–782. doi: 10.1097/CCM.0b013e318206cca9

Aloisi, M., Azzone, G., and Carafoli, E. (1960). Lesions of pigeon muscle mitochondria in avitaminosis B1 and denervation atrophy. *Arch. De Vecchi Anat. Patol.* 32:33.

Aon, M. A., Stanley, B. A., Sivakumaran, V., Kembro, J. M., O'Rourke, B., Paolocci, N., et al. (2012). Glutathione/thioredoxin systems modulate mitochondrial H2O2 emission: an experimental-computational study. *J. Gen. Physiol.* 139, 479–491. doi: 10.1085/jgp.201210772

Appell, H.-J., Duarte, J., and Soares, J. (1997). Supplementation of vitamin E may attenuate skeletal muscle immobilization atrophy. *Int. J. Sports Med.* 18, 157–160. doi: 10.1055/s-2007-972612

Arnér, E. S., and Holmgren, A. (2000). Physiological functions of thioredoxin and thioredoxin reductase. *Eur. J. Biochem.* 267, 6102–6109. doi: 10.1046/j.1432-1327.2000.01701.x

Atalay, M., Oksala, N. K., Laaksonen, D. E., Khanna, S., Nakao, C., Lappalainen, J., et al. (2004). Exercise training modulates heat shock protein response in diabetic rats. *J. Appl. Physiol.* 97, 605–611. doi: 10.1152/japplphysiol.01183.2003

Baar, K., Wende, A. R., Jones, T. E., Marison, M., Nolte, L. A., Chen, M., et al. (2002). Adaptations of skeletal muscle to exercise: rapid increase in the transcriptional coactivator PGC-1. *FASEB J.* 16, 1879–1886. doi: 10.1096/fj.02-0367com

Betters, J. L., Criswell, D. S., Shanely, R. A., Van Gammeren, D., Falk, D., Deruisseau, K. C., et al. (2004). Trolox attenuates mechanical ventilation–induced diaphragmatic dysfunction and proteolysis. *Am. J. Respir. Crit. Care Med.* 170, 1179–1184. doi: 10.1164/rccm.200407-939OC

Bodine, S. C., Stitt, T. N., Gonzalez, M., Kline, W. O., Stover, G. L., Bauerlein, R., et al. (2001). Akt/mTOR pathway is a crucial regulator of skeletal muscle hypertrophy and can prevent muscle atrophy in vivo. *Nat. Cell Biol.* 3, 1014–1019. doi: 10.1038/ncb1101-1014

Brault, J. J., Jespersen, J. G., and Goldberg, A. L. (2010). Peroxisome proliferator-activated receptor γ coactivator 1α or 1β overexpression inhibits muscle protein degradation, induction of ubiquitin ligases, and disuse atrophy. *J. Biol. Chem.* 285, 19460–19471. doi: 10.1074/jbc.M110.113092

Brocca, L., Pellegrino, M. A., Desaphy, J.-F., Pierno, S., Camerino, D. C., and Bottinelli, R. (2010). Is oxidative stress a cause or consequence of disuse muscle atrophy in mice? A proteomic approach in hindlimb-unloaded mice. *Exp. Physiol.* 95, 331–350. doi: 10.1113/expphysiol.2009.050245

Brooks, S. V., Vasilaki, A., Larkin, L. M., Mcardle, A., and Jackson, M. J. (2008). Repeated bouts of aerobic exercise lead to reductions in skeletal muscle free radical generation and nuclear factor κB activation. *J. Physiol.* 586, 3979–3990. doi: 10.1113/jphysiol.2008.155382

Cannavino, J., Brocca, L., Sandri, M., Grassi, B., Bottinelli, R., and Pellegrino, M. A. (2015). The role of alterations in mitochondrial dynamics and PGC-1alpha over-expression in fast muscle atrophy following hindlimb unloading. *J. Physiol.* doi: 10.1113/jphysiol.2014.286740. [Epub ahead of print].

Carafoli, E., Margreth, A., and Buffa, P. (1964). Early biochemical changes in mitochondria from denervated muscle and their relation to the onset of atrophy. *Exp. Mol. Pathol.* 3, 171–181. doi: 10.1016/0014-4800(64)90050-4

Cartoni, R., Léger, B., Hock, M. B., Praz, M., Crettenand, A., Pich, S., et al. (2005). Mitofusins 1/2 and ERRα expression are increased in human skeletal muscle after physical exercise. *J. Physiol.* 567, 349–358. doi: 10.1113/jphysiol.2005.092031

Chan, D. C. (2012). Fusion and fission: interlinked processes critical for mitochondrial health. *Annu. Rev. Genet.* 46, 265–287. doi: 10.1146/annurev-genet-110410-132529

Chang, N. C., Nguyen, M., Bourdon, J., Risse, P.-A., Martin, J., Danialou, G., et al. (2012). Bcl-2-associated autophagy regulator Naf-1 required for maintenance of skeletal muscle. *Hum. Mol. Genet.* 21, 2277–2287. doi: 10.1093/hmg/dds048

Criswell, D., Powers, S., Dodd, S., Lawler, J., Edwards, W., Renshler, K., et al. (1993). High intensity training-induced changes in skeletal muscle antioxidant enzyme activity. *Med. Sci. Sports Exerc.* 25, 1135–1140. doi: 10.1249/00005768-199310000-00009

Davies, K. J., Quintanilha, A. T., Brooks, G. A., and Packer, L. (1982). Free radicals and tissue damage produced by exercise. *Biochem. Biophys. Res. Commun.* 107, 1198–1205. doi: 10.1016/S0006-291X(82)80124-1

De Boer, M. D., Selby, A., Atherton, P., Smith, K., Seynnes, O. R., Maganaris, C. N., et al. (2007). The temporal responses of protein synthesis, gene expression and cell signalling in human quadriceps muscle and patellar tendon to disuse. *J. Physiol.* 585, 241–251. doi: 10.1113/jphysiol.2007.142828

Desaphy, J.-F., Pierno, S., Liantonio, A., Giannuzzi, V., Digennaro, C., Dinardo, M. M., et al. (2010). Antioxidant treatment of hindlimb-unloaded mouse counteracts fiber type transition but not atrophy of disused muscles. *Pharmacol. Res.* 61, 553–563. doi: 10.1016/j.phrs.2010.01.012

Dimmer, K. S., and Scorrano, L. (2006). (De) constructing mitochondria: what for? *Physiology* 21, 233–241. doi: 10.1152/physiol.00010.2006

Ding, H., Jiang, N., Liu, H., Liu, X., Liu, D., Zhao, F., et al. (2010). Response of mitochondrial fusion and fission protein gene expression to exercise in rat skeletal muscle. *Biochim. Biophys. Acta* 1800, 250–256. doi: 10.1016/j.bbagen.2009.08.007

Du, J., Wang, X., Miereles, C., Bailey, J. L., Debigare, R., Zheng, B., et al. (2004). Activation of caspase-3 is an initial step triggering accelerated muscle proteolysis in catabolic conditions. *J. Clin. Invest.* 113, 115–123. doi: 10.1172/JCI18330

Dupont-Versteegden, E. E. (2006). Apoptosis in skeletal muscle and its relevance to atrophy. *World J. Gastroenterol.* 12, 7463. doi: 10.3748/wjg.v12.i46.7463

Ecochard, L., Lhenry, F., Sempore, B., and Favier, R. (2000). Skeletal muscle HSP72 level during endurance training: influence of peripheral arterial insufficiency. *Pflüg. Arch.* 440, 918–924. doi: 10.1007/s004240000362

Eisele, P. S., Salatino, S., Sobek, J., Hottiger, M. O., and Handschin, C. (2013). The peroxisome proliferator-activated receptor γ coactivator 1α/β (PGC-1) coactivators repress the transcriptional activity of NF-κB in skeletal muscle cells. *J. Biol. Chem.* 288, 2246–2260. doi: 10.1074/jbc.M112.375253

Falk, D. J., Deruisseau, K. C., Van Gammeren, D. L., Deering, M. A., Kavazis, A. N., and Powers, S. K. (2006). Mechanical ventilation promotes redox status alterations in the diaphragm. *J. Appl. Physiol.* 101, 1017–1024. doi: 10.1152/japplphysiol.00104.2006

Farid, M., Reid, M. B., Li, Y.-P., Gerken, E., and Durham, W. J. (2005). Effects of dietary curcumin or N-acetylcysteine on NF-κB activity and contractile performance in ambulatory and unloaded murine soleus. *Nutr. Metab.* 2:20. doi: 10.1186/1743-7075-2-20

Feder, M. E., and Hofmann, G. E. (1999). Heat-shock proteins, molecular chaperones, and the stress response: evolutionary and ecological physiology. *Annu. Rev. Physiol.* 61, 243–282. doi: 10.1146/annurev.physiol.61.1.243

Feng, D., Liu, L., Zhu, Y., and Chen, Q. (2013). Molecular signaling toward mitophagy and its physiological significance. *Exp. Cell Res.* 319, 1697–1705. doi: 10.1016/j.yexcr.2013.03.034

Ferrando, A. A., Paddon-Jones, D., Hays, N. P., Kortebein, P., Ronsen, O., Williams, R. H., et al. (2010). EAA supplementation to increase nitrogen intake improves muscle function during bed rest in the elderly. *Clin. Nutr.* 29, 18–23. doi: 10.1016/j.clnu.2009.03.009

Fisher-Wellman, K. H., Mattox, T. A., Thayne, K., Katunga, L. A., La Favor, J. D., Neufer, P. D., et al. (2013). Novel role for thioredoxin reductase−2 in mitochondrial redox adaptations to obesogenic diet and exercise in heart and skeletal muscle. *J. Physiol.* 591, 3471–3486. doi: 10.1113/jphysiol.2013.254193

Garramone, R. R. Jr., Winters, R. M., Das, D. K., and Deckers, P. J. (1994). Reduction of skeletal muscle injury through stress conditioning using the heat-shock response. *Plast. Reconstr. Surg.* 93, 1242–1247. doi: 10.1097/00006534-199405000-00021

Gehrig, S. M., Van Der Poel, C., Sayer, T. A., Schertzer, J. D., Henstridge, D. C., Church, J. E., et al. (2012). Hsp72 preserves muscle function and slows progression of severe muscular dystrophy. *Nature* 484, 394–398. doi: 10.1038/nature10980

Glover, E. I., and Phillips, S. M. (2010). Resistance exercise and appropriate nutrition to counteract muscle wasting and promote muscle hypertrophy. *Curr. Opin. Clin. Nutr. Metab. Care* 13, 630–634. doi: 10.1097/MCO.0b013e32833f1ae5

Goll, D. E., Thompson, V. F., Li, H., Wei, W., and Cong, J. (2003). The calpain system. *Physiol. Rev.* 83, 731–801. doi: 10.1152/physrev.00029.2002

Gomez-Cabrera, M.-C., Borrás, C., Pallardó, F. V., Sastre, J., Ji, L. L., and Viña, J. (2005). Decreasing xanthine oxidase-mediated oxidative stress prevents useful cellular adaptations to exercise in rats. *J. Physiol.* 567, 113–120. doi: 10.1113/jphysiol.2004.080564

Gomez-Cabrera, M.-C., Domenech, E., Romagnoli, M., Arduini, A., Borras, C., Pallardo, F. V., et al. (2008a). Oral administration of vitamin C decreases muscle mitochondrial biogenesis and hampers training-induced adaptations in endurance performance. *Am. J. Clin. Nutr.* 87, 142–149.

Gomez-Cabrera, M.-C., Domenech, E., and Viña, J. (2008b). Moderate exercise is an antioxidant: upregulation of antioxidant genes by training. *Free Radic. Biol. Med.* 44, 126–131. doi: 10.1016/j.freeradbiomed.2007.02.001

González, B., Hernando, R., and Manso, R. (2000). Stress proteins of 70 kDa in chronically exercised skeletal muscle. *Pflüg. Arch.* 440, 42–49. doi: 10.1007/s004240051020

Gore, M., Fiebig, R., Hollander, J., Leeuwenburgh, C., Ohno, H., and Ji, L. (1998). Endurance training alters antioxidant enzyme gene expression in rat skeletal muscle. *Can. J. Physiol. Pharmacol.* 76, 1139–1145. doi: 10.1139/y98-125

Grumati, P., Coletto, L., Schiavinato, A., Castagnaro, S., Bertaggia, E., Sandri, M., et al. (2011). Physical exercise stimulates autophagy in normal skeletal muscles but is detrimental for collagen VI-deficient muscles. *Autophagy* 7, 1415–1423. doi: 10.4161/auto.7.12.17877

Gurney, M. E., Pu, H., Chiu, A. Y., Dal Canto, M. C., Polchow, C. Y., Alexander, D. D., et al. (1994). Motor neuron degeneration in mice that express a human Cu, Zn superoxide dismutase mutation. *Science* 264, 1772–1775. doi: 10.1126/science.8209258

He, C., and Klionsky, D. J. (2009). Regulation mechanisms and signaling pathways of autophagy. *Annu. Rev. Genet.* 43, 67. doi: 10.1146/annurev-genet-102808-114910

Holloszy, J. O., and Coyle, E. F. (1984). Adaptations of skeletal muscle to endurance exercise and their metabolic consequences. *J. Appl. Physiol.* 56, 831–838.

Holmgren, A. (1989). Thioredoxin and glutaredoxin systems. *J. Biol. Chem.* 264, 13963–13966.

Ichinoseki-Sekine, N., Yoshihara, T., Kakigi, R., Sugiura, T., Powers, S. K., and Naito, H. (2014). Heat stress protects against mechanical ventilation-induced diaphragmatic atrophy. *J. Appl. Physiol.* 117, 518–524. doi: 10.1152/japplphysiol.00170.2014

Iqbal, S., and Hood, D. (2014). The role of mitochondrial fusion and fission in skeletal muscle function and dysfunction. *Front. Biosci.* 20, 157–172.

Itoh, M., Oh-Ishi, S., Hatao, H., Leeuwenburgh, C., Selman, C., Ohno, H., et al. (2004). Effects of dietary calcium restriction and acute exercise on the antioxidant enzyme system and oxidative stress in rat diaphragm. *Am. J. Physiol. Regul. Integr. Comp. Physiol.* 287, R33–R38. doi: 10.1152/ajpregu.00598.2003

Jackman, R. W., and Kandarian, S. C. (2004). The molecular basis of skeletal muscle atrophy. *Am. J. Physiol. Cell Physiol.* 287, C834–C843. doi: 10.1152/ajpcell.00579.2003

Kang, C., and Ji, L. L. (2013). Muscle immobilization and remobilization down-regulates PGC-1α signaling and the mitochondrial biogenesis pathway. *J. Appl. Physiol.* 115, 1618–1625. doi: 10.1152/japplphysiol.01354.2012

Kang, P.-J., Ostermann, J., Shilling, J., Neupert, W., Craig, E. A., and Pfanner, N. (1990). Requirement for hsp70 in the mitochondrial matrix for translocation and folding of precursor proteins. *Nature* 348, 137–143. doi: 10.1038/348137a0

Kanki, T., and Klionsky, D. J. (2008). Mitophagy in yeast occurs through a selective mechanism. *J. Biol. Chem.* 283, 32386–32393. doi: 10.1074/jbc.M802403200

Kanki, T., Wang, K., Cao, Y., Baba, M., and Klionsky, D. J. (2009). Atg32 is a mitochondrial protein that confers selectivity during mitophagy. *Dev. Cell* 17, 98–109. doi: 10.1016/j.devcel.2009.06.014

Kavazis, A. N., Talbert, E. E., Smuder, A. J., Hudson, M. B., Nelson, W. B., and Powers, S. K. (2009). Mechanical ventilation induces diaphragmatic mitochondrial dysfunction and increased oxidant production. *Free Radic. Biol. Med.* 46, 842–850. doi: 10.1016/j.freeradbiomed.2009.01.002

Kayani, A. C., Close, G. L., Jackson, M. J., and Mcardle, A. (2008). Prolonged treadmill training increases HSP70 in skeletal muscle but does not affect age-related functional deficits. *Am. J. Physiol. Regul. Integr. Comp. Physiol.* 294, R568–R576. doi: 10.1152/ajpregu.00575.2007

Kirkwood, S., Packer, L., and Brooks, G. (1987). Effects of endurance training on a mitochondrial reticulum in limb skeletal muscle. *Arch. Biochem. Biophys.* 255, 80–88. doi: 10.1016/0003-9861(87)90296-7

Koesterer, T., Dodd, S. L., and Powers, S. (2002). Increased antioxidant capacity does not attenuate muscle atrophy caused by unweighting. *J. Appl. Physiol.* 93, 1959–1965. doi: 10.1152/japplphysiol.00511.2002

Kondo, H., Miura, M., and Itokawa, Y. (1991). Oxidative stress in skeletal muscle atrophied by immobilization. *Acta Physiol. Scand.* 142, 527–528. doi: 10.1111/j.1748-1716.1991.tb09191.x

Kondo, H., Miura, M., and Itokawa, Y. (1993). Antioxidant enzyme systems in skeletal muscle atrophied by immobilization. *Pflüg. Arch.* 422, 404–406. doi: 10.1007/BF00374299

Kondo, H., Miura, M., Kodama, J., Ahmed, S. M., and Itokawa, Y. (1992). Role of iron in oxidative stress in skeletal muscle atrophied by immobilization. *Pflüg. Arch.* 421, 295–297. doi: 10.1007/BF00374844

Kortebein, P., Symons, T. B., Ferrando, A., Paddon-Jones, D., Ronsen, O., Protas, E., et al. (2008). Functional impact of 10 days of bed rest in healthy older adults. *J. Gerontol. Ser. A* 63, 1076–1081. doi: 10.1093/gerona/63.10.1076

Ku, Z., Yang, J., Menon, V., and Thomason, D. (1995). Decreased polysomal HSP-70 may slow polypeptide elongation during skeletal muscle atrophy. *Am. J. Physiol. Cell Physiol.* 268, C1369–C1374.

Lambertucci, R. H., Levada-Pires, A. C., Rossoni, L. V., Curi, R., and Pithon-Curi, T. C. (2007). Effects of aerobic exercise training on antioxidant enzyme activities and mRNA levels in soleus muscle from young and aged rats. *Mech. Ageing Dev.* 128, 267–275. doi: 10.1016/j.mad.2006.12.006

Laughlin, M., Simpson, T., Sexton, W., Brown, O., Smith, J., and Korthuis, R. (1990). Skeletal muscle oxidative capacity, antioxidant enzymes, and exercise training. *J. Appl. Physiol.* 68, 2337–2343.

Lawler, J. M., Song, W., and Demaree, S. R. (2003). Hindlimb unloading increases oxidative stress and disrupts antioxidant capacity in skeletal muscle. *Free Radic. Biol. Med.* 35, 9–16. doi: 10.1016/S0891-5849(03)00186-2

Lawler, J. M., Song, W., and Kwak, H. B. (2006). Differential response of heat shock proteins to hindlimb unloading and reloading in the soleus. *Muscle Nerve* 33, 200–207. doi: 10.1002/mus.20454

Lebovitz, R. M., Zhang, H., Vogel, H., Cartwright, J., Dionne, L., Lu, N., et al. (1996). Neurodegeneration, myocardial injury, and perinatal death in mitochondrial superoxide dismutase-deficient mice. *Proc. Natl. Acad. Sci. U.S.A.* 93, 9782–9787. doi: 10.1073/pnas.93.18.9782

Lecker, S. H., Jagoe, R. T., Gilbert, A., Gomes, M., Baracos, V., Bailey, J., et al. (2004). Multiple types of skeletal muscle atrophy involve a common program of changes in gene expression. *FASEB J.* 18, 39–51. doi: 10.1096/fj.03-0610com

Lecker, S. H., Solomon, V., Mitch, W. E., and Goldberg, A. L. (1999). Muscle protein breakdown and the critical role of the ubiquitin-proteasome pathway in normal and disease states. *J. Nutr.* 129, 227S–237S.

Liang, X. H., Jackson, S., Seaman, M., Brown, K., Kempkes, B., Hibshoosh, H., et al. (1999). Induction of autophagy and inhibition of tumorigenesis by beclin 1. *Nature* 402, 672–676. doi: 10.1038/45257

Lin, J., Wu, H., Tarr, P. T., Zhang, C.-Y., Wu, Z., Boss, O., et al. (2002). Transcriptional co-activator PGC-1α drives the formation of slow-twitch muscle fibres. *Nature* 418, 797–801. doi: 10.1038/nature00904

Lira, V. A., Okutsu, M., Zhang, M., Greene, N. P., Laker, R. C., Breen, D. S., et al. (2013). Autophagy is required for exercise training-induced skeletal muscle adaptation and improvement of physical performance. *FASEB J.* 27, 4184–4193. doi: 10.1096/fj.13-228486

Liu, Y., Mayr, S., Opitz-Gress, A., Zeller, C., Lormes, W., Baur, S., et al. (1999). Human skeletal muscle HSP70 response to training in highly trained rowers. *J. Appl. Physiol.* 86, 101–104.

Locke, M., Noble, E. G., and Atkinson, B. G. (1990). Exercising mammals synthesize stress proteins. *Am. J. Physiol.* 258, C723–C729.

Lomonosova, Y. N., Shenkman, B. S., and Nemirovskaya, T. L. (2012). Attenuation of unloading-induced rat soleus atrophy with the heat-shock protein inducer 17-(allylamino)-17-demethoxygeldanamycin. *FASEB J.* 26, 4295–4301. doi: 10.1096/fj.12-204412

Maes, K., Testelmans, D., Powers, S., Decramer, M., and Gayan-Ramirez, G. (2007). Leupeptin inhibits ventilator-induced diaphragm dysfunction in rats. *Am. J. Respir. Crit. Care Med.* 175, 1134–1138. doi: 10.1164/rccm.200609-1342OC

Mangner, N., Linke, A., Oberbach, A., Kullnick, Y., Gielen, S., Sandri, M., et al. (2013). Exercise training prevents TNF-α induced loss of force in the diaphragm of mice. *PLoS ONE* 8:e52274. doi: 10.1371/journal.pone.0052274

Masiero, E., Agatea, L., Mammucari, C., Blaauw, B., Loro, E., Komatsu, M., et al. (2009). Autophagy is required to maintain muscle mass. *Cell Metab.* 10, 507–515. doi: 10.1016/j.cmet.2009.10.008

Matsushima, Y., Nanri, H., Nara, S., Okufuji, T., Ohta, M., Hachisuka, K., et al. (2006). Hindlimb unloading decreases thioredoxin-related antioxidant proteins and increases thioredoxin-binding protein-2 in rat skeletal muscle. *Free Radic. Res.* 40, 715–722. doi: 10.1080/10715760600580488

McClung, J. M., Kavazis, A. N., Deruisseau, K. C., Falk, D. J., Deering, M. A., Lee, Y., et al. (2007). Caspase-3 regulation of diaphragm myonuclear domain during mechanical ventilation-induced atrophy. *Am. J. Respir. Crit. Care Med.* 175, 150–159. doi: 10.1164/rccm.200601-142OC

Meier, P., Renga, M., Hoppeler, H., and Baum, O. (2013). The impact of antioxidant supplements and endurance exercise on genes of the carbohydrate and lipid metabolism in skeletal muscle of mice. *Cell Biochem. Funct.* 31, 51–59. doi: 10.1002/cbf.2859

Milne, K. J., and Noble, E. G. (2002). Exercise-induced elevation of HSP70 is intensity dependent. *J. Appl. Physiol.* 93, 561–568. doi: 10.1152/japplphysiol.00528.2001

Min, K., Smuder, A. J., Kwon, O. S., Kavazis, A. N., Szeto, H. H., and Powers, S. K. (2011). Mitochondrial-targeted antioxidants protect skeletal muscle against immobilization-induced muscle atrophy. *J. Appl. Physiol.* 111, 1459–1466. doi: 10.1152/japplphysiol.00591.2011

Miyabara, E. H., Nascimento, T. L., Rodrigues, D. C., Moriscot, A. S., Davila, W. F., Aitmou, Y., et al. (2012). Overexpression of inducible 70-kDa heat shock protein in mouse improves structural and functional recovery of skeletal muscles from atrophy. *Pflüg. Arch. Eur. J. Physiol.* 463, 733–741. doi: 10.1007/s00424-012-1087-x

Moriggi, M., Vasso, M., Fania, C., Capitanio, D., Bonifacio, G., Salanova, M., et al. (2010). Long term bed rest with and without vibration exercise countermeasures: effects on human muscle protein dysregulation. *Proteomics* 10, 3756–3774. doi: 10.1002/pmic.200900817

Morton, J. P., Kayani, A. C., Mcardle, A., and Drust, B. (2009). The exercise-induced stress response of skeletal muscle, with specific emphasis on humans. *Sports Med.* 39, 643–662. doi: 10.2165/00007256-200939080-00003

Mosser, D. D., Caron, A. W., Bourget, L., Meriin, A. B., Sherman, M. Y., Morimoto, R. I., et al. (2000). The chaperone function of hsp70 is required for protection against stress-induced apoptosis. *Mol. Cell. Biol.* 20, 7146–7159. doi: 10.1128/MCB.20.19.7146-7159.2000

Muller, F. L., Song, W., Jang, Y. C., Liu, Y., Sabia, M., Richardson, A., et al. (2007). Denervation-induced skeletal muscle atrophy is associated with increased

mitochondrial ROS production. *Am. J. Physiol. Reg. Integr. Comp. Physiol.* 293, R1159–R1168. doi: 10.1152/ajpregu.00767.2006

Muller, F. L., Song, W., Liu, Y., Chaudhuri, A., Pieke-Dahl, S., Strong, R., et al. (2006). Absence of CuZn superoxide dismutase leads to elevated oxidative stress and acceleration of age-dependent skeletal muscle atrophy. *Free Radic. Biol. Med.* 40, 1993–2004. doi: 10.1016/j.freeradbiomed.2006.01.036

Muscatello, U., and Patriarca, P. L. (1968). Denervation and disuse atrophy in pigeon breast muscle. An electron microscopic and biochemical study. *Am. J. Pathol.* 52, 1169.

Naito, H., Powers, S. K., Demirel, H. A., Sugiura, T., Dodd, S. L., and Aoki, J. (2000). Heat stress attenuates skeletal muscle atrophy in hindlimb-unweighted rats. *J. Appl. Physiol.* 88, 359–363.

Narendra, D. P., Jin, S. M., Tanaka, A., Suen, D.-F., Gautier, C. A., Shen, J., et al. (2010). PINK1 is selectively stabilized on impaired mitochondria to activate Parkin. *PLoS Biol.* 8:e1000298. doi: 10.1371/journal.pbio.1000298

Nelson, R. J., Ziegelhoffer, T., Nicolet, C., Werner-Washburne, M., and Craig, E. A. (1992). The translation machinery and 70 kd heat shock protein cooperate in protein synthesis. *Cell* 71, 97–105. doi: 10.1016/0092-8674(92)90269-I

Nelson, W. B., Smuder, A. J., Hudson, M. B., Talbert, E. E., and Powers, S. K. (2012). Cross-talk between the calpain and caspase-3 proteolytic systems in the diaphragm during prolonged mechanical ventilation. *Crit. Care Med.* 40, 1857–1863. doi: 10.1097/CCM.0b013e318246bb5d

Oh-Ishi, S., Kizaki, T., Nagasawa, J., Izawa, T., Komabayashi, T., Nagata, N., et al. (1997). Effects of endurance training on superoxide dismutase activiy, content and mRNA expression in rat muscle. *Clin. Exp. Pharmacol. Physiol.* 24, 326–332. doi: 10.1111/j.1440-1681.1997.tb01196.x

Oh-Ishi, S., Toshinai, K., Kizaki, T., Haga, S., Fukuda, K., Nagata, N., et al. (1996). Effects of aging and/or training on antioxidant enzyme system in diaphragm of mice. *Respir. Physiol.* 105, 195–202. doi: 10.1016/0034-5687(96)00057-6

O'leary, M. F., and Hood, D. A. (2008). Effect of prior chronic contractile activity on mitochondrial function and apoptotic protein expression in denervated muscle. *J. Appl. Physiol.* 105, 114–120. doi: 10.1152/japplphysiol.00724.2007

Perry, C. G., Lally, J., Holloway, G. P., Heigenhauser, G. J., Bonen, A., and Spriet, L. L. (2010). Repeated transient mRNA bursts precede increases in transcriptional and mitochondrial proteins during training in human skeletal muscle. *J. Physiol.* 588, 4795–4810. doi: 10.1113/jphysiol.2010.199448

Picard, M., Gentil, B. J., McManus, M. J., White, K., Louis, K. S., Gartside, S. E., et al. (2013). Acute exercise remodels mitochondrial membrane interactions in mouse skeletal muscle. *J. Appl. Physiol.* 115, 1562–1571. doi: 10.1152/japplphysiol.00819.2013

Pilegaard, H., Saltin, B., and Neufer, P. D. (2003). Exercise induces transient transcriptional activation of the PGC-1α gene in human skeletal muscle. *J. Physiol.* 546, 851–858. doi: 10.1113/jphysiol.2002.034850

Powers, S. K. (2014). Can antioxidants protect against disuse muscle atrophy? *Sports Med.* 44, 155–165. doi: 10.1007/s40279-014-0255-x

Powers, S. K., Criswell, D., Lawler, J., Martin, D., Ji, L. L., Herb, R. A., et al. (1994). Regional training-induced alterations in diaphragmatic oxidative and antioxidant enzymes. *Respir. Physiol.* 95, 227–237. doi: 10.1016/0034-5687(94)90118-X

Powers, S. K., and Jackson, M. J. (2008). Exercise-induced oxidative stress: cellular mechanisms and impact on muscle force production. *Physiol. Rev.* 88, 1243–1276. doi: 10.1152/physrev.00031.2007

Powers, S. K., Smuder, A., and Judge, A. (2012a). Oxidative stress and disuse muscle atrophy: cause or consequence? *Curr. Opin. Clin. Nutr. Metab. Care* 15, 240. doi: 10.1097/MCO.0b013e328352b4c2

Powers, S. K., Talbert, E. E., and Adhihetty, P. J. (2011). Reactive oxygen and nitrogen species as intracellular signals in skeletal muscle. *J. Physiol.* 589, 2129–2138. doi: 10.1113/jphysiol.2010.201327

Powers, S. K., Wiggs, M. P., Duarte, J. A., Zergeroglu, A. M., and Demirel, H. A. (2012b). Mitochondrial signaling contributes to disuse muscle atrophy. *Am. J. Physiol. Endocrinol. Metab.* 303, E31–E39. doi: 10.1152/ajpendo.00609.2011

Powers, S. K., Wiggs, M. P., Sollanek, K. J., and Smuder, A. J. (2013). Ventilator-induced diaphragm dysfunction: cause and effect. *Am. J. Physiol. Regul. Integr. Comp. Physiol.* 305, R464–R477. doi: 10.1152/ajpregu.00231.2013

Puigserver, P., Adelmant, G., Wu, Z., Fan, M., Xu, J., O'Malley, B., et al. (1999). Activation of PPARγ coactivator-1 through transcription factor docking. *Science* 286, 1368–1371. doi: 10.1126/science.286.5443.1368

Puigserver, P., Wu, Z., Park, C. W., Graves, R., Wright, M., and Spiegelman, B. M. (1998). A cold-inducible coactivator of nuclear receptors linked to adaptive thermogenesis. *Cell* 92, 829–839. doi: 10.1016/S0092-8674(00)81410-5

Puntschart, A., Vogt, M., Widmer, H., Hoppeler, H., and Billeter, R. (1996). Hsp70 expression in human skeletal muscle after exercise. *Acta Physiol. Scand.* 157, 411–417. doi: 10.1046/j.1365-201X.1996.512270000.x

Rando, T. A., Crowley, R. S., Carlson, E. J., Epstein, C. J., and Mohapatra, P. K. (1998). Overexpression of copper/zinc superoxide dismutase: a novel cause of murine muscular dystrophy. *Ann. Neurol.* 44, 381–386. doi: 10.1002/ana.410440315

Ristow, M., Zarse, K., Oberbach, A., Klöting, N., Birringer, M., Kiehntopf, M., et al. (2009). Antioxidants prevent health-promoting effects of physical exercise in humans. *Proc. Natl. Acad. Sci. U.S.A.* 106, 8665–8670. doi: 10.1073/pnas.0903485106

Romanello, V., Guadagnin, E., Gomes, L., Roder, I., Sandri, C., Petersen, Y., et al. (2010). Mitochondrial fission and remodelling contributes to muscle atrophy. *EMBO J.* 29, 1774–1785. doi: 10.1038/emboj.2010.60

Russell, A. P., Feilchenfeldt, J., Schreiber, S., Praz, M., Crettenand, A., Gobelet, C., et al. (2003). Endurance training in humans leads to fiber type-specific increases in levels of peroxisome proliferator-activated receptor-γ coactivator-1 and peroxisome proliferator-activated receptor-α in skeletal muscle. *Diabetes* 52, 2874–2881. doi: 10.2337/diabetes.52.12.2874

Sacheck, J. M., Hyatt, J.-P. K., Raffaello, A., Jagoe, R. T., Roy, R. R., Edgerton, V. R., et al. (2007). Rapid disuse and denervation atrophy involve transcriptional changes similar to those of muscle wasting during systemic diseases. *FASEB J.* 21, 140–155. doi: 10.1096/fj.06-6604com

Safdar, A., Bourgeois, J. M., Ogborn, D. I., Little, J. P., Hettinga, B. P., Akhtar, M., et al. (2011). Endurance exercise rescues progeroid aging and induces systemic mitochondrial rejuvenation in mtDNA mutator mice. *Proc. Natl. Acad. Sci. U.S.A.* 108, 4135–4140. doi: 10.1073/pnas.1019581108

Salo, D. C., Donovan, C. M., and Davies, K. J. (1991). HSP70 and other possible heat shock or oxidative stress proteins are induced in skeletal muscle, heart, and liver during exercise. *Free Rad. Biol. Med.* 11, 239–246. doi: 10.1016/0891-5849(91)90119-N

Saltin, B., Henriksson, J., Nygaard, E., Andersen, P., and Jansson, E. (1977). Fiber types and metabolic potentials of skeletal muscles in sedentary man and endurance runners. *Ann. N.Y. Acad. Sci.* 301, 3–29. doi: 10.1111/j.1749-6632.1977.tb38182.x

Sandri, M. (2013). Protein breakdown in muscle wasting: role of autophagy-lysosome and ubiquitin-proteasome. *Int. J. Biochem. Cell Biol.* 45, 2121–2129. doi: 10.1016/j.biocel.2013.04.023

Sandri, M., Lin, J., Handschin, C., Yang, W., Arany, Z. P., Lecker, S. H., et al. (2006). PGC-1alpha protects skeletal muscle from atrophy by suppressing FoxO3 action and atrophy-specific gene transcription. *Proc. Natl. Acad. Sci. U.S.A.* 103, 16260–16265. doi: 10.1073/pnas.0607795103

Schiaffino, S., Dyar, K. A., Ciciliot, S., Blaauw, B., and Sandri, M. (2013). Mechanisms regulating skeletal muscle growth and atrophy. *FEBS J.* 280, 4294–4314. doi: 10.1111/febs.12253

Selsby, J. T., and Dodd, S. L. (2005). Heat treatment reduces oxidative stress and protects muscle mass during immobilization. *Am. J. Physiol. Regul. Integr. Comp. Physiol.* 289, R134–R139. doi: 10.1152/ajpregu.00497.2004

Senf, S. M., Dodd, S. L., and Judge, A. R. (2010). FOXO signaling is required for disuse muscle atrophy and is directly regulated by Hsp70. *Am. J. Physiol. Cell Physiol.* 298, C38–C45. doi: 10.1152/ajpcell.00315.2009

Senf, S. M., Dodd, S. L., McClung, J. M., and Judge, A. R. (2008). Hsp70 overexpression inhibits NF-κB and Foxo3a transcriptional activities and prevents skeletal muscle atrophy. *FASEB J.* 22, 3836–3845. doi: 10.1096/fj.08-110163

Servais, S., Letexier, D., Favier, R., Duchamp, C., and Desplanches, D. (2007). Prevention of unloading-induced atrophy by vitamin E supplementation: links between oxidative stress and soleus muscle proteolysis? *Free Radic. Biol. Med.* 42, 627–635. doi: 10.1016/j.freeradbiomed.2006.12.001

Smuder, A. J., Kavazis, A. N., Hudson, M. B., Nelson, W. B., and Powers, S. K. (2010). Oxidation enhances myofibrillar protein degradation via calpain and caspase-3. *Free Radic. Biol. Med.* 49, 1152–1160. doi: 10.1016/j.freeradbiomed.2010.06.025

Smuder, A. J., Kavazis, A. N., Min, K., and Powers, S. K. (2011). Exercise protects against doxorubicin-induced oxidative stress and proteolysis in skeletal muscle. *J. Appl. Physiol.* 110, 935–942. doi: 10.1152/japplphysiol.00677.2010

Smuder, A. J., Min, K., Hudson, M. B., Kavazis, A. N., Kwon, O. S., Nelson, W. B., et al. (2012b). Endurance exercise attenuates ventilator-induced diaphragm dysfunction. *J. Appl. Physiol.* 112, 501–510. doi: 10.1152/japplphysiol.01086.2011

Smuder, A. J., Min, K., Hudson, M. B., Kavazis, A. N., Kwon, O.-S., Nelson, W. B., et al. (2012a). Endurance exercise attenuates ventilator-induced diaphragm dysfunction. *J. Appl. Physiol.* 112, 501–510. doi: 10.1152/japplphysiol.01086.2011

Spiegelman, B. M. (2007). "Transcriptional control of mitochondrial energy metabolism through the PGC1 coactivators," in *Novartis Foundation Symposium: Chichester, 1999* (New York, NY: John Wiley), 60.

Stanley, B. A., Sivakumaran, V., Shi, S., McDonald, I., Lloyd, D., Watson, W. H., et al. (2011). Thioredoxin reductase-2 is essential for keeping low levels of H2O2 emission from isolated heart mitochondria. *J. Biol. Chem.* 286, 33669–33677. doi: 10.1074/jbc.M111.284612

Stein, T., and Wade, C. (2005). Metabolic consequences of muscle disuse atrophy. *J. Nutr.* 135, 1824S–1828S.

St-Pierre, J., Lin, J., Krauss, S., Tarr, P. T., Yang, R., Newgard, C. B., et al. (2003). Bioenergetic analysis of peroxisome proliferator-activated receptor γ coactivators 1α and 1β (PGC-1α and PGC-1β) in muscle cells. *J. Biol. Chem.* 278, 26597–26603. doi: 10.1074/jbc.M301850200

Strobel, N. A., Peake, J. M., Matsumoto, A., Marsh, S. A., Coombes, J. S., and Wadley, G. D. (2011). Antioxidant supplementation reduces skeletal muscle mitochondrial biogenesis. *Med. Sci. Sports Exerc.* 43, 1017–1024. doi: 10.1249/MSS.0b013e318203afa3

Symons, T. B., Sheffield-Moore, M., Chinkes, D. L., Ferrando, A. A., and Paddon-Jones, D. (2009). Artificial gravity maintains skeletal muscle protein synthesis during 21 days of simulated microgravity. *J. Appl. Physiol.* 107, 34–38. doi: 10.1152/japplphysiol.91137.2008

Talbert, E. E., Smuder, A. J., Min, K., Kwon, O. S., and Powers, S. K. (2013a). Calpain and caspase-3 play required roles in immobilization-induced limb muscle atrophy. *J. Appl. Physiol.* 114, 1482–1489. doi: 10.1152/japplphysiol.00925.2012

Talbert, E. E., Smuder, A. J., Min, K., Kwon, O. S., Szeto, H. H., and Powers, S. K. (2013b). Immobilization-induced activation of key proteolytic systems in skeletal muscles is prevented by a mitochondria-targeted antioxidant. *J. Appl. Physiol.* 115, 529–538. doi: 10.1152/japplphysiol.00471.2013

Taylor, E. B., Lamb, J. D., Hurst, R. W., Chesser, D. G., Ellingson, W. J., Greenwood, L. J., et al. (2005). Endurance training increases skeletal muscle LKB1 and PGC-1α protein abundance: effects of time and intensity. *Am. J. Physiol. Endocrinol. Metab.* 289, E960–E968. doi: 10.1152/ajpendo.00237.2005

Thomason, D. B., and Booth, F. W. (1990). Atrophy of the soleus muscle by hindlimb unweighting. *J. Appl. Physiol.* 68, 1–12.

Tischler, M. E., Rosenberg, S., Satarug, S., Henriksen, E. J., Kirby, C. R., Tome, M., et al. (1990). Different mechanisms of increased proteolysis in atrophy induced by denervation or unweighting of rat soleus muscle. *Metab. Clin. Exp.* 39, 756–763. doi: 10.1016/0026-0495(90)90113-Q

Twig, G., Elorza, A., Molina, A. J., Mohamed, H., Wikstrom, J. D., Walzer, G., et al. (2008). Fission and selective fusion govern mitochondrial segregation and elimination by autophagy. *EMBO J.* 27, 433–446. doi: 10.1038/sj.emboj.7601963

Twig, G., and Shirihai, O. S. (2011). The interplay between mitochondrial dynamics and mitophagy. *Antioxid. Redox Signal.* 14, 1939–1951. doi: 10.1089/ars.2010.3779

Vincow, E. S., Merrihew, G., Thomas, R. E., Shulman, N. J., Beyer, R. P., Maccoss, M. J., et al. (2013). The PINK1–Parkin pathway promotes both mitophagy and selective respiratory chain turnover in vivo. *Proc. Natl. Acad. Sci. U.S.A.* 110, 6400–6405. doi: 10.1073/pnas.1221132110

Westermann, B. (2010). Mitochondrial fusion and fission in cell life and death. *Nat. Rev. Mol. Cell Biol.* 11, 872–884. doi: 10.1038/nrm3013

Wolfe, R. R. (2006). The underappreciated role of muscle in health and disease. *Am. J. Clin. Nutr.* 84, 475–482.

Wu, Z., Puigserver, P., Andersson, U., Zhang, C., Adelmant, G., Mootha, V., et al. (1999). Mechanisms controlling mitochondrial biogenesis and respiration through the thermogenic coactivator PGC-1. *Cell* 98, 115–124. doi: 10.1016/S0092-8674(00)80611-X

Yin, F., Sancheti, H., and Cadenas, E. (2012). Mitochondrial thiols in the regulation of cell death pathways. *Antioxid. Redox Signal.* 17, 1714–1727. doi: 10.1089/ars.2012.4639

Youle, R. J., and Narendra, D. P. (2011). Mechanisms of mitophagy. *Nat. Rev. Mol. Cell Biol.* 12, 9–14. doi: 10.1038/nrm3028

Zechner, C., Lai, L., Zechner, J. F., Geng, T., Yan, Z., Rumsey, J. W., et al. (2010). Total skeletal muscle PGC-1 deficiency uncouples mitochondrial derangements from fiber type determination and insulin sensitivity. *Cell Metab.* 12, 633–642. doi: 10.1016/j.cmet.2010.11.008

Zhang, J., and Ney, P. A. (2009). Role of BNIP3 and NIX in cell death, autophagy, and mitophagy. *Cell Death Differ.* 16, 939–946. doi: 10.1038/cdd.2009.16

Zhang, Y., Davis, C., Sakellariou, G. K., Shi, Y., Kayani, A. C., Pulliam, D., et al. (2013). CuZnSOD gene deletion targeted to skeletal muscle leads to loss of contractile force but does not cause muscle atrophy in adult mice. *FASEB J.* 27, 3536–3548. doi: 10.1096/fj.13-228130

Zhou, L. Z.-H., Johnson, A. P., and Rando, T. A. (2001). NFκB and AP-1 mediate transcriptional responses to oxidative stress in skeletal muscle cells. *Free Radic. Biol. Med.* 31, 1405–1416. doi: 10.1016/S0891-5849(01)00719-5

Zhu, S., Nagashima, M., Khan, M. A., Yasuhara, S., Kaneki, M., and Martyn, J. (2013). Lack of caspase−3 attenuates immobilization−induced muscle atrophy and loss of tension generation along with mitigation of apoptosis and inflammation. *Muscle Nerve* 47, 711–721. doi: 10.1002/mus.23642

Conflict of Interest Statement: The author declares that the research was conducted in the absence of any commercial or financial relationships that could be construed as a potential conflict of interest.

frontiers in Physiology

MINI REVIEW
published: 30 March 2015
doi: 10.3389/fphys.2015.00102

Uremic myopathy: is oxidative stress implicated in muscle dysfunction in uremia?

*Antonia Kaltsatou[1], Giorgos K. Sakkas[1,2], Konstantina P. Poulianiti[1], Yiannis Koutedakis[1], Konstantinos Tepetes[3], Grigorios Christodoulidis[3], Ioannis Stefanidis[4] and Christina Karatzaferi[1]**

[1] Department of Physical Education and Sport Sciences (DPESS), School of Physical Education (PE), University of Thessaly, Trikala, Greece, [2] Institute for Research and Technology-Centre for Research and Technology Hellas, Trikala, Greece, [3] Department of Surgery, Faculty of Medicine, University of Thessaly, Larissa, Greece, [4] Department of Nephrology, Faculty of Medicine, University of Thessaly, Larissa, Greece

OPEN ACCESS

Edited by:
Brian McDonagh,
University of Liverpool, UK

Reviewed by:
Laszlo Csernoch,
University of Debrecen, Hungary
David Sheehan,
University College Cork, Ireland
Brian McDonagh,
University of Liverpool, UK

***Correspondence:**
Christina Karatzaferi,
Muscle Physiology and Mechanics Group, Department of Physical Education and Sport Sciences (DPESS), School of Physical Education (PE), University of Thessaly, Tmima Epistimis Fysikis Agogis kai Athlitismou - Panepistimio Thessalias, Karyes 42100, Trikala, Thessaly, Greece
ck@pe.uth.gr

Specialty section:
This article was submitted to Striated Muscle Physiology, a section of the journal Frontiers in Physiology

Received: 01 December 2014
Accepted: 13 March 2015
Published: 30 March 2015

Citation:
Kaltsatou A, Sakkas GK, Poulianiti KP, Koutedakis Y, Tepetes K, Christodoulidis G, Stefanidis I and Karatzaferi C (2015) Uremic myopathy: is oxidative stress implicated in muscle dysfunction in uremia? Front. Physiol. 6:102. doi: 10.3389/fphys.2015.00102

Renal failure is accompanied by progressive muscle weakness and premature fatigue, in part linked to hypokinesis and in part to uremic toxicity. These changes are associated with various detrimental biochemical and morphological alterations. All of these pathological parameters are collectively termed uremic myopathy. Various interventions while helpful can't fully remedy the pathological phenotype. Complex mechanisms that stimulate muscle dysfunction in uremia have been proposed, and oxidative stress could be implicated. Skeletal muscles continuously produce reactive oxygen species (ROS) and reactive nitrogen species (RNS) at rest and more so during contraction. The aim of this mini review is to provide an update on recent advances in our understanding of how ROS and RNS generation might contribute to muscle dysfunction in uremia. Thus, a systematic review was conducted searching PubMed and Scopus by using the Cochrane and PRISMA guidelines. While few studies met our criteria their findings are discussed making reference to other available literature data. Oxidative stress can direct muscle cells into a catabolic state and chronic exposure to it leads to wasting. Moreover, redox disturbances can significantly affect force production *per se*. We conclude that oxidative stress can be in part responsible for some aspects of uremic myopathy. Further research is needed to discern clear mechanisms and to help efforts to counteract muscle weakness and exercise intolerance in uremic patients.

Keywords: oxidative stress, uremia, muscle dysfunction, uremic myopathy, premature fatigue, muscle weakness

Introduction

Among the clinical entities affecting thousands of patients, chronic kidney disease (CKD) is a silent epidemic expected to influence more than 50% of the Americans born today (Grams et al., 2013) and approximately 40% of the population in Europe (Zoccali et al., 2010). Muscular weakness, muscle wasting, limited endurance, exercise intolerance, and fatigue are components of the functional and morphological abnormalities collectively termed uremic myopathy, which often also includes uremic cardiomyopathy (Campistol, 2002). While the pathogenesis of uremic myopathy is not clear, it is thought that an interplay of uremic toxicity and hypokinesis guide these abnormalities in patients with CKD and especially in end-stage renal disease (ESRD) patients undergoing

hemodialysis (HD) therapy. Observations of a significant correlation between glomerular filtration rate (GFR) and exercise tolerance (e.g., Clyne et al., 1987, 1994) led to studies revealing the very low activity levels and poor functional capacity of renal patients (Kouidi et al., 1998; Johansen et al., 2003; Sakkas et al., 2003a). Moreover, various groups turned their attention to exercise and other interventions to remedy or halt muscle deterioration in pre-dialysis (e.g., Clyne et al., 1991) and dialysis patients (e.g., Sakkas et al., 2003b; Johansen et al., 2006). Despite the evident improvements in exercise capacity and muscle morphology (Sakkas et al., 2003b, 2008a), in increasing muscle mass with steroid supplementation (Topp et al., 2003), in improving sleep and overall quality of life (Sakkas et al., 2008c) it appears that interventions so far cannot restore muscle functionality in ESRD patients to the level of age-matched healthy sedentary individuals (Sakkas et al., 2003b, 2008a; Giannaki et al., 2011).

Components of Uremic Myopathy

Loss of skeletal muscle strength in renal patients, contributes to easy fatigability, and can be linked to loss of muscle fibers and atrophy of the remaining fibers (Porter et al., 1995; Sakkas et al., 2003a). In cross-sectional studies, comparing age-matched controls and end-stage patients, atrophy and loss of type IIα and IIx fibers, reduced muscle fiber capillarization and peripheral activation (Sakkas et al., 2003a), and a significant decrease in the mean diameter of both fiber types (Crowe et al., 2007) has been observed. However, not all functional consequences can be attributed to atrophy. Interventions to improve muscle mass indicate that there is a functional deficit in the existing muscle mass. Dialysis patients present with rapid and large accumulation of inorganic phosphate during submaximal exercise, lower oxidative potential, larger phosphocreatine reduction with slower recovery but also with evidence of central activation failure, all these factors contributing to early and excess fatigue (Johansen et al., 2005). Abnormal mitochondria respiratory capacity, is also a factor responsible for easily fatigability in CKD patients, as mitochondrial morphology is disturbed in patients with CKD (Kouidi et al., 1998), while alterations in respiratory chain proteins likely enhance reactive oxygen species (ROS) production which has been seen in a rat uremia model (Yazdi et al., 2013).

CKD patients, especially the end-stage ones, lead a very sedentary lifestyle. Morphological abnormalities however have been observed in both locomotory and non-locomotory muscles (Sakkas et al., 2003a) thus not all of the dysfunction can be attributed to inactivity.

Biochemical and nutritional changes occurring through the progression of CKD can stimulate protein losses and can contribute to the development of muscle wasting. This has grave significance as catabolic conditions increase the risk of morbidity and mortality (Griffiths, 1996; Gordon et al., 2007).

Pro-dialysis and dialysis patients face increasing dietary restrictions. Malnutrition is associated with hypoalbuminemia, which is inversely correlated with mortality in uremic patients (Lowrie and Lew, 1990), and it is also used as a marker of depleted protein stores (Carrero et al., 2008).

Metabolic acidosis, which is commonly associated with CKD, stimulates the breakdown of muscle proteins resulting in loss of muscle mass (Hu et al., 2013). Furthermore, the observation that insulin resistance, is common in patients with CKD, suggests that impaired insulin signaling could also contribute to protein losses (Sakkas et al., 2008b; Zhang et al., 2009). Moreover, CKD is associated with an increase in circulating levels of inflammatory cytokines. Specifically, levels of circulating IL-6, TNF-α, serum amyloid A, and C-reactive protein are increased in patients with CKD (Zhang et al., 2009, 2011; Cheung et al., 2010). Notably, it is contested that in well-dialyzed patients, circulating proinflammatory markers are the main cause for hypoalbuminemia rather than malnutrition (Kaysen et al., 2004). The possibility of an accelerated protein degradation in CKD mediated by the ubiquitin-proteasome system (UPS) (Wang and Mitch, 2013) should also be considered.

Apart from a compounded or accelerated muscle loss, a reduction in the ability to anabolize muscle could be an issue in CKD. Still, interventions with nandrolone decanoate were successful in increasing muscle mass, albeit without improving muscle strength (Topp et al., 2003), pointing to an available anabolic response. However, there are suggestions that CKD may dampen the function of satellite cells. Zhang et al. (2010) using a mouse model of CKD reported a delayed regeneration of damaged muscle and reductions in MyoD protein and the myogenin expression, indicating a decreased satellite cell proliferation and differentiation (Zhang et al., 2010).

To compound the above, in dialyzed patients, the HD procedure *per se* stimulates protein degradation and reduced protein synthesis with the effect persisting for 2 h following dialysis (Ikizler et al., 2002). Thus, while blunting of anabolic responses can't be excluded, a multitude of factors can promote protein loss, especially in the end-stage patients.

Is there a Role for Oxidative Stress in Uremic Muscle Dysfunction?

Oxidative stress promotes catabolic state and accelerates muscle atrophy (Moylan and Reid, 2007). But it can also affect contractility of the available muscle and sarcomeric protein expression.

Many studies have found that oxidative stress can cause long-term effects and acute effects (Lamb and Westerblad, 2011) on contractility. Long-term effects include altered gene and protein expression or damages in lipids and proteins that are irreversible, while acute effects are reversible. The decrease in Ca^{2+} sensitivity which contributes to muscle fatigue is considered as an acute effect of oxidative stress (Lamb and Westerblad, 2011).

A key mechanism that has been proposed to explain the ROS contribution in muscle fatigue is the reduced myofibrillar Ca^{2+} sensitivity and/or sarcoplasmic reticulum Ca^{2+} release (Allen et al., 2008). Moreover, an increase in NO during fatigue in fast twitch muscle fibers contribute in decreased myofibrillar Ca^{2+} sensitivity (Lamb and Westerblad, 2011). However, in slow-twitch fibers NO donors, did not affect myofibrillar Ca^{2+} sensitivity (Spencer and Posterino, 2009). Also, a study by Reardon and Allen (2009), showed that iron can increase ROS production at high temperature in the skeletal muscle cells, accelerating muscle fatigue.

Moreover, ROS generation can acutely affect contractile function and disturbs structural transition within the actomyosin complex which is crucial for force generation. Exposure to low or high concentrations of peroxide (5 or 50 mM) reduces maximum force and velocity of contraction, with the high peroxide resulting in irreversible loss of calcium regulation of force mediated by oxidation of methionines in the heavy and essential light chains (Prochniewicz et al., 2008a). More elegant work from same group, examining structural dynamics of actin and myosin pointed to an effect of oxidation on weak-to-strong structural transition and by using site-directed mutagenesis of *Dictyostelium* (*Dicty*) myosin II oxidation, a redistribution of existing structural states of the actin-binding cleft was implicated (Prochniewicz et al., 2008b; Klein et al., 2011). Alterations in myosin heavy chain expression in uremic animals have also been reported (Taes et al., 2004).

Many studies have observed increased levels of oxidative stress biomarkers in blood samples of CKD patients (Samouilidou and Grapsa, 2003; Filiopoulos et al., 2009). In the literature, there are sufficient studies with different technical approaches in which the activity and role of ROS and reactive nitrogen species (RNS) in skeletal muscle has been studied using both *in vivo* and *in vitro* methods in a variety of contexts (Powers et al., 2011). Thus, based on recent advances in our understanding of how ROS and RNS affect muscle function, this mini-review aimed to examine if oxidative stress can contribute to muscle dysfunction in ESRD.

Methods

A systematic review was conducted searching PubMed and Scopus by using the Cochrane and PRISMA guidelines. A comprehensive literature search was conducted from September 2014 until November 2014. We used PubMed, ScienceDirect and Scopus or Google Scholar to search for studies that investigated the relationship among (i) oxidative stress and uremic myopathy in humans, and (ii) markers of oxidative stress in the skeletal muscle of uremic patients on HD. Eligibility of the studies based on titles, abstracts and full-text articles was determined by two reviewers. Studies were selected using inclusion and exclusion criteria. We included only those studies that met the following criteria: they assessed oxidative stress markers in the skeletal muscle of patients on HD; they used human biopsies; they addressed randomized control trials, controlled trials, or clinical trials designed to evaluate oxidative stress in skeletal muscle in uremic patients on HD therapy; they were written in English.

Results and Discussion

Only three studies have examined the oxidative damage in human skeletal muscle of uremic patients on HD (**Table 1**). Their findings are discussed with reference to renal human blood findings and/or animal muscle findings either models of CKD or models of other conditions.

Lim et al. (2002a) found increased malondialdehyde (MDA) and protein carbonyls (PC) levels reflecting extensive oxidative damage to total protein content and lipids, in muscle suggested by the authors to be due to increased levels of inflammatory cytokines and to increased protein degradation. Increased levels of lipid peroxidation in blood samples of CKD patients during HD treatment has also been found elsewhere (Varan et al., 2010) and could enhance the susceptibility of LDL oxidation which is a major contributor in the genesis of atherosclerosis. The above observations, together with animal findings in the role of carbonyl stress in vascular injury (Chen et al., 2013) concur to a role of protein oxidation in long-term vascular damage which could impact overall vessel functionality and thus striated muscle's bioenergetics and function.

The same group also reported increased mitochondrial protein and lipid oxidative damage in skeletal muscle of uremic patients compared to age-matched controls (Lim et al., 2002b). The authors also reported mitochondrial DNA mutations, and overall oxidative damage to total cellular DNA, supporting a notion of attenuating regenerative and bioenergetics capacities of the skeletal muscles of renal patients. Also, mitochondrial DNA deletions have been observed in the skeletal muscle of ESRD patients similar with these found in the skeletal muscle of elderly subjects due to oxidative damage which probably contribute to the impaired mitochondrial energy metabolism that characterizes uremic patients (Lim et al., 2000).

It is considered that mitochondrial membranes are more likely to develop oxidative damage due to the relatively high amounts of lipid containing polyunsaturated fatty acids that they possess (Laganiere and Yu, 1993) and this would explain their increased oxidative damage. Given that mitochondria are considered the predominant source of ROS in muscle fibers (Davies et al., 1982; McArdle et al., 2001; Jackson, 2009), due to the elevated oxygen consumption that occurs with increased mitochondrial activity, especially during exercise (Powers et al., 2011) it is conceivable that damage to the mitochondria membrane might further compound their function as a ROS source causing more leaking. Moreover, it has been suggested that mitochondrial ROS leaking depends on fiber type both at resting basal respiration and at an increased respiration (as in exercise). In an animal saponin-treated muscle study of mitochondrial respiration, type IIb skeletal muscle fibers showed significantly higher free radical leaking compared to type IIa and I fibers at basal respiration (Anderson and Neufer, 2006).

If indeed the ROS load in the late stages renal skeletal muscle is high, that might in part explain the higher susceptibility of type II fibers to atrophy observed in end stage patients, where not only generalized muscle atrophy was observed but more prominent atrophy was seen in type II (especially IIx) vs type I fibers either in non-locomotory (Sakkas et al., 2003a) or locomotory muscle samples. Furthermore, on the possible role of the mitochondrial dysfunction in renal muscle atrophy it should be noted that de-innervation studies show that denervated muscle mitochondria release fatty acid hydro peroxides, mediated by calcium dependent phospholipase A_2 (Bhattacharya et al., 2009). Such observations together with observations of an increased sensitivity of human aged mitochondria to apoptosis (Gouspillou et al., 2014), and the findings of Lim et al. (2002b) reviewed above, can collectively substantiate an important role

TABLE 1 | Summary results of the studies meeting the criteria of the present systematic review.

References	Total glutathione nmol/mg protein	GSS Gnmol/mg protein	SOD U/mg protein	MDA nmol/mg protein	CAT U/mg protein	PC nmol /mg of protein	Thiols nmol/mg protein
MARKERS OF OXIDATIVE STRESS IN MUSCLE TISSUE OF UREMIC PATIENTS							
Lim et al., 2002a	–	–	–	0.065 ± 0.009↑	–	3.78 ± −0.14↑	–
Lim et al., 2002b	–	–	–	23.76 ± 6.06↑	–	24.9 ± 4.00↑	–
Crowe et al., 2007	≈ 24↑	≈ 2.6	≈ 20	≈ 0.28↓	≈ 11↓	–	≈ 79
MARKERS OF OXIDATIVE STRESS IN MUSCLE TISSUE OF HEALTHY CONTROLS							
Lim et al., 2002a	–	–	–	0.043 ± 0.005	–	2.97 ± −0.28	–
Lim et al., 2002b	–	–	–	7.67 ± 0.95	–	3.78 ± 0.14	–
Crowe et al., 2007	≈ 5	≈ 3.3	≈ 27	≈ 0.52	≈ 34	–	≈ 60

GSH, glutathione; GSSG, oxidized glutathione; SOD, superoxide dismutase; MDA, malondialdehyde; CAT, catalase; PC, protein carbonyl; Thiols, protein thiol content. Arrows indicate statistically significant differences reported by authors.

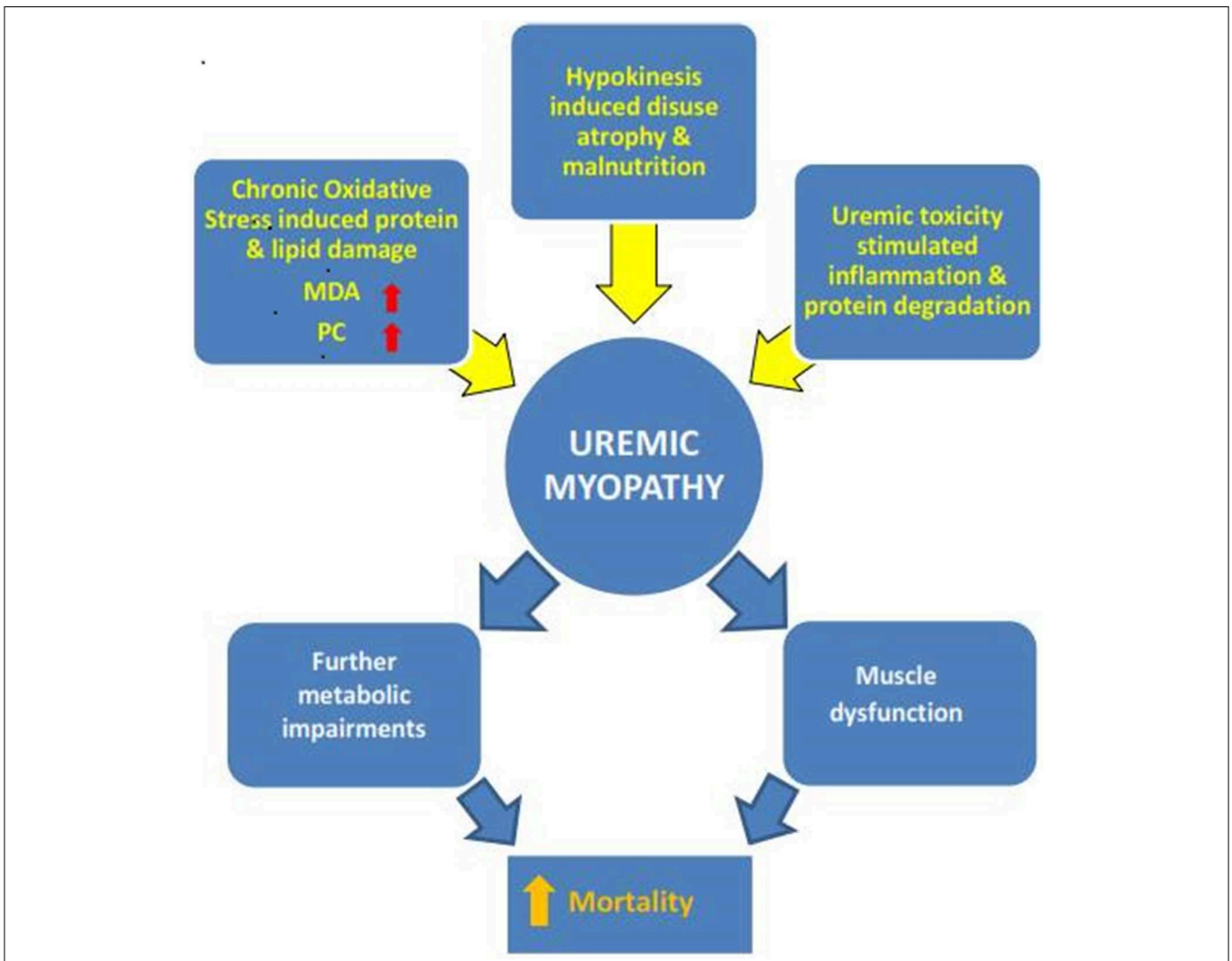

FIGURE 1 | The multifactorial nature of uremic myopathy. Many specific disease-related but also lifestyle factors (e.g., physical inactivity) contribute to the pathological muscle state. Exactly when one factor reaches critical importance cannot be surmised so far. The results of this systematic mini review do point to oxidative stress as a contributor to the development of uremic myopathy. MDA, malondialdehyde; PC, protein carbonyls.

for mitochondrial dysfunction, in the pathogenesis of uremic myopathy.

In contrast to the findings of Lim et al. and Crowe et al. (2007), reported decreased MDA content, increased total glutathione and no change in protein thiols content, superoxide dismutase (SOD), oxidized glutathione (GSSG) and catalase activity and concluded that there is no evident connection between oxidative stress and muscle atrophy in uremia. However, if one considers the age difference in the subjects of the conflicting studies one cannot discount the possibility that the much younger subjects, which also had spent less time on dialysis, of the Crowe et al. study had better preserved mitochondrial status. Adaptation of various antioxidant mechanisms can also explain some of the above differences. It should also be noted that in transgenic mice studies, the model overexpressing phospholipid hydroperoxide glutathione peroxidase, Gpx4-Tg (which is associated with mitochondrial and other membranes) protected against denervation atrophy and not the manganese superoxide dismutase (Sod2-Tg) or copper-zinc superoxide dismutase (Sod1-Tg) models, suggesting that the release of fatty acid hydroperoxides from mitochondria may be a more important factor in denervation-induced atrophy than superoxide and hydrogen peroxide (Bhattacharya et al., 2009).

The above discourse further highlights the difficulty faced by researchers in renal patient studies. Many confounding factors such as years in dialysis, nutrition, physical activity levels, level of treatment, and comorbidities can affect muscle status and accelerate or decelerate disease and aging effects (**Figure 1**).

Conclusions

CKD has a high and increasing prevalence not only in the old retirees but also in the middle-aged Europeans (Zoccali et al., 2010). Skeletal muscle dysfunction is a ubiquitous finding in CKD patients on advanced stages of the disease. The impact is grave as the statistics are implacable. Muscle loss and weakness contribute to the high morbidity and mortality of these patients, especially at the end-stage renal failure. Many specific disease-related but also lifestyle factors (such as physical inactivity) can be seen as contributors to the pathological muscle state. Exactly when one factor reaches critical importance cannot be surmised so far. The few studies meeting our search criteria while not agreeing, do point to a possibly important role for oxidative stress in uremic myopathy. It is not known if hypothesized oxidative stress mediated effects on muscle function are more of an acute or a chronic nature. *In vitro* studies however show clearly that oxidative stress does have a role whether via chronic, protein and other modifications or acute contractility effects. If anything the three studies and the peripheral literature highlight the need for a systematic study of the disease mechanisms affecting skeletal muscle performance in renal disease.

As long as great unknowns remain on the mechanisms and modulation of uremic myopathy, which leads to debilitation and premature death, progress in the management of this new epidemic is the least slowed down. We suggest that more muscle research, human and animal, should be done on pro-dialysis stages including work on the role of oxidative stress. This would allow researchers to decipher early changes, and perhaps identify susceptible individuals for accelerated muscle loss, before moving into the end-stage situation which on its own has detrimental effects on muscle status.

Acknowledgments

This work has been co-financed by the European Union (European Social Fund—ESF) and Greek national funds through the Operational Program "Educational and Lifelong Learning" of the National Strategic Reference Framework (NSRF)—Research Funding Program: Thales (MuscleFun Project-MIS 377260) Investing in knowledge society through the European Social Fund.

References

Allen, D. G., Lamb, G. D., and Westerblad, H. (2008). Skeletal muscle fatigue: cellular mechanisms. *Physiol. Rev.* 88, 287–332. doi: 10.1152/physrev.00015.2007

Anderson, E. J., and Neufer, P. D. (2006). Type II skeletal myofibers possess unique properties that potentiate mitochondrial H(2)O(2) generation. *Am. J. Physiol. Cell Physiol.* 290, C844–C851. doi: 10.1152/ajpcell.00402.2005

Bhattacharya, A., Muller, F. L., Liu, Y., Sabia, M., Liang, H., Song, W., et al. (2009). Denervation induces cytosolic phospholipase A2-mediated fatty acid hydroperoxide generation by muscle mitochondria. *J. Biol. Chem.* 284, 46–55. doi: 10.1074/jbc.M806311200

Campistol, J. M. (2002). Uremic myopathy. *Kidney Int.* 62, 1901–1913. doi: 10.1046/j.1523-1755.2002.00614.x

Carrero, J. J., Chmielewski, M., Axelsson, J., Snaedal, S., Heimburger, O., Barany, P., et al. (2008). Muscle atrophy, inflammation and clinical outcome in incident and prevalent dialysis patients. *Clin. Nutr.* 27, 557–564. doi: 10.1016/j.clnu.2008.04.007

Chen, X., Mori, T., Guo, Q., Hu, C., Ohsaki, Y., Yoneki, Y., et al. (2013). Carbonyl stress induces hypertension and cardio-renal vascular injury in Dahl salt-sensitive rats. *Hypertens. Res.* 36, 361–367. doi: 10.1038/hr.2012.204

Cheung, W. W., Paik, K. H., and Mak, R. H. (2010). Inflammation and cachexia in chronic kidney disease. *Pediatr. Nephrol.* 25, 711–724. doi: 10.1007/s00467-009-1427-z

Clyne, N., Ekholm, J., Jogestrand, T., Lins, L. E., and Pehrsson, S. K. (1991). Effects of exercise training in predialytic uremic patients. *Nephron* 59, 84–89. doi: 10.1159/000186524

Clyne, N., Jogestrand, T., Lins, L. E., and Pehrsson, S. K. (1994). Progressive decline in renal function induces a gradual decrease in total hemoglobin and exercise capacity. *Nephron* 67, 322–326. doi: 10.1159/000187987

Clyne, N., Jogestrand, T., Lins, L. E., Pehrsson, S. K., and Ekelund, L. G. (1987). Factors limiting physical working capacity in predialytic uraemic patients. *Acta Med. Scand.* 222, 183–190. doi: 10.1111/j.0954-6820.1987.tb10657.x

Crowe, A. V., McArdle, A., McArdle, F., Pattwell, D. M., Bell, G. M., Kemp, G. J., et al. (2007). Markers of oxidative stress in the skeletal muscle of patients on haemodialysis. *Nephrol. Dial. Transplant.* 22, 1177–1183. doi: 10.1093/ndt/gfl721

Davies, K. J., Quintanilha, A. T., Brooks, G. A., and Packer, L. (1982). Free radicals and tissue damage produced by exercise. *Biochem. Biophys. Res. Commun.* 107, 1198–1205. doi: 10.1016/S0006-291X(82)80124-1

Filiopoulos, V., Hadjiyannakos, D., Takouli, L., Metaxaki, P., Sideris, V., and Vlassopoulos, D. (2009). Inflammation and oxidative stress in end-stage renal

disease patients treated with hemodialysis or peritoneal dialysis. *Int. J. Artif. Organs* 32, 872–882.

Giannaki, C. D., Stefanidis, I., Karatzaferi, C., Liakos, N., Roka, V., Ntente, I., et al. (2011). The effect of prolonged intradialytic exercise in hemodialysis efficiency indices. *ASAIO J.* 57, 213–218. doi: 10.1097/MAT.0b013e318215dc9e

Gordon, P. L., Sakkas, G. K., Doyle, J. W., Shubert, T., and Johansen, K. L. (2007). Relationship between vitamin D and muscle size and strength in patients on hemodialysis. *J. Ren. Nutr.* 17, 397–407. doi: 10.1053/j.jrn.2007.06.001

Gouspillou, G., Bourdel-Marchasson, I., Rouland, R., Calmettes, G., Biran, M., Deschodt-Arsac, V., et al. (2014). Mitochondrial energetics is impaired *in vivo* in aged skeletal muscle. *Aging Cell* 13, 39–48. doi: 10.1111/acel.12147

Grams, M. E., Chow, E. K. H., Segev, D. L., and Coresh, J. (2013). Lifetime Incidence of CKD Stages 3-5 in the United States. *Am. J. Kidney Dis.* 62, 245–252. doi: 10.1053/j.ajkd.2013.03.009

Griffiths, R. D. (1996). Muscle mass, survival, and the elderly ICU patient. *Nutrition* 12, 456–458. doi: 10.1016/S0899-9007(96)00141-4

Hu, W. T., Shelnutt, M., Wilson, A., Yarab, N., Kelly, C., Grossman, M., et al. (2013). Behavior Matters-Cognitive Predictors of Survival in Amyotrophic Lateral Sclerosis. *PLoS ONE* 8:e57584. doi: 10.1371/journal.pone.0057584

Ikizler, T. A., Pupim, L. B., Brouillette, J. R., Levenhagen, D. K., Farmer, K., Hakim, R. M., et al. (2002). Hemodialysis stimulates muscle and whole body protein loss and alters substrate oxidation. *Am. J. Physiol. Endocrinol. Metab.* 282, E107–E116.

Jackson, M. J. (2009). Redox regulation of adaptive responses in skeletal muscle to contractile activity. *Free Radic. Biol. Med.* 47, 1267–1275. doi: 10.1016/j.freeradbiomed.2009.09.005

Johansen, K. L., Doyle, J., Sakkas, G. K., and Kent-Braun, J. A. (2005). Neural and metabolic mechanisms of excessive muscle fatigue in maintenance hemodialysis patients. *Am. J. Physiol. Regul. Integr. Comp. Physiol.* 289, R805–R813. doi: 10.1152/ajpregu.00187.2005

Johansen, K. L., Painter, P. L., Sakkas, G. K., Gordon, P., Doyle, J., and Shubert, T. (2006). Effects of resistance exercise training and nandrolone decanoate on body composition and muscle function among patients who receive hemodialysis: a randomized, controlled trial. *J. Am. Soc. Nephrol.* 17, 2307–2314. doi: 10.1681/ASN.2006010034

Johansen, K. L., Shubert, T., Doyle, J., Soher, B., Sakkas, G. K., and Kent-Braun, J. A. (2003). Muscle atrophy in patients receiving hemodialysis: effects on muscle strength, muscle quality, and physical function. *Kidney Int.* 63, 291–297. doi: 10.1046/j.1523-1755.2003.00704.x

Kaysen, G. A., Dubin, J. A., Muller, H. G., Rosales, L., Levin, N. W., and Mitch, W. E. (2004). Inflammation and reduced albumin synthesis associated with stable decline in serum albumin in hemodialysis patients. *Kidney Int.* 65, 1408–1415. doi: 10.1111/j.1523-1755.2004.00520.x

Klein, J. C., Moen, R. J., Smith, E. A., Titus, M. A., and Thomas, D. D. (2011). Structural and functional impact of site-directed methionine oxidation in myosin. *Biochemistry* 50, 10318–10327. doi: 10.1021/bi201279u

Kouidi, E., Albani, M., Natsis, K., Megalopoulos, A., Gigis, P., Guiba-Tziampiri, O., et al. (1998). The effects of exercise training on muscle atrophy in haemodialysis patients. *Nephrol. Dial. Transplant.* 13, 685–699. doi: 10.1093/ndt/13.3.685

Laganiere, S., and Yu, B. P. (1993). Modulation of membrane phospholipid fatty acid composition by age and food restriction. *Gerontology* 39, 7–18. doi: 10.1159/000213509

Lamb, G. D., and Westerblad, H. (2011). Acute effects of reactive oxygen and nitrogen species on the contractile function of skeletal muscle. *J. Physiol.* 589, 2119–2127. doi: 10.1113/jphysiol.2010.199059

Lim, P. S., Cheng, Y. M., and Wei, Y. H. (2000). Large-scale mitochondrial DNA deletions in skeletal muscle of patients with end-stage renal disease. *Free Radic. Biol. Med.* 29, 454–463. doi: 10.1016/S0891-5849(00)00334-8

Lim, P. S., Cheng, Y. M., and Wei, Y. H. (2002a). Increase in oxidative damage to lipids and proteins in skeletal muscle of uremic patients. *Free Radic. Res.* 36, 295–301. doi: 10.1080/10715760290019318

Lim, P. S., Ma, Y. S., Cheng, Y. M., Chai, H., Lee, C. F., Chen, T. L., et al. (2002b). Mitochondrial DNA mutations and oxidative damage in skeletal muscle of patients with chronic uremia. *J. Biomed. Sci.* 9, 549–560. doi: 10.1007/BF02254982

Lowrie, E. G., and Lew, N. L. (1990). Death risk in hemodialysis patients: the predictive value of commonly measured variables and an evaluation of death rate differences between facilities. *Am. J. Kidney Dis.* 15, 458–482. doi: 10.1016/S0272-6386(12)70364-5

McArdle, A., Pattwell, D., Vasilaki, A., Griffiths, R. D., and Jackson, M. J. (2001). Contractile activity-induced oxidative stress: cellular origin and adaptive responses. *Am. J. Physiol. Cell Physiol.* 280, C621–C627.

Moylan, J. S., and Reid, M. B. (2007). Oxidative stress, chronic disease, and muscle wasting. *Muscle Nerve* 35, 411–429. doi: 10.1002/mus.20743

Porter, M. M., Vandervoort, A. A., and Lexell, J. (1995). Aging of human muscle: structure, function and adaptability. *Scand. J. Med. Sci. Sports* 5, 129–142. doi: 10.1111/j.1600-0838.1995.tb00026.x

Powers, S. K., Ji, L. L., Kavazis, A. N., and Jackson, M. J. (2011). Reactive oxygen species: impact on skeletal muscle. *Compr. Physiol.* 1, 941–969. doi: 10.1002/cphy.c100054

Prochniewicz, E., Lowe, D. A., Spakowicz, D. J., Higgins, L., O'conor, K., Thompson, L. V., et al. (2008a). Functional, structural, and chemical changes in myosin associated with hydrogen peroxide treatment of skeletal muscle fibers. *Am. J. Physiol. Cell Physiol.* 294, C613–C626. doi: 10.1152/ajpcell.00232.2007

Prochniewicz, E., Spakowicz, D., and Thomas, D. D. (2008b). Changes in actin structural transitions associated with oxidative inhibition of muscle contraction. *Biochemistry* 47, 11811–11817. doi: 10.1021/bi801080x

Reardon, T. F., and Allen, D. G. (2009). Time to fatigue is increased in mouse muscle at 37 degrees C; the role of iron and reactive oxygen species. *J. Physiol.* 587, 4705–4716. doi: 10.1113/jphysiol.2009.173005

Sakkas, G. K., Ball, D., Mercer, T. H., Sargeant, A. J., Tolfrey, K., and Naish, P. F. (2003a). Atrophy of non-locomotor muscle in patients with end-stage renal failure. *Nephrol. Dial. Transplant.* 18, 2074–2081. doi: 10.1093/ndt/gfg325

Sakkas, G. K., Hadjigeorgiou, G. M., Karatzaferi, C., Maridaki, M. D., Giannaki, C. D., Mertens, P. R., et al. (2008a). Intradialytic aerobic exercise training ameliorates symptoms of restless legs syndrome and improves functional capacity in patients on hemodialysis. *ASAIO J.* 54, 185–190. doi: 10.1097/MAT.0b013e3181641b07

Sakkas, G. K., Karatzaferi, C., Zintzaras, E., Giannaki, C. D., Liakopoulos, V., Lavdas, E., et al. (2008b). Liver fat, visceral adiposity, and sleep disturbances contribute to the development of insulin resistance and glucose intolerance in nondiabetic dialysis patients. *Am. J. Physiol. Regul. Integr. Comp. Physiol.* 295, R1721–R1729. doi: 10.1152/ajpregu.00935.2007

Sakkas, G. K., Liakopoulos, V., Karatzaferi, C., and Stefanidis, I. (2008c). Sleep quality and dialysis efficacy affect functional capacity in patients receiving haemodialysis therapy. *Nephrol. Dial. Transplant.* 23, 2703–2704. doi: 10.1093/ndt/gfn048

Sakkas, G. K., Sargeant, A. J., Mercer, T. H., Ball, D., Koufaki, P., Karatzaferi, C., et al. (2003b). Changes in muscle morphology in dialysis patients after 6 months of aerobic exercise training. *Nephrol. Dial. Transplant.* 18, 1854–1861. doi: 10.1093/ndt/gfg237

Samouilidou, E., and Grapsa, E. (2003). Effect of dialysis on plasma total antioxidant capacity and lipid peroxidation products in patients with end-stage renal failure. *Blood Purif.* 21, 209–212. doi: 10.1159/000070691

Spencer, T., and Posterino, G. S. (2009). Sequential effects of GSNO and H2O2 on the Ca2+ sensitivity of the contractile apparatus of fast- and slow-twitch skeletal muscle fibers from the rat. *Am. J. Physiol. Cell Physiol.* 296, C1015–C1023. doi: 10.1152/ajpcell.00251.2008

Taes, Y. E. C., Speeckaert, M., Bauwens, E., De Buyzere, M. R., Libbrecht, J., Lameire, N. H., et al. (2004). Effect of dietary creatine on skeletal muscle myosin heavy chain isoform expression in an animal model of uremia. *Nephron Exp. Nephrol.* 96, E103–E110. doi: 10.1159/000077376

Topp, K. S., Painter, P. L., Walcott, S., Krasnoff, J. B., Adey, D., Sakkas, G. K., et al. (2003). Alterations in skeletal muscle structure are minimized with steroid withdrawal after renal transplantation. *Transplantation* 76, 667–673. doi: 10.1097/01.TP.0000076096.45542.1B

Varan, H. I., Dursun, B., Dursun, E., Ozben, T., and Suleymanlar, G. (2010). Acute effects of hemodialysis on oxidative stress parameters in chronic uremic patients: comparison of two dialysis membranes. *Int. J. Nephrol. Renovasc. Dis.* 3, 39–45.

Wang, X. H., and Mitch, W. E. (2013). Muscle wasting from kidney failure-a model for catabolic conditions. *Int. J. Biochem. Cell Biol.* 45, 2230–2238. doi: 10.1016/j.biocel.2013.06.027

Yazdi, P. G., Moradi, H., Yang, J. Y., Wang, P. H., and Vaziri, N. D. (2013). Skeletal muscle mitochondrial depletion and dysfunction in chronic kidney disease. *Int. J. Clin. Exp. Med.* 6, 532–539.

Zhang, L., Du, J., Hu, Z., Han, G., Delafontaine, P., Garcia, G., et al. (2009). IL-6 and serum amyloid A synergy mediates angiotensin II-induced muscle wasting. *J. Am. Soc. Nephrol.* 20, 604–612. doi: 10.1681/ASN.2008060628

Zhang, L., Rajan, V., Lin, E., Hu, Z., Han, H. Q., Zhou, X., et al. (2011). Pharmacological inhibition of myostatin suppresses systemic inflammation and muscle atrophy in mice with chronic kidney disease. *FASEB J.* 25, 1653–1663. doi: 10.1096/fj.10-176917

Zhang, L., Wang, X. H., Wang, H., Du, J., and Mitch, W. E. (2010). Satellite cell dysfunction and impaired IGF-1 signaling cause CKD-induced muscle atrophy. *J. Am. Soc. Nephrol.* 21, 419–427. doi: 10.1681/ASN.2009060571

Zoccali, C., Kramer, A., and Jager, K. J. (2010). Epidemiology of CKD in Europe: an uncertain scenario. *Nephrol. Dial. Transplant.* 25, 1731–1733. doi: 10.1093/ndt/gfq250

Conflict of Interest Statement: The authors declare that the research was conducted in the absence of any commercial or financial relationships that could be construed as a potential conflict of interest.

Advantages of publishing in Frontiers

OPEN ACCESS
Articles are free to read, for greatest visibility

COLLABORATIVE PEER-REVIEW
Designed to be rigorous – yet also collaborative, fair and constructive

FAST PUBLICATION
Average 85 days from submission to publication (across all journals)

COPYRIGHT TO AUTHORS
No limit to article distribution and re-use

TRANSPARENT
Editors and reviewers acknowledged by name on published articles

SUPPORT
By our Swiss-based editorial team

IMPACT METRICS
Advanced metrics track your article's impact

GLOBAL SPREAD
5'100'000+ monthly article views and downloads

LOOP RESEARCH NETWORK
Our network increases readership for your article

Frontiers
EPFL Innovation Park, Building I • 1015 Lausanne • Switzerland
Tel +41 21 510 17 00 • Fax +41 21 510 17 01 • info@frontiersin.org
www.frontiersin.org

Find us on